# Uptake and accumulation of silver nanoparticles by wheat (*Triticum aestivum L.*)

Denitsa Nikolaeva Rigby

Imperial College London

Department of Earth Science and Engineering

South Kensington Campus

London SW7 2AZ, UK




A thesis submitted for the degree of Doctor of Philosophy


R
M
S

# Statement of originality

I certify that the content of this thesis is my original work unless otherwise stated and that contributions and assistance received in preparing this thesis are fully and appropriately acknowledged and referenced.




# Copyright Declaration

The copyright of this thesis rests with the author. Unless otherwise indicated, its contents are licensed under a Creative Commons Attribution-Non-Commercial 4.0 International Licence (CC BY-NC).

Under this licence, you may copy and redistribute the material in any medium or format. You may also create and distribute modified versions of the work. This is on the condition that: you credit the author and do not use it, or any derivative works, for a commercial purpose.

When reusing or sharing this work, ensure you make the licence terms clear to others by naming the licence and linking to the licence text. Where a work has been adapted, you should indicate that the work has been changed and describe those changes.

Please seek permission from the copyright holder for uses of this work that are not included in this licence or permitted under UK Copyright Law.

# Acknowledgements

First, I would like to say a massive thank you to my supervisors Mark, Claus, Marianne and Amaia for their everlasting support, encouragement and enthusiasm. Thank you for all of your guidance, expertise and patience. Mark, you have always had my back and I cannot be more grateful to have had such an amazing supervisor. Claus, Marianne and Amaia, thank you so much for your valuable help, outstanding assistance and advice and for pushing me to give so many presentations.

Next, I would like to thank the fantastic MAGIC and ecotoxicology groups at Imperial College and UK CEH for a supportive and wonderful environment. I cannot thank enough the Ecotox group, and Amaia specifically, for the many root washing sessions and help with my experimental setups and takedowns over Harry Potter. Special thanks to Tabea, who patiently passed on her knowledge down to me.

Also, I would like to thank the laboratory managers who have helped throughout this PhD – I have learned so much from you and I will always be very grateful. Special thanks to Katharina, Rudo, Elma and Carolin for all of their patience and for teaching me so many valuable techniques and methods.

I would like to thank my office buddies – Holly and Elmer – for all of the times they helped out, listened and cheered me up. Thanks for all of our lunchtime breaks, walks, book club meetings, pub evenings, wine sessions, BBQs and tea breaks. Also, thanks to Sarah, Ilse, Arran, Jordan and Hollie.

Special thanks to my friends for all of our chats, rendezvous' and for the lovely distractions.

Ben, you have been my absolute rock (compliment of the highest order) throughout and have always encouraged me. I honestly think I have put you through more severe mental obstacles than what you endured during your Royal Marines Officers training. Thank you ever so much!

Last, but not least, I would like to thank my family for their never stopping encouragement and for pushing me forward. You must be glad to know that I am finally done with education. Thank you, mum, dad, Yana, Vesko, Sarah, Jeremy and Lizzy for all of your love and support!


R
M
S

# Abstract

The rapid product development and intense production, consumer use, and disposal of engineered nanomaterials like silver nanoparticles (Ag NPs) are leading to increased levels of Ag NP-containing waste. This waste can enter natural ecosystems by direct release or when biosolids from sewage sludge are applied on agricultural land as fertilisers. Silver NPs display physicochemical properties that differ from their bulk materials and their physical and chemical interactions with the environment are often poorly understood. As such, there is an urgent need for exposure studies of Ag NPs that can be used for comprehensive risk assessments. Recent research shows that Ag from Ag NPs enters roots through vascular tissues and is translocated to the stem, leaves and fruit of plants. Previous studies have reported that Ag from Ag NPs can have an impact on the cell structures of plants and their physiological and biochemical functions.

This thesis focusses on the uptake, translocation and accumulation of Ag from Ag NPs and their ready soluble form ($AgNO_3$) by wheat (*Triticum aestivum L.*) and their effects on a biological level in a series of exposures. In detail, the work presented in this thesis aims to: (i) provide quantitative data on the uptake and accumulation of Ag from Ag NPs and $AgNO_3$ on wheat in an environmentally relevant exposure; (ii) focus on the effects of Ag on a biological level in an environmentally relevant Ag NP and $AgNO_3$ exposure; (iii) delve into the uptake of Ag from Ag NPs, $Ag_2S$ NPs and $AgNO_3$ in a multimedia exposure and into the use of hydroponic systems as a substitute for soil testing; and (iv) identify the mechanisms of Ag uptake from Ag NPs and $AgNO_3$ under water stress through split root experiments.

# TABLE OF CONTENTS

**List of tables** ..... **11**

**List of figures** ..... **13**

**Chapter 1: Introduction & literature review** ..... **18**

**1.1. Reasons for research** ..... 18
**1.2. Thesis aims & structure** ..... 19
**1.3. Literature review** ..... 19
*1.3.1. Nanomaterials & the environment* ..... 19
*1.3.1.1. Nanomaterials* ..... 19
*1.3.1.2. Nano-ecotoxicology* ..... 20
*1.3.2. Ag NPs* ..... 21
*1.3.2.1. Ag* ..... 21
*1.3.2.2. Properties & applications of Ag NPs* ..... 21
*1.3.3. Release of Ag NPs into the environment* ..... 22
*1.3.4. Fate of Ag NPs in the environment* ..... 24
*1.3.5. Predicted environmental concentrations for Ag NPs* ..... 26
*1.3.6. Ag NP exposures on plants* ..... 27
*1.3.7. Wheat & Ag uptake* ..... 28
*1.3.7.1. Wheat* ..... 28
*1.3.7.2. Wheat plant anatomy & physiology* ..... 28
*1.3.7.3. Wheat development & nutrient transport* ..... 30
*1.3.7.4. Potential pathway for the uptake, translocation & accumulation of Ag by wheat* ..... 31
*1.3.7.5. Ag speciation within plants* ..... 33
*1.3.8. Effects of Ag from Ag NPs on plants* ..... 33

**Chapter 2: Stable isotope tracing of silver nanoparticles through a full wheat life cycle exposure; Part 1: Uptake, accumulation & translocation** ... **44**

**2.1. Introduction** ..... 44
**2.2. Experimental design & methodology** ..... 46
*2.2.1. Isotopically labelled $^{109}Ag$ NPs & $^{109}AgNO_3$* ..... 46
*2.2.1.1. Synthesis* ..... 46
*2.2.1.2. Characterisation of the labelled $^{109}Ag$ NPs* ..... 48

*2.2.2. Exposure* ..... 48
*2.2.2.1. Preparation of the soils* ..... 48
*2.2.2.2. Dosing of the soils* ..... 49
*2.2.2.3. Planting of wheat* ..... 51
*2.2.2.4. Exposure conditions* ..... 51
*2.2.3. Sample collection* ..... 52
*2.2.3.1. Plant tissues* ..... 52
*2.2.3.2. Soils & soil pore waters* ..... 53
*2.2.4. Sample analyses* ..... 54
*2.2.4.1. Digestion & initial treatment* ..... 55
*2.2.4.2. Separation of Ag* ..... 55
*2.2.5. Mass spectrometry* ..... 56
*2.2.5.1. Instrumentation* ..... 56
*2.2.5.2. Preliminary assessment of Ag concentrations* ..... 57
*2.2.5.3. Ag isotope measurements* ..... 57
*2.2.5.4. Data reduction* ..... 58
*2.2.5.5. Quality control* ..... 59
*2.2.6. Statistical analyses* ..... 59
**2.3. Results** ..... 60
*2.3.1. Characterisation of the $^{109}$Ag NPs* ..... 60
*2.3.2 Validity of the exposure experiment* ..... 62
*2.3.3. Soils* ..... 62
*2.3.4. Soil pore waters* ..... 62
*2.3.5. Plant tissues* ..... 65
**2.4. Discussion** ..... 67
*2.4.1. Ag mass balance of soils* ..... 67
*2.4.2. Total Ag & truly dissolved Ag in soil pore waters* ..... 68
*2.4.3. Ag uptake by & translocation in wheat* ..... 70
*2.4.4. Implications* ..... 73
**2.5. Conclusion** ..... 74

**Chapter 3: Stable isotope tracing of silver nanoparticles in a full wheat life cycle exposure; Part 2: Influence on the biology** ..... **76**
**3.1. Introduction** ..... 76
**3.2. Experimental design & methodology** ..... 78

*3.2.1. Exposure conditions* ..... 78
*3.2.2. Sample collection & measurements* ..... 78
**3.3. Results** ..... 80
*3.3.1. Germination rate* ..... 80
*3.3.2. Dry & wet plant biomass & plant osmotic balance* ..... 80
*3.3.3. Length of wheat shoots & grains* ..... 84
*3.3.4. Plant growth rates* ..... 85
**3.4. Discussion** ..... 85
*3.4.1. No effects of $^{109}$Ag-E on dry biomass* ..... 86
*3.4.2. Possible effects of $^{109}$Ag-E on grains & shoots* ..... 86
*3.4.3. Impact of $^{109}$Ag-E on plant development* ..... 89
**3.5. Conclusion** ..... 90
**Chapter 4: Silver nanoparticle accumulation: Assessing different hydroponic media as a proxy for soil** ..... **91**
**4.1. Introduction** ..... 91
**4.2. Experimental design & methodology** ..... 92
*4.2.1. Ag NPs, $Ag_2S$ NPs & $AgNO_3$* ..... 92
*4.2.2. Exposure* ..... 92
*4.2.2.1. Preparation of the media* ..... 92
*4.2.2.2. Exposure systems* ..... 95
*4.2.2.3. Dosing of the media* ..... 96
*4.2.2.4. Planting of wheat* ..... 97
*4.2.2.5. Exposure conditions* ..... 98
*4.2.3. Sample collection* ..... 98
*4.2.3.1. Plant tissues* ..... 98
*4.2.3.2. Soils & soil pore waters* ..... 99
*4.2.3.3. Hydroponic media* ..... 99
*4.2.4. Sample analysis* ..... 100
*4.2.4.1. Sample preparation* ..... 100
*4.2.4.2. Graphite furnace atomic absorption spectroscopy (GF AAS)* ..... 100
*4.2.4.3. Flame AAS* ..... 101
*4.2.5. Statistical analyses* ..... 102
**4.3. Results** ..... 102
*4.3.1. Characterisation of the nanoparticles* ..... 102

*4.3.2. Validity of the exposure experiment* ..... 102
*4.3.3. Exposure media* ..... 103
*4.3.4. Plant tissues* ..... 105
*4.3.4.1. Root tissues* ..... 105
*4.3.4.2. Shoot tissues* ..... 107
*4.3.5. Dry plant biomass* ..... 109
**4.4. Discussion** ..... 110
*4.4.1. Ag concentration in the media* ..... 110
*4.4.1.1. Ag concentration of the Lufa soil & LUPW* ..... 111
*4.4.1.2. Ag concentration of the hydroponic media* ..... 112
*4.4.2. Ag associated with the roots* ..... 114
*4.4.3. Ag uptake & translocation* ..... 116
**4.5. Conclusion** ..... 119

**Chapter 5: Xylem- & phloem-based transport of Ag NPs in wheat** ..... **122**
**5.1. Introduction** ..... 122
**5.2. Experimental design & methodology** ..... 123
*5.2.1. Ag NPs* ..... 124
*5.2.2. Soil* ..... 125
*5.2.3. Exposure system* ..... 125
*5.2.4. Planting of wheat* ..... 125
*5.2.5. Experimental design & test conditions* ..... 126
*5.2.6. Sample collection* ..... 126
*5.2.7. Ag NP exposure* ..... 127
*5.2.7.1. Soil preparation* ..... 127
*5.2.7.2. Sample collection* ..... 128
*5.2.8. Time series exposure* ..... 128
*5.2.8.1. Soil preparation* ..... 128
*5.2.8.2. Sample collection* ..... 129
*5.2.9. Sample analysis* ..... 129
*5.2.9.1. Sample preparation* ..... 129
*5.2.9.2. Graphite furnace atomic absorption spectroscopy (GF AAS)* ..... 130
*5.2.9.3. Flame AAS* ..... 131
*5.2.10. Statistical analyses* ..... 132
**5.3. Results** ..... 132

*5.3.1. Characterisation of the Ag NPs* ..... 132
*5.3.2. Validity of the exposure experiment* ..... 132
*5.3.3. Ag NP exposure* ..... 133
*5.3.3.1. Soils* ..... 133
*5.3.3.2. Plant tissues* ..... 134
*5.3.4. Time series exposure* ..... 136
*5.3.4.1. Soils* ..... 136
*5.3.4.2. Soil pore waters* ..... 137
*5.3.4.3. Roots* ..... 138
*5.3.4.4. Shoots* ..... 139
**5.4. Discussion** ..... 140
*5.4.1. Ag NP exposure* ..... 141
*5.4.1.1. Soils* ..... 141
*5.4.1.2. Roots from treated soils* ..... 141
*5.4.1.3. Shoots & xylem-based transport of Ag* ..... 142
*5.4.1.4. Roots in untreated soils & phloem-based transport of Ag* ..... 145
*5.4.2. Time series exposure* ..... 147
*5.4.2.1. Soils* ..... 147
*5.4.2.2. Soil pore waters* ..... 148
*5.4.2.3. Treated roots* ..... 149
*5.4.2.4. Shoots & xylem-based transport of Ag* ..... 150
*5.4.2.5. Untreated roots & phloem-based transport of Ag* ..... 153
**5.5. Conclusion** ..... 154
**Chapter 6: Summary & outlook** ..... 156
**Bibliography** ..... 159
**Appendices** ..... 183
**Appendix A** ..... 183
**Appendix B** ..... 185
**Appendix C** ..... 188
**Appendix D** ..... 195

# List of tables


**Chapter 1** **Page**

*Table 1.1.* Predicted environmental concentrations of Ag NP concentrations in different compartments for 2017, 2030 and 2050 (Giese et al., 2018). 26

*Table 1.2.* Review table of Ag NP exposures in different media and at different exposure concentrations. 35

**Chapter 2**

*Table 2.1.* Reagents used for preparation and results of the characterisation for the two batches of labelled $^{109}$Ag NPs that were employed in this study. 47

*Table 2.2.* Chemical composition of the 25% Hoagland solution. 49

*Table 2.3.* Growth stages (GSs) according to the Zadoks scale (Zadoks et al., 1974) with days in brackets, which represent the time that the samples were collected in this experiment. 52

*Table 2.4.* Types of biological tissues collected for each growth stage. 53

*Table 2.5.* Summary of the anion exchange chromatography protocol for Ag separation developed by Junk et al. (2019). 56

*Table 2.6.* Mean bioaccumulation ratios for $^{109}$Ag-E determined for samples from GSs 4, 6 and 8 (n = 2). 71

*Table 2.7.* Mean translocation ratios for $^{109}$Ag-E determined for samples from GSs 4, 6 and 8 (n = 2). 72

**Chapter 4**

*Table 4.1.* Chemical composition of 1L artificial pore water. 94

*Table 4.2.* Chemical composition of 1L 25% Hoagland solution. 94

*Table 4.3.* Spiking volumes and concentrations used for the experiment. The V* indicates the total volume of spike added to each medium and mg $L^{-1}$** signifies the concentration of spike used for each treatment and medium. 97

*Table 4.4.* Mean Ag concentrations (in mg $kg^{-1}$ or mg $L^{-1}$) and per cent of the nominal Ag concentrations at day 0 for all media including the Lufa soil, Lufa hydroponic solution, artificial pore water and Hoagland solution (n = 3). 111

**Chapter 5**

*Table 5.1*. Mean Ag concentrations determined for the treated and untreated soils (in mg kg-1) of the wet-wet and wet-dry exposure systems of the Ag NP exposure at day 0 and day 7. BLOD: Ag concentrations below the limit of detection. The uncertainties signify the calculated standard deviations of three replicates (n = 3). 133

*Table 5.2*. Mean total and truly dissolved Ag concentrations (in µg $L^{-1}$) determined for the soil pore waters of the untreated dry soils during the course of the Ag time series exposure. The uncertainties represent the calculated standard deviations (n = 3). 138

*Table 5.3*. Mean $[Ag]_{Shoot}/[Ag]_{T\text{-}root}$ and $[Ag]_{U\text{-}root}/[Ag]_{Shoot}$ ratios for the Ag NP exposure. The uncertainties denote the calculated standard deviations (n = 3). 143

*Table 5.4*. The $[Ag]_{Root}/[Ag]_{Tot\text{-}PW}$ and $[Ag]_{Root}/[Ag]_{TrD\text{-}PW}$ ratios are calculated from the Ag concentrations of roots grown in the TW soils as well as the total (Tot-PW) or truly dissolved (TrD-PW) Ag concentrations of soil pore waters from the treated wet (TW) soils. The uncertainties signify the calculated standard deviation (n = 3). 150

*Table 5.5*. Mean $[Ag]_{Tot\text{-}PW\text{-}Ag\ NP}/[Ag]_{Tot\text{-}PW\text{-}AgNO3}$, $[Ag]_{T\text{-}root\text{-}AgNP}/[Ag]_{T\text{-}root\text{-}AgNO3}$ and $[Ag]_{Shoot\text{-}AgNP}/[Ag]_{Shoot\text{-}AgNO3}$ ratios for day 7 of the time series Ag exposure. The uncertainties denote the calculated standard deviation (n = 3). 151

*Table 5.6*. Mean $[Ag]_{Shoot}/[Ag]_{T\text{-}Root}$ and $[Ag]_{U\text{-}Root}/[Ag]_{Shoot}$ ratios for the time series exposure. The uncertainties signify the calculated standard deviation (n = 3). 152

# List of figures


**Chapter 1** **Page**

*Figure 1.1*. Simplified overview of the release of Ag NPs into the environment. Figure reproduced and adjusted after Hartmann et al. (2014). 23

*Figure 1.2.* An overview of the anatomy of wheat (adjusted after Aslam et al. 2018 and Carver 2009). Panel A displays the anatomy of the seed, B shows the germination of wheat, while C presents the overall anatomy of a mature wheat plant. 29

*Figure 1.3*. Simplified overview of the uptake of Ag NPs by different wheat plant tissues. Little root tissues pictures were adapted and adjusted after Kim et al. (2018). 32

**Chapter 2**

*Figure 2.1.* Schematic of setup. Polypropylene plastic pint cups (133 mm in height, top diameter of 97 mm and a base diameter of 63 mm) with 0.7 kg soil capacity and three holes for wicks, 20 mm in diameter each, were used as pots. 50

*Figure 2.2.* DLS data for size distribution determined for the $^{109}$Ag NPs of batch #1 (A) and batch #2 (B). Sample measurements were repeated 5 times. 60

*Figure 2.3.* Frequency plot for the diameters (in nm) of the $^{109}$Ag NPs as determined by TEM imaging. The mean particle diameter is 19.62 ± 6.45 nm (n = 873). 61

*Figure 2.4.* TEM micrographs of the $^{109}$Ag NPs. A and B: TEM images of batch #1; C and D: TEM images of batch #2. 61

*Figure 2.5.* $^{109}$Ag-E concentrations for the spiked Lufa soils determined at day 0 and for GSs 1, 2, 4, 6 and 8. The symbols on the graph show the two individual data points (n = 2). 64

*Figure 2.6.* Total $^{109}$Ag-E (A) and truly dissolved $^{109}$Ag-E (B) concentrations in Lufa soil pore water for GSs 4, 6 and 8 (n = 3). The error bars signify standard deviations of two or three samples. The $^{109}$Ag-E concentrations for the $^{109}$Ag NP treatment were found to be significantly higher than those of the $^{109}AgNO_3$ treatment for both the total $^{109}$Ag-E concentrations (A) (p = 0.03) and the truly dissolved $^{109}$Ag-E concentrations (B) (p = 0.01). 64

*Figure 2.7.* Simple linear regression for (A) total $^{109}$Ag-E concentrations for the $^{109}$Ag NP treatment, (B) truly dissolved $^{109}$Ag-E for the $^{109}$Ag NP treatment, (C) 65

total $^{109}$Ag-E for the $^{109}AgNO_3$ treatment and (D) truly dissolved $^{109}$Ag-E for the $^{109}AgNO_3$ treatment, when plotted versus the number of sampling days (n = 3). The total and truly dissolved $^{109}$Ag-E concentrations of the pore waters showed no significant temporal trends, with p-values exceeding 0.46 and 0.58, respectively.

*Figure 2.8*. $^{109}$Ag-E concentrations for roots (A), shoots (B), seeds (C) and grains (D) of wheat plotted versus the GS of sampling. The symbols on the graph show the two individual data points (n = 2) and the ⊕ symbol denotes the mean values. 66

**Chapter 3**

*Figure 3.1.* Total (A) and aboveground (B) dry biomass yield (DBY) for wheat plants sampled at GS 1 to GS 8. The individual points represent the results for individual samples, whilst the red line marks the 100% DBY value defined by the average blank control result for a given GS (n = 5 for the Ag treatements; n = 3 for the controls). The error bars denote 1 standard deviation for each dataset. The only significant difference between the treatments was found at GS 5 for the $^{109}AgNO_3$ and the blank control treatments (*p=0.04). 81

*Figure 3.2.* Shoot tissue dry biomass (g) (A) and shoot length (cm) (B) for the different treatments at GSs 1 to 8 (n = 5 for the Ag treatements; n = 3 for the controls). The individual data points represent the results for individual plant samples, whilst the error bars denote 1 standard deviation for each dataset. The purple square boxes indicate the mean values in panel B. In panel (A), there are no significant differences between the samples from different treatments (p>0.07). In panel (B), the box plots show the length measured for the longest shoot leaf and indicate a single statistical increase at GS 5 for the $^{109}AgNO_3$ treatments when compared to the citrate control (*p=0.02). 82

*Figure 3.3.* Grain dry biomass (g) (A) and grain head length (cm) (B) for the four treatments at GSs 6 to 8 (n = 5 for the Ag treatements; n = 3 for the controls). The individual data points represent the results for individual samples, whilst the error bars denote 1 standard deviation for each dataset. The purple square boxes indicate the mean values in panel B. In panel (A) there are significant differences between Ag NP and $AgNO_3$ treatments versus the citrate control treatment at GS 8 (*p = 0.001). In panel (B) the single significant difference between treatments is also at GS 8, between the AgNO3 and the citrate control treatment (*p = 0.01). 83

*Figure 3.4*. Plant osmotic balance for the different treatments at GS 1 to GS 8. The individual points represent the results for individual samples (n = 5 for the 84

Ag treatments; n = 3 for the controls). The error bars denote 1 standard deviation for each dataset.

*Figure 3.5.* Plant growth rate determined for the four treatments for GSs 1 to 8 (n = 10 for the Ag treatments and n = 6 for the control treatments for GSs 1 – 3, while n = 5 for the Ag treatments; n = 3 for the controls for GSs 4 – 8). The box plots show how long it took plants to reach each GS (in number of days). The individual data points represent the results for individual samples, whilst the error bars denote 1 standard deviation for each dataset. There are significant differences between the results of the two Ag treatments versus the two control results at GS 5 (*p = 0.001) and GS 7 (**p = 0.03). 85

**Chapter 4**

*Figure 4.1.* Schematic of the soil (left) and hydroponic (right) setup. 95

*Figure 4.2.* Silver concentrations measured for the Lufa soil where the error bars signify standard deviation (n = 3). Means with different letters are significantly different. 104

*Figure 4.3.* Silver concentrations measured for Lufa soil pore water (LUPW), Lufa soil hydroponic solutions (LUHS), artificial pore water (APW) and Hoagland solution (HS) following treatment with Ag NPs (A), $Ag_2S$ NPs (B) and $AgNO_3$ (C). The error bars indicate standard deviation (n = 3) and the means with different letters are statistically different. 104

*Figure 4.4.* Mean Ag concentrations determined for the wheat roots exposed to Ag NPs (A), $Ag_2S$ NPs (B and C; note different scale in the latter panel) and $AgNO_3$ (D) for the different media including the Lufa soil, Lufa soil hydroponic solution (LUHS), artificial pore water (APW) and Hoagland solution (HS). The error bars convey standard deviation (n = 3) and the means with different letters are significantly different. 106

*Figure 4.5.* Mean Ag concentrations measured for the shoots exposed to Ag NPs (A), $Ag_2S$ NPs (B) and $AgNO_3$ (C) for the different media including the Lufa soil, Lufa soil hydroponic solution (LUHS), artificial pore water (APW) and land solution (HS). Here, the error bars signify standard deviation (n = 3) and the means with different letters are statistically different. 108

*Figure 4.6.* Total dry biomass recorded for the plants grown in Lufa 2.2 soil, Lufa 2.2 soil hydroponic solution (LUHS), artificial pore water (APW) and Hoagland solution (HS) at day 14. The error bars signify standard deviation (n = 3) where the means with different letters are significantly different. 109

*Figure 4.7.* Mean Ag distribution for the Lufa soil, Lufa hydroponic solution (LUHS), artificial pore water (APW) and Hoagland solution (HS) systems for days 7 and 14 (n = 3). The distributions were determined by mass balance calculations for the different compartments, which are exposure medium (soil or hydroponic solution) as well as root and shoot tissues. For each system, the maximum value of 100% was defined by the Ag mass that was introduced into the system at the beginning of the exposure. Any Ag that was not found in any of the medium or plant tissue compartments was assumed to be adsorbed to the container walls. As the extracted LUPW contains less than 0.01% of the Ag for exposures carried out in Lufa soil, this reservoir cannot be seen at the scale of the figure and it is hence ignored. 113

*Figure 4.8.* Plots of $[Ag]_{Shoot}/[Ag]_{Root}$ ratios determined for samples from days 7 and 14 (n = 6). 117

*Figure 4.9.* Plots of $[Ag]_{Shoot}/[Ag]_{Medium}$ ratios that characterise bioaccumulation of Ag in the wheat seedlings determined for samples collected at days 7 and 14 (n = 6). 118

**Chapter 5**

*Figure 5.1.* Schematic diagram of the hypothesis (A), the exposure experiments (B), and experimental setup (C). 124

*Figure 5.2.* Mean Ag concentrations measured for the treated (A) and untreated (B) roots from the wet-wet and wet-dry systems of the Ag NP exposures, which were dosed with 10 mg kg-1 and 50 mg kg-1 of Ag NPs. The error bars signify standard deviation (n = 3). Different letters denote mean values that are statistically different. Note that panels A and B use scaling which differs by a factor of x100. 135

*Figure 5.3.* Mean Ag concentrations measured for shoots for the wet-wet and wet-dry conditions of the Ag NP exposure, which were dosed with 10 mg kg-1 and 50 mg kg-1 of Ag NPs. Panel (A) shows the mean results for each exposure type. Panel (B) shows the results when the data for wet-wet and wet-dry conditions at a single dosing concentration are pooled. For panel A, the error bars signify standard deviation with n = 3, while for panel B n = 6. Different letters denote mean values that are statistically different. 135

*Figure 5.4.* Mean Ag concentrations measured for the treated wet soils of the time series exposure. The error bars signify standard deviation (n = 3). Different letters denote mean values that are statistically different. 136

*Figure 5.5.* Total (A) and truly dissolved (B) Ag concentrations measured for the soil pore waters extracted from the treated soils of the time series exposure. The error bars signify standard deviation (n = 3). Different letters denote mean values that are statistically different. Note that the scaling of panels A and B differs by about a factor of x10. 137

*Figure 5.6.* Mean Ag concentrations measured for the roots grown in the treated soils (A) and untreated (B) soils of the time series exposure. The error bars signify standard deviation (n = 3). Means with different letters are significantly different. Note that the scaling of panels A and B differs by about a factor of x10. 139

*Figure 5.7.* Mean Ag concentrations measured for shoots from the time series exposure. The error bars signify standard deviation (n = 3). Different letters denote mean values that are statistically different. 140

*Figure 5.8.* Silver distribution for the wheat seedlings of the Ag NP exposure (n = 3). 144

# Chapter 1: Introduction & literature review

## 1.1. Reasons for research

The exponential growth in production and use of engineered nanomaterials (ENMs) is resulting in their increasing release into the environment (Ray et al., 2009). The novel properties of ENMs that makes them attractive for nanotechnology development is the foundation for concern since they have been reported to react differently to their bulk counterparts (Lowry et al., 2012; Jeevanandam et al., 2018). Among other ENMs, silver nanoparticles (Ag NPs) are of particular interest because of their wide-spread use in a variety of commercial products (Gottschalk et al., 2009; Giese et al., 2018; Hood 2004; Wijnhoven et al., 2009). A major source of Ag NP deposition in terrestrial environments is through the application of sewage sludge as a fertiliser (Pradas del Real et al., 2017). Although research has detected Ag NPs in sewage sludge, the concentrations of Ag from Ag NPs are currently increasing the potential for Ag NP contamination of terrestrial environments and their interaction with local biota (Mueller and Nowack 2008). Recently, Ag from Ag NPs has been reported to enter roots of plants through vascular tissues and to be translocated to the stem, leaves and fruit of plants (Geisler-Lee et al., 2014; Ma et al., 2010; Dietz and Herth 2011). As such the research on the uptake, translocation and accumulation of Ag by edible crops such as wheat is vitally important in terms of animal and human health. Excessive intake of Ag can have toxic effects in humans and can cause argyria (blue skin condition), renal, pulmonary and gastrointestinal irritation (NCCIH, 2017).

Previous nano-ecotoxicology studies have reported Ag uptake and effects on all biological levels of plants (Tkalec et al., 2019; Yan and Chen 2019; Ma et al., 2010; Dietz and Herth 2011; Lv et al., 2019). Hence, the current thesis delves into the uptake, translocation and accumulation of Ag from Ag NPs by wheat. The current thesis can help the expansion of the present knowledgebase of Ag uptake by plants and will ultimately aid Ag NP risk assessments and guidelines for future regulation and monitoring schemes.

## 1.2. Thesis aims & structure

This PhD project aimed to (i) investigate the uptake, translocation and accumulation of Ag from Ag NPs and the ready soluble form ($AgNO_3$) by wheat (specifically *Triticum aestivum L.*) in a series of exposures and (ii) identify their effects on a biological level. In the following, the key aims of each chapter are outlined.

In Chapter 1 of this thesis, an introduction into the release and fate of Ag NPs in the environment is provided, and current plant research on their uptake and effects is addressed. The key aims of Chapter 2 are to provide quantitative data on the uptake and accumulation of Ag from Ag NPs and $AgNO_3$ on wheat at environmentally relevant concentrations under realistic conditions in terms of exposure medium and exposure length. Chapter 3 focuses on biological effects of the environmentally relevant Ag NP and $AgNO_3$ exposure. Chapter 4 delves into the use of hydroponic systems as a substitute for soil testing and compares the uptake of Ag from Ag NPs, $Ag_2S$ NPs and $AgNO_3$. The last research chapter – Chapter 5 – aims to identify the mechanisms of Ag uptake and translocation following exposure to Ag NPs and $AgNO_3$ under water stress. Chapter 6 summarises the main findings from Chapters 2 – 5 and outlines the approaches needed for further research.

## 1.3. Literature review

### *1.3.1. Nanomaterials & the environment*

#### *1.3.1.1. Nanomaterials*

Nanotechnology can be defined as the manipulation of matter on an atomic and molecular level (Rauscher et al., 2014; Klaine et al., 2013). Nanomaterials are materials with structured components with at least one dimension that is less than 100 nm (Klaine et al., 2008; Christian et al., 2008; BSI 2007; American Society for Testing and Materials 2006; SC on Emerging and Newly Identified Health Risks 2007; The RC and RAE 2004). They are commonly included in electronic components, consumer, agricultural and biomedical products such as

cosmetics, antimicrobial and stain-resistant fabrics and sprays, pesticides, sunscreens, cleaning products, tyres, paints, and diesel additives (Rauscher et al., 2014; Florini et al., 2006). Although, nano-sized particulates can occur both naturally and anthropogenically, of particular interest are the manmade or ENMs designed for the improvement of various industrial and commercial products.

Engineered NMs can be carbon-based or metal-based (Peralta-Videa et al., 2011; Handy et al., 2008) and have different properties to their bulk counterparts due to their nanoscale. Previous studies have reported the following main reasons for these properties: (i.) increased surface area to volume ratio; and (ii.) new quantum effects (Klaine et al., 2013; Rauscher et al., 2014; COT 2005; Christian et al., 2008). In detail, these two properties have been reported to result in higher chemical reactivity (Klaine et al., 2013; COT 2005; Christian et al., 2008) and new electrical, optical, and magnetic behaviours (Klaine et al., 2013; Rauscher et al., 2014). These unique properties make ENMs attractive for new product development. A report published in March 2015, based on the Nanotechnology Consumer Products Inventory, shows that ENMs in consumer products have increased from as many as 54 recorded products in 2005 to 1814 commercial products and processes in 2014 (Vance et al., 2015). This intensive use, production and disposal of medical, industrial and agricultural ENMs, is (i) leading to an increase in the amount of ENM-containing waste emitted to the environment, and (ii) contributing to the contamination of the atmosphere, sediments, soils, surface and ground waters.

*1.3.1.2. Nano-ecotoxicology*

Ecotoxicology is the field of research that combines ecology and toxicology to study the effects of environmental pollutants on ecosystems. As a result of the quick development of nanotechnology, the field of nano-ecotoxicology has arisen to assess the toxicity of ENMs in the ecosystem (Handy et al., 2008). As some NPs have proven to be toxic in different environments and scenarios, quantitative data is required for risk assessment and regulatory purposes. Engineered NMs have been shown to have various toxic effects on invertebrates (Tourinho et al., 2012; Croteau et al., 2011), algae (Aruoja et al., 2009; Navarro et al., 2008), fish (Federici et al., 2007; Handy et al., 2008), plants (Navarro et al., 2008; Lin and

Xing 2007; Rico et al., 2015), phytoplankton (Miao et al., 2007), fungi (Navarro et al., 2008), bacteria (Pal et al., 2007; Sondi et al., 2004) as well as mammals (Handy et al., 2008; Bermudez et al., 2004). Nano-ecotoxicological studies of different organisms have furthermore revealed effects such as cytotoxicity (Brunner et al., 2006), genotoxicity (Dhawan et al., 2009), extracellular toxic effects (Sun et al., 2016), inflammation (Borm et al., 2006), physiological and biochemical stress (Lin and Xing 2007), photosynthetic (Lin and Xing 2007) and plant growth stress (Lin and Xing 2007; Miao et al., 2007) and respiratory problems (Borm et al., 2006). The toxicity of ENMs is thought to be dependent on the size, shape, chemical composition, solubility, aggregation state, surface structure and area of the ENM (Navarro et al., 2008).

### *1.3.2. Ag NPs*

#### *1.3.2.1. Ag*

Silver is a precious transition metal that is soft, ductile, reflective and non-corrodible. Natural Ag is comprised of two stable isotopes encompassing $^{107}$Ag and $^{109}$Ag that occur in almost equal amounts with abundance of about 52% and 48%, respectively (de Laeter et al., 2003). The high electrical and thermal conductivities of Ag have transformed this metal from a decorative to a mainly industrial material (Blaser et al., 2008). It was discovered roughly 4,000 BC and was mainly used as a medium of exchange and as a jewellery material (Kabata-Pendias and Pendias 2011). Currently, Ag is used in photographic manufacture, medical products, batteries, electronics, jewellery, brazing etc. (Alloway 2013).

The abundance of naturally occurring Ag in the environment is in the μg $kg^{-1}$ range. To put this into context, Ag concentrations of roughly 75 μg $kg^{-1}$ have been reported for the Earth's crust and about 100 μg $kg^{-1}$ for soils (Alloway 1990; 2013).

#### *1.3.2.2. Properties & applications of Ag NPs*

The first Ag NP synthesis, in the form of colloidal Ag, was reported in 1889 (Lea 1889). Since then, the synthesis of Ag NPs has evolved and various properties have been reported including relatively high thermal and electrical conductivity; low contact resistance; large surface area; high surface energy; surface plasmon

resonance under irradiation of light; antimicrobial activity; and antiviral properties (Gottschalk et al., 2009).

With their various properties, and the quick advancement of nanotechnology in the past two decades, Ag NPs are one of the most used ENMs (Vance et al., 2015). Although historically colloidal Ag was mainly used for medical purposes including treatment of wounds and infections (Fung and Bowen 1996), nowadays Ag NPs are widely used in a variety of products mainly due to their antimicrobial and conductive properties. These encompass (i) electronics such as optoelectronics, data storage devices, washing machines; (ii) photographic devices, sensing and imaging applications; (iii) medical applications such as surgical instruments, wound dressing, bone cement; (iv) fungicide products; (v) food packaging and food storage materials; (vi) various textiles such as odour-resistant clothing; (vii) cosmetics such as lotions and soaps; (viii) laundry detergents; and (ix) paints (Gottschalk et al., 2009).

As a result of this wide use of Ag NPs, it has been suggested that Ag NPs are amongst the most produced and used metal-based ENMs (Keller et al., 2013; Hansen et al., 2020). In 2015 the Nanotechnology Consumer Products Inventory reported that 435 products or 24% out of 1,814 consumer products contain Ag NPs (Vance et al., 2015). By 2020, the number of products increased to about 5,000 of which roughly 10% were reported to contain Ag NPs (Hansen et al., 2020). Recently, Giese et al. (2018) suggested that the current annual production volume of Ag NPs is below 1,000 t and reported that the main use of Ag NPs is in electronics, textiles and for medical products.

### *1.3.3. Release of Ag NPs into the environment*

This widespread use of Ag NPs is the basis for concern as their release in the environment is increasing the potential for Ag NP contamination of terrestrial environments (Mueller and Nowack 2008). Giese et al. (2018) estimated Ag NP release of about 6 t $a^{-1}$ into soils, waters and air, as well as roughly 12 t $a^{-1}$ into the technosphere (landfills, recycling, waste incineration, and sewage treatment) by 2030 and predicts a 3-fold increase by 2050.

There are several processes during which Ag NPs are released into the terrestrial environment encompassing (i) production and synthesis; (ii) product manufacturing; (iii) transport; (iv) product use; and (v) disposal and recycling (Blaser et al. 2008; Gottschalk et al., 2011; Giese et al., 2018; Kaegi et al., 2010). One of the primary pathways for Ag NP discharge is through the washing and use of consumer products such as textiles, which are introduced to fight odours and prevent infections (Figure 1.1) (Blaser et al., 2008). Other major contributing products to this release include cleaning agents, cosmetics and medical products (Giese et al., 2018). As much as 100 µg $L^{-1}$ of Ag NPs are released into wash water during laundering (Luoma 2008; Benn et al., 2008; 2010). To put this into context, other products like food containers contribute only to 3.1 ng $cm^{-2}$ of total Ag after 10 days, whilst toothbrushes as much as 10.2 ng of Ag per toothbrush (Mackevica et al., 2016; 2017).

These washed down-the-drain Ag NPs can either be discharged directly into landfills from consumer and professional product use or transported to a wastewater treatment plant (WWTP) for wastewater processing, where Ag NPs are deposited in sewage sludge (Fabrega et al., 2011). Often these sewage sludges are used as a fertiliser on agricultural lands (Fabrega et al., 2011; Blaser et al., 2008; Gottschalk et al., 2013). In the UK, the majority of sewage sludge is applied to agricultural soils (Schlich et al., 2013) and it has been suggested that increased Ag concentrations in sewage sludges might increase the environmental risks in terrestrial and aquatic ecosystems (Luoma 2008; Blaser et al., 2008).

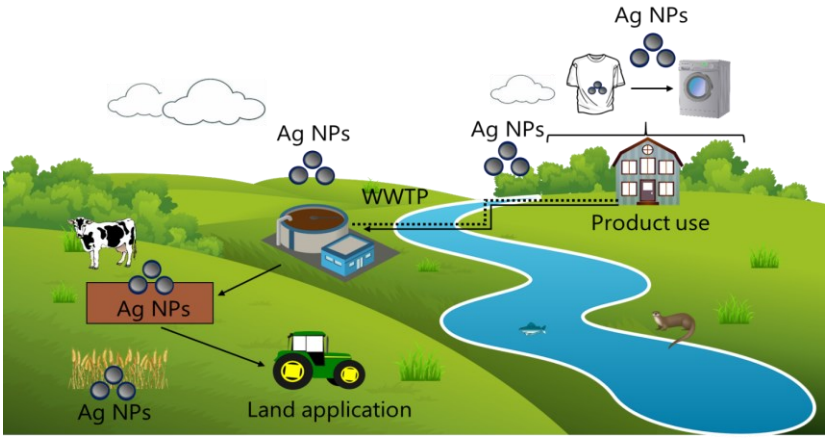



*Figure 1.1*. Simplified overview of the release of Ag NPs into the environment. Figure reproduced and adjusted after Hartmann et al. (2014).

### *1.3.4. Fate of Ag NPs in the environment*

Once Ag NPs enter the environment a series of chemical transformations occur including (i) dissolution to $Ag^+$ ions; (ii) change in chemical speciation; (iii) degradation; and (iv) alterations in surface properties by precipitation and sorption (McGillicuddy et al., 2017). These transformations are controlled by both particle properties and environmental factors (Bundschuh et al., 2018). The fate of Ag NPs and their transformations in soil govern to a large extent the bioavailability, uptake and toxicity mechanisms of Ag in plants.

In soil, Ag NPs are subjected to both liquid and solid phases and some of the more important physicochemical reactions that occur include dissolution (reduction and oxidation), organic matter complexation, soil particle sorption and aggregation/ agglomeration (Bundschuh et al., 2018; Klitzke et al., 2015). The fate of Ag NPs in soils is mainly governed by the physicochemical properties of the soil. In this context, factors including cation exchange capacity, ionic strength, pH, presence of organic matter and particle size distribution of the soil are vital for understanding the reactions that occur in soils (Lowry et al. 2012; Mahdi et al. 2018). The processes are explained in the following.

The release of $Ag^+$ ions from Ag NPs is often linked to both particle physicochemical properties like surface charge and coating, size, shape and particle aggregation and environmental factors such as temperature, pH and dissolved organic carbon (DOC) (Mitrano et al., 2014; Metreveli et al., 2016). In detail, Ag NPs can dissolve into $Ag^+$ in soil as $Ag^0$ oxidises, a process affected by pH, presence of natural organic matter (NOM) and cations, and transforms to Ag(I) to dissolved $Ag^+$ ions (Liu and Hurt, 2010). Most $Ag^+$ ions can be released at low pH (pH 4) and in the absence of NOM wherein the presence of cations can speed up Ag oxidation and dissolution (Li et al., 2010; Klitzke et al., 2015).

Notably, Ag binds strongly to both organic and inorganic sulphur, hence the stability of Ag NPs is influenced largely by the coating of dissolved organic matter (DOM) and NOM and can lead to an increase or decrease in Ag NP colloidal stability (Lecoanet et al., 2004; Klitzke et al., 2015). Previous studies have reported that Ag NP sorption to fulvic and humic acid can increase the stability of Ag NPs (Li et al., 2010; 2018). In this context, the mechanism of Ag NP activity is

closely related to the reaction of $Ag^+$ ions or Ag NPs with sulfhydryl groups (Levard et al., 2011; 2012; Cornelis et al., 2014; Gan et al., 2011) and the sulphidation of either $Ag^+$ ions or Ag NPs can lead to the formation of either $Ag_2S$ or $Ag_2S$ NP. This process is mainly governed by soil properties like the presence of NOM, DOM, and soil pH (Cornelis et al., 2014). The formation of such sulphide shells on the particle surfaces may lead to surface charge change and increase aggregation (Levard et al., 2011). Both $Ag_2S$ and $Ag_2S$ NPs are relatively insoluble and inert, and have also been shown to decrease toxicity and availability but still show toxic properties to microorganisms (Tkalec et al., 2019; Kraas et al., 2017).

Aggregates and agglomerates may form as either Ag NPs or $Ag^+$ ions collide with other particles via Brownian motion to form particles of a larger size. Aggregates form by the association of particles by strong binding (irreversible), whilst agglomerates form by the association through weak bonding by Van der Waals forces (reversible) (Levard et al., 2012; Tourinho et al., 2012). In the environment, Ag NP aggregation and agglomeration are often affected by (i) physical forces including Brownian motion, gravity and fluid movement; and (ii) Ag NP characteristics encompassing size, charge and coating stability (Farré et al., 2009). In this context, two important processes occur in soils including (i) homoaggregation where Ag NPs eventually aggregate with each other and (ii) heteroaggregation where Ag NPs react with other environmental particles (Cornelis et al., 2014). Heteroaggregation is considered the more environmentally relevant process of the two and the collision of NPs with soil colloids has been identified to increase the mobility of NPs, while the presence of NOM can reduce the process (Cornelis et al., 2013; 2014; Quik et al., 2014). Notably, Ag reacts readily with chloride and it has been shown that $Cl^-$ can increase the aggregation of Ag NPs, while low chloride ($Cl^-$) concentrations may lead to precipitation of negatively charged particles (Metreveli et al., 2016; Levard et al., 2013). The formation of AgCl is a process that is generally governed by the pH of the soils (Sekine et al., 2015). The above-mentioned processes can cause a difference in surfaces (size and charge), concentration and bioavailability to plants (Pachapur et al., 2016).

Although soil is the more environmentally relevant exposure medium in ecotoxicology, plant studies often employ hydroponic media as plants tend to grow faster than those grown in soils (Tkalec et al., 2019). It is widely known that the transformations of Ag NPs in hydroponic media differ to these in soils which in turn, would influence the bioavailability of Ag to plants (Tkalec et al., 2019). Admittedly, the release of $Ag^+$ ions from the Ag NP, Ag-NOM binding, and the formation of Ag aggregates/agglomerates are considered as more relevant reactions in hydroponic systems (Li et al., 2018). Silver NPs in hydroponic solutions though, are thought to release more metal ions than their bulk counterparts caused by the higher specific surface areas (Li et al., 2018).

### *1.3.5. Predicted environmental concentrations for Ag NPs*

The predicted environmental concentrations (PECs) for Ag from Ag NPs in soils are at a range of ng $kg^{-1}$ to µg $kg^{-1}$ (Table 1.1). A study modelling the European PECs of Ag from Ag NPs between 2017 and 2050 estimated a range of Ag concentrations for environmental and WWTP compartments (Giese et al., 2018). The study reported PECs for agricultural soils of between 9 ng $kg^{-1}$ and 792 ng $kg^{-1}$ for Ag from Ag NPs for 2017 and predicted a 5-fold increase by 2050 (Giese et al., 2018).

*Table 1.1.* Predicted environmental concentrations of Ag from Ag NPs in different compartments for 2017, 2030 and 2050 (Giese et al., 2018).

| Compartment | PECs of Ag NPs | Unit |
|---|---|---|
| **2017** | | |
| Agricultural soils | 9.4 – 792.2 | ng $kg^{-1}$ |
| Sewage sludge treated soils | 0.5 – 24.9 | µg $kg^{-1}$ |
| Sewage sludge | 32.4 – 2730.3 | µg $kg^{-1}$ |
| **2030** | | |
| Agricultural soils | 18.5 – 1736.7 | ng $kg^{-1}$ |
| Sewage sludge treated soils | 0.9 – 53.3 | µg $kg^{-1}$ |
| Sewage sludge | 62.3 – 4554.0 | µg $kg^{-1}$ |
| **2050** | | |
| Agricultural soils | 53.4 – 4756.1 | ng $kg^{-1}$ |
| Sewage sludge treated soils | 2.3 – 128.1 | µg $kg^{-1}$ |
| Sewage sludge | 187.9 – 11669.2 | µg $kg^{-1}$ |

All PECs are for 100% persistent Ag NP (no-degradation scenario)

Although the PECs for sewage sludge were estimated to be an order of magnitude higher with Ag concentrations ranging between 32 µg $kg^{-1}$ and 2730 µg $kg^{-1}$ for 2017, a similar 5-fold increase by 2050 was calculated (Giese et al., 2018). Of particular interest are the sewage sludge treated soils, which were estimated to vary between 0.5 µg $kg^{-1}$ and 25 µg $kg^{-1}$ for 2017. These concentrations are predicted to double to 0.9 µg $kg^{-1}$ and 53 µg $kg^{-1}$ by 2030 and to further increase between 2.3 µg $kg^{-1}$ and 128 µg $kg^{-1}$ of Ag from Ag NPs by 2050 (Giese et al., 2018).

*1.3.6. Ag NP exposures on plants*

The uptake and translocation of Ag from Ag NPs by plants is closely correlated to transformations and bioavailability of Ag in the exposure medium and these are controlled by both particle properties (e.g., size, charge) and environmental factors (Bundschuh et al., 2014). Toxicological effects to plants have been linked to both Ag NPs and dissolved $Ag^+$ ions released from Ag NPs, whereby tests species are often exposed to Ag NPs and $Ag^+$ ions to distinguish and compare the uptake, accumulation and toxicity between the two Ag forms. Some of the more important factors that affect Ag NP and $Ag^+$ ion toxicity, uptake and bioavailability to plants include exposure plant species, length, medium and concentration (Gubbins et al., 2011; Lee et al., 2012; Geisler-Lee et al., 2014). These factors will be discussed in the following.

The most frequently used plant species include *Arabidopsis thaliana*, maize *(Zea mays)* and wheat (*Triticum aestivum)*. In terms of exposure length and medium, about 70% of the current nano-ecotoxicology literature for plants focuses on standard short-term experiments between 3 and 28 days based in aqueous test media due to the straightforward nature of short-term hydroponic exposures. Previous studies have used Ag exposure concentrations from Ag NPs and their readily soluble form ($AgNO_3$) between 0.1 and 1,000 mg $L^{-1}$ for hydroponic studies and 10 to 2,000 mg $kg^{-1}$ for soil exposures. Lee et al. (2012) used Ag NP concentrations between 0 and 2,000 mg $kg^{-1}$ (dry weight) in a soil exposure and found Ag concentrations of up to 22 mg $kg^{-1}$ in mung beans (*Phaseolus radiatus*) and sorghum (*Sorghum bicolor*). To compare, the uptake of Ag for the same plant

species in an agar exposure of up to 40 mg of Ag NP $L^{-1}$ was determined to be between 3 and 5 mg $kg^{-1}$ (Lee et al., 2012).

### *1.3.7. Wheat & Ag uptake*

#### *1.3.7.1. Wheat*

Field crop plants account for over 50% of the human food consumption where over 40% is provided from wheat and rice (Poehlman 2013). Wheat is considered as one of the most important and wide-grown crops in the world (Wan and Layton, 2006). Historically, wheat has been domesticated for 10,000 years before present in efforts to reduce hunger (Weiss and Zohary 2011). Today, wheat is the most important grain worldwide in terms of grain acreage and is the second most-produced cereal crop in the world with a global production of more than 765 million metric tons for 2019/2020 (Shahbandeh 2020). By 2050, the human population is estimated to rise to 10.5 billion, which would increase the demand for wheat consumption as well as the need for Ag-based nanotechnology. As such, the risk of Ag uptake to the grain from Ag NPs is escalating. As a major agricultural plant, wheat (*Triticum aestivum L.*) was chosen as a test species for this project.

#### *1.3.7.2. Wheat plant anatomy & physiology*

The anatomy and physiology of wheat has been discussed in detail by Percival (1974) but will be described in brief in the following. Wheat plants consist of a grain head (which consists of seeds), roots, stem, leaves, and tillers (Figure 1.2).

Wheat seeds typically have three parts: (i) testa or seed coat; (ii) the endosperm; and (iii) the germ or embryo (Figure 1.2A). The testa covers the embryo and endosperm and consists of two layers (outer and inner layer) of elongated cells. The endosperm makes up the majority of the seed (87 – 89%) and encompasses the floury part where the starch/gluten for the nutrition of the embryo are stored (when germination starts). The germ lies at the base of the grain and makes up only 2.8 – 3.5% of the seed. It is comprised of a short cotyledon (the part of the stem of an embryo plant); the plumule (primary bud) composed of immature leaves; and at its base, a radicle which develops into the primary roots (Figure 1.2B).

Germination of a wheat seed begins by absorption of water and seed swelling. Next, a radicle commences to emerge and forms the first root (Figure 1.2B). In quick succession another two radicles burst through the testa, establishing the main (primary) root system, while root hairs develop on the upper regions of the organ. This primary root system is also referred to as the seminal roots. In the meantime, the plumule, wrapped around a protective sheath (the coleoptile), grows in an upright direction. Once it has emerged above the soil, the first leaves grow out of the coleoptile, which remains as a protective sheath round the base of the leaves. Following this stage, wheat seedlings consist of five main parts – roots, stems, tillers, shoots (leaves), and grain heads.

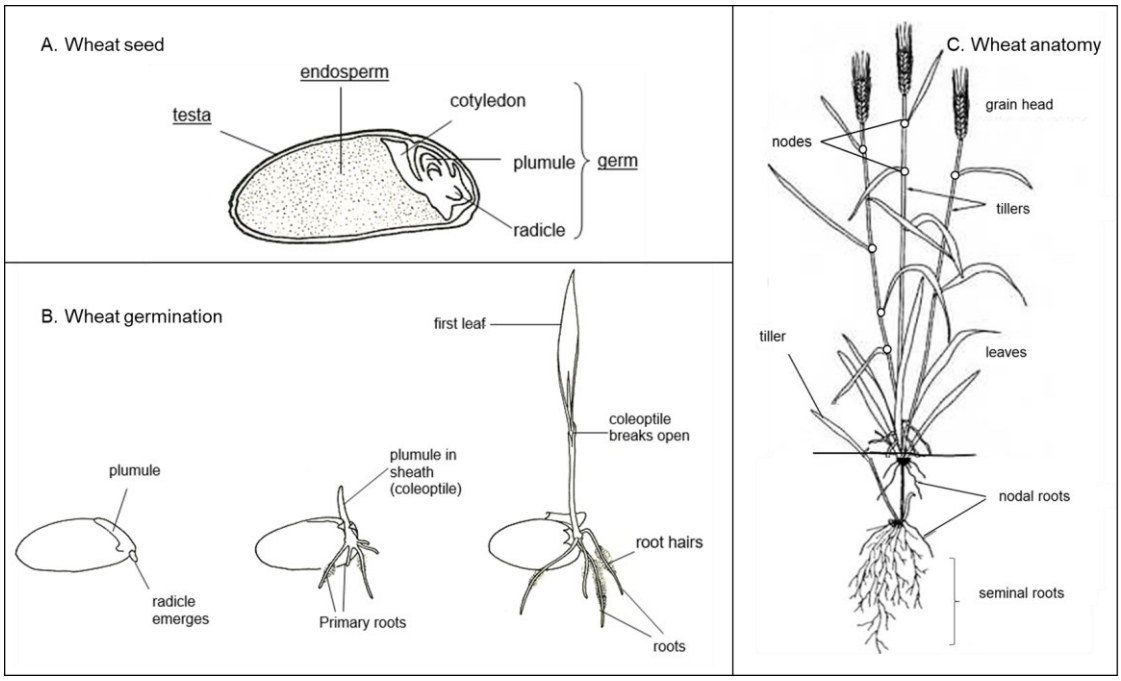



*Figure 1.2.* An overview of the anatomy of wheat (adjusted after Aslam et al. 2018 and Carver 2009). Panel A displays the anatomy of the seed, B shows the germination of wheat, while C presents the overall anatomy of a mature wheat plant.

The root system of wheat plants includes seminal and nodal roots (Figure 1.2C). The seminal roots, developed from the seed embryo, consist of five roots – a primary root; two pairs of lateral roots; and a sixth root that often grows at a later point (Percival 1974). Full-grown wheat plants then consist of two root systems: (i) seminal roots developed from the seed germ (Perry and Belford 2000) and (ii) nodal or crown roots produced at the time that tiller development starts (Kirby 2002).

The stems are erect and cylindrical – like a straw – with smooth surfaces (Percival 1974). The mature wheat plant consists of a central stem from which shoots grow on opposite sides (Figure 1.2C). The stem is constructed of repeating segments including a node and internode (hollow), a shoot and a tiller bud (Kirby 2002), and it terminates at the wheat grain head/ear. The leaf sheath weaves around the stem for support (Setter and Carlton 2000). The main stem is the first to emerge, usually the strongest culm, once the seed has germinated.

The tillers branch out from the main stem and serve to increase the number of grain heads of the mature wheat crop (Figure 1.2C). The tillers are the lateral branches, off the main stem, which produce shoots on opposite sides in the same way that the main stem produces them (Kirby 2002). Tillers are also able to produce a grain head/ear, which is thought to be linked to competition for light and nutrients (Kirby 2002).

*1.3.7.3. Wheat development & nutrient transport*

Wheat development includes three main crop phases – vegetative, flowering, and grain formation phases. These crop phases are split into ten principal cereal growth stages: 0 – Germination; 1 – Seeding growth; 2 – Tillering; 3 – Stem elongation; 4 – Booting; 5 – Awn emergence; 6 – Flowering (anthesis); 7 – Milk development; 8 – Dough development; 9 – Ripening. For assessment of wheat development in a standardised manner, the Zadoks scale for cereal growth is widely used as it details developmental changes by the use of 99 sub-growth stages (Zadoks et al., 1974).

For the development of healthy wheat plants, transportation of nutrients is key. The uptake of nutrients has been heavily studied and as such a brief overview is presented in the following. Generally, the uptake of nutrients from soils and begins by adsorption of nutrients to the root surfaces by electrostatic attraction from the soil solution. These nutrients are then internalised via the apoplastic and symplastic pathways. In the apoplastic pathway, solutes are generally transported in intercellular spaces toward the stele through free spaces and cell walls of the epidermis and cortex (Barberon and Geldner 2014). In the symplastic pathway, solutes are generally selectively taken up into cells and then transported from one cell to another through the plasmodesmata (Barberon and

Geldner 2014). In contrast, the trans-cellular pathway, the third nutrient transport pathway, is normally disregarded due to analytical limitations (Barberon and Geldner 2014).

The apoplastic and symplastic pathways merge at the Casparian strip and once passed this dense tissue, nutrients enter the vascular tissues of the plant. The vascular system consists of the xylem and phloem conductive tissues. The xylem system uses root-to-shoot flow direction, while the phloem transports solutes from shoot-to-root. The xylem provides an open route for water, ions and nutrients, which are delivered non-selectively by the xylem sap as water is pulled through the plant by transpiration (Grusak et al., 2002; Ueno et al., 2008; Uraguchi et al., 2009). Once in the shoots, nutrients are transported to the phloem via the apoplastic and symplastic pathways. The phloem moves sugars, amino acids, carbohydrates, certain minerals and secondary metabolites from the photosynthetic “source” organs (e.g., shoots) to “sink” areas (e.g., young developing shoots and roots) through a hydrostatic pressure gradient. The vascular system runs through the whole plants, including the roots, stems, shoots and grains and is non-circulatory, such that solutes do not circulate back to their original sources (Barberon and Geldner 2014).

*1.3.7.4. Potential pathway for the uptake, translocation & accumulation of Ag by wheat*

The potential pathway for Ag uptake has been displayed in Figure 1.3. The uptake, translocation and accumulation of Ag from Ag NPs and $Ag^+$ ions starts with the adsorption of Ag to the root surface (Yin et al., 2011; Stegemeier et al., 2015; Vannini et al., 2014). Silver from Ag NPs and readily soluble Ag adsorb to root surfaces by electrostatic attraction in a similar manner to copper (Cu) and cadmium (Cd) (Figure 1.3A). This attraction occurs when positively charged Ag species adsorb to negatively charged root surfaces (-COOH, -OH, $-NH_2$, and $-H_2PO_4$) (Wu and Hendershot 2009; Liu et al., 2017). The adsorbed Ag is internalised through the root tips, rhizodermis/cortex, any lateral root junctions, or root wounding (Yin et al., 2011). At a cellular level, the main site through which the Ag can enter plant root cells is the cell wall (Tripathi et al., 2017) whereby Ag first penetrates through the cell wall then into the plasma membranes of the

epidermis (Yan and Chen 2019). Notably, the cell wall acts as a natural sieve and allows penetration of smaller NPs (<20 nm) through the pores but sieves out any larger particles (Tripathi et al., 2017). Other possible pathways encompass the formation of new larger-sized pores (Navarro et al., 2008) or through the 50 – 60 nm pore openings of the plasmodesmata which connect neighbouring cell walls.

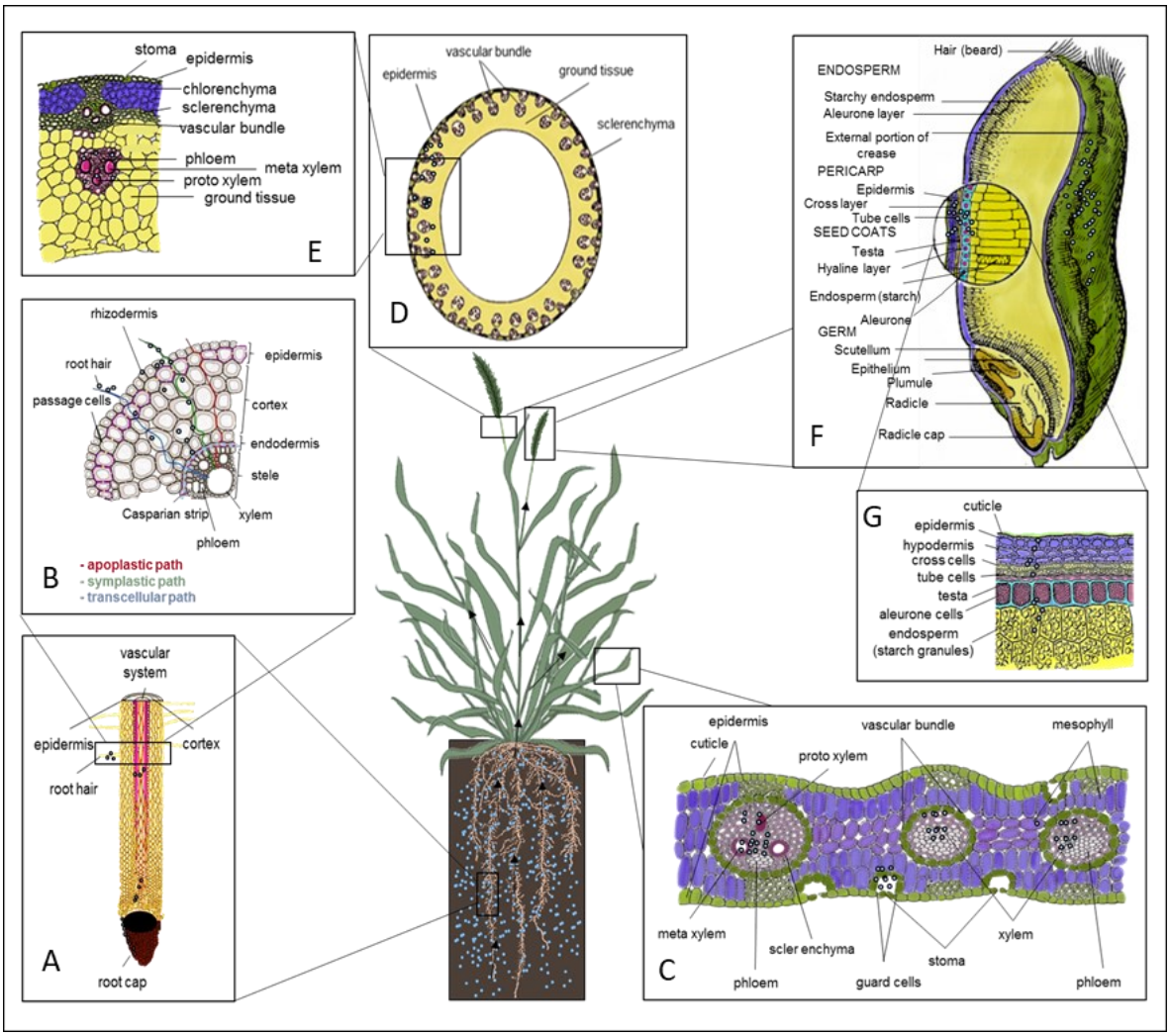



*Figure 1.3*. Simplified overview of the uptake of Ag NPs by different wheat plant tissues. Little root tissues pictures were adapted and adjusted after Kim et al. (2018) and Lv et al. (2019).

The exact mechanism for Ag movement via the phloem is largely unknown, but perhaps Ag transport is similar to that of Cu. Wang et al. (2012) proposed that the mechanism for Cu transport within the phloem is associated with the movement of carbohydrates during whole-plant carbohydrate partitioning. The Cu is loaded into the phloem sap together with sugars, amino acids, certain minerals and

secondary metabolites. Once in the phloem sap, it is moved cell-to-cell from photosynthetic “source” organs (e.g. shoots) to “sink” areas (e.g., young developing shoots and roots) through a hydrostatic pressure gradient. Previous studies by Tripathi et al. (2017) have reported the presence of Ag in the phloem. Notably, Ag from Ag NPs and $Ag^+$ ions has been documented in the grain (Yang et al., 2018) and it is most likely that Ag enters the grains of wheat during the foundation phase and when grain head/ear initiation is being completed during stem elongation through the phloem (Pérez-de-Luque 2017). Silver can then enter the individual seeds of the grain head (Figure 1.3F and G).

*1.3.7.5. Ag speciation within plants*

Once internalised, Ag from Ag NPs and $Ag^+$ ions has been widely recorded to form subsequent secondary complexes *in planta* including AgCl (Larue et al., 2014) and thiol-based complexes (Adams and Kramer 1999). Previously, aggregation of Ag NPs at the plasmodesmata of the roots has also been recorded (Geisler-Lee et al., 2014). These complexes are often inert and insoluble and less bioavailable to the rest of the plant.

Once transported to the shoot, Ag from Ag NPs has been reported to aggregate around the cell wall (parenchyma) and in the vacuole of the leaf (Bao et al., 2016), the guard cells, and sub-stomatal chamber (Larue et al., 2014). Similar to the roots, it has been widely reported that Ag from Ag NPs can form secondary species such as $Ag^+$ ions, Ag-thiol and AgCl in the shoots (Tkalec et al., 2019, Pradas del Real et al., 2017).

*1.3.8. Effects of Ag from Ag NPs on plants*

Currently, there are roughly 60 Ag NP exposure studies published on plants with a wide variety of negative, positive and neutral effects (Table 1.2). Generally, effects on biological plant level are reported by experimental observations on seed germination, germination rate, fresh and dry biomass, transpiration rate, reactive oxygen species analysis, chlorophyll contents, root and shoot length. Comprehensive literature reviews have been provided by Ma et al. (2010), Dietz and Herth (2011) and Tkalec et al. (2019) Lv et al. (2019).

Most of the literature reports negative effects of Ag NPs on plants at high exposure levels, as shown by Table 1.2. However, it is worth noting that most of the studies to date are ecotoxicological investigations that specifically aim to trigger effects. For example, at Ag NP concentrations of up to 1,000 mg $L^{-1}$, undertaken by Babu et al. (2008), Kumari et al. (2009), Barrena et al. (2009) and Stampoulis et al. (2009) negative effects and phytotoxicity on plants were reported based on the germination index, mitotic index, metaphase, chromosomes, cell walls, transpiration and biomass. Several studies investigating the effects of Ag from Ag NPs upon plants suggest that Ag NPs at concentrations of up to 750 mg $L^{-1}$ can affect seed germination (Hawthorne et al., 2012), plant growth (Hawthorne et al., 2012) and biomass (Hawthorne et al., 2012), transpiration rates (Hawthorne et al., 2012), protein content (Salama 2012), cell structures (Jiang et al., 2014) and processes (Kumari et al., 2009). Studies also suggest that Ag from Ag NPs at concentrations of up to 100 mg $kg^{-1}$ can be genotoxic and can lead to oxidative stress (Salama 2012). On a physiological level, research has found that Ag from Ag NPs can aggregate on the surface of the root causing cell-level morphological changes to plant roots (Geisler-Lee et al., 2014). The reported discolouration of the root cap and columella, referred to as “brown tips” (Geisler-Lee et al., 2014), at Ag concentrations of 0.7 mg $kg^{-1}$ was explained by Ag accumulation from Ag NPs and/or in combination with cell wall activity (Geisler-Lee et al., 2014; Ma et al., 2010). Geisler-Lee et al. (2014) found that Ag NPs can aggregate in the plasmodesmata and the cell wall affecting nutrient transporter proteins and intercellular transport caused by wall leakage and blockage of intercellular communication (Geisler-Lee et al., 2014).

*Table 1.2.* Review table of Ag NP exposures in different media and at different exposure concentrations.

| Particle size (nm) | Concentration ($mg\ L^{-1}$; $mg\ kg^{-1}$) | Medium | Exposure time (days) | Plant species | Physiological/ biochemical effects | Reference |
|---|---|---|---|---|---|---|
| 30 | 62, 100, and 116 | Hydroponic solution | 7 | Cucumber (*Cucumis sativus*) and lettuce (*Lactuca sativa*) | Reduction effect on germination index; negative influence on cucumber root growth | Barrena et al., 2009 |
| 0.6–2 and 20 | 20, 40, 60, 80, and 100 | Hydroponic solution | 7 | Flax (*Linum usitatissimum L.*), ryegrass (*Lolium perenne L.*), and barley (*Hordeum vulgare L.*) | Reduction on germination, shoot length, transpiration and biomass | El-Temsah and Joner, 2010 |
| 20, 40, 80 | 667, 1334, 267 and 535 | Hydroponic solution | 14 | *Arabidopsis thaliana* | Roots developed brown tips; transportation of NPs to the internal root tissue | Geisler-Lee et al., 2012 |
| 20 and 100 | 5, 10, 20, 40, 80 and 160 | Hydroponic solution | 14 | Duckweed (*Lemma minor*) | Plant growth dependent of NP size; reduction in dry weight; significant effect of dose upon frond number | Gubbins et al., 2011 |
| <100 | 250 and 750 | Hydroponic solution | 7 | Courgette (*Cucurbita pepo*) | Reduction on plant biomass and transpiration rate | Hawthorne et al., 2012 |
| 6 and 20 | 0.5, 1, 5, and 10 | Hoagland solution | 7 | Duckweed (*Spirodela polyrhiza*) | Dose-dependent increase of ROS and protein content; change in antioxidant enzymes, substance and chloroplast ultrastructure; induction of oxidative stress | Jiang et al., 2014 |

| Particle size (nm) | Concentration (mg $L^{-1}$; mg $kg^{-1}$) | Medium | Exposure time (days) | Plant species | Physiological/ biochemical effects | Reference |
|---|---|---|---|---|---|---|
| <100 | 25, 20, 75, and 100 | Hydroponic solution | 4 h | Onion (*Allium cepa*) | Decrease in the mitotic index; disturbed metaphase; chromosomal aberrations such as stickiness, chromosomal breaks, gaps, disturbed metaphase, and cell wall disintegration at different doses | Kumari et al., 2009 |
| 20, 40 and 80 | 0.34 and 0.68 | Hoagland solution | 28 | *Arabidopsis thaliana* | Uptake and accumulation of Ag NPs was detected in plant roots and vascular tissues | Ma et al., 2010 |
| 20 | 0.05, 0.5, and 1 | Hoagland solution | 12 | Rice (*Oryza sativa*) | Damage to external and internal portions of cells; breakage of cell wall and vacuoles in root cells; depositions of Ag NPs inside the root cell | Mazumdar and Ahmed, 2011 |
| <50 and <100 | 100 and 500 | Hoagland solution | 14 | Yellow squash (*Cucurbita pepo*) | Reduction in squash biomass; transpiration effects on seedlings | Musante and White, 2012 |
| 60 | 12.5, 25, 50 and 100 | Hydroponic solution | 4 h | Broad bean (*Vicia faba*) root tips | Increase in chromosomal aberrations, micronuclei; decrease in mitotic index; genotoxicity | Patlolla et al., 2012 |
| 56 | 73 | Petri dish | 7 | Maize (*Zea mays L.*) and cabbage (*Brassica oleracea*) | Inhibition upon germination in maize; erosion of apical meristem cells; reduced root growth | Pokhrel and Dubey, 2013 |

| Particle size (nm) | Concentration ($mg\ L^{-1}$; $mg\ kg^{-1}$) | Medium | Exposure time (days) | Plant species | Physiological/ biochemical effects | Reference |
|---|---|---|---|---|---|---|
| <100 | 10, 15, and 20 | Petri dish | At 80% of the control seeds germination | Tomato (*Lycopersicon esculentum*) and corn (*Zea mays*) | Inhibition upon root length and germination; reduction in germination index | Ravindran et al., 2012 |
| 25 | 20, 40 and 60 | Not specified | 14 | Borage plant (*Borago officinalis L.*) | Improvement in seed yield; effect on Ag concentration in the plant shoot, the number of leaves, the height of the plant, plant dry weight, inflorescence dry weight, seed yield, seed weight, polyphenol and tannin content in shoot; no effect on the length, width and greenness of leaves | Sah et al., 2011 |
| 190-1100 | 25, 50, 100, 200 and 400 | Hydroponic solution | 7 | Mustard (*Brassica juncea*) | Positive effect on fresh weight, root and shoot length, and vigour index of seedlings; improved photosynthetic quantum efficiency and higher chlorophyll contents in leaves; increase in root length; modulation antioxidant status | Sharma et al., 2012 |
| 10-15 | 50, 100, 500, 1000 and 5000 for petri dish and 100, or 1000 for hydroponics | Petri dish germination tests/Hoagland solution | 6 | Tomato (*Lycopersicon esculentum*) | Decreased root elongation; lower chlorophyll contents; higher superoxide dismutase activity and less fruit productivity | Song et al., 2013a,b |

| Particle size (nm) | Concentration ($mg\ L^{-1}$; $mg\ kg^{-1}$) | Medium | Exposure time (days) | Plant species | Physiological/ biochemical effects | Reference |
|---|---|---|---|---|---|---|
| **20** | 0.2, 0.5 and 1 | Hoagland solution | 7 | Jasmine rice (*Oryza sativa L.*) | Reduction in root elongation, shoot and root fresh weights, total chlorophyll and carotenoids contents; increase in hydrogen peroxide formation and lipid peroxidation in shoots and roots, increased foliar proline accumulation and decreased sugar contents; oxidative stress and induction oxidative stress tolerance mechanisms; changes in the relative mRNA expression | Nair and Chung, 2014 |
| **20** | 5, 10, 20 and 50 | Agar | 21 | Mung bean (*Vigna radiata L.*) | Reduction in shoot length and weight, chlorophyll content; reduction in root elongation and weight; hydrogen peroxide level and lipid peroxidation levels increased significantly in roots | Nair and Chung, 2015 |
| 13 | 20 and 50 | Hydroponic solution | 5 | Pearl millet (*Pennisetum glaucum*) | Increased the rate of germination; effects the shoot and root length | Parveen and Rao, 2015 |
| 85 and 17 | 6 ($Ag_2S$ NPs) and 0.6 (Ag NPs) | Hydroponic solution | 14 | Cowpea (*Vigna unguiculata L. Walp.*) and wheat (*Triticum aestivum L.)* | No toxicity observed within 24 h; direct uptake in plant tissues; $Ag_2S$ NPs are toxic to plants over a 2-week period; Ag-NPs are more toxic to cowpea growth than the release of dissolved Ag; formation of ruptures in roots | Wang et al., 2015 |
| 70 | 10 | Hydroponic solution | 7 | Cucumber (*Cucumis sativus*) and wheat (*Triticum aestivum L.*) | NPs with sizes up to 120 nm can be taken up by plant roots and translocated to leaves without substantial transformation or dissolution | Wang et al., 2017 |

| Particle size (nm) | Concentration (mg $L^{-1}$; mg $kg^{-1}$) | Medium | Exposure time (days) | Plant species | Physiological/ biochemical effects | Reference |
|---|---|---|---|---|---|---|
| 100 | 1.0, 10, 50, 100, 500 and 1000 | Hoagland solution | 15 | Zucchini (*Cucurbita pepo*) | Reduced transpiration and biomass | Stampoulis et al., 2009 |
| 20- 150 | 0.1,1,10,100 and 1000 | Hydroponic solution | 21 | Jasmine rice (*Oryza sativa L.*) | Larger Ag NPs had more negative effects on seedling growth; decrease in seed germination and subsequent growth of those seedlings; leaf cell deformation | Thuesombat et al., 2014 |
| 10 and 25 | 0.01 to 100 | Hoagland solution | 11 | Poplars (*Populus deltoids*) and *Arabidopsis thaliana* | Increased root and stem biomass, enhanced evapotranspiration at low concentrations; reduced fresh weights of roots, stems, and leaves at high concentrations | Wang et al., 2013 |
| 100 | 5 to 11 | Hoagland solution | 10 | *Arabidopsis thaliana* | Decrease in chlorophyll content; Ag contents in roots were far higher than that in leaves | Wen et al., 2016 |
| <100 | 100, 200, 500, 1,000, 2,000, and 4,000 | Petri dish | 7 | Castor bean, (*Ricinus communis L.)* | No significant effects on seedling growth; enhanced enzymatic activity of ROS enzymes and phenolic content in castor seedlings; enhanced content of parahydroxy benzoic acid; Ag NP have lesser toxicity in comparison to other particles in castor seeds | Yasur and Rani, 2013 |

| Particle size (nm) | Concentration (mg $L^{-1}$; mg $kg^{-1}$) | Medium | Exposure time (days) | Plant species | Physiological/ biochemical effects | Reference |
|---|---|---|---|---|---|---|
| 6 and 25 | 1, 5, 10, 20 and 40 | Hydroponic solution | 7 | Common grass (*Lolium multiflorum*) | Reduction in growth and root biomass; shorter shoots and roots; Ag NP treated roots had no root hairs; highly vacuolated and collapsed cortical cells which collapsed; broken epidermis and root cap | Yin et al., 2011 |
| 2 | 125, 250 and 500 | Hydroponic solution | 5 | Radish (*Raphanus sativus*) | Germination not affected, diminished root and shoot length; concentration-dependent reduction in seedling elongation and water content; reduction in biomass; impairment of the absorption of nutritional elements; induced conformational changes in carbohydrates, lignin, and lipids | Zuverza-Mena et al., 2016 |
| 23 and 57 | 3 (Ag NP) and 7 (Ag2S NPs) | Hydroponic solution | 21 | Wheat (*Triticum aestivum L.*) | Uptake and translocation of Ag was lower for $Ag_2S$ NPs exposure compared to the Ag NP; $Ag_2S$ NPs are not as stable as expected; distribution of Ag species probably evolves over time | Pradas del Real et al., 2017 |
| 18 | 0.030 and 0.060 | Hydroponic solution and agar | 21 | Jasmine rice (*Oryza sativa L.)* | Significant effect on root branching and dry weight; root growth acceleration/restriction depending on concentrations; decrease of soluble carbohydrates; production of ROS and local root tissue death | Mirzajani et al., 2013 |

| Particle size (nm) | Concentration (mg $L^{-1}$; mg $kg^{-1}$) | Medium | Exposure time (days) | Plant species | Physiological/ biochemical effects | Reference |
|---|---|---|---|---|---|---|
| 20 | 25, 50, 75, 100, 125 and150 | Soil | At flag leaf stage | Wheat (*Triticum aestivum L*.) | Enhanced growth and yield attributes (NPK uptake and nutrient efficiency); improvement in maximum leaf area and highest grain yield | Jhanzab et al., 2015 |
| 39 | 1, 10 and 100 | Fertilised compost | 7 | Lettuce (*Lactuca sativa*) | No sign of phytotoxicity; Ag effectively trapped on lettuce leaves and washing did not decrease Ag content significantly; entrapment of Ag-NPs by cuticle and penetration in the leaf tissue through stomata | Larue et al., 2014 |
| 5–50 | 0.1 and 0.9 | Autoclaved loam and sandy soil | 35 | Faba bean (*Vicia faba L.)* | Declined germination; retarded nodulation; early senescence of root nodules; decreased shoot and root length; decreased leaf area | Abd-Alla et al., 2016 |
| 20 | 0.3 and 0.8 | FafardR 4M Mix potting soil | 42 | *Arabidopsis thaliana* | Loss of belowground function of the primary root meristem; prolonged vegetative development; shortened reproductive growth; decreased germination rates of offspring after three generations; shorter rosette growth; brown tips | Geisler-Lee et al., 2014 |
| 10 | 100, 300, 500, 1000 and 2000 | OECD artificial soil | 5 | Mung bean (*Phaseolus radiatus*) and sorghum (Sorghum bicolor) | Effects on seedling growth; growth rate not affected; the root and shoot growths of *P. radiatus* were not observed to be reduced; plants exposed to Ag NPs had much shorter roots and fewer rootlets | Lee at al., 2012 |

| Particle size (nm) | Concentration (mg $L^{-1}$; mg $kg^{-1}$) | Medium | Exposure time (days) | Plant species | Physiological/ biochemical effects | Reference |
|---|---|---|---|---|---|---|
| 20 | 100 | Agricultural soil | 75 | Maize (*Zea mays*) | Higher dry biomass of the aboveground and belowground plant parts; no trend of decreased biomass | Sillen et al., 2015 |
| 10 | 5 | Sand matrix | 14 | Wheat (*Triticum aestivum*) | Dose-dependent reduction in shoot and especially the root lengths; dose-dependent elevation in the accumulation of oxidised glutathionemand induction in the expression of a gene encoding a metallothionein | Dimkpa et al., 2013 |
| Not specified | 10, 20, 40 and 50 | Sandy soil | 4 h | Onions (*Allium cepa L.)* | Dose- as well as duration-dependent decreases in the mitotic index root meristems; reduction in the frequency of mitotic index; chromosomal and mitotic abnormalities on fragments, C-metaphase, sticky metaphase, laggard chromosomes, anaphasic bridge, and disturbed anaphase were identified in the treated meristem cells | Babu et al., 2008 |
| 20 | 20, 40, 60, 80 and 100 | Fertile loam soil | 12 | Common bean (*Phaseolus vulgaris*) and corn (*Zea mays*) | Retardation in shoots length; common bean showed increase/decrease in fresh weight and dry weight according to concentrations; decrease in fresh and dry weight in; increase in protein content | Salama, 2012 |

In more recent years, positive effects have also been recorded, encompassing improvements in seed yield (Parveen and Rao 2015), fresh weight (Sharma et al., 2012), root and shoot length (Sah et al., 2011) and vigour index of seedlings (Sillen et al., 2016; Sah et al., 2011). Furthermore, positive effects were reported for photosynthetic quantum efficiency, chlorophyll content in leaves and root length (Sah et al., 2011; Sharma et al., 2012). Several studies reported that exposure to Ag NPs resulted in neutral effects on germination and dry biomass (El-Temsah et al., 2012; Abdel-Azeem and Elsayed, 2013; Sharma et al., 2012; Yasur et al., 2013; Zuverza-Mena et al., 2016; Qian et al., 2013; Vannini et al., 2014).

# Chapter 2: Stable isotope tracing of silver nanoparticles through a full wheat life cycle exposure

# Part 1: Uptake, accumulation & translocation

## 2.1. Introduction

Once deposited into sewage sludge, silver nanoparticles (Ag NPs) can enter agricultural soils by direct application of sludge as a fertiliser (Sun et al., 2016). As soon as Ag NPs enter the environment, they are subject to chemical transformation. One of the most common transformations is thought to be the oxidative dissolution of Ag NPs, which leads to the release of $Ag^+$ ions, whereby the speciation of the latter is further affected and altered depending on the environment. Toxicological effects to plants have been linked to both Ag NPs and dissolved $Ag^+$ ions released from Ag NPs, whereby tests species are often exposed to Ag NPs and $Ag^+$ ions to distinguish and compare the uptake, accumulation and toxicity between the two Ag forms.

Previous work has shown that the uptake and toxicity of Ag NPs and $Ag^+$ ions to plants are governed primarily by the Ag speciation and NP properties (e.g. size and charge) as well as environmental factors, such as exposure concentration, duration and medium (Gubbins et al., 2011; Lee et al., 2012; Geisler-Lee et al., 2014; Bundschuh et al., 2018). Most published plant ecotoxicology studies thereby applied Ag NPs and $Ag^+$ ions at concentrations approximately 100 to 10,000 times higher than the predicted environmental concentrations (PECs) to trigger toxicological effects and enable reliable detection of Ag in the exposed plants with commonly available atomic absorption spectroscopy (AAS) techniques, which have Ag detection limits of about 1 µg $L^{-1}$ or higher (Hernández et al., 2019). In detail, the Ag NP and $Ag^+$ ion concentrations of plant exposures typically range from 0.1 to 1000 mg $L^{-1}$ for hydroponic studies and from 10 to 2000 mg $kg^{-1}$ for soil exposures. For example, Lee et al. (2012) used Ag NP concentrations of between 0 and 2000 mg $kg^{-1}$ (dry weight) in a soil exposure and found Ag concentrations of up to 22 mg $kg^{-1}$ in mung bean (*Phaseolus radiatus*) and sorghum (*Sorghum bicolor*). To compare, the uptake of Ag for the same plant

species in an agar exposure of up to 40 mg of Ag NP $L^{-1}$, the Ag concentrations were determined to be between 3 and 5 mg $kg^{-1}$ (Lee et al., 2012). However, PECs of 0.46 to 25.0 µg $kg^{-1}$ (Giese et al., 2018) are given for sludge treated agricultural soils, so it is hard to predict the uptake at more environmentally realistic conditions.

To understand the environmental effects of Ag NPs, studies should ideally be carried out at environmentally realistic exposure conditions with Ag concentrations close to the calculated PECs. In terms of the relevance of the exposure length and medium, about 70% of the current nano-ecotoxicology literature for plants focuses on standard short-term experiments between 3 and 28 days based in liquid solutions due to the straightforward nature of short-term hydroponic exposures. Currently, there is little focus on soil as an exposure medium due to its complex physicochemical interactions with Ag, even though Ag NPs and $Ag^+$ ions react very differently in aquatic and terrestrial systems in terms of physicochemical reactions (e.g. dissolution, adsorption and speciation). In this context, full life cycle plant experiments are necessary to evaluate Ag uptake from Ag NPs and $Ag^+$ ions by important crops like wheat. Silver NPs and $Ag^+$ ions have been reported to accumulate in edible parts of plants like wheat (Rui et al., 2017; Yang et al., 2018) and this indicates the possibility of introduction of those chemicals to the food chain. Although Ag is not currently a banned substance by EU or US regulatory bodies, excessive intake of Ag can have toxic effects in humans and cause argyria. Wheat is the second most important crop in the world (FAO 2020) and the uptake and accumulation of Ag by wheat hence may have an impact on the health of animals and humans.

In more recent years, more environmentally relevant studies have begun to occur. In a wheat life cycle study in a soil medium at concentrations of 20 mg Ag NP $kg^{-1}$, wheat roots, shoots and grains had Ag concentrations of roughly 11 mg $kg^{-1}$, 0.3 mg $kg^{-1}$ and 0.02 mg $kg^{-1}$ respectively at harvest (Yang et al., 2018). In comparison, at 20 times lower Ag NP concentrations (1 mg $kg^{-1}$ of Ag NPs), wheat tissues exhibited Ag concentrations more than 1000 times lower of about 0.4 µg $kg^{-1}$ for the roots and 0.3 µg $kg^{-1}$ for the shoots in a soil exposure (Liu et al., 2017). In a dual stable isotope co-exposure to $^{107}Ag^+$ ions and $^{109}Ag$ NPs at concentrations of 50 µg $L^{-1}$, hydroponic rice had Ag concentrations of 1000 mg of

$^{109}Ag\ kg^{-1}$ and 600 mg of $^{107}Ag\ kg^{-1}$ in the roots and 1.5 mg $^{109}Ag\ kg^{-1}$ and 1 mg $^{107}Ag\ kg^{-1}$ in the shoots.

The current investigation features a long-term exposure of wheat to environmentally realistic concentrations of Ag NPs and $Ag^+$ ions in soil which is made possible by employing Ag NPs and $AgNO_3$ that are produced from and hence labelled with highly enriched stable $^{109}Ag$ ($^{109}Ag$-E). The analytical techniques allow detection limits to be pushed down to the low ng $kg^{-1}$ level. In detail, 20 nm-sized citrate-capped $^{109}Ag$ NPs and dissolved $^{109}AgNO_3$ were introduced to Lufa soil at an environmentally relevant concentration of 72 µg $kg^{-1}$, equivalent to roughly x3 the maximum PECs. Winter wheat (*Triticum aestivum L.*) was then grown in these soils to maturity and plant tissues (seeds, roots, shoots and grains) were taken at different growth stages (GSs) and analysed for $^{109}Ag$-E content. In this chapter, the plant uptake, accumulation and translocation of $^{109}Ag$-E from added $^{109}Ag$ NPs and $^{109}AgNO_3$ is discussed.

## 2.2. Experimental design & methodology

### *2.2.1. Isotopically labelled $^{109}Ag$ NPs & $^{109}AgNO_3$*

#### *2.2.1.1. Synthesis*

The NP synthesis aimed to produce ~2 mg of 20 nm $^{109}Ag$ NPs with citrate coating in aqueous suspension with a polydispersity index (PDI) of less than ~0.2 (Danaei et al. 2018). The synthesis methods were adapted from those reported by Römer et al. (2011) and Laycock et al. (2014). First, a Ag metal strip enriched to 99.7% in $^{109}Ag$ (Isoflex, USA) was converted to $^{109}AgNO_3$ by dissolution in distilled 16 M $HNO_3$ and subsequent evaporation to dryness. For the synthesis, solid anhydrous trisodium citrate (99%, Alfa Aesar), referred to Na-citrate, was used as a capping agent and $NaBH_4$ (98%, Alfa Aesar) was used as a reductant. Millipore water with a resistivity of ≤18.2 MΩ.cm (at 25°C) was employed throughout.

To produce enough $^{109}Ag$ NPs for the exposure study, two batches were synthesised and mixed before spiking. For the wet syntheses, 100 mL aqueous

solutions of Na-citrate at concentrations 0.25 mM for batch #1 and 0.31 mM for batch #2 and 100 mL of $AgNO_3$ at 0.3 mM for batch #1 and 0.25 mM for batch #2 were cooled at 4°C in the dark and then mixed in a round bottom flask and vigorously stirred for 10 min while heating the solution. 6 mL of aqueous $NaBH_4$ (1 mM for batch #1 and 0.25 mM for batch #2) was then added and the mixture was boiled for 90 mins. The suspensions were removed from the heat and allowed to cool overnight at room temperature in the dark.

The particle suspensions were filtered through 0.1 µm pore-size cellulose acetate (MF-Millipore) filters to remove any larger particulates. The suspensions were then purified by dialysis to remove non-reacted reagents. For the dialysis, the NP suspensions were transferred into 1 kDa molecular weight cut-off dialysis bags (Spectra/Por) and placed in 4 L aqueous Na-citrate (at concentrations equivalent to the Na-citrate concentrations added to the batch) reservoirs for 72 h.

The $^{109}$Ag-E concentrations of each batch were initially measured using MC-ICP-MS (Table 2.1). Finally, prior to the exposure experiment, the two $^{109}$Ag NP batches were combined to produce a single NP suspension with a total volume of approximately 410 mL at which point the final $^{109}$Ag-E concentration was measured again and were recorded at 1.51 mg $L^{-1}$. This suspension was stored in the dark at 4°C.

*Table 2.1.* Reagents used for preparation and results of the characterisation for the two batches of labelled $^{109}$Ag NPs that were employed in this study.

| Batch # | Reagents (mM) | | | DLS (nm) | PdI | Yield | |
|---|---|---|---|---|---|---|---|
| | Na-citrate | $^{109}AgNO_3$ | $NaBH_4$ | | | % | mg |
| 1 | 0.25 | 0.3 | 1 | 23.1±0.6 | 0.178 | 33 | 0.8 |
| 2 | 0.31 | 0.25 | 0.25 | 21.2±0.4 | 0.156 | 46 | 1.3 |

Dynamic Light Scattering (DLS) data for the average diameter in nm and their polydispersity index (PdI), as well as the MC-ICP-MS data (under yield). Batch #1 was adapted after Laycock et al. (2014) and batch #2 after Römer et al. (2011).

For the comparative exposures with $^{109}AgNO_3$, about 3 mg of $^{109}AgNO_3$ was dissolved in 350 mL of Millipore water and stored in the dark at 4°C. Before the beginning of the experiment, the $^{109}$Ag-E concentration of the solution was

determined by MC-ICP-MS at 2.38 mg $L^{-1}$.

*2.2.1.2. Characterisation of the labelled $^{109}Ag$ NPs*

Dynamic Light Scattering (DLS) and transmission electron microscopy (TEM) analysis were performed at the Department of Materials at Imperial College London. The DLS analyses were carried out on a Malvern Zetasizer Nano S. For TEM imaging, the NP suspensions were sonicated for 15 mins and a drop of each suspension was dried on a carbon-coated copper grid and micrographs were produced on JEOL STEM/TEM 2100 Plus. The particles from the TEM images were analysed with ImageJ version 1.50 (Wagner et al., 2013). The Ag concentrations of the $^{109}Ag$ NP suspensions and the $^{109}AgNO_3$ solution were determined by a Nu Plasma HR MC-ICP-MS instrument at the Imperial College MAGIC Laboratories with Pd added as an internal standard.

*2.2.2. Exposure*

*2.2.2.1. Preparation of the soils*

The exposures were carried out in Lufa 2.2 (LUFA Speyer, Germany) soil. The soil was sieved to a particle size of 2 mm by the distributer and air-dried prior to the exposure. Lufa 2.2 is an agricultural, standard loamy sand soil with a total organic carbon of 1.61 ± 0.15 %; a $pH_{CaCl2}$ value of 5.4 ± 0.2; and a cation exchange capacity of 9.7 ± 0.4 meq per 100 g. A water holding capacity (at 100%) of 42 mL for 100 g of soil was determined for Lufa 2.2 using standard techniques (Priha and Smolander, 1999).

Following air-drying, the soil was supplemented with 50 mL 25% Hoagland solution (Hoagland No. 2 Basal Salt Mixture, Sigma Aldrich) to prevent nutrient depletion (Fyson and Oaks, 1990) during this long-term study and equilibrated for seven days before spiking. To prepare 25% Hoagland solution, 0.41 g of dehydrated Hoagland No. 2 basal salt mixture (Sigma Aldrich) with macro- and micronutrients, as described by Hoagland and Arnon (1950), was suspended in 1 L deionised water. The solution was mixed for 30 mins until the powder dissolved completely at which point the pH was adjusted to 5.5 with HCl. Finally, the solution was sterilised by autoclaving at 121°C for 30 mins. Table 2.2 shows the chemical composition of the solution.

*Table 2.2.* Chemical composition of the 25% Hoagland solution.

| 25% Hoagland No. 2 Basal Salt Mixture | |
|---|---|
| **Chemical** | **Concentration (M)** |
| $KNO_3$ | 6 mM |
| $Ca(NO_3)_2$ | 4 mM |
| $MgSO_4$ | 2 mM |
| $NH_4H_2PO_4$ | 1 mM |
| $MnCl_2.4H_2O$ | 9.2 µM |
| $H_3BO_3$ | 460 µM |
| $MoO_3$ | 0.11 µM |
| $ZnSO_4.7H_2O$ | 0.77 µM |
| $CuSO_4.5H_2O$ | 0.32 µM |
| $Fe_2(C_4H_4O_6)_3$ | 0.013 µM |

*2.2.2.2. Dosing of the soils*

Exposures were set up in polypropylene plastic pots (133 mm in height, top diameter of 97 mm and a base diameter of 63 mm) with three holes (20 mm in diameter) for wicks (Figure 2.1) for constant water supply throughout the test.

Prior to the dosing of the soils, the $^{109}Ag$ NP suspension was sonicated for 30 mins to reduce agglomeration of the NPs. Each of the 30 exposure setups contained 0.7 kg, which were individually spiked with 10 mL of 1.51 mg $L^{-1}$ $^{109}Ag$ NPs for a final $^{109}Ag$-E concentration of 72.0 µg $kg^{-1}$. In a similar manner, 10 mL 2.38 mg $L^{-1}$ of the $^{109}AgNO_3$ solution were added to 30 individual pots each containing 0.7 kg of soil to achieve $^{109}Ag$-E concentrations of 72.0 µg $kg^{-1}$. The citrate control treatment matched the Na-citrate concentration for the $^{109}Ag$ NP treatment and was prepared by the addition of 10 mL 1.08 mg $kg^{-1}$ of an aqueous Na-citrate solution to the Lufa soils. Following dosing, the soils were thoroughly mixed in bowls by breaking wet clumps with the back of a spoon for > 3 mins until they were visibly homogenised with no remaining wet clumps. All treatments were initially wetted to 60% water holding capacity with deionised water and were then transferred to the prepared pots. The soils were then left to equilibrate for seven days so that soil-water (via the wicking system) and chemistry equilibrium were reached before wheat seeds were planted.

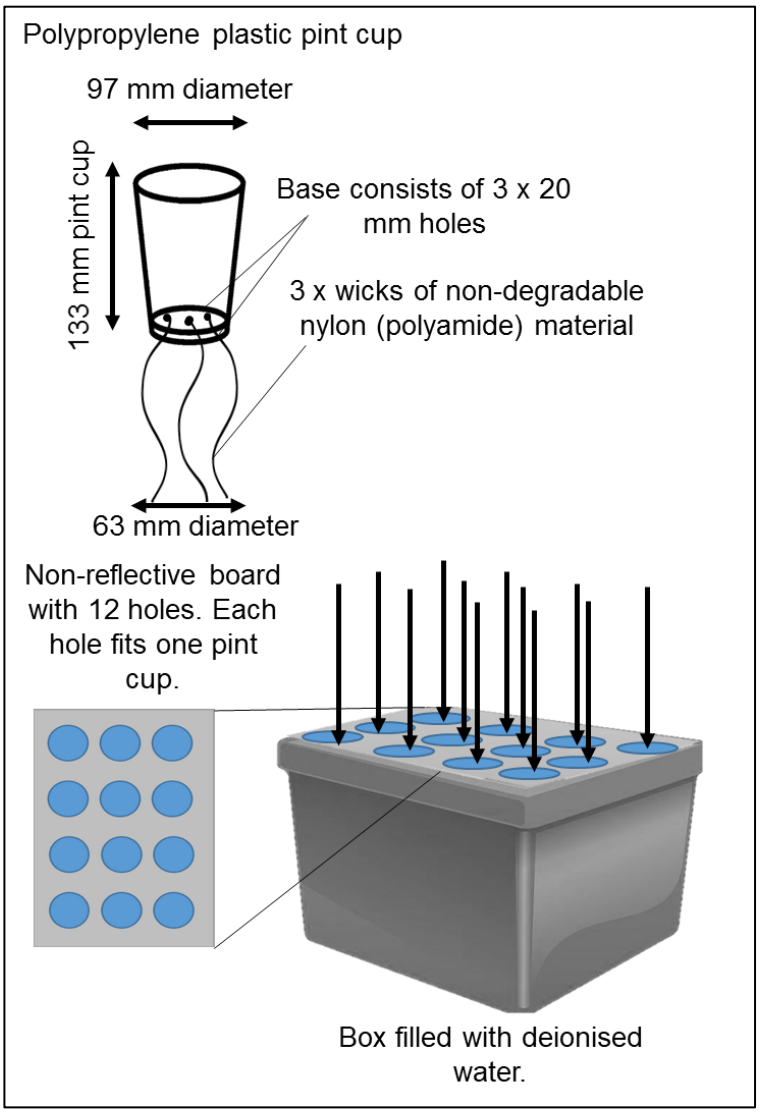



*Figure 2.1.* Schematic of setup. Polypropylene plastic pint cups (133 mm in height, top diameter of 97 mm and a base diameter of 63 mm) with 0.7 kg soil capacity and three holes for wicks, 20 mm in diameter each, were used as pots.

For comparison with the exposures that employed $^{109}$Ag NPs and $^{109}AgNO_3$, two control treatments were carried out. One was a 'blank control', to which no Ag was added, and a 'citrate control'. Na-citrate was employed as coating and stabiliser for the $^{109}$Ag NPs, the purpose of this control is to check if Na-citrate has any effect on plant growth in the applied concentrations. Both controls were treated with Hoagland solution in same manner outlined for the Ag treatments. Here, all concentrations refer to dry weight (dw) soil.

To ensure sufficient plant tissue was available for analysis, all four treatments

encompassed 16 replicates for GSs 1 and 2, for a total of 128 individual samples. For GSs 3 to 8, there were five replicates each for the $^{109}Ag$ NP and $^{109}AgNO_3$, treatments (60 pots in total) and three replicates for the blank and citrate controls (36 pots in total).

*2.2.2.3. Planting of wheat*

Untreated organic winter wheat (*Triticum aestivum L.,* Variety: KWS Dacanto) sourced by Københavns Universitet was used in the experiment. The seeds were kept refrigerated at 4°C in the dark and were not pre-treated in any way.

Seeds of similar size and visual intactness (~0.8 cm in length and ~0.5 cm in width) were chosen for the plant exposure experiment. The wheat seeds were planted at 2 cm depth as per OECD protocols (208 and 227). A total of five seeds were planted in each pot.

*2.2.2.4. Exposure conditions*

The exposure was performed at 20°C temperature, a 16 h light/8 h dark photoperiod at a light intensity of 350 ± 50 $\mu E/m^2/s$ in a controlled greenhouse chamber at the UK Centre for Ecology and Hydrology, Wallingford. It is important to note that, after the collection of the GS 7 samples, the automated lighting and temperature control system experienced a seven day fault. During this period, the average light intensity and temperature conditions were reduced to 48 $\mu E/m^2/s$ and 16°C respectively, with a 14 h light/10 h dark photoperiod. This affected all remaining plant replicates in the experiment.

The soil in the pots was consistently kept at 65 to 70% water holding capacity via the installed wicking system. Nutrient depletion during the full plant growth cycle was prevented by adding 50 mL 25% Hoagland solution every four weeks to each of the exposure sets.

The positions of the pots, including the water tanks for the wicking system, were randomised once a week to minimise position effects and variability in plant growth (Measures et al., 1973). The tanks were cleaned with water every four weeks to prevent microbial biofilm formation that can potentially affect plant growth. No antimicrobial or pesticide products were used for tank washing.

### *2.2.3. Sample collection*

Plant and soil samples were taken during the three main crop phases (vegetative phase, flowering and grain formation) in a standardised manner according to the Zadoks growth scale of cereal crop development (Zadoks et al., 1974). In detail, samples were taken at eight GSs according to the Zadoks scale: 1 – Seeding growth; 2 – Tillering; 3 – Stem elongation; 4 – Booting; 5 – Awn emergence; 6 – Flowering (anthesis); 8 – Dough development; 9 – Ripening (Table 2.3).

*Table 2.3.* Growth stages (GSs) according to the Zadoks scale (Zadoks et al., 1974) with days in brackets, which represent the time that the samples were collected in this experiment.

| Growth stage | Growth stage description | Growth stage | Growth stage description |
|---|---|---|---|
|  | First leaf unfolded (11)<br>***GS1 (6 – 7 days )*** |  | Flag leaf sheath opening (47)<br>***GS5 (102 – 125 days)*** |
|  | Three leaves unfolded (13), Main shoot and 1 tiller (21)<br>***GS2 (14 – 16 days)*** |  | Emergence of inflorescence complete (59)<br>***GS6 (111 – 135 days)*** |
|  | Five leaves unfolded (15), Main shoot and 3 tillers (23)<br>***GS3 (29 – 41 days)*** |  | Anthesis complete (69)<br>***GS7 (124 – 135 days)*** |
|  | Second node detectable (32), Eight leaves unfolded (18), Main shoot and 3 tillers (23)<br>***GS4 (94 – 119 days)*** |  | Caryopsis hard (92)<br>***GS8 (149 – 191 days)*** |

The small figures were modified from Tottman and Makepeace 1979

#### *2.2.3.1. Plant tissues*

Plant tissues were collected at all GSs from 1 to 8, and the number of days taken to complete the growth period was recorded. For GS 1 and GS 2, approximately two whole plant samples (if emerged) were collected from each pot to allow sufficient biomass for analysis. Subsequently, only one growing plant remained in each pot and samples were collected when the required GS was reached. On collection days, the samples were first obtained either by careful digging around the roots at GS 1 and GS 2 or by emptying the pot onto a workstation for GS 3 to GS 8. The plants were then photographed with a Canon DSLR 50D and split into

their representative plant tissues: roots, shoots and, if present, seeds or grains (Table 2.4). Root samples were washed thoroughly at least three times with deionised water until all roots appeared clean and free of soil particles.

*Table 2.4.* Types of biological tissues collected for each growth stage.

| Growth stage No | Shoot | Root | Seed | Grain |
|---|---|---|---|---|
| 1 & 2 | X | X | X | |
| 3, 4 & 5 | X | X | | |
| 6, 7 & 8 | X | X | | X |

The collected tissues were dried to constant weight at 70ºC (Thermo scientific, Heratherm OGS180). Once dry, the GS 1 to GS 3 samples were stored at room temperature, whilst samples from GS 4 to GS 8 were ground into a powder using a plastic garlic crusher (ToJI) to ensure homogeneity.

*2.2.3.2. Soils & soil pore waters*

Soil samples were obtained at GS 1, GS 2, GS 4, GS 6 and GS 8 by the collection of 7 g of soil after plant collection. The collected samples were dried at 70ºC (Thermo scientific, Heratherm OGS180) for seven days and were stored at room temperature.

The $^{109}$Ag-E concentrations of the soil pore waters were determined for GS 4, GS 6 and GS 8. The sampling protocol is described in detail by Lahive et al. (2017). To summarise, 34 g of soil were collected in 50 mL polypropylene centrifuge tubes, transferred to a dark controlled temperature room (20°C) overnight, before determination of the water content on a small (7 g) aliquot. The 34 g of soil were then saturated to 100% water holding capacity, stirred gently and left to equilibrate overnight in a dark room at 20°C.

Then, 31 g of the water-saturated soil samples were centrifuged for 1 h at 2000 g at 4°C through preconditioned 25 mL filter inserts (0.45 µm PVDF filter membranes) filled with preconditioned glass wool and housed into a 50 mL centrifuge system (Thermo Scientific F2519-6). The glass wool and filter inserts were preconditioned by soaking overnight in 0.1 M $CuSO_4$ solution (99.995%

purity, Sigma Aldrich) in order to reduce $Ag^+$ ion adsorption and Ag losses (Diez-Ortiz et al., 2015; Cornelis et al., 2010). After the extraction, between 5 and 7 mL of soil pore water were collected, and analyses of these samples yielded the total Ag contents of the soil pore waters. Small (1.5 ml) aliquots of the centrifuged soil pore waters were further centrifuged for 3 h at 20800 g. The top 1 mL of supernatant was then withdrawn for the determination of the truly dissolved concentrations of $^{109}$Ag-E in the soil pore water. Following collection, all soil pore water samples were acidified to 2 M $HNO_3$ with 16 M $HNO_3$ and were kept in the dark at 4°C.

In the following, the 'total' Ag contents of the soil pore waters refer to the Ag concentrations determined for the soil solutions following filtration through the 0.45 µm membranes. In contrast, the 'truly dissolved' Ag concentrations represent the Ag concentrations that were measured for the pore waters following 0.45 µm filtration and subsequent centrifugation of the filtered pore waters.

*2.2.4. Sample analyses*

The sample preparation and the subsequent Ag isotope measurements by MC-ICP-MS are time-consuming, with about two weeks needed to complete the analyses of about 30 samples. Hence, Ag isotope analyses were only carried out for a subset of samples. In detail for each of the two $^{109}$Ag treatments and the two control treatments, the following samples were analysed: (i) a duplicate set of plant tissues from GSs 1, 2, 4, 6 and 8; (ii) duplicate soil samples on the initial day of spiking and from GSs 1, 2, 4, 6 and 8; (iii) three soil pore water samples from GSs 4, 6 and 8.

The sample preparation was carried out in the Imperial College MAGIC Laboratories in an ISO Class 6 cleanroom, using ISO Class 4 laminar flow benches for critical steps. All mineral acids used were prepared from sub-boiling distilled 6 M HCl, 16 M $HNO_3$ and 27 M HF (prepared from VWR reagent-grade acids), whilst all water was of ≥18.2 MΩ.cm quality from Millipore purification systems.

*2.2.4.1. Digestion & initial treatment*

For the plant tissues, up to 500 mg of sample (dw) were weighed into the microwave Teflon vessels. Seven mL of 16 M $HNO_3$ and 3 mL Suprapur $H_2O_2$ (VWR) were added to each vessel, which was left covered but unsealed overnight to release gaseous reaction products. The vessels were then sealed and the samples digested in an Ethos EZ microwave system (Milestone Inc.) with a temperature program that featured an initial 15 min temperature increase to 200°C and a further 15 mins at constant 200°C. Following cooling, the sample solutions were transferred to 7 mL Savillex Teflon beakers and evaporated to dryness. The samples were then dissolved in 1 mL 1 M $HNO_3$, dried down and repeatedly dried down with a few drops of 6 M HCl for conversion to the chloride form. Finally, the samples were dissolved in 1 mL 0.5 M HCl in preparation for the ion exchange chemistry.

For the soil digestions, approximately 100 mg of soil (dw) was weighed into the microwave Teflon vessels. Eight mL of distilled 16 M $HNO_3$ and 2 mL $H_2O_2$ were added to each vessel and left unsealed overnight to release gases. The soil samples were then digested in the microwave oven in the same manner as the plant tissues. After this, the solutions were transferred to 7 mL Savillex Teflon beakers and evaporated to dryness. To ensure full digestion of the silicate soil components, the samples were then treated with 1 mL 16 M $HNO_3$ and 2 mL of 28 M HF and refluxed at 180°C for 48 h. The samples were then dissolved in 1 ml 1 M $HNO_3$ and further treated in the same manner as the plant tissues.

For both the total and truly dissolved soil pore water samples, 500 µl aliquots were transferred and dried in 7 ml Savillex Teflon beaker. Both 0.8 mL 16 M $HNO_3$ and 0.2 total and then refluxed on a hot plate overnight at 200°C. The solutions were then evaporated to dryness, dissolved in 1 mL 1 M $HNO_3$ and further treated in the same manner as the plant and soil samples.

*2.2.4.2. Separation of Ag*

The Ag isotope measurements by MC-ICP-MS require purified Ag that is separated from the sample matrix. This separation was achieved by a one-step gravity-flow anion exchange chromatography protocol developed by Junk et al.

(2019), as summarised in Table 2.5. The procedure involves loading of the 0.5 M HCl sample solutions onto Bio-Rad Poly-Prep chromatography columns containing 1 mL AG1-X8 (100 – 200 mm mesh) resin, pre-cleaned and pre-conditioned with 9 M HCl and 0.5 M HCl. To remove matrix elements, the columns were washed with HCl of decreasing molarity (0.1, 0.005 and 0.001 M) and finally with 0.5 M $HNO_3$. Silver was then eluted from the resin and collected by addition of 12 mL 0.5 M $HNO_3$ and a further 5 mL 0.5 M $HNO_3$ after leaving the resin to rest for at least an hour. As outlined by Junk et al. (2019), this method successfully separates Ag at high yield from elements that form problematic spectral interferences, such as $[^{64}ZnAr]^+$, $[^{88}SrO]^+$ on $^{104}Pd^+$, $[^{65}CuAr]^+$ on $^{105}Pd^+$ and $[^{67}ZnAr]^+$ on $^{107}Ag^+$.

*Table 2.5.* Summary of the anion exchange chromatography protocol for Ag separation developed by Junk et al. (2019).

| Column chemistry | | |
|---|---|---|
| **Volume [mL]** | **Acid** | **Step** |
| **2** | - | Load resin AG1-X8 |
| **16** | 9 M HCl | Clean resin |
| **24** | 0.5 M HCl | Precondition resin |
| **-** | 0.5 M HCl | Load samples |
| **27** | 0.1 M HCl | Matrix washing |
| **28** | 0.005 M HCl | Matrix washing |
| **16** | 0.001 M HCl | Matrix washing |
| **3.5** | 0.5 M $HNO_3$ | Ag elution |
| **12** | 0.5 M $HNO_3$ | Ag elution |
| **5** | 0.5 M $HNO_3$ | Ag elution |
| Evaporate samples and re-dissolve in 0.1 M $HNO_3$. | | |

### *2.2.5. Mass spectrometry*

#### *2.2.5.1. Instrumentation*

The Ag isotope measurements were carried on with a Nu Plasma HR MC-ICP-MS at Imperial College MAGIC Laboratories using an Aridus II (CETAC) desolvation system with MicroMist glass nebulisers and a CETAC ASX-100 autosampler, as described by Junk et al. (2019). The isotope analyses were

performed by static multiple collection using Faraday cups equipped with $10^{11}$ Ω resistors to simultaneously monitor mass numbers 107 and 109 for Ag, as well as 104 and 105 for Pd. The Pd ion beams were monitored to enable correction of the raw measured $^{109}Ag/^{107}Ag$ ratios for instrumental mass discrimination relative to $^{104}Pd/^{105}Pd$.

*2.2.5.2. Preliminary assessment of Ag concentrations*

A small (≤5%) aliquot of the purified Ag from each sample after the column chemistry was doped with a 100 µg $L^{-1}$ Pd solution to a concentration of 10 µg $L^{-1}$ and diluted to 1 mL for a preliminary Ag concentration assessment, following Junk et al. (2019). The Ag concentrations of the sample solutions were thereby determined by using an external calibration relative to three standard solutions of natural Ag with concentrations of 1, 10 and 20 µg $L^{-1}$ that were prepared in 0.1 M $HNO_3$ and doped to 10 µg $L^{-1}$ with Pd.

*2.2.5.3. Ag isotope measurements*

The results of the preliminary analyses were employed to determine the final dilution (with 0.1 M $HNO_3$) of the sample Ag fractions for the subsequent isotopic analysis and the order in which the samples were analysed (from low to high Ag concentrations). Silver standard solutions with concentrations that were similar to those of the sample solutions were prepared from more concentrated Ag stock solutions by dilution with 0.1 M $HNO_3$. Both the sample and the Ag standard solutions were doped with a freshly prepared 100 µg $L^{-1}$ Pd solution to a Pd concentration of 10 µg $L^{-1}$.

As outlined by Junk et al. (2019), samples with only natural Ag were analysed relative to Ag standard solutions prepared from a concentrated stock solution of natural Ag. In contrast, samples containing the $^{109}$Ag-E were measured relative to Ag standard solutions that were diluted from a concentrated stock that was prepared by mixing natural Ag with $^{109}$Ag-E to obtain a $^{109}Ag/^{107}Ag$ ratio of about 18. The $^{109}Ag/^{107}Ag$ of this stock solution was accurately determined by repeated (n > 10) mass spectrometric analyses at high ion beam intensities. The same procedure outlined by Junk et al. (2019) was followed for the isotopic measurements. To summarise, following tuning of the instrument, Ag standard

solutions were run to ensure the instrument was working appropriately for sample analyses. Procedural blanks were then analysed first so that memory effects were at the lowest possible level. The samples were then analysed in order of increasing Ag concentration, whereby samples containing natural and spiked Ag were run on different days to avoid detrimental memory effects. All sample runs were bracketed by at least two runs of an appropriate Ag standard solution. Between each sample/standard run, the sample introduction system was flushed for 2 mins with 0.1 M $HNO_3$ to ensure Ag ion beam intensities declined to a satisfactory level of less than 5 mV. After each wash and prior to each sample/Ag standard run, the memory effects were recorded by carrying out an analysis whilst 0.1 M $HNO_3$ was flushed through the system. All concentrations are reported for dry weight material.

*2.2.5.4. Data reduction*

The detailed data reduction procedure is outlined in Junk et al. (2019) and only a summary is provided below. After the 'raw' data of $^{107}Ag$, $^{109}Ag$, $^{105}Pd$ signal intensities and $^{105}Pd/^{104}Pd$ ratios were collected in a run, six offline data reduction steps were employed:

1. Memory correction: Correction of the residual instrumental memory by subtracting the raw $^{107}Ag$ and $^{109}Ag$ signal intensities recorded for the analysed 0.1 M $HNO_3$ (after the wash and before standard/sample measurement) from the recorded $^{107}Ag$ and $^{109}Ag$ signal intensities of samples and standards. This was done for all samples and standard analyses to determine memory-corrected ratios of $^{109}Ag/^{107}Ag$ and $^{109}Ag/^{105}Pd$.
2. Instrumental mass bias correction: The above-corrected ratios of $^{109}Ag/^{107}Ag$ and $^{109}Ag/^{105}Pd$ were corrected for instrumental mass bias by external normalisation relative to the measured $^{105}Pd/^{104}Pd$ ratio. For this calculation, the exponential law was utilised (Wombacher and Rehkämper, 2003).
3. Standard offset correction: Any offset in the mass bias-corrected $^{109}Ag/^{107}Ag$ data recorded for the bracketing standard runs was used to empirically correct the mass bias-corrected $^{109}Ag/^{107}Ag$ result for the

bracketed sample, following the procedure of Junk et al. (2019).

4. Mass and molar ratio calculation: By employing a calculation described by Laycock et al. (2014), the mass and molar ratio of $^{109}$Ag-E relative to the total Ag present in each sample was determined.
5. Total Ag mass and molar concentration: The total mass and molar Ag content were then calculated for each sample by use of a calibration line that is set up with standard analyses that relate the $^{109}$Ag concentration to the measured and mass bias-corrected $^{109}$Ag/$^{105}$Pd ratio (Step 2). After accounting for dilution factors, the moles of $^{109}$Ag present in a sample were determined which together with the known isotope compositions of $^{109}$Ag-E and natural Ag as well as the standard corrected $^{109}$Ag/$^{107}$Ag ratio of the sample, provided the total sample Ag content.
6. Procedural blank correction: The procedural blanks were treated and processed in the same manner as all other samples and analysed for $^{109}$Ag and $^{107}$Ag contributions as well as for $^{109}$Ag/$^{107}$Ag ratio. This final correction was calculated by subtraction of the procedural blanks from the sample Ag contents.

*2.2.5.5. Quality control*

For quality control, additional larger plant samples from the experiment were spiked with $^{109}$Ag-E and were analysed repeatedly (> x10) using the same methods that were applied for the samples. These analyses revealed that the employed methods achieved performance characteristics similar to those documented by Junk et al. (2019), whereby the $^{109}$Ag/$^{107}$Ag ratios were determined with a precision (2 SD) of ± 0.6%. The detection limit was determined by multiple measurements (n = 32) of the blank, established at 5.1 ± 3.1 pg.

*2.2.6. Statistical analyses*

All statistical analyses were performed using Minitab 18. Variations between the treatments were tested by two sample T-tests using a one-way analysis of variance (ANOVA) with a significance level of $p < 0.05$. First, the Ag concentrations between the control and Na-citrate treatments were compared. Once no differences were established between the controls, the control data were

compared to the results for the Ag treatments. All errors are reported as 1 SD (standard deviation).

## 2.3. Results

### *2.3.1. Characterisation of the $^{109}$Ag NPs*

The DLS analysis showed that the $^{109}$Ag NPs of batches #1 and #2 had average hydrodynamic diameters of 23 nm and 21 nm respectively and PDI values of 0.178 and 0.156 (Table 2.1). Figure 2.2 shows the DLS size distribution by intensity for batches #1 and #2. As expected, the TEM micrographs showed a slightly smaller average diameter of 19.6 ± 6.5 nm (n = 873; Figure 2.3) for both batches, whereby the discrepancy in diameters of approximately 1 – 3 nm reflects the limitations of the DLS technique (Baalousha et al., 2012). Micrographs of the two suspensions presented in Figure 2.4 show particles of spherical shape and consistent size distribution.

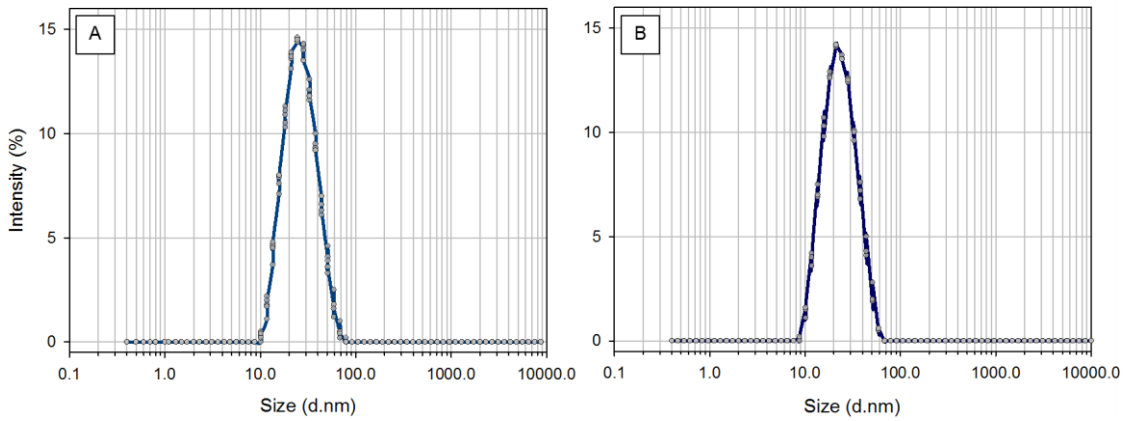



*Figure 2.2.* DLS data for size distribution determined for the $^{109}$Ag NPs of batch #1 (A) and batch #2 (B). Sample measurements were repeated 5 times.

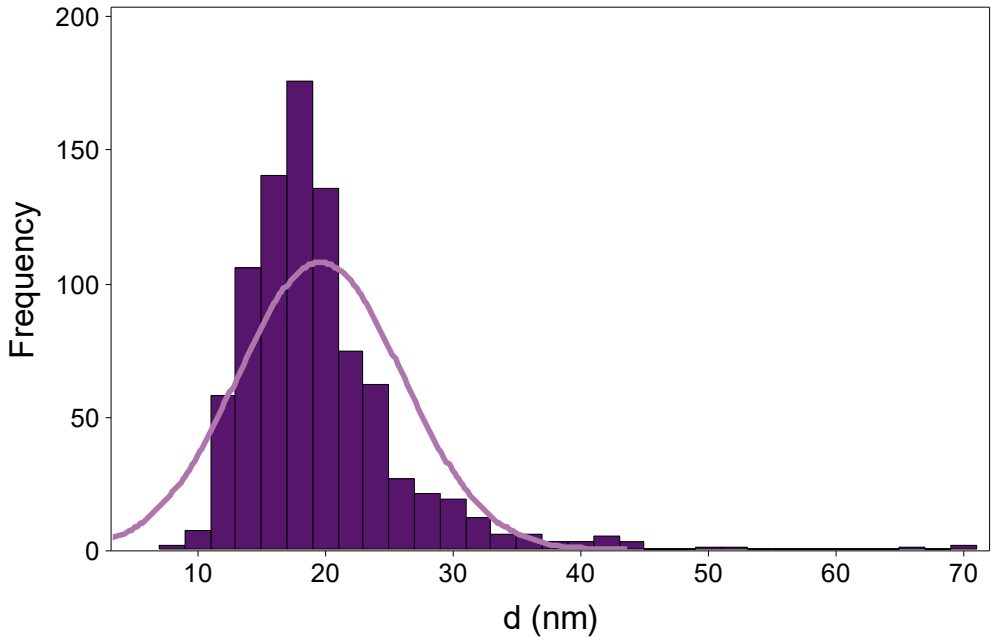



*Figure 2.3.* Frequency plot for the diameters (in nm) of the $^{109}$Ag NPs as determined by TEM imaging. The mean particle diameter is 19.62 ± 6.45 nm (n = 873).

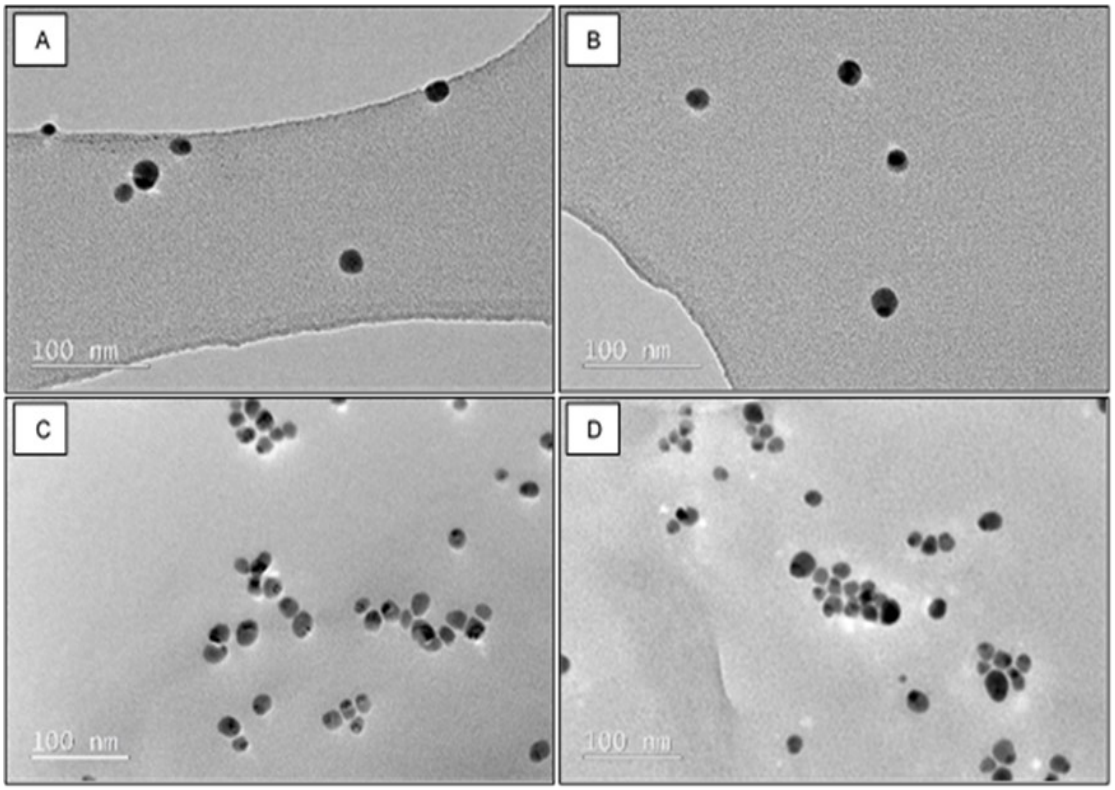



*Figure 2.4.*TEM micrographs of the $^{109}$Ag NPs. A and B: TEM images of batch #1; C and D: TEM images of batch #2.

The final $^{109}$Ag NP suspension with a volume of ~410 mL had a $^{109}$Ag-E concentration of 1.52 mg $L^{-1}$, while the $^{109}AgNO_3$ solution with a volume of ~350 mL featured a $^{109}$Ag-E concentration of 2.38 mg $L^{-1}$.

*2.3.2 Validity of the exposure experiment*

Following the OECD guidelines (OECD 208 and 227) for chemical testing of terrestrial plants, the experiment fulfils all required quality criteria so that the test can be considered as valid. Across the experiment, approximately 98% of all seedlings emerged. For the 2% of seedlings that did not emerge, there was no apparent pattern between the Ag NPs, $AgNO_3$, blank control and citrate control treatments. The controls showed no visible phytotoxic effects such as chlorosis, necrosis, wilting, shoot or stem deformations. The mean plant survival for all treatments was 100% for the duration of the experiment.

*2.3.3. Soils*

Similar temporal changes were observed for the $^{109}$Ag-E concentrations for both treatments in the soils (Figure 2.5, Table 1A, Appendix A). In summary, the $^{109}$Ag-E concentrations for the $^{109}$Ag NP treatment reduced gradually from about 69 µg $kg^{-1}$ after initial spiking to about 65 µg $kg^{-1}$ at GS 2. Even lower, and approximately constant, $^{109}$Ag-E concentrations of about 51 µg $kg^{-1}$ were found for GSs 4 to 8. The $^{109}$Ag-E concentrations for the $^{109}AgNO_3$ treatment decreased in a similar manner from about 68 µg $kg^{-1}$ after the dosing, to about 56 µg $kg^{-1}$ at GS2, and then to nearly constant values of about 51 µg $kg^{-1}$ at GSs 4 to 8. The biggest difference between the $^{109}$Ag NP and the $^{109}AgNO_3$ treatments was found for GS 2, whereby the former is clearly associated with higher soil $^{109}$Ag-E concentrations (of about 5 µg $kg^{-1}$) than the latter (with about 56 µg $kg^{-1}$). For the two controls, the $^{109}$Ag-E concentrations were between 0.5 and 2.8 ng $kg^{-1}$. As such, the controls established unproblematic background $^{109}$Ag-E concentrations that were more than three orders of magnitude lower than those found for the two $^{109}$Ag treatments (Table 1A, Appendix A).

*2.3.4. Soil pore waters*

Before statistical evaluation and interpretation, the results of four samples were excluded from the pore water dataset for data quality reasons. This encompasses

the total $^{109}$Ag-E data for one GS 4 sample from the $^{109}$Ag NP treatment as well one sample each for GSs 4 and 8 of the $^{109}AgNO_3$ treatment. These results were excluded because they featured total $^{109}$Ag-E concentrations that were lower, by a factor of 3.5 or more, than the truly dissolved $^{109}$Ag-E fraction of the same samples. In addition, a single truly dissolved $^{109}$Ag-E result was eliminated (for GS 8 of the $^{109}AgNO_3$ treatment) because this was more than all other comparable data ($p < 0.01$). Most likely, these clearly erroneous results reflect a loss of Ag from the solutions as a result of precipitation or adsorption reactions during sample preparation. In contrast, the remaining samples show fairly consistent $^{109}$Ag-E concentrations, suggesting that the data are robust and not subject to significant analytical artefacts.

The truly dissolved $^{109}$Ag-E concentrations in the soil pore water were found to be about 15 times lower than the total $^{109}$Ag-E concentrations for both $^{109}$Ag treatments for GSs 4 to 8 (Figure 2.6B, Table 3A, Appendix A). Similar to the total $^{109}$Ag-E concentrations of the soil pore water, the truly $^{109}$Ag-E concentrations in the soil pore water for the $^{109}$Ag NP treatment were found to be significantly higher ($p = 0.009$) compared to those for the $^{109}AgNO_3$. Mimicking the total $^{109}$Ag-E concentrations, the truly dissolved $^{109}$Ag-E concentrations for the $^{109}$Ag NPs were once again recorded to be about 3 times higher than those of $^{109}AgNO_3$ treatment. The truly dissolved $^{109}$Ag-E concentrations for the $^{109}$Ag NP were recorded at approximately 0.1 µg $L^{-1}$ and at about 0.03 µg $L^{-1}$ for the $^{109}AgNO_3$ treatment. The truly dissolved $^{109}$Ag-E concentrations for the two $^{109}$Ag treatments (Figure 2.7B and D) also showed no significant temporal relationship ($p > 0.58$).

For the blank control, the total $^{109}$Ag-E concentrations were found to be more than 7 times lower than the two $^{109}$Ag treatments with $^{109}$Ag-E concentrations of 1.5 ng $L^{-1}$. The truly dissolved $^{109}$Ag concentrations for the blank control were recorded to be 20 lower times than the two $^{109}$Ag treatments with measured concentrations of 1.4 ng $L^{-1}$. As the citrate control soil samples showed very low $^{109}$Ag-E concentrations (0.5 – 2.8 ng $kg^{-1}$) it may be reasoned that analysis of citrate control samples would have also shown negligible $^{109}$Ag concentrations, similar to those of the blank control soil pore waters (0.8 – 1.5 ng $L^{-1}$).

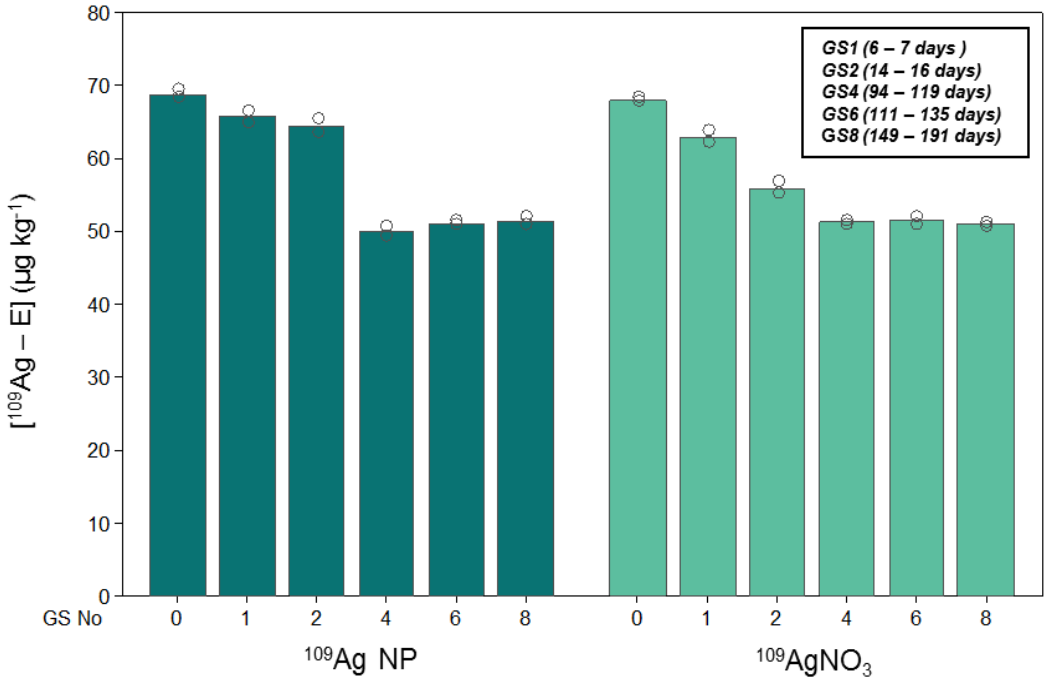



*Figure 2.5.* $^{109}$Ag-E concentrations for the spiked Lufa soils determined at day 0 and for GSs 1, 2, 4, 6 and 8. The symbols on the graph show the two individual data points (n = 2).

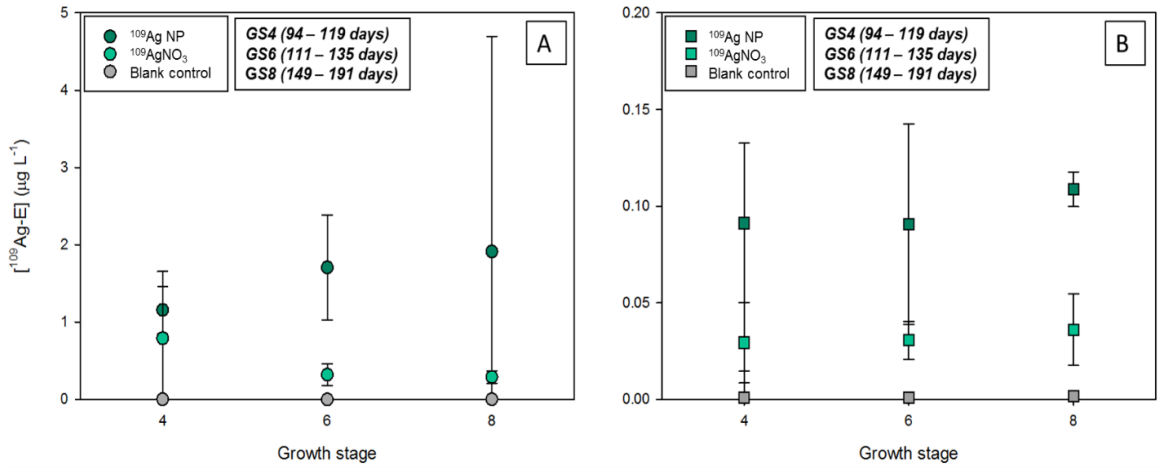



*Figure 2.6.* Total $^{109}$Ag-E (A) and truly dissolved $^{109}$Ag-E (B) concentrations in Lufa soil pore water for GSs 4, 6 and 8 (n = 3). The error bars signify standard deviations of two or three samples. The $^{109}$Ag-E concentrations for the $^{109}$Ag NP treatment were found to be significantly higher than those of the $^{109}AgNO_3$ treatment for both the total $^{109}$Ag-E concentrations (A) ($p = 0.03$) and the truly dissolved $^{109}$Ag-E concentrations (B) ($p = 0.01$).

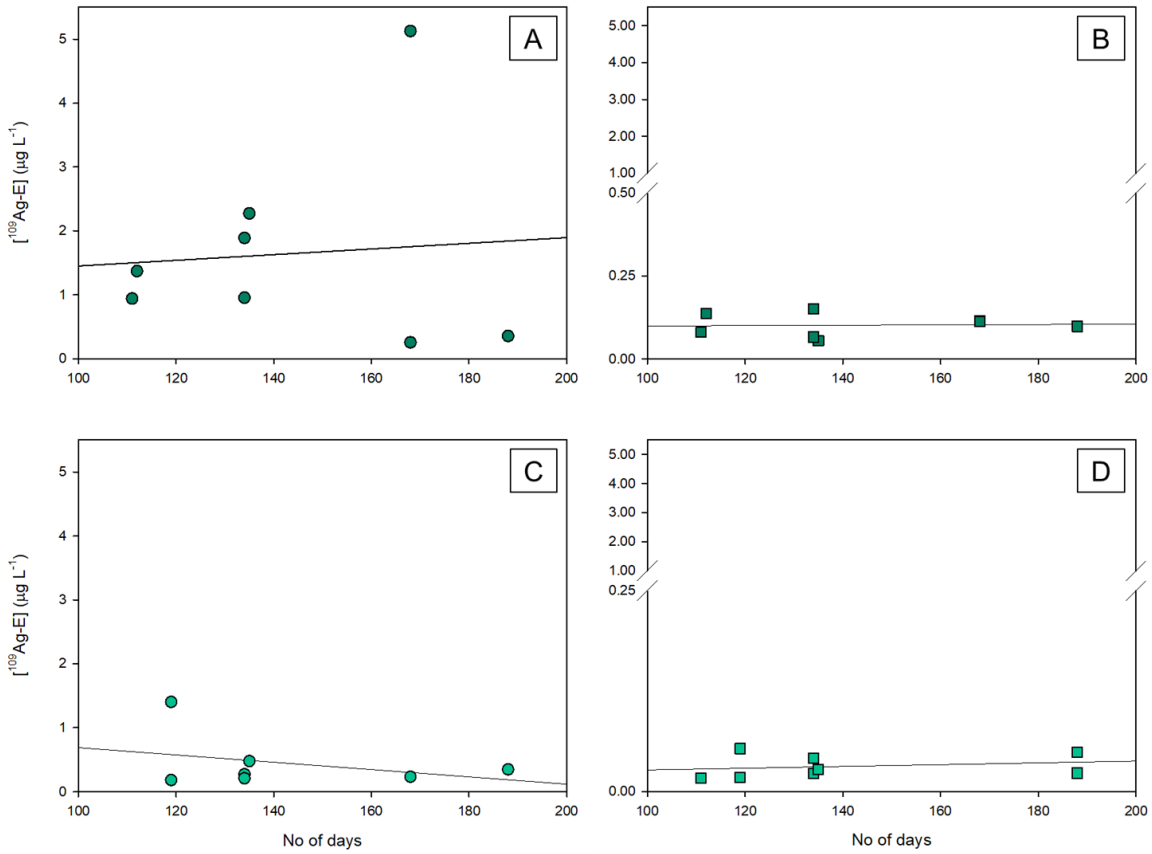



*Figure 2.7.* Simple linear regression for (A) total $^{109}$Ag-E concentrations for the $^{109}$Ag NP treatment, (B) truly dissolved $^{109}$Ag-E for the $^{109}$Ag NP treatment, (C) total $^{109}$Ag-E for the $^{109}AgNO_3$ treatment and (D) truly dissolved $^{109}$Ag-E for the $^{109}AgNO_3$ treatment, when plotted versus the sampling days (n = 3). The total and truly dissolved $^{109}$Ag-E concentrations of the pore waters showed no significant temporal trends, with p-values exceeding 0.46 and 0.58, respectively.

### *2.3.5. Plant tissues*

For both Ag treatments, $^{109}$Ag-E concentrations were found in all plant tissues. The $^{109}$Ag-E concentrations decreased in the order roots > seeds ≈ shoots > grains (Figure 2.8, Table 4A, Appendix A). Considering changes in $^{109}$Ag-E concentration in the tissues with time, the roots concentrations decrease; whilst the shoot, seed and grain concentrations appear to remain roughly constant, but clear temporal trends are difficult to discern for the latter two tissues as results are only available for two GSs (Figure 2.8, Table 4A, Appendix A). The following results of the plant tissues focus on the data obtained for GSs 4, 6 and 8 because these best capture the uptake and translocation of $^{109}$Ag-E for nearly mature wheat rather than at the early GSs.

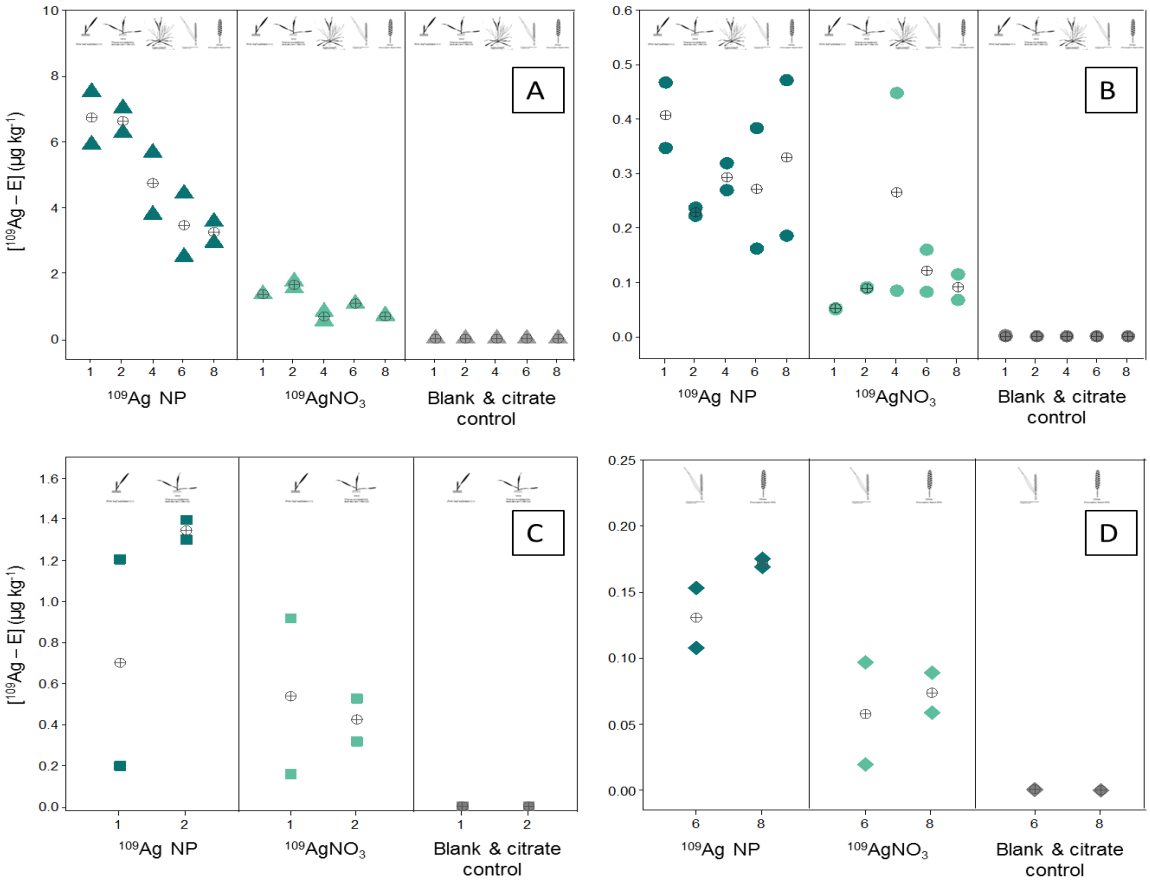



*Figure 2.8*. $^{109}$Ag-E concentrations for roots (A), shoots (B), seeds (C) and grains (D) of wheat plotted versus the GS of sampling. The symbols on the graph show the two individual data points (n = 2) and the ⊕ symbol denotes the mean values.

Notably, the plant tissues from the $^{109}$Ag NP treatment ubiquitously have higher mean $^{109}$Ag-E concentrations by a factor of x2 (for shoots and grains) to more than x3 (for roots and total plants) compared to the tissues from the $^{109}AgNO_3$ treatment. These consistently exceed the combined standard deviation uncertainties of the mean values and, considering the populations, they are highly significant for the roots ($p < 0.01$), clearly significant for the total plants ($p = 0.05$) and moderately significant for the grains ($p = 0.06$) and shoots ($p = 0.07$) (Figure 2.8, Table 4A, Appendix A).

In detail, wheat treated with $^{109}$Ag NPs had a mean $^{109}$Ag-E concentration of 3.8 µg kg$^{-1}$ for the roots, 0.30 µg kg$^{-1}$ for the shoots, 0.15 µg kg$^{-1}$ for the grains and hence of about 1.8 µg kg$^{-1}$ for the total plants. In contrast, for the $^{109}AgNO_3$ treatment the same tissues recorded mean $^{109}$Ag-E concentrations of 0.82 µg kg$^{-1}$, 0.16 µg kg$^{-1}$, 0.07 µg kg$^{-1}$, and 0.32 µg kg$^{-1}$, respectively (Figure 2.8, Table 4A,

Appendix A).

The plant tissues from the two control exposures had very low $^{109}$Ag-E background levels of about 0.1 to 2 ng kg$^{-1}$ (Figure 2.8, Table 4A, Appendix A). As such the $^{109}$Ag-E concentration in the control tissues were significantly lower ($p < 0.001$), typically 3 orders of magnitude or lower, than those determined for the two $^{109}$Ag-E treatments.

## 2.4. Discussion

### *2.4.1. Ag mass balance of soils*

The $^{109}$Ag-E concentrations determined for soils (Figure 2.5) that were sampled directly after treatment with $^{109}$Ag NPs and $^{109}$Ag $NO_3$ (on day 0) reveal similar and consistent results with $^{109}$Ag-E recoveries of between 94% and 97%. This indicates that the initial dosing was carried out accurately and in a consistent manner. This conclusion is further supported by the observation that all $^{109}$Ag-E treated soils show similar patterns of decreasing or constant $^{109}$Ag-E concentrations with time. Notably, both the $^{109}$Ag NPs and $^{109}AgNO_3$ treatment reveal decreasing $^{109}$Ag-E contents from day 0 to GS 4, whereby a faster loss of $^{109}$Ag-E is recorded for the latter at GS 2. Furthermore, at GSs 4 to 8, all soils show similar and nearly constant $^{109}$Ag-E concentrations with recoveries of 70 to 72%. As such, the soils record a significant reduction ($p= 0.04$) in $^{109}$Ag-E concentrations of about 25%, which might be caused by (i) plant uptake, (ii) Ag sequestration by remaining soil material or (iii) adsorption to the pot walls and wicks.

An investigation of the mass balance for the Ag present in soils showed that these lost approximately 18 µg of $^{109}$Ag-E from the initial dosing to GS 8. In contrast, the plants took up a maximum of 37 ng of $^{109}$Ag-E, which is equivalent to less than 1% of the original soil budget. This demonstrates that the uptake of Ag by the wheat plants cannot be responsible for reduced recovery for either of the $^{109}$Ag-E treatments. Furthermore, previous work has shown that after partial soil digestions that are carried out without HF, the remaining silicate materials can adsorb about 10 to 30% of the Ag released from added Ag NPs (Kvitek et al.,

2011). To avoid this pitfall, the current study employed an HF step to achieve full digestions of the soil samples. As such, the decreasing soil $^{109}$Ag-E contents with time cannot be attributed to sorption onto soil material remaining after mineralisation.

Considering the above, it is hence most likely that the loss of $^{109}$Ag-E from the soils during the exposure is caused by $^{109}$Ag adsorption to the walls of the polypropylene pots and the polyamide wicks used for plant watering. This conclusion is in accordance with previous work, which has shown that dissolved Ag can adsorb readily to plastics, including polycarbonate and polypropylene, which in turn may lead to Ag reduction in the exposure medium (Sekine et al., 2015). In particular, it was shown that Ag solution concentrations in polypropylene containers over a 72 h test period were reduced by 10% (Sekine et al., 2015). In the current study, approximately 25% of the $^{109}$Ag-E that was initially added to the soils was lost to adsorption, probably as dissolved $^{109}$Ag-E in the pore waters adsorbed to the polypropylene pot walls and polyamide wicks. The relatively constant $^{109}$Ag-E concentrations at GSs 4 to 8 indicate that the surfaces of the pot walls and wicks were most likely saturated with adsorbed $^{109}$Ag-E by GS 4.

### *2.4.2. Total Ag & truly dissolved Ag in soil pore waters*

In an attempt to unravel the bioavailability of Ag NP and $Ag^+$ ions in soils, the total and truly dissolved $^{109}$Ag-E concentrations of pore waters were studied. Overall, the pore waters of both treatments featured low total and truly dissolved $^{109}$Ag-E concentrations, whereby the former ranged from about 0.2 to 2 µg $L^{-1}$. This attests to low overall solubility of $^{109}$Ag-E in the soil solutions, regardless whether added as $^{109}$Ag NPs or $^{109}AgNO_3$. In detail, at any one time, less than 0.15% of the $^{109}$Ag-E present in the soil-pore water system was present in the latter. Limited solubility of Ag in soil solutions was previously reported by Waalewijn-Kool et al. (2014), who found that about 1.5% of the Ag added to soils as Ag NPs and $AgNO_3$ was present in pore waters in a 28-day exposure study that was conducted at much higher Ag levels of 30 to 200 mg $kg^{-1}$.

Notably, both the total and truly dissolved $^{109}$Ag-E pore water concentrations were constant, within error, with time from GS 4 to 8 (Figure 2.6). This

observation is confirmed by a plot of $^{109}$Ag-E pore water concentrations versus sampling days, which revealed no temporal changes in $^{109}$Ag-E levels within uncertainty (Figure 2.7). As such, the pore waters of both $^{109}$Ag treatments appear to have (near-) steady-state $^{109}$Ag-E concentrations, which record the equilibrium between dissolved $^{109}$Ag and $^{109}$Ag that is in the solid-state, which might reflect undissolved $^{109}$Ag NPs, precipitated $^{109}$Ag species and/or $^{109}$Ag that is adsorbed to the soils and container walls.

It is well known that Ag undergoes complex physicochemical interactions and transformations in soils. The oxidative dissolution of Ag NPs to $Ag^+$ ions has been studied by in-depth and is affected by pH, the presence of natural organic matter and cations ($Ca^{2+}$, $Mg^{2+}$, $Na^+$ and $K^+$) (Bundschuh et al., 2018; Mitrano et al., 2014; Metreveli et al., 2016; Rayment and Higginson 1992). Furthermore, numerous reactions promote the loss of dissolved Ag from soil solutions or readily soluble Ag NPs from soils. One common reaction is the formation of highly insoluble AgCl precipitates. In addition, both $Ag^+$ ions and Ag NPs can react with the sulfhydryl groups of organic matter (Qing et al., 2018), to form either $Ag_2S$ NPs or $Ag_2S$, both of which are highly insoluble, inert and hence have very limited bioavailability (Pradas del Real et al., 2017). It also possible that dissolved $Ag^+$ ions were bound strongly to reactive surfaces of organic matter, soil particles and the container walls (Coutris et al., 2012; Diez-Ortiz et al., 2015A; 2015B). Finally, dissolved $Ag^+$ ions and Ag NPs may have formed aggregates and agglomerates of a larger size (Jiang et al., 2009; Tourinho et al., 2012).

In this context, it is significant that the soils treated with $^{109}$Ag NPs have total and truly dissolved $^{109}$Ag-E pore water concentrations, which both exceed those of the $^{109}AgNO_3$ treatments by about a factor of x3, and this difference is statistically significant with $p \leq 0.02$. Most likely, this reflects that the $^{109}$Ag-E from the $^{109}AgNO_3$ treatments reacted to a larger extent to form highly insoluble Ag species, such as AgCl and $Ag_2S$ or by sorption to organic matter. In detail, this may reflect that the added $^{109}AgNO_3$ first dissolved rapidly but the $Ag^+$ ions were subsequently removed from solution nearly quantitatively by the formation of highly insoluble Ag species. In contrast, the $^{109}$Ag NPs reacted more slowly to form highly insoluble $^{109}$Ag species, such that remaining NPs were able to

maintain higher concentrations of dissolved $^{109}$Ag in the soil solutions.

Two further observations are of interest about the pore waters. First, the measured $^{109}$Ag-E pore water concentrations show significant variability, even for the three replicate samples that were taken for each treatment at each GS (Table 2A and 3A, Appendix A). Whilst it is possible that this variability is an artefact of our sampling and analytical techniques, it is more likely a characteristic of the soil – pore water systems of the experiment. In particular, the variability may reflect that the $^{109}$Ag-E pore water concentrations record the spatially heterogeneous character of the soil – pore water equilibrium that is established for Ag within each pot. It is significant in this context that only about 35 g of soil were sampled from each pot (with a total of 700 g of soil) for the extraction of pore water samples. Secondly, both $^{109}$Ag treatments produced statistically identical concentration ratios of truly dissolved to total $^{109}$Ag-E for the pore waters, albeit at significantly different $^{109}$Ag-E levels (Table 5A, Appendix A). This observation suggests that speciation of both the total and the truly dissolved $^{109}$Ag-E is essentially identical for both treatments. To confirm this observation, further studies of Ag speciation in soil pore waters is desirable.

### *2.4.3. Ag uptake by & translocation in wheat*

The discussion on the uptake and translocation of $^{109}$Ag-E is focused on GSs 4, 6 and 8 as these GSs best characterise $^{109}$Ag-E transfer for the fully, or nearly fully, developed wheat plant. In the current study, the roots presented the highest $^{109}$Ag-E concentrations of the plant tissues and accrued the majority of the plant – accumulated $^{109}$Ag-E, which corresponds to published findings in the plant literature (Wen et al., 2016; Wang et al., 2012; Yin et al., 2011; Stegemeier et al., 2015A; Ma et al., 2010; Geisler-Lee et al., 2014; Lowry et al., 2012; Vannini et al., 2014; Yang et al., 2018). Notably, $^{109}$Ag NP consistently had higher $^{109}$Ag-E concentrations for both the roots and the total plants when compared to the $^{109}AgNO_3$ treatments (Figure 2.8, Table 4A, Appendix A).

Interestingly, the dissolved $^{109}$Ag-E concentrations of pore waters associated with the $^{109}$Ag NP treatment were also higher compared to the $^{109}AgNO_3$ exposure (Figure 2.6, Table 2A and 3A, Appendix A), whilst the $^{109}$Ag-E soil contents of both treatments were essentially identical (Figure 2.5, Table 1A, Appendix A). As

such, it could be argued that the higher $^{109}$Ag-E concentrations of pore waters from the $^{109}$Ag NP treatment enabled increased $^{109}$Ag-E uptake by the roots, which then produced significantly higher $^{109}$Ag-E concentrations for the whole plants. To further evaluate the bioaccumulation of $^{109}$Ag-E by the wheat, an assessment was carried out for the $^{109}$Ag-E concentrations of the roots and total plants relative to the total and truly dissolved $^{109}$Ag-E contents of the pore waters (Table 2.6). Notably, all four ratios are statistically identical for the two treatments, with T-test p-values of between 0.15 and 0.73. These observations provide strong evidence that the $^{109}$Ag-E uptake by the wheat was primarily governed by the concentration of the total and truly dissolved $^{109}$Ag-E in the pore waters. In addition, the findings support the previous conclusion that the speciation of dissolved pore water $^{109}$Ag-E was similar for both $^{109}$Ag-E treatments.

To put these findings into perspective, it is of interest to compare the measured bioaccumulation ratios of $[^{109}Ag\text{-}E]_{Root}/[^{109}Ag\text{-}E]_{TD\text{-}Pw}$ = 2.2 and $[^{109}Ag\text{-}E]_{Plant}/[^{109}Ag\text{-}E]_{TD\text{-}Pw}$ = 0.77 with results for other elements (Table 2.6). For wheat grown on natural soils, the $[Cd]_{Root}/[Cd]_{TD\text{-}Pw}$ and $[Cd]_{Plant}/[Cd]_{TD\text{-}Pw}$ ratios were both at about 15 to 20 and thus exceeded our results for Ag by a factor of about x10 to x20 (Imseng et al., 2018). Even higher root-to-pore water and plant-to-pore water bioaccumulation factors were observed for As in rice, with results that exceeded the Ag data by factors of between x30 to x1500 (Somenahally et al., 2011). In comparison to cadmium (Cd) and arsenic (As), the accumulation of Ag in wheat from the soil pore waters is therefore comparatively inefficient.

*Table 2.6.* Mean bioaccumulation ratios for $^{109}$Ag-E determined for samples from GSs 4, 6 and 8 (n = 2).

| Bioaccumulation ratios | Treatment | | |
|---|---|---|---|
| | $^{109}$Ag NPs | $^{109}AgNO_3$ | p-value |
| $[^{109}Ag\text{-}E]_{Root}/[^{109}Ag\text{-}E]_{Total\ PW}$ | 2.6±1.1 | 2.2±1.0 | 0.7 |
| $[^{109}Ag\text{-}E]_{Root}/[^{109}Ag\text{-}E]_{TrD\ PW}$ | 39.9±9.0 | 25.9±6.9 | 0.2 |
| $[^{109}Ag\text{-}E]_{Plant}/[^{109}Ag\text{-}E]_{Total\ PW}$ | 1.3±0.8 | 0.8±0.4 | 0.5 |
| $[^{109}Ag\text{-}E]_{Plant}/[^{109}Ag\text{-}E]_{TrD\ PW}$ | 18.9±8.8 | 10.2±4.1 | 0.3 |

The quoted uncertainties represent 1 standard deviation 'Total PW' stands for total $^{109}$Ag-E in pore waters. 'TrD PW' stands for truly dissolved $^{109}$Ag-E in pore waters.

Following uptake from the soil solutions, the internalised $^{109}$Ag-E in the roots was translocated to the shoots and grains. To assess this internal transport, the translocation factors $[^{109}Ag\text{-}E]_{Shoot}/[^{109}Ag\text{-}E]_{Root}$, $[^{109}Ag\text{-}E]_{Grain}/[^{109}Ag\text{-}E]_{Root}$ and $[^{109}Ag\text{-}E]_{Grain}/[^{109}Ag\text{-}E]_{Shoot}$ were assessed for both $^{109}$Ag-E treatments (Table 2.7). Notably, the results reveal that the two $^{109}$Ag-E treatments produced statistically identical ratios, with p-values of between 0.22 and 0.55. This suggests that the two distinct $^{109}$Ag treatments are associated with essentially identical translocation within the wheat plants. These findings also indicate that there is no difference in Ag speciation within the plants for the different $^{109}$Ag-E treatments, an interpretation that is in accord with the previous inference of similar $^{109}$Ag-E speciation within the pore waters. To confirm this finding, further investigations of Ag speciation in both soil solutions and plant tissues is needed.

*Table 2.7.* Mean translocation ratios for $^{109}$Ag-E determined for samples from GSs 4, 6 and 8 (n = 2).

| Translocation ratios | Treatment | | |
|---|---|---|---|
| | $^{109}$Ag NPs | $^{109}AgNO_3$ | p-value |
| $[^{109}Ag\text{-}E]_{Shoot}/[^{109}Ag\text{-}E]_{Root}$ | 0.09±0.01 | 0.12±0.01 | 0.3 |
| $[^{109}Ag\text{-}E]_{Ab\text{-}Gr\ plant}/[^{109}Ag\text{-}E]_{Root}$ | 0.08±0.01 | 0.12±0.01 | 0.2 |
| $[^{109}Ag\text{-}E]_{Grain}/[^{109}Ag\text{-}E]_{Shoot}$ | 0.50±0.02 | 0.65±0.17 | 0.6 |
| $[^{109}Ag\text{-}E]_{Grain}/[^{109}Ag\text{-}E]_{Root}$ | 0.05±0.01 | 0.08±0.03 | 0.4 |

The quoted uncertainties represent 1 standard deviation 'Ab-G' stands for the above-ground plant tissues.

Also of interest is the observation that the observed $[^{109}Ag\text{-}E]_{Shoot}/[^{109}Ag\text{-}E]_{Root}$ ratios are relatively small, with mean values of about 0.1 for both $^{109}$Ag-E treatments (Table 2.7). This result is comparable to data from a hydroponic study, which determined an average $[Ag\text{-}E]_{Shoot}/[Ag\text{-}E]_{Root}$ ratio of 0.04 for wheat exposed to Ag NP concentrations of 1 and 10 mg $L^{-1}$ (Vannini et al., 2014). Furthermore, low Ag translocation factors of less than 1 were also reported for Alfalfa (Stegemeier et al., 2015) and common grass (Yin et al., 2011). To put these data for Ag into perspective, previous studies of wheat plants observed a root-to-shoot translocation factor of 20 for the essential element potassium (K), whilst a value of 43 was observed for Cd, which is non-essential but chemically similar to the essential element zinc (Zn) (Wang et al., 2020; Hart et al., 1998). In comparison to these and other elements, the root-to-shoot translocation of Ag

within wheat plants is clearly much more inefficient. Notably, the grains feature the lowest $^{109}$Ag-E concentrations of the wheat plants, as a consequence of limited shoot-to-grain translocation, which is documented by statistically identical [$^{109}$Ag-E]$_{Grain}$/[$^{109}$Ag-E]$_{Shoot}$ ratios of about 0.55 for both $^{109}$Ag-E treatments.

*2.4.4. Implications*

In terms of $^{109}$Ag-E transfer to the edible part of wheat, a key observation is that the grains had the lowest $^{109}$Ag-E levels of the wheat plants, with concentrations of about 0.05 to 0.15 µg kg$^{-1}$ for both $^{109}$Ag-E treatments. These low concentrations are a consequence of multiple factors. First, they reflect the low solubility of the $^{109}$Ag-E added to the soils in the soil solutions, as the $^{109}$Ag-E uptake by wheat was shown to scale with the $^{109}$Ag-E concentrations of the soil pore waters. This is demonstrated by the statistically similar [$^{109}$Ag-E]$_{Plant}$/[$^{109}$Ag-E]$_{Pw}$ and [$^{109}$Ag-E]$_{Plant}$/[$^{109}$Ag-E]$_{TrD\ Pw}$ ratios for the two $^{109}$Ag treatments (Table 2.6). Second, the uptake of Ag from soil pore waters by the wheat roots was found to be relatively inefficient compared to observations made for other elements in wheat and other plants (Imseng et al., 2018). Third, the translocation of Ag within the wheat plants, from the roots-to-shoots and from shoots-to-grains, was also found to be relatively inefficient, in comparison to results obtained for other elements in wheat (Liu et al., 2009; Guo et al., 2018; Wiggenhauser et al., 2016; Imseng et al., 2018). As such, the low $^{109}$Ag-E concentrations observed for wheat grains in this study are a consequence of both poor Ag uptake by and limited Ag translocation in the wheat plants.

From a regulatory perspective, Ag is not currently officially approved as a direct additive to food nor is it listed as a banned substance by EU or US regulatory bodies. Instead, Ag has been classified as a non-essential substance that has no known physiological benefits (NCCIH, 2017). Excessive intake of Ag can have toxic effects in humans and can cause argyria (blue skin condition), renal, pulmonary and gastrointestinal irritation (NCCIH, 2017). For this reason, the European Food Safety Authority (EFSA) suggested a guideline of 50 µg Ag kg$^{-1}$ of food (EFSA, 2011). As such, the $^{109}$Ag-E concentrations recorded for the grains in this study are more than 300 times below the EFSA guideline value. Notably, this result was obtained even though the wheat plants were exposed to

Ag levels which exceeded the PECs by a factor of x3 or more. This suggests that the projected increase in Ag levels in agricultural soils from sewage sludge that contains Ag NPs or Ag derived from the materials is unlikely to lead to Ag levels in grains which are problematic for human consumption.

## 2.5. Conclusion

The current study was the first to investigate the uptake and translocation of Ag by wheat from soils treated with Ag NPs and $AgNO_3$ at an environmentally relevant concentration of 72 µg $kg^{-1}$ and which was carried out over the full life cycle of wheat. This was enabled by carrying out the exposure with Ag NPs and $AgNO_3$ that were prepared from highly enriched $^{109}$Ag-E. The following conclusions can be drawn from this study:

- The $^{109}$Ag-E concentrations of the soils dropped by about 25% during the exposure, most likely due to adsorption of Ag to the surface of the polypropylene pots and polyamide wicks.
- The overall solubility of the $^{109}$Ag-E added to the soils in the soil pore waters was very low, as documented by pore water $^{109}$Ag-E concentrations that were typically less than 0.1% of the soil $^{109}$Ag-E levels. The $^{109}AgNO_3$ soil treatments were associated with significantly lower pore water $^{109}$Ag-E concentrations compared to the $^{109}$Ag NP exposures, most likely due to the enhanced formation of insoluble Ag species.
- The wheat roots and total wheat plants from the exposures to $^{109}$Ag NPs exhibited higher $^{109}$Ag concentrations compared to those produced by the $^{109}AgNO_3$ treatments. However, both treatments were associated with statistically identical bioaccumulation ratios of $[^{109}Ag\text{-}E]_{Root}/[^{109}Ag\text{-}E]_{TD\text{-}Pw}$ and $[^{109}Ag\text{-}E]_{Plant}/[^{109}Ag\text{-}E]_{TD\text{-}Pw}$. This provides strong evidence that the $^{109}$Ag-E uptake by wheat was primarily governed by the concentration of truly dissolved $^{109}$Ag-E in the pore waters. In addition, it indicates that the speciation of pore water $^{109}$Ag-E was similar for both $^{109}$Ag-E treatments.
- Similarly, both $^{109}$Ag-E treatments were associated with similar translocation of Ag within the plants, as documented by statistically identical [$^{109}$Ag-

$E]_{Shoot}/[^{109}Ag\text{-}E]_{Root}$ and $[^{109}Ag\text{-}E]_{Grain}/[^{109}Ag\text{-}E]_{Shoot}$ ratios. This suggests that Ag speciation within wheat was also identical for both treatments.

- Overall, the uptake of Ag by the roots from pore water and the translocation of Ag within the plants from roots-to-shoots and grains was found to be relatively inefficient, compared to observations made for different elements for wheat and other plants.
- The wheat grains had the lowest $^{109}Ag\text{-}E$ concentrations of the plant tissues and these were well below the maximum guideline concentrations set by EFSA. Notably, these low levels were obtained in exposures that applied Ag at soil levels that exceeded the PECs by a factor of x3 or more. This indicates the application of sewage sludge, which contains Ag NPs (or Ag derived from these), to agricultural soils is unlikely to generate Ag levels in grains that are problematic for human consumption.

In addition to the work summarised in this chapter, it is important to study and understand whether the biological parameters of wheat and its development were affected in this environmentally relevant exposure. The next chapter delves into the biological influence of the $^{109}Ag\text{-}E$ that accumulated in the wheat plants and aims to explain how these treatments may affect plant growth, development and health.

# Chapter 3: Stable isotope tracing of silver nanoparticles in a full wheat life cycle exposure

## Part 2: Influence on the biology

### 3.1. Introduction

In Chapter 2, the uptake and accumulation of silver (Ag) by wheat from soils dosed with Ag nanoparticles (Ag NPs) or $AgNO_3$ at environmentally relevant concentrations were investigated and quantified. This work showed that uptake of Ag by wheat plants was governed primarily by the Ag concentration of the soil pore waters. Furthermore, once taken up by the roots, the Ag was translocated to the shoots and edible grains of the wheat plants, albeit with limited efficiency.

Previous investigations have shown that the uptake and accumulation of Ag can cause morphological changes to plants, such as reduction of seed germination and leaf area, as well as lower root and shoot growth (Stampoulis et al., 2019; Dimkpa et al., 2013; Nair and Chung 2014; Kaveh et al., 2013; Jiang et al., 2014). Furthermore, discoloured root caps and columella, referred to as 'brown tips' (Dietz et al., 2011), were identified in exposures of plants to Ag NPs and linked to the aggregation of Ag NPs or Ag complexes at the root tips (Hawthorne et al., 2012). At a cellular level, Ag from Ag NPs were found to aggregate in the plasmodesmata, which can cause wall leakage, block intercellular communication and affect nutrient transport (Geisler-Lee et al., 2012). Uptake of Ag from hydroponic solutions by plants at Ag NP exposure concentrations of 10 to 1000 mg $L^{-1}$ has also been linked to phytotoxicity based on changes observed for the germination and mitotic index, metaphase, chromosomes, cell walls, transpiration rate and biomass (Babu et al., 2008; Kumari et al., 2009; Barrena et al., 2009; Stampoulis et al., 2009). Furthermore, most published studies agree that exposure of plants to Ag NPs can significantly enhance the production of reactive oxygen species (ROS). Notably, ROS production is a key stress-induced morphogenic response of plants, which can affect plant growth and cellular viability (Oukarroum et al., 2013). However, exposure of plants to Ag NPs has also been associated with beneficial effects. This includes improvements in seed

yield and vigour index of seedlings as well as increases in fresh weight, root and shoot length, photosynthetic efficiency and the chlorophyll content of leaves (Sah et al., 2011; Sharma et al., 2012). An observed increase in maize biomass exposed to 100 mg $kg^{-1}$ of Ag NPs in soils was linked to changes of the bacterial community in the rhizosphere (Sillen et al., 2015).

Understanding the biological changes induced in plants by the accumulation of Ag from Ag NPs can improve our understanding of how the yields of important crops, such as wheat, may be impacted by the dispersal of Ag NPs in the environment. Several toxicity studies have addressed this goal but due to analytical limitations, these applied Ag NP exposure concentrations, which exceeded the predicted environmental concentrations (PECs) by at least a factor of x10 to x100, with many conducted at x1000 to x10,000 PEC levels (Gubbins et al., 2011; Lee et al., 2012; Geisler-Lee et al., 2014). Furthermore, most published investigations were carried out in hydroponic media rather than soils and only for short periods (seven days, 21 days and 28 days) rather than over full plant life cycles. These gaps in knowledge are addressed by the current study, which complements Chapter 2, as it investigates how the exposure of wheat plants to low, environmentally relevant levels of Ag NPs and ionic $Ag^{+}$ can affect the biological parameters of wheat plants, including biomass and rate of growth and development.

To enable tracing of the Ag in the plants at low concentrations, the exposures were carried out with Ag NPs and $AgNO_3$ that were prepared from and hence labelled with highly enriched stable $^{109}Ag$ (denoted as $^{109}Ag$-E in the following). The reagents were employed to produce $^{109}Ag$-E concentrations of 72 µg $kg^{-1}$ in the soils, which were then used to grow wheat to maturity. This chapter explores whether any distinct biological effects were induced by the presence of Ag NPs and $AgNO_3$ in the soils as a consequence of Ag uptake and accumulation by the wheat plants.

## 3.2. Experimental design & methodology

The preparation of the labelled $^{109}Ag$ NPs and $^{109}AgNO_3$, the exposure conditions, and sample collection procedures were previously described in detail in Chapter 2. Only a brief summary is thus given here. In addition, methods and issues that are particularly relevant to this Chapter are highlighted.

### *3.2.1. Exposure conditions*

Winter wheat (*Triticum aestivum L.*) was grown to maturity under controlled greenhouse conditions in pots with Lufa 2.2 soil that was subjected to four different treatments. Treatments (i) and (ii) encompassed soils treated with citrate-capped $^{109}Ag$ NPs and $^{109}AgNO_3$, respectively, to produce soils with $^{109}Ag$-E concentrations of 72 µg $kg^{-1}$. Treatments (iii) and (iv) were a blank control and a 'citrate control', whereby the latter introduced citrate ions to the soils at the same level as the $^{109}Ag$ NP treatment. Samples were collected at eight different biological growth stages (GSs). All four treatments encompassed 16 replicates for GSs 1 and 2, for a total of 128 individual samples while for GSs 3 to 8, there were five replicates each for the $^{109}Ag$ NP and $^{109}AgNO_3$, treatments (60 pots in total) and three replicates for the blank and citrate controls (36 pots in total).

Notably, the automated lighting and temperature control system experienced a fault for seven days during the exposure, whilst the remaining plants were at GS 7 affecting all treatments in GS 7 and GS 8. During the fault, the available lighting was at 48 µE/$m^2$/s (instead of the 350 ± 50 µE/$m^2$/s set value), the temperature was at 16°C (rather than the 20°C set value) with a reduced day/night regime of 14 h light/10 h dark.

### *3.2.2. Sample collection & measurements*

To determine the plant growth rates, the day of sampling was recorded at each different GS. The germination rate was calculated by recording the successfully germinated seeds. The collected wheat samples were first photographed (Canon EOS 50D DSLR) and then split into the representative plant tissues, encompassing seeds, roots, shoots and grains. The longest leaf and grain head of each plant sample were measured by analysing plant images with ImageJ

version 1.50. In summary, for each image, a new scale was set by drawing a line across a known scale. Next, by using the line drawing tool, a series of lines were drawn along the longest leaf/grain head which were subsequently summed to give a total leaf/grain head length.

All plant tissue samples were subsequently dried for analysis. Roots were collected from all plants and for all GSs but the washing of root samples to remove soil particles led to biomass loss of the fine root hairs that could not be adequately quantified. As such, the data discussion places only limited focus on the root mass data. The dry and wet biomass of plant tissues were recorded using a Sartorius Toploader 140 MP8 balance. The dry biomass of plant tissues from each treatment was summed to determine both the total dry biomass (seed, roots, shoots and grain) and the total mass of the above-ground tissues (shoots and grain). The same summation was performed for the wet biomass. These totals were then used to determine the dry biomass yield (DBY) and the wet biomass yield (WBY), which express the relative difference in the mass of a given sample (in %) when compared to the average biomass determined for the plants of the blank control treatment for the same GS:

$$DBY\ or\ WBY(\%) = \left[\frac{Dry\ or\ wet\ biomass\ of\ \ plant}{Average\ dry\ or\ wet\ biomass\ of\ blank\ control\ plant}\right] \times\ 100$$

The total dry and wet biomass data were also used to calculate the plant osmotic balance, which records the difference between wet and dry biomass (in %) relative to the total wet biomass:

$$Osmotic\ balance(\%) = \left[\frac{Total\ wet\ biomass - Total\ dry\ biomass}{Total\ wet\ biomass}\right] \times\ 100$$

All statistical analyses were performed using Minitab 18. For analyses of differences between treatments, one-way ANOVA tests with a significance level of $p < 0.05$ were used. First, the biological parameters between the control and citrate were compared. After no difference was established between the controls, the control and citrate data were compared to the Ag treatments. All errors have been reported as standard deviations.

## 3.3. Results

In this study, eleven biological parameters are discussed including the germination rate, DBYs, WBYs, plant osmotic balance, shoot and grain dry biomass, shoot and grain wet biomass, shoot and grain lengths, as well as the plant growth rate. The results obtained are displayed in the following.

### *3.3.1. Germination rate*

The germination rates recorded for the wheat plants were 99% for the $^{109}AgNO_3$ and citrate control treatments, 98% for the $^{109}Ag$ NP treatment, and 96% for the blank control. A statistical analysis of these germination rates revealed that they were identical for all four treatments, with $p = 0.12$.

### *3.3.2. Dry & wet plant biomass & plant osmotic balance*

The DBYs and WBYs were determined for both the total dry and wet plant biomass as well as the dry and wet biomass of the aboveground plant tissues. The total DBY and WBY data for the treatments showed no trends over the eight GSs and with only a single exception, all results obtained for the different treatments were identical with $p \geq 0.07$ (Figure 3.1A and C, Table 1B, Appendix B). The only exception was identified for GS 5, where the DBYs determined for the $^{109}AgNO_3$ and the blank control treatment were statistically different with $p = 0.04$. The DBY and WBY data for the aboveground plant tissues (Figure 3.1B and D), which excludes the roots, also showed constant and steady values for the different treatments and GSs and all results (including those for GS 5) were statistically identical with $p \geq 0.06$ (Figure 3.1B, Table 2B, Appendix B).

For all four treatments, the shoot dry biomass increased from less than 0.2 g for GS 1 to 3 to relatively constant values of between 3 – 4 g for GS 4 and beyond (Figure 3.2A, Table 3B, Appendix B). Similar to the aboveground DBY, the shoot tissue dry biomass was statistically identical for all four treatments, with $p \geq 0.07$.

Grains were only present on the plants from GS 6 onwards, with the grain dry biomass increasing continually from about 0.3 g at GS 6 to approximately 0.9 g at GS 8 (Figure 3.3A, Table 4B, Appendix B). For GSs 6 and 7, the grain dry biomass was statistically identical for all four treatments ($p \geq 0.21$). At GS 8,

however, the grain dry biomass for the citrate control treatment was significantly larger (with $p \leq 0.001$) than the grain biomasses obtained from the two $^{109}Ag$ treatments.

The plant osmotic balance was found to be stable throughout the experiment with an average of about 82% for all treatments (Figure 3.4). The data showed no trends over time or between the treatments with $p \geq 0.12$. Notably, the plants exhibited essentially identical osmotic balance results of approximately 82% for GSs 1 to 3 (with $p \geq 0.44$). Following this, the plants showed larger deviations between individual samples, which is reflected in lower p-values of $p \geq 0.12$ for GSs 4 to 8.

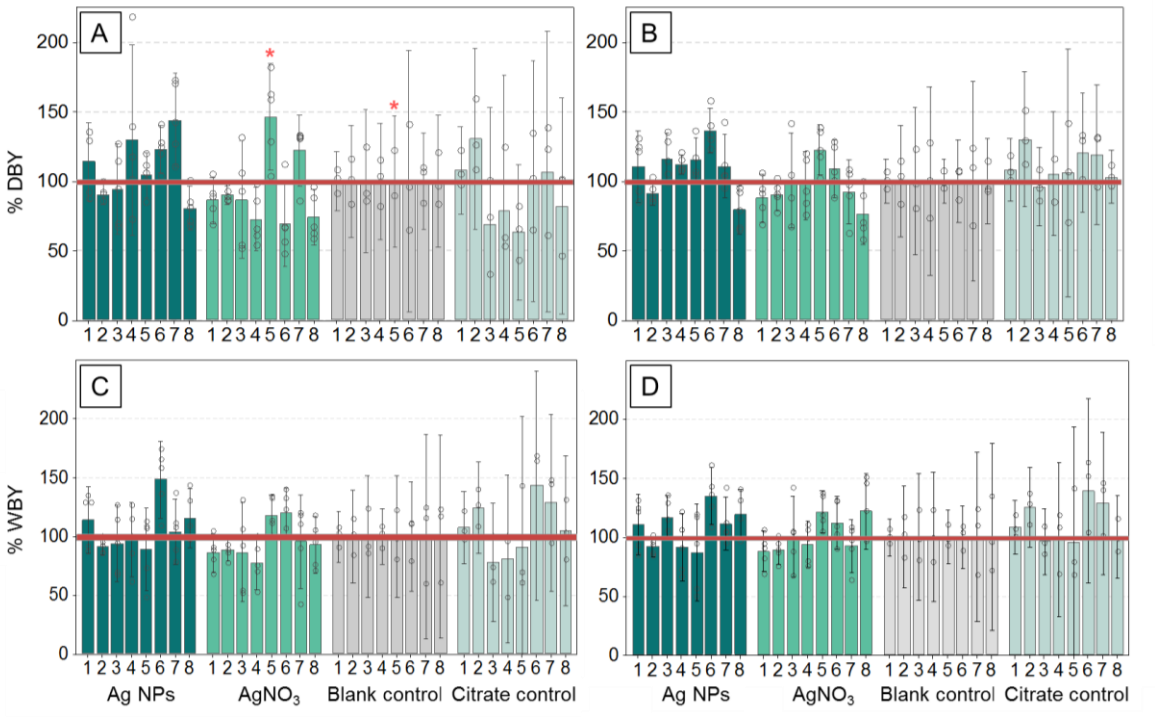



*Figure 3.1.* Total (A), aboveground (B) dry biomass yield (DBY) and total (C) and aboveground (D) wet biomass yield for wheat plants sampled at GS 1 to GS 8. The individual points represent the results for individual samples, whilst the red line marks the 100% BY value defined by the average blank control result for a given GS (n = 5 for the Ag treatments; n = 3 for the controls). The error bars denote 1 standard deviation for each dataset. The only significant difference between the treatments was found at GS 5 for the $^{109}AgNO_3$ and the blank control treatments (*p = 0.04).

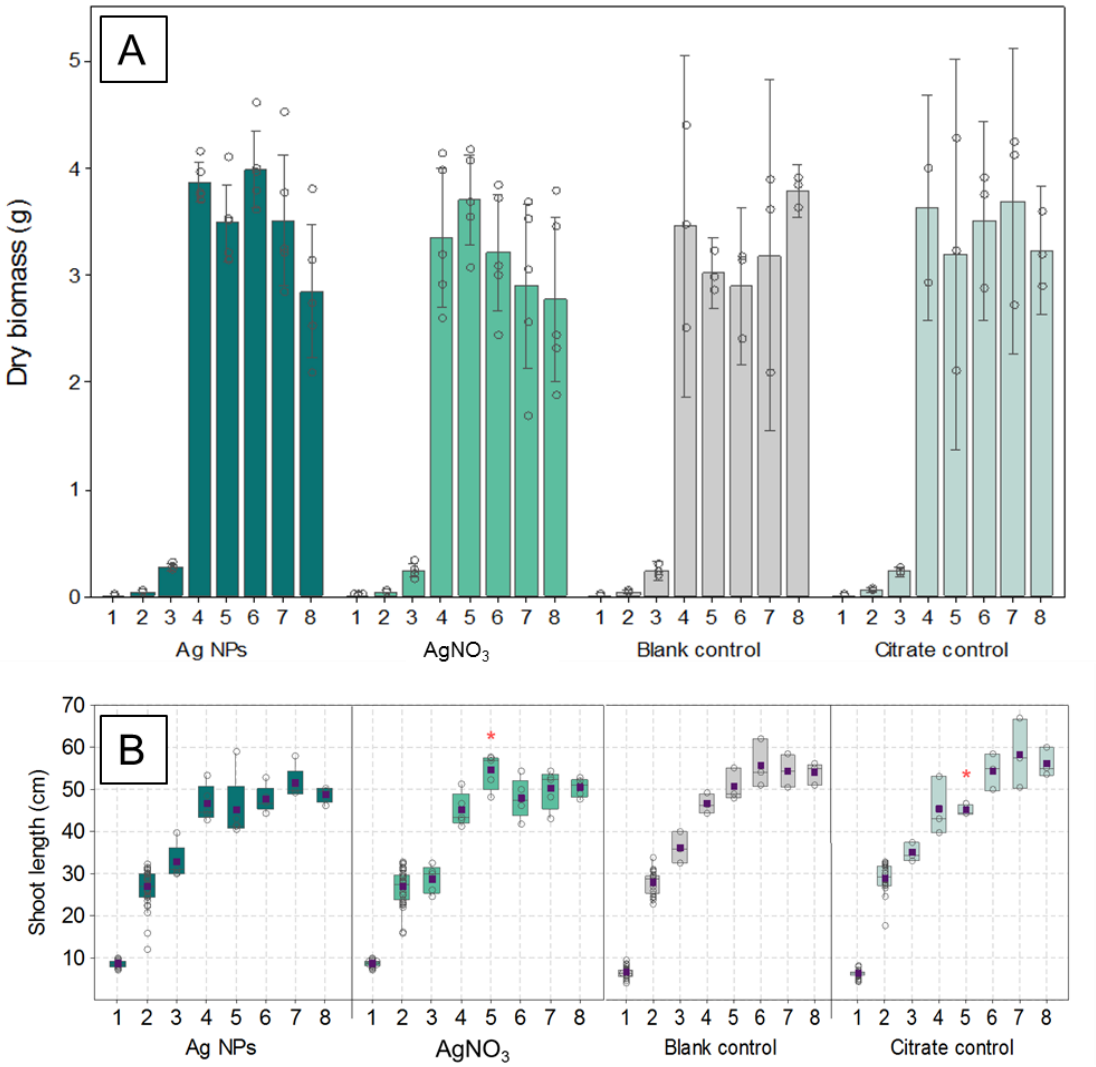



*Figure 3.2.* Shoot tissue dry biomass (g) (A) and shoot length (cm) (B) for the different treatments at GSs 1 to 8 (n = 5 for the Ag treatments; n = 3 for the controls). The individual data points represent the results for individual plant samples, whilst the error bars denote 1 standard deviation for each dataset. The square boxes indicate the mean values in panel B. In panel (A), there are no significant differences between the samples from different treatments ($p > 0.07$). In panel (B), the box plots show the length measured for the longest shoot leaf and indicate a single statistical increase at GS 5 for the $^{109}AgNO_3$ treatments when compared to the citrate control (*$p = 0.02$).

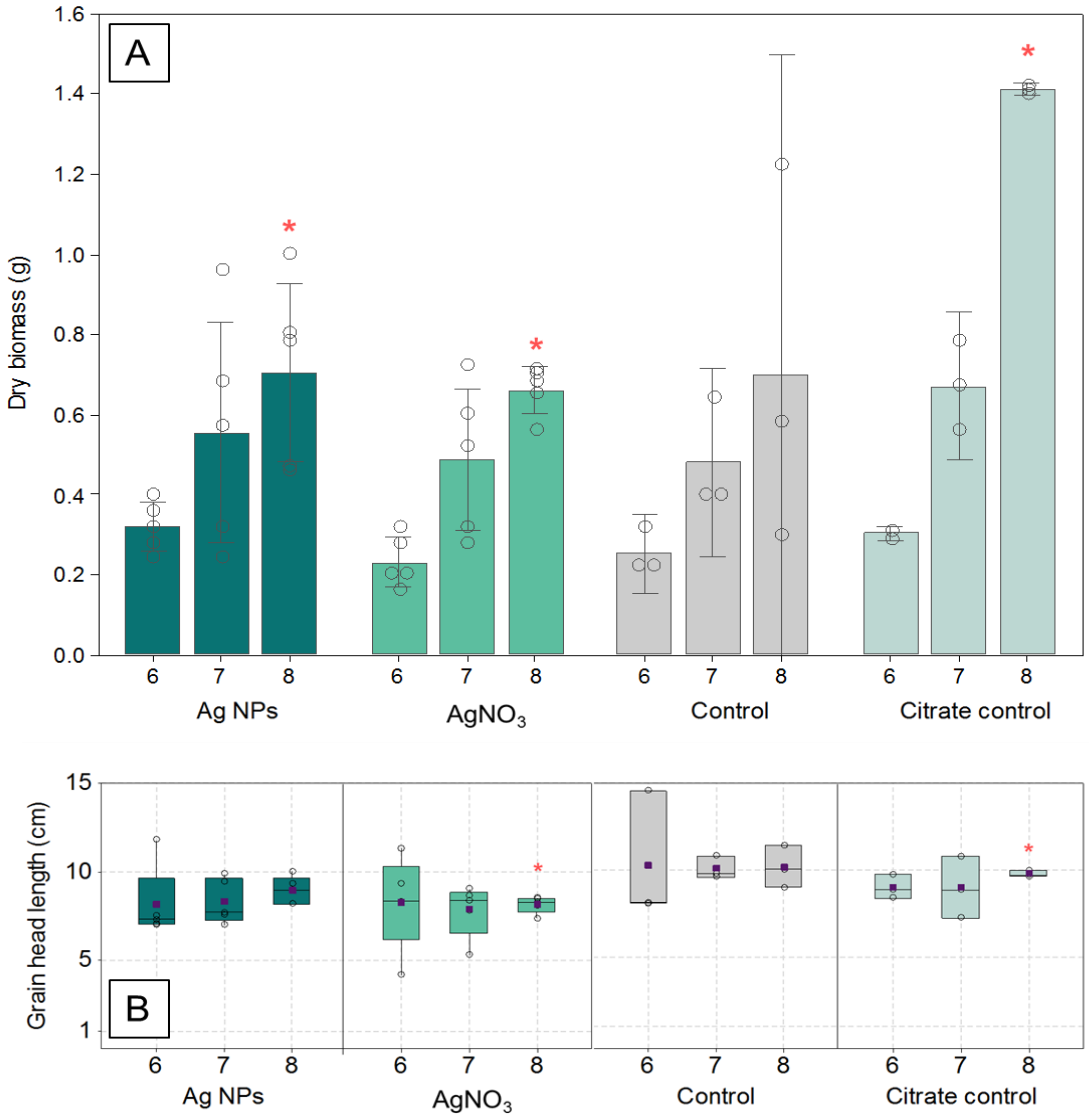



*Figure 3.3.* Grain dry biomass (g) (A) and grain head length (cm) (B) for the four treatments at GSs 6 to 8 (n = 5 for the Ag treatments; n = 3 for the controls). The individual data points represent the results for individual samples, whilst the error bars denote 1 standard deviation for each dataset. The purple square boxes indicate the mean values in panel B. In panel (A) there are significant differences between Ag NP and $AgNO_3$ treatments versus the citrate control treatment at GS 8 (*p = 0.001). In panel (B) the single significant difference between treatments is also at GS 8, between the $AgNO_3$ and the citrate control treatment (*p = 0.01).

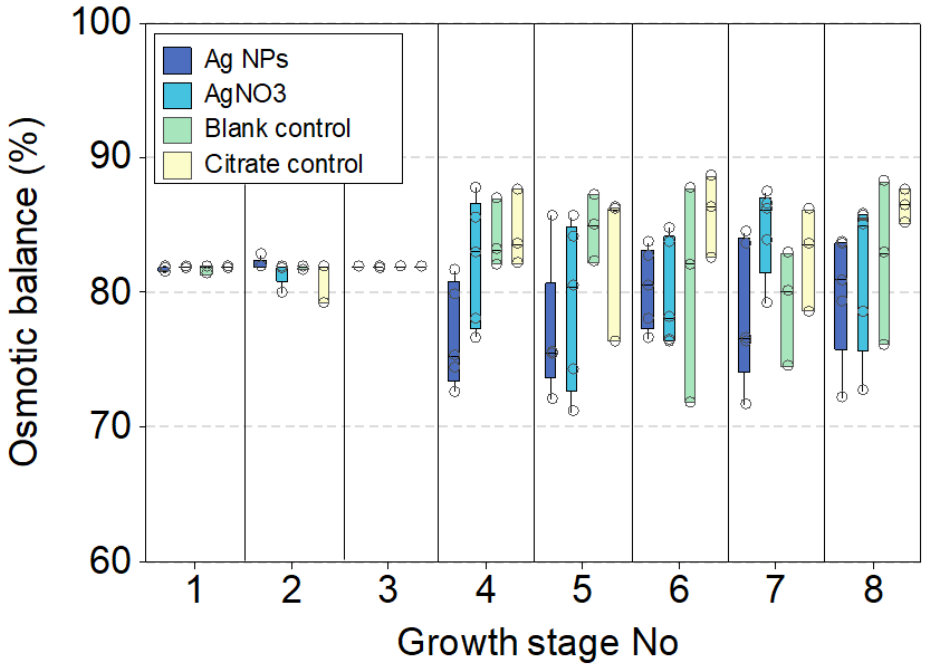



*Figure 3.4.* Plant osmotic balance for the different treatments at GS 1 to GS 8. The individual points represent the results for individual samples (n = 5 for the Ag treatments; n = 3 for the controls). The error bars denote 1 standard deviation for each dataset.

### *3.3.3. Length of wheat shoots & grains*

The shoot lengths of the wheat plants increased continually until GS 4 and then remained approximately constant until GS 8 (Figure 3.2B, Table 5B, Appendix B). With one exception, the shoot lengths were statistically identical for plants from the different treatments during all GSs (with $p \geq 0.06$). The exception is found at GS 5, where the shoots of the plants treated with $^{109}AgNO_3$ were significantly longer (with $p = 0.02$) than those of the citrate control treatment.

The measured grain head lengths remained approximately constant during GSs 6, 7 and 8 (Figure 3.3B, Table 6B, Appendix B). For GSs 6 and 7, all four treatments furthermore revealed grain lengths that were statistically identical (with $p \geq 0.1$). At GS 8, however, the grains obtained from the $^{109}AgNO_3$ treatment were significantly shorter (with $p = 0.01$) than the grains from the citrate control treatment.

### *3.3.4. Plant growth rates*

The plant growth rates are measured by the number of days it took plants to reach a given GS. For GSs 1 to 3, the plants from all four treatments revealed statistically identical growth rates, with $p \geq 0.6$ (Figure 3.5, Table 7B, Appendix B). At GS 4, however, the plants from the $^{109}$Ag-E treatments showed signs of growth retardation, as they reached this GS about 12 days later compared to the plants from the two control treatments ($p = 0.09$). This difference in plant growth for the $^{109}$Ag-E relative to the control treatments was statistically most significant at GSs 5 and 7, where the lag was about 20 days (with $p \leq 0.001$) and 16 days (with $p \leq 0.03$), respectively. This lag in growth rates was also evident for GS 8, which the plants from the $^{109}$Ag-E treatments reached about 15 days later than the control treatment plants but this difference was only marginally significant (with $p = 0.15$).

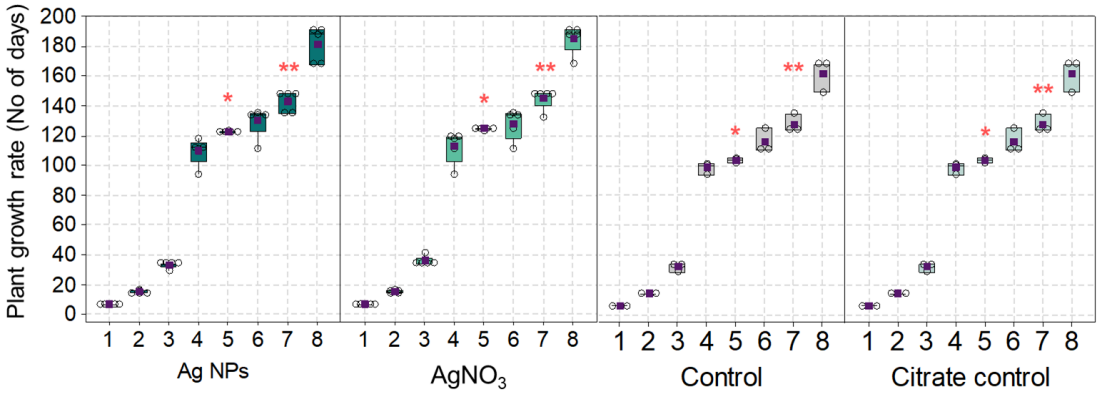



*Figure 3.5*. Plant growth rate determined for the four treatments for GSs 1 to 8 (n = 10 for the Ag treatments and n = 6 for the control treatments for GSs 1 – 3, while n = 5 for the Ag treatments; n = 3 for the controls for GSs 4 – 8). The box plots show how long it took plants to reach each GS (in number of days). The individual data points represent the results for individual samples, whilst the error bars denote 1 standard deviation for each dataset. There are significant differences between the results of the two Ag treatments versus the two control results at GS 5 (*p = 0.001) and GS 7 (**p = 0.03).

## 3.4. Discussion

Among the eleven biological properties studied, six showed no effects for the $^{109}$Ag-E treatments, whilst four showed possible and one showed clear evidence of changes linked to the presence of $^{109}$Ag-E in the soils. The results obtained are

discussed in three separate sections according to this below.

### *3.4.1. No effects of $^{109}$Ag-E on dry biomass*

For six of the eleven biological parameters, germination, aboveground DBY, total and aboveground WBY, osmotic balance and shoot dry biomass, the statistical analyses revealed no significant impact of $^{109}$Ag NPs and $^{109}AgNO_3$.

To put this finding into perspective, previous soil studies have also reported no effects on germination rate (El-Temsah and Joner 2012; Liu et al., 2017; Yang et al., 2018) and the above-ground dry biomass (Doolette et al., 2015; Larue et al., 2014) at much higher exposure concentrations of up to 100 mg kg$^{-1}$. For example, Lee et al. (2012) documented that the growth of mung beans (*P. radiatus*) and sorghum (*S. bicolor*) was not inhibited by exposure to Ag NPs concentrations of 100 mg kg$^{-1}$ in soils. Notably, this Ag exposure concentration exceeds the $^{109}$Ag-E concentrations employed in this study (of 72 µg kg$^{-1}$) by more than three orders of magnitude. Lee et al. (2012) also found, however, that growth of the same plant species was reduced when exposed to 40 mg L$^{-1}$ Ag NPs in agar as an exposure medium. This demonstrates that both exposure medium and concentration have an impact on the biological effects and highlights the importance of the current investigation, which was carried out in soils at an environmentally relevant exposure concentration, with the aid of stable isotope labelled $^{109}$Ag-E.

### *3.4.2. Possible effects of $^{109}$Ag-E on grains & shoots*

Four biological parameters, encompassing total DBY, grain dry biomass as well as grain and shoot lengths hint at possible impacts from the presence of $^{109}$Ag-E in the soils. An evaluation of the results for these properties revealed statistically significant differences ($p \leq 0.05$) between the two $^{109}$Ag-E treatments and the controls. These possible effects are discussed below.

The grain dry biomass at GS 8 was recorded to be lower for the $^{109}$Ag NPs and the $^{109}AgNO_3$ treatments than for the citrate control (Figure 3.3A). Similarly, the $^{109}AgNO_3$ treatment revealed grains that were shorter compared to those of the citrate treatment, also at GS 8. It is possible that these statistically significant differences reflect the presence of $^{109}$Ag-E in the soils but additional observations

cast serious doubt on this interpretation.

First, if the biological effects were indeed significant, they should be clearly apparent in differences between the $^{109}$Ag-E treatments relative to both the blank and the citrate control treatments but this was not observed. This conclusion is supported by a consideration of the possible role of citrate on plant growth. In detail, the added citrate provides an additional carbon (C) contribution to the soil and it may alter the soil pH value. For example, the C derived from the citrate could promote the growth of rhizobacteria (Marschner 1995; Lugtenberg and Kamilova 2009). Such bacteria release exudates that can increase the availability of essential nutrients for plant growth and hinder the growth of plant pathogens (Lugtenberg and Kamilova 2009). A calculation shows, however, that the added citrate contributed only about 0.18 mg kg$^{-1}$ of C to the soils. This is a negligible contribution as it increased the total C reserve of the soils by less than 0.15%. Similarly, identical soil pH values of 5.5 ± 0.4 were recorded for all four treatments, regardless of whether citrate was present or not. Consequently, it can be concluded that the citrate present in the respective control exposures is unlikely to have had an impact on plant growth parameters such as grain dry biomass and length.

Second, if any biological parameters are indeed impacted by the presence of $^{109}$Ag-E in the soils and plants, they should be more severe for the $^{109}$Ag NP treatment, and this was also not observed. Previous soil studies have reported significantly enhanced growth yield and improvement in leaf area and grain yield of wheat (*Triticum aestivum L.*) when exposed to Ag NPs at concentrations of up to 150 mg kg$^{-1}$ (Jhanzab et al., 2015). In contrast, some soil studies report severe retardation in shoots length and decrease in fresh and dry weight dependant on Ag concentrations in the soils (Salama, 2012). The latter conclusion reflects that the uptake of Ag by the plants was found to be effectively limited by the concentration of dissolved Ag in the soil pore waters (see Chapter 2). Furthermore, the work of Chapter 2 demonstrates that the $^{109}$Ag NP treatments were associated with dissolved pore water $^{109}$Ag-E concentrations, which exceeded those of the $^{109}AgNO_3$ treatments by a factor of about x3. As a consequence, the plants from the $^{109}$Ag NP treatments also featured higher $^{109}$Ag-E concentrations.

Considering the above, it is very unlikely that the differences in grain dry biomass and length at GS 8 between the $^{109}$Ag-E and the citrate control treatments are caused by the presence of $^{109}$Ag-E in the soils. Furthermore, it is also unlikely that the effects are in any way related to the seven day technical fault of the environmental control system, which occurred after the collection of the GS 7 samples. Whilst this fault will have had an impact on plant growth, all remaining plants will have been impacted in the same or a very similar manner. As such, the technical fault is unlikely to be responsible for differences in plant growth parameters between plants from the $^{109}$Ag-E and the control treatments. As such, it is most likely that the observed effects for the grain dry biomass and length are due to a sampling bias, which is related to the limited number of plants and plant tissues that were monitored in the current study. In this context, it is notable that the blank and citrate controls consisted of only three replicates, whilst five replicates were sampled for the two $^{109}$Ag-E treatments.

The above considerations are also important for an evaluation of the possible effects seen for the shoot lengths and total DBY values at GS 5. In detail, the shoots from the $^{109}AgNO_3$ treatments were found to be longer compared to the citrate control shoots, whilst the total DBY of the wheat exposed to $^{109}AgNO_3$ was found to be larger compared to the results for the blank control treatment. Given that no significant impacts were seen for the plants treated with $^{109}$Ag NPs relative to either the blank or citrate control treatments, the observed effects are also most likely caused by a sampling bias. This conclusion is thereby particularly relevant for the possible difference in total DBY observed at GS 5 (Figure 3.1A). In this case, the total DBY results were impacted by root mass, which typically contributed more than 25% to the total DBY (Table 1B, Appendix B). The root masses, however, were found to be highly variable, most likely due to tissue loss during the root washing procedure. The conclusion that this shortcoming may have contributed to the sampling bias is supported by the observation that the aboveground DBY values of the plants show no significant differences between the $^{109}$Ag-E treatments and the controls (Figure 3.1B).

In summary, the above considerations indicate that the total DBY of the plants, grain dry biomass and length, and shoot length were most likely not impacted by the presence of $^{109}$Ag-E in the soils. Rather, the observed effects are more likely

to be a consequence of a sampling bias.

### *3.4.3. Impact of $^{109}$Ag-E on plant development*

The current study revealed clear and statistically significant differences in plant growth rates between the $^{109}$Ag-E and the control treatments at GSs 5 and 7, as well as smaller, less significant differences at GSs 4, 6 and 8 (Figure 3.5, Table 8B, Appendix B). In detail, for the first three GSs, the plants from all treatments showed similar growth rates. However, at GS 4 the plants exposed to the $^{109}$Ag-E treatments demonstrated a delay in growth of about 10 to 12 days. At GSs 5 to 7 this retardation is more pronounced, with a delay between 15 to 20 days for the wheat plants treated with $^{109}$Ag-E relative to the control treatments. At GS 8, a difference in growth rate for the plants of different treatments is still apparent but the difference is less significant ($p = 0.15$). Most likely, the observed differences in wheat growth rates are linked to the uptake of $^{109}$Ag-E by the plants, as reported in Chapter 2. In this context, it is important to note that both $^{109}$Ag-E treatments seem to cause similar retardation of growth relative to the controls. This observation is in accord with the findings of Chapter 2, which suggested that the two $^{109}$Ag-E treatments were associated with similar speciation of Ag within the soils and the plants. Furthermore, whilst the $^{109}$Ag-E concentrations were higher for the plants exposed to $^{109}$Ag NPs rather than $^{109}AgNO_3$, this difference in concentration was probably too small to generate clearly distinct biological effects.

In summary, the observations demonstrate that the uptake of Ag from Ag NPs and $AgNO_3$ in soils can delay the growth and development of wheat plants, even if the materials are present in soils in low, but environmentally relevant, levels. This conclusion is in accord with previous work, which has shown that exposure of rice seedlings to C nanotubes can be associated with a delay in development and growth (Hao et al., 2016). In this latter study, the growth delay was linked to a reduction in the levels of plant hormones that impact development, including gibberellin, indole-3-acetic acid and isopentenyl adenosine (Hao et al., 2016). The current study, however, does not address the mechanisms responsible for the slower growth rates of plants exposed to low Ag levels in soils. Further research is hence needed to understand how Ag NPs and $AgNO_3$ can trigger the

observed effects even at such low exposure levels.

## 3.5. Conclusion

For the first time, this study investigated whether a wheat soil exposure to Ag NPs and $AgNO_3$ at an environmentally relevant Ag concentration of 72 µg $kg^{-1}$ had an impact on biological parameters over the full life cycle of the plants. The current work provided several important findings:

- Germination of the seeds, aboveground DBY, total and aboveground WBY, plant osmotic balance, and shoot dry biomass were clearly not impacted by the exposure to $^{109}$Ag-E in soils.
- Initial analyses of the data revealed that (i) grain dry biomass and length, (ii) shoot length and (iii) total plant DBY were possibly impacted in the plants exposed to $^{109}$Ag-E. Detailed scrutiny of the results revealed, however, that the possible effects are most likely a consequence of a sampling bias, which reflects that only 5 and 3 replicate samples were analysed for the $^{109}$Ag-E and the control treatments, respectively.
- At GSs 5 and 7, the plants exposed to both $^{109}$Ag-E treatments recorded a clearly resolved retardation in development by about 15 to 20 days. This impact on plant development is most likely related to the uptake of Ag by the wheat plants from the Ag NPs and $AgNO_3$ present in the soils.

Importantly, the latter result demonstrates a clear impact of even low Ag concentrations in soils on the growth rate of wheat plants. This is an important result with significant economic implications. In particular, the slower growth may delay the wheat harvest, which increases the chances of crop damage by, for example, harsh weather or fungal growth. Alternatively, or in addition, slower wheat growth may be associated with reduced grain yields or lead to poor grain quality due to grain sprouting. Given these possible impacts, it will be worthwhile to conduct further studies to both substantiate the results of the current study and reveal the mechanisms that are responsible for the delayed growth.

# Chapter 4: Silver nanoparticle accumulation: Assessing different hydroponic media as a proxy for soil

## 4.1. Introduction

Once Ag NPs are released into the environment, they undergo a series of physicochemical transformations such as oxidative dissolution, sorption, change in chemical speciation and precipitation (Tkalec et al., 2019). Among the most common transformations are the oxidative dissolution of Ag NPs to form ionic $Ag^+$ and sorption of the Ag NPs to organic and inorganic sulphur species. Notably, the fate of Ag NPs in soils and hydroponic media governs the bioavailability to plants and toxicity mechanisms (Coutris et al., 2012). In particular, sulfidation of $Ag^+$ ions and Ag NPs can lead to the formation of either $Ag_2S$ or $Ag_2S$ NPs, both of which are highly insoluble, inert and have been shown to decrease toxicity (Qing et al., 2018).

The uptake and accumulation of Ag NPs, $Ag_2S$ NPs and $Ag^+$ ions by plants and their toxicity are governed primarily by Ag speciation and Ag NP properties (e.g. size and charge) as well as environmental factors and in particular the exposure medium (Gubbins et al., 2011; Lee et al., 2012; Geisler-Lee et al., 2014; Bundschuh et al., 2014). Clear evidence for the latter was provided by Lee et al. (2012), who found that mung beans (*Phaseolus radiatus*) and sorghum (*Sorghum bicolor)* exposed to Ag NPs recorded more Ag uptake in an agar medium than in soils. This was thought to reflect that more $Ag^+$ ions were released from the Ag NPs in the agar medium. Despite this difference, nano-ecotoxicological studies of plants most commonly employ hydroponic media even though soil is the more environmentally relevant substrate (Tkalec et al., 2019). As a consequence, there are questions to what extent the results of hydroponic studies are applicable to and relevant for actual agronomic systems where crops are grown in soils. This is especially important in terms of risk and hazard assessment of Ag from Ag NPs to plants.

The current study addresses this uncertainty with exposure studies that enable a direct Ag uptake comparison from Ag NPs by plants grown in soils and three

hydroponic media. In detail, winter wheat (*Triticum aestivum L.*) was grown in soil and three different hydroponic media dosed with Ag NPs, $Ag_2S$ NPs and $AgNO_3$ for 14 days under controlled conditions. Plant tissues, as well as soil and three hydroponic solutions, were collected at four-time points and analysed for Ag concentrations. The three hydroponic solutions encompassed a (i) pore water solution extracted from the soil, (ii) artificial pore water prepared from pure reagents to mimic a soil solution composition and (iii) a 25% strength Hoagland solution. With this approach, the experiment aims to (i) quantify and compare uptake of Ag from relevant Ag species by wheat in soil versus hydroponic media; and (ii) assess the suitability of hydroponic exposures as a substitute for soil systems.

## 4.2. Experimental design & methodology

### *4.2.1. Ag NPs, $Ag_2S$ NPs & $AgNO_3$*

Three different species of Ag were employed in the exposures: Ag NPs, $Ag_2S$ NPs, which are known to form from Ag NPs in wastewater treatment plants and soils, and for comparison, readily soluble $AgNO_3$. The 20 nm polyvinylpyrrolidone (PVP) coated Ag NPs and 20 nm $Ag_2S$ NPs were supplied and synthesised by Applied Nanoparticles, Barcelona, Spain. The Ag NPs were characterised by the Department of Materials, Oxford. The hydrodynamic diameter of the NPs was measured using a Dynamic Light Scattering (DLS) on a Malvern Zetasizer Nano ZS90 (Malvern Instruments) where size and distribution were determined by JEOL1010 Transmission Electron Microscope (TEM) (JEOL). The $AgNO_3$ (≥ 99% purity; ACS reagent grade) was purchased from Sigma Aldrich.

### *4.2.2. Exposure*

#### *4.2.2.1. Preparation of the media*

Four different exposure media types were used in this study, one soil and three different hydroponic solutions (i) the Lufa soil is a reference soil commonly employed in plant research; (ii) a pore water solution extracted from the Lufa soil also referred to as Lufa hydroponic solution (LUHS); (iii) an artificial pore water

(APW) prepared from pure reagents to mimic a soil solution composition; (iv) a 25% strength Hoagland solution (HS), which is commonly employed in experimental hydroponic systems.

The soil was sieved to a particle size of 2 mm by the distributer and air-dried prior to the exposure. Lufa 2.2 soil (LUFA-Speyer 2.2, Germany, 2018) is a loamy sand with a total organic carbon content of 1.61 ± 0.15%, a $pH_{CaCl2}$ value of 5.4 ± 0.2 and a cation exchange capacity of 9.7 ± 0.4 meq per 100 g. A 100% water holding capacity of 40 mL per 100 g of soil was determined for Lufa 2.2 using standard techniques (Priha and Smolander, 1999).

For the LUHS medium, 400 mL of deionised water were added to 1 kg batches of air-dried Lufa soil (100% water holding capacity of the soil). The saturated soil was left to equilibrate for 72 h at 20°C in the dark to avoid algae growth and the breakdown of components through UV. The saturated soil was then filtered through three different stages: a 1.6 µm glass microfiber membrane (Whatman), a 0.45 µm polyvinylidene fluoride (PVDF) filter (Merck Millipore) and a 0.22 µm PVDF membrane (Merck Millipore) to ensure removal of bacteria. This alternative method to autoclaving was used to sterilise the solution, whilst retaining the organic matter content, to mimic the Lufa soil environment as closely as possible. At this point, the solution was aerated for 12 h to equilibrate the dissolved $CO_2$ concentration and a pH value of 5.5 was measured. The solution was then stored at 4°C in the dark.

The APW was prepared following Tyne et al. (2013) to produce an artificial soil pore water. In summary, the APW was made up from reagent grade $NaHCO_3$, $Ca(NO_3)_2$, anhydrous $KNO_3$, $HNO_3$, $MgSO_4 \cdot 7H_2O$, $Na_2HPO_4 \cdot 12H_2O$ (Sigma Aldrich), Fe and Al standard solutions (1 g $L^{-1}$; VWR) and Pahokee Peat Standard II fulvic acid (International Humic Substance Society) that were dissolved and mixed in deionised water in defined proportions (Table 4.1). The pH of the solution was then reduced from 7 to 5.5 by the addition of HCl, to match the pH of the Lufa soil and LUHS. Finally, the solution was sterilised by autoclaving at 121°C for 30 mins, aerated for 12 h to equilibrate the dissolved $CO_2$ concentration prior to storage at 4°C in the dark.

To prepare the 25% Hoagland solution, 0.41 g of dehydrated Hoagland No. 2

basal salt mixture (Sigma Aldrich) was suspended in 1000 mL deionised water (Table 4.2) (Hoagland and Arnon, 1950). The solution was then mixed for 30 mins until the powder dissolved completely and the pH was adjusted from 6 to 5.5 to match the pH of the other media. Finally, the solution was sterilised by autoclaving at 121°C for 30 mins and stored at 4°C in the dark.

*Table 4.1.* Chemical composition of 1L artificial pore water.

| **Artificial pore water** | |
|---|---|
| **Chemical** | **Concentration (M)** |
| $NaHCO_3$ | 0.1 |
| $Ca(NO_3)_2$ | 0.1 |
| $KNO_3$ | 0.1 |
| $HNO_3$ | 0.1 |
| $MgSO_4$ | 0.1 |
| $Na_2HPO_4$ | 0.1 |
| Fe(III) | 0.0179 |
| Al | 0.037 |
| Fulvic acid | 50 mg dw |

*Table 4.2.* Chemical composition of 1L 25% Hoagland solution.

| **25% Hoagland No. 2 Basal Salt Mixture** | |
|---|---|
| **Chemical** | **Concentration (M)** |
| $KNO_3$ | 6 mM |
| $Ca(NO_3)_2$ | 4 mM |
| $MgSO_4$ | 2 mM |
| $NH_4H_2PO_4$ | 1 mM |
| $MnCl_2.4H_2O$ | 9.2 µM |
| $H_3BO_3$ | 460 µM |
| $MoO_3$ | 0.11 µM |
| $ZnSO_4.7H_2O$ | 0.77 µM |
| $CuSO_4.5H_2O$ | 0.32 µM |
| $Fe_2(C_4H_4O_6)_3$ | 0.013 µM |

*4.2.2.2. Exposure systems*

For the exposures, the soils were held in individual polyvinylchloride semi-column containers with a length of 320 mm length and a diameter of 24 mm. Each container held 150 g soil and a mesh attached to the bottom of the semi-column allowed drainage (Figure 4.1). The flat surface of the semi-column was sealed with a clear Perspex sheet with dimensions of 320 mm x 50 mm x 14.5 mm (length x width x depth). The Perspex was secured using cable ties and covered with a black film to obscure light. Each soil container was then added to a rack.

The hydroponic media with a volume of 45 mL were held in 50 mL polypropylene centrifuge tubes with conical V-bottoms (SLS) to reduce Ag adsorption to the walls of the containers (Sekine et al., 2015). Each hydroponic container was equipped with a conical cork plug (32 mm diameter at the top and 30 mm diameter on the bottom) with a hole through which each seedling was threaded (Figure 4.1). To avoid Ag agglomeration and aggregation, each tube was supplied with a winged magnetic stirrer (VWR) with the following dimensions: 16 mm triangle sides, 10 mm topside and 5 mm wings.

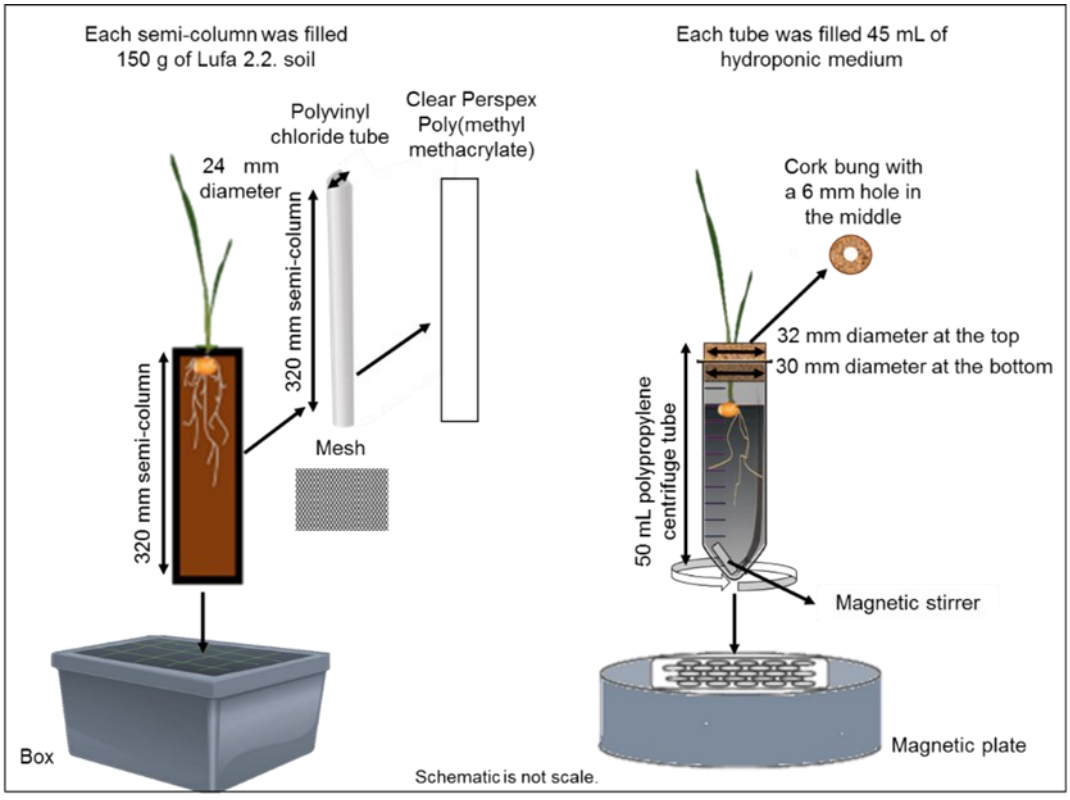



*Figure 4.1.* Schematic of the soil (left) and hydroponic (right) setup.

*4.2.2.3. Dosing of the media*

A key aim of this study was to provide approximately similar Ag uptake conditions for wheat grown in soils that were dosed with 10 mg of Ag $kg^{-1}$ from Ag NPs, $Ag_2S$ NPs and $AgNO_3$ and wheat grown in hydroponic systems to which the same Ag species were added. To this end, preliminary experiments were carried out to determine the Ag concentrations of pore waters that had equilibrated with Lufa soil following the addition of the three Ag species. Based on these experiments, the three hydroponic media were dosed with 0.02 mg Ag $kg^{-1}$ for the Ag NPs and $AgNO_3$ treatments and with 0.01 mg Ag $kg^{-1}$ for the $Ag_2S$ NP treatment to match the soil pore water concentration of the Lufa soil.

The dosing of the soils and hydroponic media was accomplished using freshly prepared aqueous solutions of $AgNO_3$ as well as freshly prepared aqueous suspensions of Ag NPs and $Ag_2S$ NPs, which were sonicated for 30 mins before use to reduce agglomeration (Table 4.3). For the soil exposures, a 2.5 kg batch of Lufa soil was spiked to a nominal Ag concentration of 10 mg $kg^{-1}$ with the prepared Ag NP and $Ag_2S$ NP suspensions and $AgNO_3$ solution. The dosed soils were thoroughly mixed by breaking wet clumps with the back of a spoon until they were visibly homogenised with no remaining clumps. Following dosing, all soils were wetted to 60% water holding capacity with deionised water and left to equilibrate for 72 h at 20°C in the dark. The hydroponic media were dosed immediately before the exposure to avoid premature Ag adsorption and agglomeration or dissolution of the NPs. Large initial volumes of the three hydroponic media (LUHS, APW and HS) were split into batches of 685 mL and dosed with appropriate volumes of the two NP suspensions and an $AgNO_3$ solution to achieve final Ag concentrations of 0.02 mg $L^{-1}$ for the Ag NP and $AgNO_3$ treatments and of 0.01 mg $L^{-1}$ for the $Ag_2S$ NP treatment (Table 4.3).

'Coating control' treatments for both the soil and the hydroponic media, which approximately matched the PVP concentrations of the respective Ag NP exposures, were obtained in the following manner.
Following initial centrifugation of the PVP-coated Ag NP suspension, an aliquot of the supernatant was first collected and then subjected to ultracentrifugation at 41000 rpm for 1 h at 4°C to prepare a suitable 'PVP-containing supernatant'.

Appropriate volumes (9 mL) of this supernatant were then added to Lufa soil and the three hydroponic media to prepare the respective coating control treatments.

A 'blank control' with no added test substance was also included for each of the different exposure media.

*Table 4.3.* Spiking volumes and concentrations used for the experiment. The V* indicates the total volume of spike added to each medium and mg $L^{-1}$** signifies the concentration of spike used for each treatment and medium.

| Medium type | Total V of media (g or mL) | Ag NPs | | $Ag_2S$ NPs | | $AgNO_3$ | |
|---|---|---|---|---|---|---|---|
| | | V * | mg $L^{-1}$ ** | V * | mg $L^{-1}$ ** | V * | mg $L^{-1}$ ** |
| **Lufa soil** | 2500 | 21.64 | 1167 | 59.76 | 422.5 | 53.34 | 473.4 |
| **Lufa soil pore water** | 685 | 1.76 | 7.78 | 0.16 | 2.82 | 1.45 | 9.47 |
| **Artificial pore water** | 685 | 1.76 | 7.78 | 0.16 | 2.82 | 1.45 | 9.47 |
| **Hoagland solution** | 685 | 1.76 | 7.78 | 0.16 | 2.82 | 1.45 | 9.47 |

#### *4.2.2.4. Planting of wheat*

Winter wheat (*Triticum aestivum L.*, Variety: KWS Dacanto) sourced from Københavns Universitet was used in the experiment. Prior to use, the seeds were not pre-treated in any way and were kept refrigerated at 4°C in the dark. Seeds of similar size (~0.8 cm in length and ~0.5 cm in width) and visual intactness were chosen for the experiment. Seeds were germinated on filter paper wetted with deionised water under controlled conditions (16 h light/8 h dark photoperiod; 20°C temperature). After 10 days, seedlings of similar weight (≥ 0.3 g fresh weight) and size were transferred to either the soil or hydroponic containers where seedlings were grown for further 14 days. Each container thereby held one seedling and represented a single replicate, and each treatment and timepoint encompassed three replicates.

For the soil medium, the seedlings were transferred by first laying the roots onto about 120 g of soil in open soil containers and then covering them with the remaining 30 g of soil to make up a total soil weight of 150 g. Each soil container was then closed with a Perspex sheet, covered with a black film to obscure light and placed in a rack. For the hydroponic experiments, the seedlings were transferred to hydroponic containers, filled with 45 mL of the hydroponic solution, whereby the stems were threaded through the holes of the plugs. The plugholes

were then filled with cotton wool (SLS) to support the vertical position of the seedling and to reduce evaporation, whilst leaving enough space to ensure that growth of the seedling was not affected. The plant root and seed were then suspended in the hydroponic medium. Finally, the containers were covered in Al foil to obscure light and the media were continuously stirred on magnetic plates at 750 – 800 rpm.

*4.2.2.5. Exposure conditions*

The exposure was performed at controlled conditions of 20°C temperature, a 16 h light/8 h dark photoperiod at a light intensity of 350 ± 50 $\mu E/m^2/s$ in a climate chamber at the UK Centre for Ecology and Hydrology, Wallingford. The soil media were maintained at 60% water holding capacity by weighing the containers and adding deionised water as required every 48 h. The hydroponic media were replenished to 45 mL once, at day 7, with deionised water. The positions of the containers and container racks were randomised every three days to minimise position effects in plant growth (Measures et al., 1972).

*4.2.3. Sample collection*

Plant tissues, soil, soil pore waters and media samples were collected on days 1, 3, 7 and 14 for the Ag NP, $Ag_2S$ NP, $AgNO_3$ and blank control treatments. For the coating control treatment, samples were only collected on days 1 and 14.

*4.2.3.1. Plant tissues*

Following collection, each seedling was first photographed with a Canon DSLR 50D and then split into root and shoot tissues. Root samples were first washed thoroughly with deionised water, soaked in 0.1 M aqueous ethylenediaminetetraacetic acid (EDTA) solution for approximately 3 mins, and then washed again at least three times with deionised water. The EDTA solution was prepared by dissolving the solid reagent (Fisher BioReagents) in Millipore water and adjustment of the pH value to 8 using NaOH. Prior to use, the EDTA solution was autoclaved at 121°C for 30 mins. The solution was used as it is a well-known chelator that complexes a wide variety of metals (Flora and Pachauri 2010).

The collected tissues were dried at 70ºC in an oven (Heratherm OGS180,

Thermo Scientific) for seven days. Once dry, the samples were weighed with a Sartorius electronic Toploader 140 MP8 balance and then stored at room temperature.

*4.2.3.2. Soils & soil pore waters*

Soil samples were dried at 70°C (Heratherm OGS180, Thermo Scientific) for seven days and subsequently stored at room temperature. Soil pore waters were obtained using a sampling protocol described in detail by Lahive et al. (2017). To summarise, 34 g of soil was collected in a 50 mL polypropylene centrifuge tube, transferred to a dark controlled temperature room (20°C) overnight, prior to the determination of the water holding capacity on an additional small (7 g) aliquot. The 34 g of soil were then saturated to 100% water holding capacity, stirred gently and left to equilibrate overnight in a dark room at 20°C.

Approximately 31 g of the water-saturated soil samples were centrifuged for 1 h at 2000 g at 4°C through preconditioned 25 mL filter inserts (with 0.45 µm PVDF filter membranes) filled with preconditioned glass wool (Sigma Aldrich) and housed in a 50 mL centrifuge system (Thermo Scientific F2519-6). The glass wool and filter inserts were preconditioned by soaking overnight in 0.1 M $CuSO_4$ solution (99.995% purity, Sigma Aldrich) to reduce Ag adsorption. After the extraction, between 5 and 7 mL of soil pore water were collected and analyses of these samples yielded the total Ag contents of the soil pore waters. Following collection, all soil pore water samples were acidified with an equal volume of *aqua regia* (3-parts concentrated HCl (≥ 37% purity, TraceSELECT grade, Honeywell) + 1-part concentrated $HNO_3$ (≥ 69% purity, TraceSELECT grade, Honeywell) and stored at 4°C in the dark.

*4.2.3.3. Hydroponic media*

The total Ag concentrations of the hydroponic media were determined on 2 mL unfiltered aliquots of the respective solutions. Following collection, all soil pore water samples were acidified with an equal volume of *aqua regia* (3-parts concentrated HCl (≥ 37% purity, TraceSELECT grade, Honeywell) + 1-part concentrated $HNO_3$ (≥ 69% purity, TraceSELECT grade, Honeywell)) and stored at 4°C in the dark.

### *4.2.4. Sample analysis*

#### *4.2.4.1. Sample preparation*

The samples were processed and analysed at the Department of Animal Ecology, Vrije Universiteit Amsterdam. The sample preparation for the plant and soil samples encompassed two steps:

*Step 1.* For the plant and soil samples, less than 100 mg and 130 mg of material respectively, were digested without HF for analysis. The samples were first weighed to about ± 0.1 mg accuracy (Sartorius Type 1712 Analytical Balance) on weighing paper and transferred to digestion bombs. To each sample, 2 mL of a mixture consisting of 4-parts concentrated HCl (32 – 35%, Ultrex II Ultrapure, J.T. Baker) and 1-part concentrated $HNO_3$ (70%, Ultrex II Ultrapure, J.T. Baker) was added. The samples were left open under an extraction hood for 15 mins to release acid fumes. The bomb vessels were then tightly sealed with a wrench and placed in a Binder furnace at 140°C for a digestion time of 7 h. After digestion, the samples were left overnight to cool down to room temperature.

*Step 2.* The bombs were carefully opened with a wrench and any acid droplets on the tops or lids of the bombs were collected with a pipette. After this, 4 mL of deionised water were added to each bomb and the solutions were transferred into polystyrene tubes and left to stand for approximately 6 h. The sample tubes were then covered and stored at 4°C in the dark.

All concentrations of the soils and plant tissues are reported for dry weight material.

The acidified extracted soil pore water samples, hydroponic and truly dissolved solutions were not digested in any way; but simply diluted as required with Millipore water on the day of analysis.

#### *4.2.4.2. Graphite furnace atomic absorption spectroscopy (GF AAS)*

All plants, hydroponic media and extracted soil pore water samples were analysed with a Perkin Elmer graphite furnace atomic absorption spectrometer (GF AAS) (PinAAcle 900Z) equipped with a PinAAcle 900Z autosampler system. For the analyses, the instrument was first set for Ag measurements and the

autosampler tip was cleaned with 96% ethanol and aligned within the graphite furnace. To improve instrument performance and data quality, a matrix modifier consisting of $Mg(NO_3)_2$ and $Pd(NO_3)_2$ was injected with each sample and standard solution.

Instrument calibration was achieved with four freshly prepared standard solutions with Ag concentrations of 10, 20, 30 and 40 µg $L^{-1}$, which were prepared from a common 4 mg $L^{-1}$ Ag stock (SCP Science). Sample analyses began once a calibration curve with a correlation coefficient of $R^2 > 0.98$ was obtained. The samples were analysed in order of increasing Ag concentrations – to avoid error during analysis – and sample solutions that exceeded the calibration range were further diluted with 1 M HCl (Ultrex II Ultrapure, J.T. Baker). Between samples, the introduction system was rinsed with 10 µL of a mixture of ethanol and $HNO_3$.

The following quality control measures were adopted during the analyses. The tip alignment in the furnace was checked after every 20 analyses, to ensure samples were dispensing correctly. After every 7 to 13 sample analyses, as per instrumental protocols, the 20 µg $L^{-1}$ Ag standard was measured again and the calibration curve was adjusted if necessary or re-determined if the $R^2$ value was less than 0.98. Furthermore, fresh dilute Ag standard solutions were prepared and analysed to define a new calibration curve after every 80 analyses. For further quality control, additional reference material DOLT4 (NRC – CNRC) for plants was analysed repeatedly (> x10) using the same methods that were applied for the samples/standards. These analyses revealed that the employed methods achieved performance characteristics in terms of reproducibility ± 0.02 µg $L^{-1}$. The Ag detection limit of the instrument was found to be 0.03±0.01 µg $L^{-1}$.

*4.2.4.3. Flame AAS*

Due to the high Ag concentrations of the dosed soils, all soil samples were analysed with a Perkin Elmer AAnalyst 100 flame atomic absorption spectrometer. For the analyses, a calibration curve was produced by measurements of dilute Ag standard solutions with concentrations of 0.5, 1, 2 and 3 mg $L^{-1}$ that were prepared from a common Ag stock solution with a concentration of 1000 mg Ag $L^{-1}$ (SCP Science). After a calibration curve with a correlation coefficient of $R^2 > 0.98$ was achieved, samples were analysed in order

of increasing Ag concentration. Any samples with Ag concentrations that exceeded the calibration range were diluted with Millipore water. For quality control, additional soil reference material ISE 989 (Wepal/Quasimeme) was analysed repeatedly (> x10) using the same methods that were applied for the samples/standards. These analyses revealed that the employed methods achieved performance characteristics in terms of reproducibility ± 0.05 mg $L^{-1}$. The detection limit of the instrument was 0.05 ± 0.02 mg $L^{-1}$.

*4.2.5. Statistical analyses*

All statistical analyses were performed with SigmaPlot 13.0 and Minitab 18. For analyses of differences between treatments, media and Ag type, one-way ANOVA and two-way ANOVA analyses with a significance level of $p < 0.05$ were used. First, the Ag concentrations between the control and Na-citrate were compared. After no differences were established between the controls, the control data was compared to the Ag treatments. All errors have been reported as standard deviations.

## 4.3. Results

*4.3.1. Characterisation of the nanoparticles*

The NPs were supplied as an aqueous suspension of 20 nm PVP-coated Ag NPs and 20 nm $Ag_2S$ NPs with PVP coating. The TEM micrographs revealed average diameters of 21.6 ± 6.0 nm and 18.5 ± 12.9 nm for the Ag NPs and the $Ag_2S$ NPs, respectively and particles of spherical shape with a consistent size distribution (Figure 1C, Appendix C).

The DLS analyses provided average hydrodynamic diameters of 20.6 ± 5.7 nm and 26.8 ± 2.8 nm for the Ag NPs and the $Ag_2S$ NPs, respectively, with PdI values of 0.28 ± 0.03 and 0.17 ± 0.05, respectively.

*4.3.2. Validity of the exposure experiment*

According to criteria set out in the OECD guidelines (OECD 208 and 227) for chemical testing of terrestrial plants, the experiment was valid as (i) the

germination rate was 99%, (ii) the controls showed no visible phytotoxic effects such as chlorosis, necrosis, wilting, shoot and stem deformation throughout the experiment and (iii) the mean plant survival was 100% for the duration of the experiment.

*4.3.3. Exposure media*

The Ag concentrations were determined for all media at all five-time points during the experiment. The extracted soil pore water from the Lufa soil will be referred to as Lufa pore water (LUPW), in contrast to the Lufa hydroponic solution (LUHS), which was extracted from Lufa soil prior to the experiment as plant growth medium.

In the following, the results of the Ag concentration measurements for the media are presented first for the Lufa soil and the associated LUPW; the results for the three hydroponic media are presented thereafter. For each media, the data that were obtained for the three Ag treatments, with Ag NPs, $Ag_2S$ NPs and $AgNO_3$ are presented prior to the results for the two controls (blank and coating control).

The Ag concentrations of the Lufa soils appear to decrease slightly for all three Ag treatments during the course of the experiment but the statistical significance of the changes are limited, with p-values of 0.16 (Figure 4.2, Table 1C, Appendix C). In detail, the Ag concentrations of the Ag NP treated soils decreased from 9.8 ± 0.8 mg $kg^{-1}$ after spiking (day 0) to 7.6 ± 0.3 mg $kg^{-1}$ at the end of the experiment at day 14. For the same time period, the Ag concentrations of the soils dosed with $Ag_2S$ NPs and $AgNO_3$ declined from 11.7 ± 1.0 mg $kg^{-1}$ to 10.2 ± 0.6 mg $kg^{-1}$ and from 9.4 ± 0.4 mg $kg^{-1}$ to 7.2 ± 0.5 mg $kg^{-1}$, respectively. Both the blank and the coating controls for the Lufa soil medium had Ag concentrations below the limit of detection (less than 0.05 ± 0.02 µg $kg^{-1}$).

The LUPW Ag concentrations (Figure 4.3A, B and C, Table 1C, Appendix C) were constant ($p = 0.12$) of Ag for the duration of the experiment. Specifically, throughout the experiment, the LUPW exhibited constant Ag concentrations with mean values of 0.03 mg $L^{-1}$ for the Ag NPs, 0.01 mg $L^{-1}$ for $Ag_2S$ NPs and 0.02 mg $L^{-1}$ for the $AgNO_3$ treatment. The Ag concentrations measured for the LUPW controls were 0.03 ± 0.01 µg $L^{-1}$.

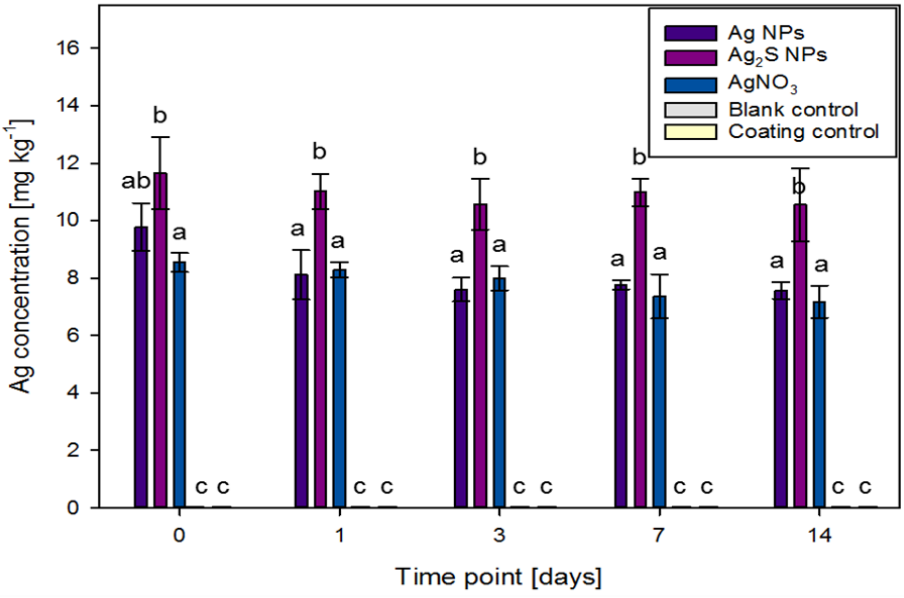



*Figure 4.2.* Silver concentrations measured for the Lufa soil where the error bars signify standard deviation (n = 3). Means with different letters are significantly different.

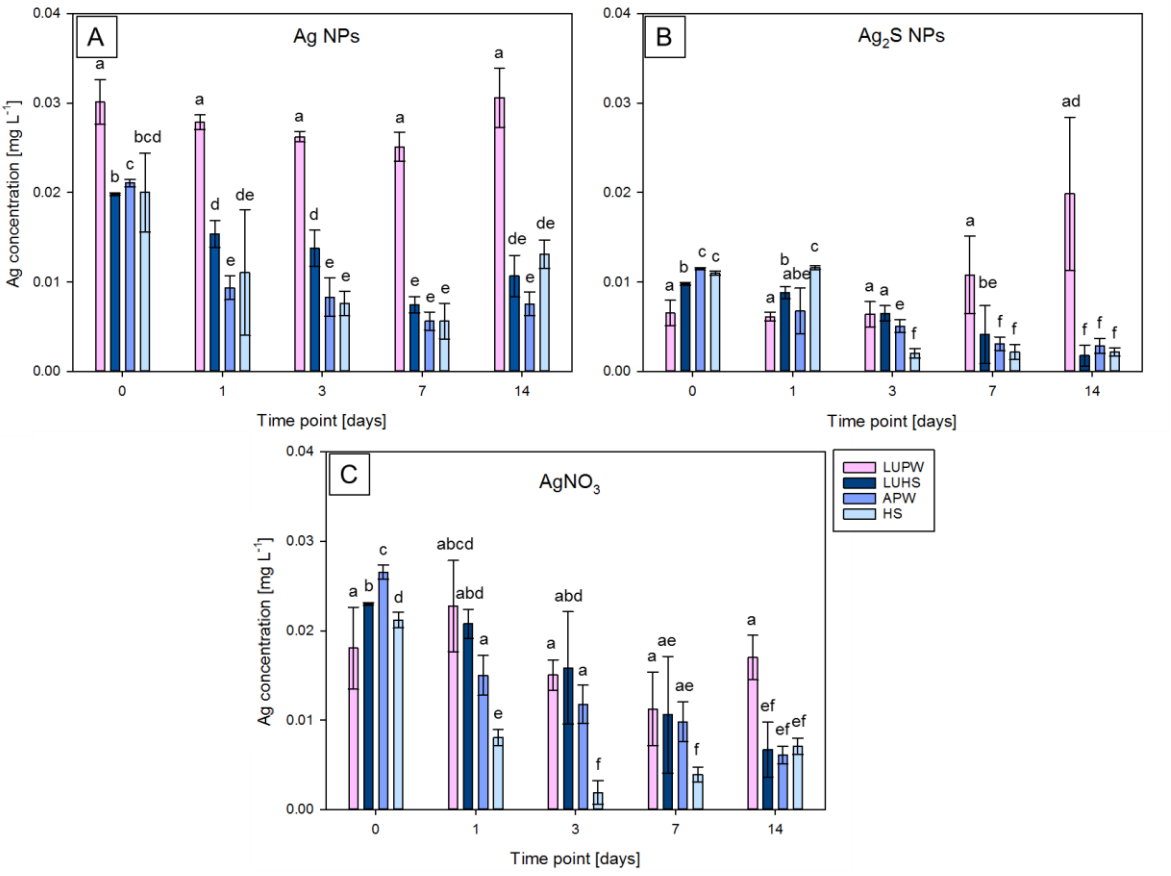



*Figure 4.3.* Silver concentrations measured for Lufa soil pore water (LUPW), Lufa soil hydroponic solutions (LUHS), artificial pore water (APW) and Hoagland solution (HS) following treatment with Ag NPs (A), $Ag_2S$ NPs (B) and $AgNO_3$ (C). The error bars indicate standard deviation (n = 3) and the means with different letters are statistically different.

The Ag concentrations determined for the hydroponic media (Figure 4.3A, B and C, Table 1C, Appendix C) differed for the three Ag treatments but exhibited a general decline during the course of the experiment. Specifically, for all three treatments, the Ag concentrations of the hydroponic media are significantly lower ($p < 0.04$) at day 14 compared to day 0. In detail, from day 0 to day 14, the Ag concentrations of the Ag NP and the $Ag_2S$ NP treatments declined from about 0.02 mg $L^{-1}$ to 0.01 mg $L^{-1}$ and from 0.01 mg $L^{-1}$ to 0.005 mg $L^{-1}$, respectively. In a similar manner, the Ag concentrations of the three hydroponic media treated with $AgNO_3$ declined from approximately 0.02 mg $L^{-1}$ at day 0 to about 0.01 mg $L^{-1}$ at day 14. The Ag concentrations for the blank and coating controls were either below or close to the limit of detection with an average concentration of 0.94 ± 0.26 µg $L^{-1}$.

*4.3.4. Plant tissues*

In the following, the presentation of the Ag concentration data for the plant tissues is structured according to the different Ag and control treatments. Prior to the statistical evaluation of the data, the results for two individual sample analyses were excluded: (i) a day 1 root sample result for the APW treated with $AgNO_3$ and (ii) a day 3 shoot sample results for the Lufa soil dosed with Ag NPs. In both cases, the measured Ag concentrations exceeded the results obtained for the two additional replicates by more than a factor of x5, most likely due to an analytical or procedural error.

*4.3.4.1. Root tissues*

The roots exposed to the Ag NP treatment in Lufa soil exhibited an overall increase in Ag concentrations from day 1 to day 14, whilst the roots from the hydroponic media showed more constant Ag concentrations (Figure 4.4, Table 2C, Appendix C). Specifically, the Ag concentrations of roots exposed to Ag NPs in the Lufa soil showed identical ($p > 0.4$) Ag concentrations for the first two time points (6.9 ± 1.6 µg $g^{-1}$) but the Ag concentrations were significantly higher ($p < 0.03$) at day 7 and again at day 14 ($p < 0.01$; 56.2 ± 9.5 µg $g^{-1}$) (Figure 4.4A, Table 2C, Appendix C). In contrast, the roots from the hydroponic solutions exhibited similar ($p > 0.2$) and stable Ag concentrations throughout the experiment for the Ag NPs (Figure 4.3A, Table 2C, Appendix C). In detail, the

roots exposed to the Ag NP treatment in the hydroponic solutions displayed Ag concentrations of 4.1 ± 1.6 – 5.2 ± 0.8 µg $g^{-1}$ for the LUHS, of 5.8 ± 1.5 – 9.6 ± 2.5 µg $g^{-1}$ for the APW, and of 6.8 ± 1.9 – 12.4 ± 3.1 µg $g^{-1}$ for the HS.

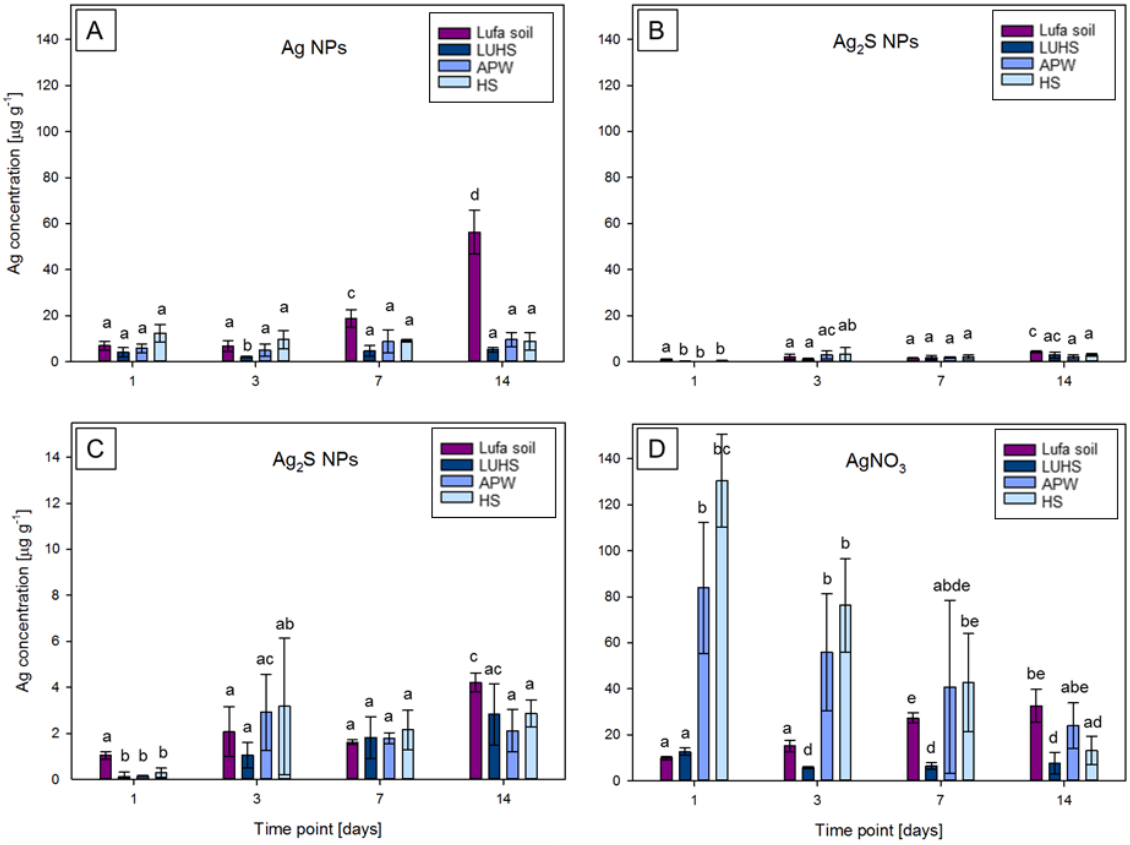



*Figure 4.4.* Mean Ag concentrations determined for the wheat roots exposed to Ag NPs (A), $Ag_2S$ NPs (B and C; note different scale in the latter panel) and $AgNO_3$ (D) for the different media including the Lufa soil, Lufa soil hydroponic solution (LUHS), artificial pore water (APW) and Hoagland solution (HS). The error bars convey standard deviation (n = 3) and the means with different letters are significantly different.

Generally, the roots exposed to the $Ag_2S$ NPs in all four media exhibited an overall increase in Ag concentrations during the experiment (Figure 4.4B, Table 2C, Appendix C). Specifically, the roots exposed to $Ag_2S$ NPs in Lufa soil display approximately stable Ag concentrations of about 1.2 ± 0.2 µg $g^{-1}$ between day 1 and 7; at day 14, however, a significantly higher ($p < 0.04$) Ag concentration of 4.2 ± 0.3 µg $g^{-1}$ was recorded. The Ag concentrations measured for the roots exposed to $Ag_2S$ NPs in the hydroponic solutions were identical at day 1 but they were significantly higher ($p < 0.03$) by more than a factor of x15 at day 3 (Figure 4.4B, Table 2C, Appendix C). After day 3, the Ag concentrations of the roots

grown in the hydroponic media remained constant for the remainder of the experiment with average Ag concentrations of 2.8 ± 1.1 µg $g^{-1}$ for the LUHS, of 2.1 ± 0.8 µg $g^{-1}$ for the APW, and of 2.9 ± 0.5 µg $g^{-1}$ for the HS (Figure 4.4B, Table 2C, Appendix C).

The roots exposed to $AgNO_3$ in Lufa soil showed small increases in Ag concentration with time (Figure 4.4C, Table 2C, Appendix C). In detail, the roots in the Lufa soil showed Ag concentrations of about 12.6 ± 1.3 µg $g^{-1}$ on days 1 and 3; the Ag concentrations increased thereafter ($p < 0.02$) and reached a maximum of 32.5 ± 5.9 µg on day 14. In contrast, the Ag concentrations of the roots exposed to $AgNO_3$ in LUHS remained nearly constant and low throughout, ranging between 5.7 ± 0.3 and 12.7 ± 1.3 µg $g^{-1}$. The roots of wheat grown in APW and HS showed very high initial (day 1) Ag concentrations of 83.8 ± 20.1 µg $g^{-1}$ for the APW and 130.3 ± 11.6 µg $g^{-1}$ for the HS. In both cases, the root Ag concentrations decreased gradually with time to levels of 24.0 ± 8.1 µg $g^{-1}$ for the APW and of 13.1 ± 5.0 µg $g^{-1}$ for the HS at day 14.

The mean Ag concentrations of the roots for the blank and coating control treatments (Table 2C, Appendix C) were 1.8 ± 0.4 µg $kg^{-1}$ for all media.

*4.3.4.2. Shoot tissues*

Overall, the Ag concentrations of the shoots exposed to all three Ag treatments in the four different media are lower by about a factor of x80 compared to the roots and less variable during the exposure (Figure 4.5, Table 3C, Appendix C). Notably, there is a clear systematic difference in shoot Ag concentrations at the end of the exposure between the treatments with decreasing concentrations in the order Ag NPs > $Ag_2S$ NPs > $AgNO_3$.

The Ag concentrations for the shoots from wheat exposed to the Ag NPs show no statistically significant ($p > 0.5$) changes for the duration of the experiment, with the exception of the shoots grown in APW at day 3, which were significantly higher ($p < 0.04$) (Figure 4.5A, Table 3C, Appendix C). In detail, the shoots exposed to Ag NPs showed mean Ag concentrations for days 1 to 14 of 0.51 ± 0.15 µg $g^{-1}$ for the Lufa soil, of 0.27 ± 0.17 µg $g^{-1}$ for the LUHS, of 0.88 ± 0.46 µg $g^{-1}$ for the APW and of 0.94 ± 0.23 µg $g^{-1}$ for the HS.

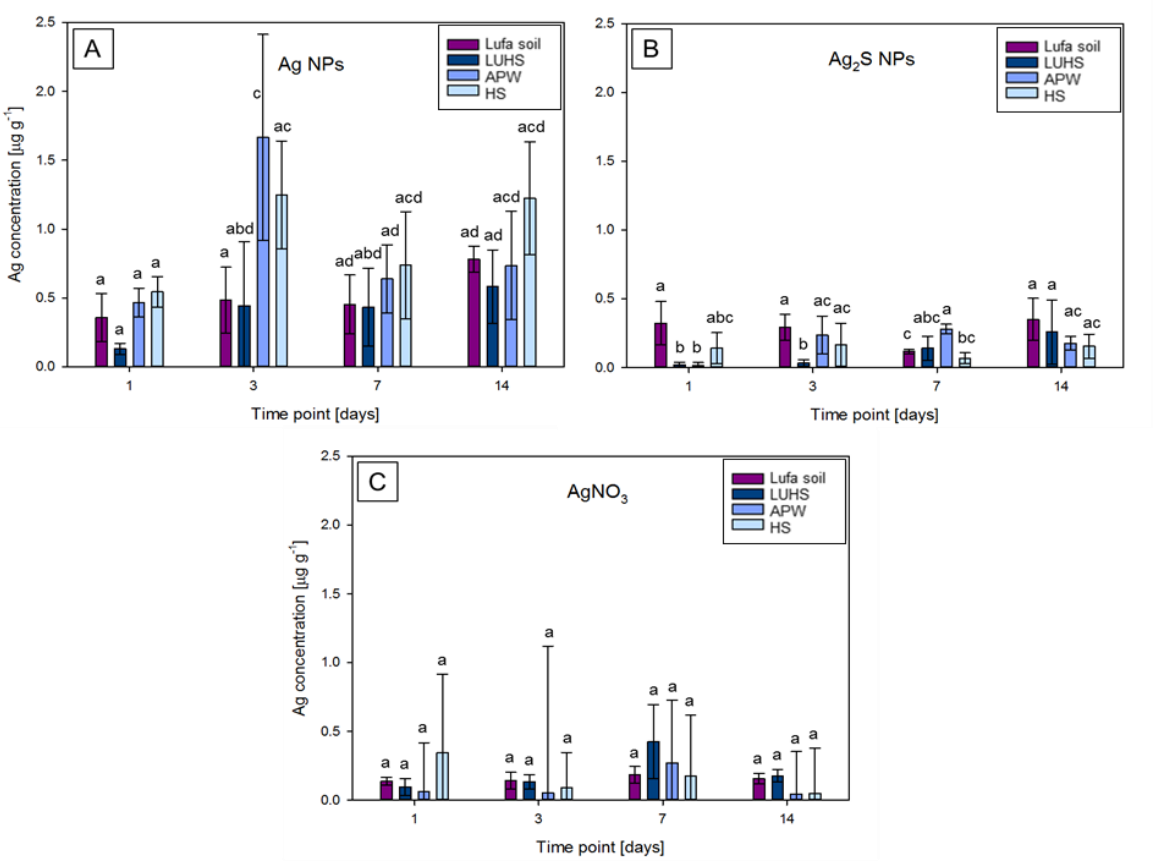



*Figure 4.5.* Mean Ag concentrations measured for the shoots exposed to Ag NPs (A), $Ag_2S$ NPs (B) and $AgNO_3$ (C) for the different media including the Lufa soil, Lufa soil hydroponic solution (LUHS), artificial pore water (APW) and Hoagland solution (HS). Here, the error bars signify standard deviation (n = 3) and the means with different letters are statistically different.

In comparison, the shoots exposed to the $Ag_2S$ NPs in all media generally had lower Ag concentrations (Figure 4.5B, Table 3C, Appendix C). In addition, the different media yield more variable results, except for day 14, when the shoots grown in all four media have statistically indistinguishable Ag concentrations ($p > 0.1$). Specifically, at this final time point, the shoot Ag concentrations for the $Ag_2S$ NP treatment are 0.28 ± 0.10 µg $g^{-1}$ for the Lufa soil, 0.11 ± 0.09 µg $g^{-1}$ for the LUHS, 0.18 ± 0.04 µg $g^{-1}$ for the APW and 0.13 ± 0.04 µg $g^{-1}$ for the HS.

The Ag concentrations of the shoots exposed to $AgNO_3$ in all four media were statistically identical ($p > 0.2$) throughout the 14-day experiment (Figure 4.5C, Table 3C, Appendix C). The shoot Ag concentrations were thereby similar but with more variation to those observed for the shoots exposed to $Ag_2S$ NPs, with

average values (for days 1 to 14) of between 0.15 ± 0.02 µg $g^{-1}$ and 0.55 ± 0.33 µg $g^{-1}$ for all media.

The Ag concentrations of the shoots from the two control treatments were close to or lower than the analytical detection limit, with mean results of 0.87 ± 0.41 µg $kg^{-1}$ for all media (Table 3C, Appendix C).

*4.3.5. Dry plant biomass*

The dry plant biomass encompasses the masses of both wheat root and shoot and the data presentation focuses on the final values for day 14 but the results for all time points are available in the Appendix (Figure 4.6, Table 4C, Appendix C).

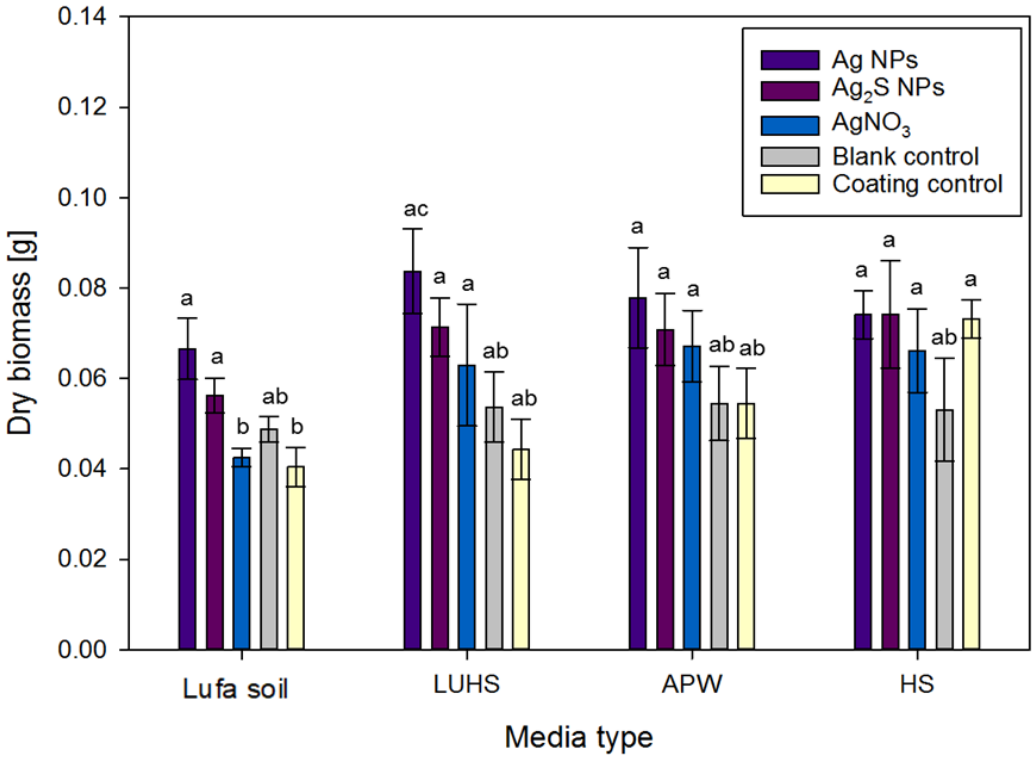



*Figure 4.6.* Total dry biomass (in g) recorded for the plants grown in Lufa soil, Lufa soil hydroponic solution (LUHS), artificial pore water (APW) and Hoagland solution (HS) at day 14. The error bars signify standard deviation (n = 3) where the means with different letters are significantly different.

The plants exposed to the Ag NPs and $Ag_2S$ NPs grown in the Lufa soil medium showed statistically increased ($p < 0.001$) dry biomasses compared to the $AgNO_3$ treatment and the blank and coating controls. Unlike the other two Ag treatments,

the dry biomass for the plants exposed to $AgNO_3$ in the Lufa soil medium indicated similar ($p = 1.0$) weight of 0.04 g to that of the two controls.

The dry biomass for the plants grown LUHS treated with Ag NPs demonstrated heightened biomass with $p < 0.04$ compared to the blank and coating controls. In contrast to the Ag NPs, the biomass for the plants treated with $Ag_2S$ NPs and $AgNO_3$ showed identical ($p > 0.07$) weight of approximately 0.05 g.

Unlike the Lufa soil and LUHS media, the biomass of the plants in the APW medium exhibited identical dry weight of about 0.06 g between all treatments with $p > 0.08$.

In a similar manner to the APW, the plants grown in the HS comprised of statistically similar ($p > 0.17$) dry biomass between all treatments with a mean weight of 0.07 g.

## 4.4. Discussion

### *4.4.1. Ag concentration in the media*

With one exception, all media sampled directly after spiking (day 0) with Ag NPs, $Ag_2S$ NP and $AgNO_3$, revealed consistent Ag concentrations with average recoveries of 96%, 95% and 98%, respectively. This is indicative of precise and suitably accurate dosing (Table 4.4). The single exception was observed for the initial Ag concentration of the Lufa soil medium spiked with $Ag_2S$ NPs. In this case, the day 0 Ag concentration was elevated by about 17% (or 1.7 mg $kg^{-1}$) relative to the nominal concentration of 10 mg $kg^{-1}$ (Figure 4.2). Most likely, this is either related to a soil weighing inaccuracy prior to dosing, or a pipetting error during dosing. However, this error is not deemed to be problematic as the LUPW extracted from the soils treated with $Ag_2S$ NPs had a Ag concentration of about 0.01 mg $L^{-1}$ as originally intended.

*Table 4.4.* Mean Ag concentrations (in mg $kg^{-1}$ or mg $L^{-1}$) and per cent of the nominal Ag concentrations at day 0 for all media including the Lufa soil, Lufa hydroponic solution, artificial pore water and Hoagland solution (n = 3).

| Media type | Ag NPs | | $Ag_2S$ NPs | | $AgNO_3$ | |
|---|---|---|---|---|---|---|
| | mg $kg^{-1}$ | % | mg $kg^{-1}$ | % | mg $kg^{-1}$ | % |
| **Lufa soil** | 9.8 | 98 | 11.7 | 117 | 9.4 | 95 |
| **Lufa soil pore water** | 0.02 | 84 | 0.01 | 88 | 0.02 | 102 |
| **Artificial pore water** | 0.02 | 105 | 0.01 | 104 | 0.02 | 100 |
| **Hoagland solution** | 0.02 | 100 | 0.01 | 92 | 0.02 | 106 |

#### *4.4.1.1. Ag concentration of the Lufa soil & LUPW*

Over the duration of the experiment, the Ag concentrations of the Lufa soils dosed with Ag NPs, $Ag_2S$ NPs and $AgNO_3$ showed a slight decline for all Ag treatments. In detail, the soils exhibited a reduction in Ag concentration of about 13% after day 1 and this reached approximately 15% by day 14 (Figure 4.2). The LUPW extracted from the soils of all three Ag treatments had essentially constant ($p = 0.12$) Ag concentrations for the duration of the experiment (Figure 4.3). The latter observation, most likely reflects equilibration of the soils with the soil solutions and replenishment of any Ag lost from the pore water phase by further dissolution of soil-bound Ag. However, less than 0.1% of the Ag present in the soil-plant systems was found in the analysed LUPW. As such, the release of soil-bound Ag into the LUPW phase alone cannot account for the low and declining Ag concentrations of the Lufa soils.

Given that the Lufa soils were not completely mineralised using HF prior to analysis but only partially digested using HCl and $HNO_3$, it is conceivable that the declining soil Ag concentrations reflect incomplete dissolution and/or reaction of the Ag with undigested soil particles. In this context, it is relevant that previous work has shown that Ag bound to undigested silicate particles of soils can contain up to 30% of the total Ag budget of a soil (Kvitek et al., 2011). Silver losses exceeding 5% due to these processes are unlikely for the current experiment, however, as soils that were analysed directly after the addition of the three Ag treatments (on day 0) exhibited Ag recoveries of > 95%. Furthermore, such

reactions are unlikely to generate soil Ag concentration that declines essentially systematically from day 0 to day 14 (Figure 4.2).

Close inspection of the Ag distribution in the Lufa soil systems treated with Ag NPs, $Ag_2S$ NPs and $AgNO_3$ at day 14 reveals that plant accumulation of Ag constitutes a negligible fraction of the total system Ag budget (Figure 4.7). In detail, the maximum plant uptake of 1.5 µg Ag is equivalent to less than 0.15% of the total Ag present in the systems (Figure 4.7, Table 5C, Appendix C). As such, uptake of Ag by the wheat seedlings cannot be the cause for the declining Ag concentrations of the soils. Given this, the most plausible explanation for the 15% decrease of soil Ag concentrations during the experiment is progressive adsorption of Ag from the soils via the soil solutions to the walls of the polyvinyl chloride containers (Figure 4.7, Table 5C, Appendix C). This agrees with the findings of Chapter 2, which revealed that about 25% of the Ag that was added to soils in the form of Ag NPs and $AgNO_3$ was later adsorbed to the walls of the exposure containers.

*4.4.1.2. Ag concentration of the hydroponic media*

The LUHS, APW and HS media that were dosed with the three Ag treatments demonstrated a gradual temporal decrease in Ag concentrations between day 0 and day 14, whereby the total loss of Ag by day 14 was much more severe than that observed for the soil medium (Figure 4.3). In detail, the Ag concentrations of the hydroponic media at day 14 had decreased relative to the initial concentration at day 0 by about 57% for the Ag NP treatment, by 73% for the $Ag_2S$ NP treatment and by 80% for the $AgNO_3$ treatment. The possible reasons for this decline are discussed in the following.

For the hydroponic solutions, incomplete digestion and adsorption onto undigested soil particles cannot be responsible for the decreasing Ag concentrations. However, in contrast to the soil pore waters, the Ag distribution for the hydroponic systems at days 7 and 14 reveals that a large proportion of the Ag is present in the wheat plants. In detail, up to 37%, 36% and 70% of the Ag present in the hydroponic systems was concentrated in the plants for the Ag NP, the $Ag_2S$ NP and the $AgNO_3$ treatments, respectively (Figure 4.7). Notably, a large proportion of the Ag found in the plants was associated with the roots,

where the Ag can be either adsorbed onto the root surfaces or internalised. Regardless of where the Ag was located, Ag associated with the plants played an important role in the Ag distribution of the hydroponic exposure systems. Despite of this, between 9% and 42% of the days 7 and 14 Ag budgets of the hydroponic systems were not present in the plants or the exposure media. By exclusion, this Ag was most likely lost from the solutions to adsorption onto the walls of the polypropylene containers. This is in accord with previous work, which showed that dissolved Ag readily adsorbs to plastics, such as polycarbonate and polypropylene, whereby such adsorption reactions can readily reduce the Ag concentrations of hydroponic media by approximately 20% (Sekine et al., 2015).

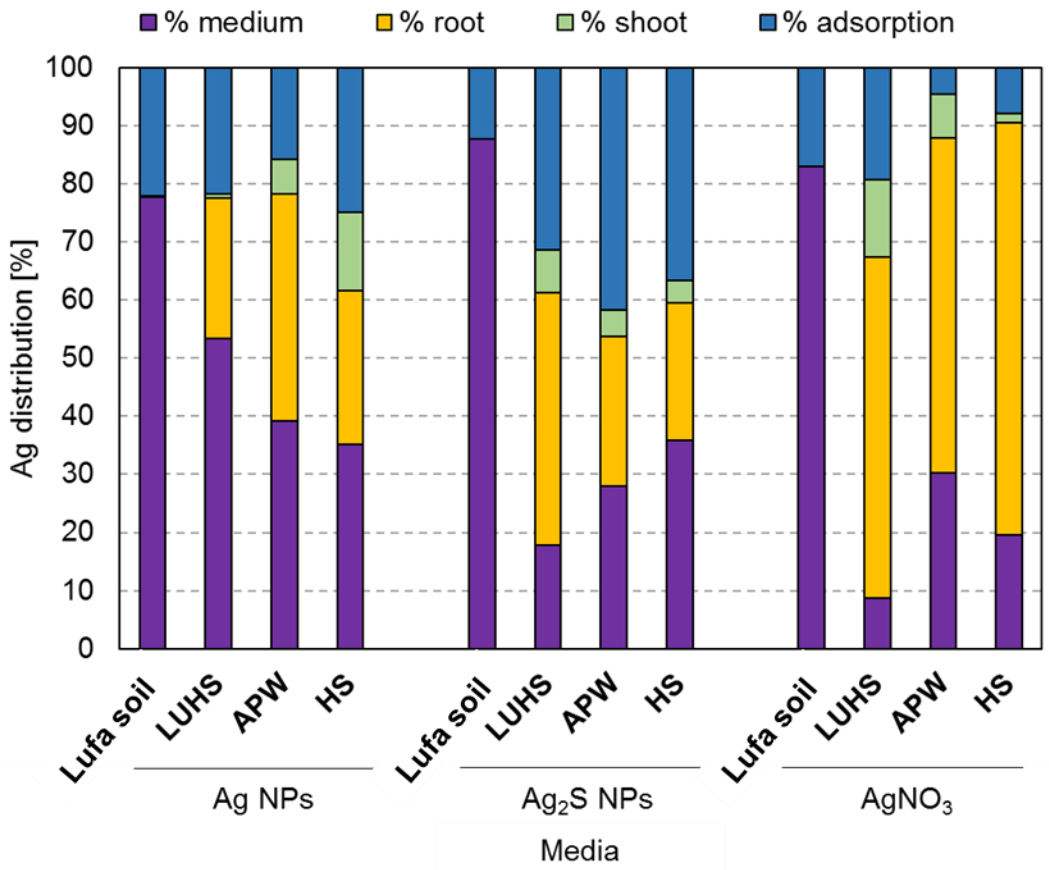



*Figure 4.7.* Mean Ag distribution for the Lufa soil, Lufa hydroponic solution (LUHS), artificial pore water (APW) and Hoagland solution (HS) systems for days 7 and 14 (n = 3). The distributions were determined by mass balance calculations for the different compartments, which are exposure medium (soil or hydroponic solution) as well as root and shoot tissues. For each system, the maximum value of 100% was defined by the Ag mass that was introduced into the system at the beginning of the exposure. Any Ag that was not found in any of the medium or plant tissue compartments was assumed to be adsorbed to the container walls. As the extracted LUPW contains less than 0.01% of the Ag for exposures carried out in Lufa soil, this reservoir cannot be seen at the scale of the figure and it is hence ignored.

*4.4.2. Ag associated with the roots*

The roots had the highest Ag concentrations of the plant tissues and as such comprised of about 90% of the total Ag present in the wheat seedlings for all media and Ag treatments (Figure 4.7). This is in accord with previous work (Wang et al., 2012; Yin et al., 2011; Stegemeier et al., 2015; Ma et al., 2010; Geisler-Lee et al., 2014; Lowry et al., 2012). In this context, it should be noted that it remains unclear whether the majority of the Ag associated with the roots is adsorbed or internalised even though the roots were thoroughly washed with both deionised water and EDTA to remove any adsorbed Ag. However, a previous foliar exposure study showed that the washing of lettuce leaves treated with Ag NPs removed only about 2% of the total deposited Ag from the leaf surfaces (Larue et al., 2014).

In general, the roots exposed to Ag NPs showed low and stable Ag concentrations for all media until day 3, at which point the Ag concentrations increased by approximately x7 for the Lufa soil but remained stable and relatively unchanged for the hydroponic media (Figure 4.4A). In this case, the Ag concentrations determined for the roots seem to reflect the Ag concentrations of the exposure media. In detail, the increasing Ag concentrations of the roots grown in the Lufa soil reflect the high and stable Ag concentrations found for the extracted LUPW, whereby the latter is a consequence of constant replenishment of the Ag budget from the large Ag reservoir of the soil phase (Figures 4.2 and 4.3). In contrast, the lower Ag concentrations of the roots exposed to Ag NPs grown in the hydroponic media can be attributed to the decreasing Ag concentrations in the media, which were up to 3x lower compared to those of the LUPW (Figure 4.3A). In this case, up to about 25% of the Ag present in the systems was inferred to be adsorbed to the exposure containers, with more Ag of up to nearly 40% probably adsorbed to the root surfaces (Figure 4.7). The similar Ag concentrations that were recorded for the roots of the hydroponic media dosed with Ag NPs furthermore suggest that these systems were associated with similar speciation of Ag, both within the solutions as well as on, and within, the wheat roots. This speculative conclusion, however, requires further confirmation from more detailed experiments.

The roots exposed to the $Ag_2S$ NPs consistently showed the lowest Ag concentrations among the three Ag treatments and only limited variations in Ag abundances (Figure 4.4B and C). The former observation, most likely reflects the comparatively low solubility of the $Ag_2S$ NPs in the media (Figure 4.3). This finding is in accord with previous work, which also found relatively low Ag concentrations for plant tissues exposed to $Ag_2S$ NPs in a soil medium (Doolette et al., 2015; Wang et al., 2016). In the current study, the wheat roots exposed to $Ag_2S$ NPs had somewhat higher Ag concentrations at day 14 when they were grown in Lufa soil compared to the hydroponic media (Figures 4.4B and C). Most likely this can be attributed to the higher Ag concentrations found in the extracted LUPW compared to the hydroponic solutions, as the former was constantly replenished from the large Ag inventory present in the soils (Figures 4.2 and 4.3). Furthermore, the Ag distribution for the hydroponic systems indicates that between 24% and 43% of the Ag present in the experiments was adsorbed to the walls of the exposure containers (Figure 4.7). Due to the particularly high extent of this adsorption for the $Ag_2S$ NP treatment, less total Ag was available in the media for root adsorption and internalisation (Figure 4.7).

The Ag concentrations of roots from the $AgNO_3$ treatment showed quite divergent results during the course of the experiment for the different media. However, on day 14 the roots from all four media had comparatively similar Ag concentrations of between 7.7 μg $g^{-1}$ and 32.5 μg $g^{-1}$ (Figure 4.4D). In detail, the roots grown in the Lufa soil revealed gradually increasing Ag contents, from about 10 μg $g^{-1}$ at day 1 to approximately 33 μg $g^{-1}$ at day 14. This steady increase is well explained by the relatively stable Ag concentrations of the extracted LUPW, which are maintained by the release of Ag from the large soil reservoir to the pore water phase. The roots from the LUHS consistently have the lowest Ag concentrations for the $AgNO_3$ treatment. Most likely, this reflects increasing Ag adsorption from the medium to the surfaces of the polypropylene containers (Figure 4.7, Table 5C, Appendix C) in combination with limited Ag adsorption to and uptake by the wheat roots until day 14.

The roots exposed to $AgNO_3$ in APW and HS show a similar and significant decrease in Ag concentrations from roughly 100 μg $g^{-1}$ at day 1 to about 20 μg $g^{-1}$ at day 14. This intriguing trend is most likely a consequence of adsorption and re-

equilibration reactions within the hydroponic systems. Initially, large amounts of Ag were quickly adsorbed to the roots of the wheat seedlings, leading to very high root Ag concentrations at the start of the experiment. With time, the high Ag concentrations associated with the roots declined due to growth of the roots, which increased in mass by about x3 to x5 during the exposure (Table 4C, Appendix C), whilst the amount of root-adsorbed Ag remained either relatively constant or decreased with time (Figure 2C C and D, Appendix C). The latter observation indicates that Ag initially adsorbed to the roots was released back into the hydroponic solutions to be re-adsorbed onto the container walls. Most likely, this reflects that kinetic factors (faster adsorption) favoured high initial Ag roots concentrations, whilst thermodynamic factors (stronger adsorption) favoured more adsorption to the container walls during the course of the exposure.

*4.4.3. Ag uptake & translocation*

Compared to the roots, the Ag concentrations of the shoots grown in the four media and exposed to the different Ag treatments were relatively low and stable throughout the exposure with no clear temporal trends (Figure 4.5). In detail, the shoots exposed to Ag NPs showed the highest day 14 Ag concentrations of about 0.7 µg $g^{-1}$, whereas the shoots from the $Ag_2S$ NP and the $AgNO_3$ treatments had Ag concentrations that were roughly x3 lower ($p = 0.03$) with a mean of about 0.3 µg $g^{-1}$. This small but significant difference most likely reflects that the Ag NP treatments maintained the highest Ag concentrations in both the pore water phase (for the Lufa soil medium) and the hydroponic media (Figure 4.3).

To compare the uptake and accumulation of Ag by the shoots grown in soils versus those grown in hydroponics, the mean $[Ag]_{Shoot}/[Ag]_{Root}$ and the $[Ag]_{Shoot}/[Ag]_{Medium}$ ratios determined for days 7 and 14, were investigated. In this case, the compilation of data from two subsequent days served to improve the statistical significance of the results. Inspection of the $[Ag]_{Shoot}/[Ag]_{Root}$ data reveals consistently low ratios of between 0.01 and 0.12 (Figure 4.8, Table 6C, Appendix C). These results are unsurprising, however, because they reflect the high Ag concentrations of the roots, which are caused by both Ag adsorption to

the root surfaces and internalisation. Notably, the extent of Ag adsorption versus internalisation is uncertain and likely variable for the different media and treatments. As such, the $[Ag]_{Shoot}/[Ag]_{Root}$ ratios that were determined here are not suitable for robust evaluation of Ag translocation within the seedlings and the results will therefore not be considered further in the following.

However, the $[Ag]_{Shoot}/[Ag]_{Medium}$ ratios that were determined for the samples from days 7 and 14 enable a robust evaluation of the uptake and accumulation of Ag by the wheat seedlings because they do not encompass the Ag data for the roots (Figure 4.9, Table 7C, Appendix C). To enable a meaningful comparison of the results obtained for the exposures carried out in Lufa soil versus the hydroponic media, the LUPW Ag concentrations were used as the medium concentrations for the former. The use of LUPW for these ratio calculations is in agreement with the results of the current experiment, Chapter 2 and published studies (Lee et al., 2011; Tangahu et al., 2011), which show that plant uptake of Ag from soils is governed by the Ag concentrations of the soil solutions.

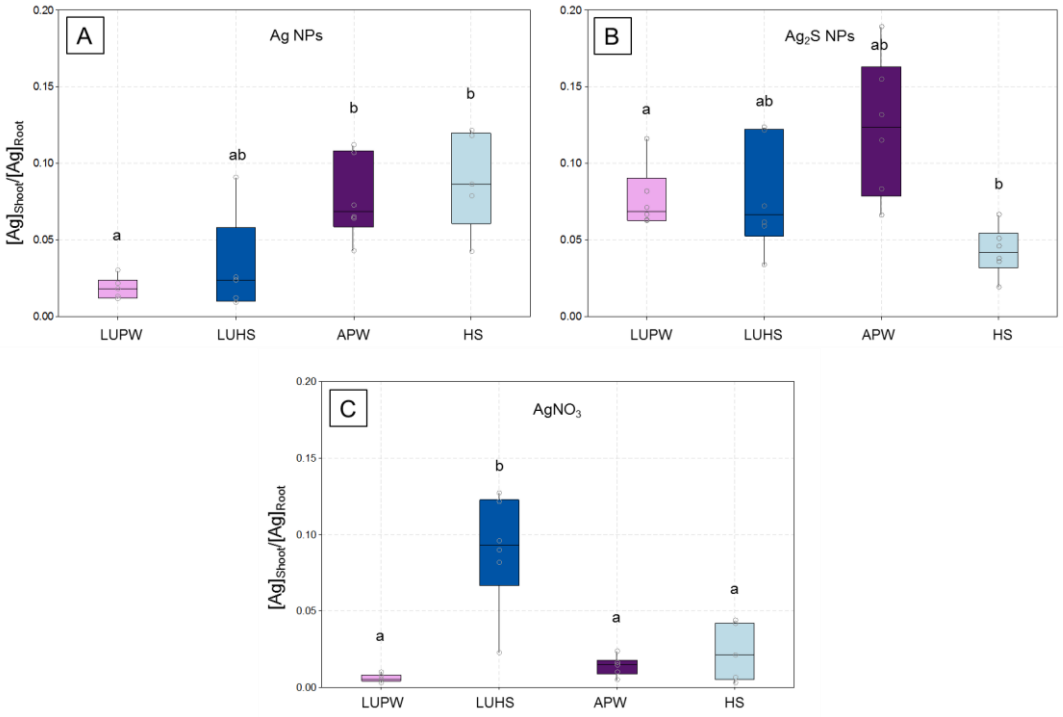



*Figure 4.8.* Plots of $[Ag]_{Shoot}/[Ag]_{Root}$ ratios determined for samples from days 7 and 14 (n = 6).

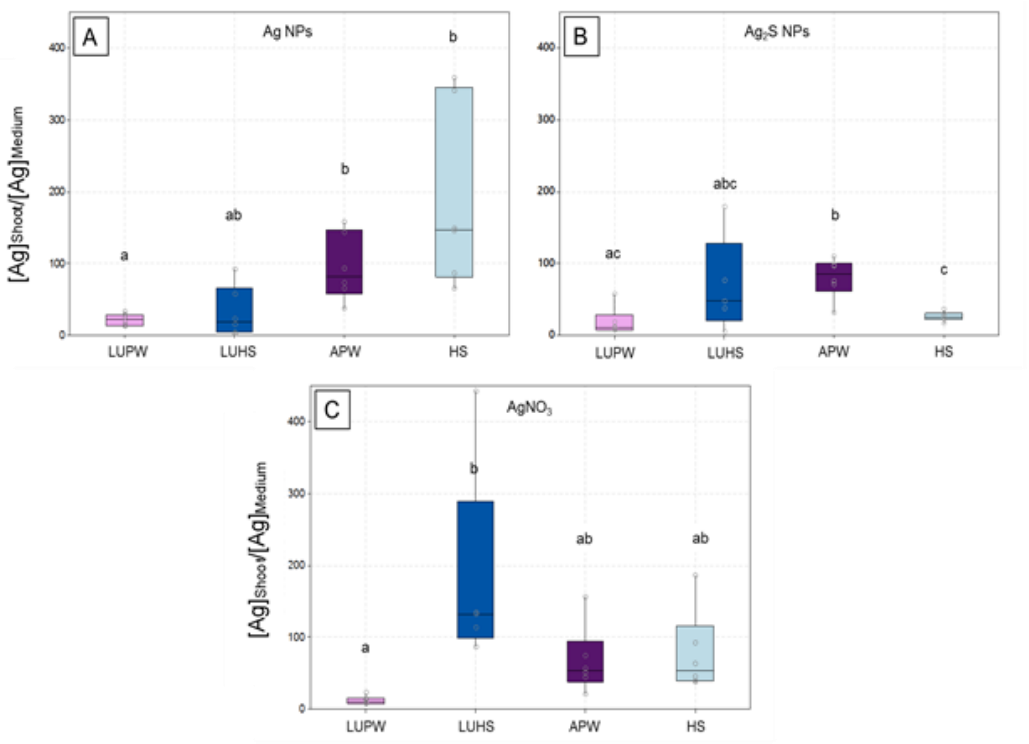



*Figure 4.9.* Plots of $[Ag]_{Shoot}/[Ag]_{Medium}$ ratios that characterise bioaccumulation of Ag in the wheat seedlings determined for samples collected at days 7 and 14 (n = 6).

Overall, the $[Ag]_{Shoot}/[Ag]_{Medium}$ ratios for the Ag treatments in the LUPW are similarly low, with a mean value of 18. In contrast, the hydroponically grown plants exhibit more variable and generally higher $[Ag]_{Shoot}/[Ag]_{Medium}$ ratios of between 4 and 442. To place these new results into context, previous Ag studies also found low $[Ag]_{Shoot}/[Ag]_{Medium}$ ratios of 0.06 to 5.04 for grasses grown on natural soils, whilst much higher ratios ranging between 2,100 and 124,000 were determined for grasses grown in hydroponic systems (Ratte et al., 1999).

In the current study, the $[Ag]_{Shoot}/[Ag]_{Medium}$ data for the Ag NP treatment reveal low ratios of about 22 for the LUPW medium and similar results (with $p > 0.05$) were obtained for the LUHS (Figure 4.9). As such, the data indicate that bioaccumulation of Ag from Ag NPs in these two media was similar, with no evidence for significant differences in Ag speciation between the two systems. Further research is required, however, to confirm the latter conclusion. In comparison, the Ag NP treatments in APW and HS were associated with more variable and statistically higher $[Ag]_{Shoot}/[Ag]_{Medium}$ ratios of between 38 and 358.

The $[Ag]_{Shoot}/[Ag]_{Medium}$ ratios for the $Ag_2S$ NP treatments in LUPW and HS are both low and statistically identical ($p > 0.4$) with individual results of between about 20 and 30 (Figure 4.9). In contrast, the $[Ag]_{Shoot}/[Ag]_{Medium}$ ratios for the $Ag_2S$ NP treatments in LUHS and APW were more variable and generally higher, with mean values of approximately 76. As such, these results are indicative of similar Ag accumulation behaviour, and possibly similar Ag speciation, in the LUPW and HS hydroponic systems.

For the $AgNO_3$ treatments, the lowest and least variable mean $[Ag]_{Shoot}/[Ag]_{Medium}$ ratio of about 13 was obtained for the LUPW medium (Figure 4.9). In contrast more variable and generally higher $[Ag]_{Shoot}/[Ag]_{Medium}$ ratios were determined for the three hydroponic media with mean results of between 13 and 182. Nevertheless, the results obtained for the APW and HS media were found to be statistically similar ($p > 0.1$) to the data for the LUHS. This observation indicates that uptake and accumulation of Ag derived from $AgNO_3$ by the wheat seedlings was similar for all three hydroponic media.

## 4.5. Conclusion

This is the first study to directly compare the Ag uptake by wheat plants grown in soil versus different hydroponic media in order to assess the relevance of hydroponic studies in nano-ecotoxicological exposures. To this end, wheat seedlings were exposed to three different Ag treatments, with Ag NPs, $Ag_2S$ NPs and $AgNO_3$, in Lufa soil and three different hydroponic media for 14 days. Analyses of the Ag concentrations of the media and plant tissues collected during and after the conclusion of the exposure offer several important observations and conclusions.

The Ag concentrations of the soils and the hydroponic media from all Ag treatments declined during the course of the experiment, by a total of about 15% for the soils and by up to nearly 80% for the hydroponic media. Inspection of the Ag distribution revealed that the decrease in soil Ag concentrations was caused by adsorption of Ag to the surfaces of the exposure containers. In contrast, the Ag distributions in the hydroponic systems showed that up to nearly 75% of the

Ag loss from the media was due to adsorption to or uptake by plant tissues, whilst up to 45% of the loss was from adsorption to the exposure containers.

Overall, up to 90% of the Ag budget determined for the plant tissues were associated with the roots, which had variable final (day 14) Ag concentrations of between 2.1 and 56.2 µg $g^{-1}$. The remaining 10% of the plant Ag budget was concentrated in the shoots, which had day 14 Ag concentrations, which were roughly 40x lower than those of the roots, with values of 0.1 to 1.2 µg $g^{-1}$. In detail, the final Ag concentrations for the roots from plants grown in Lufa soil were generally higher than those of plants cultured in the hydroponic media, whereby the latter revealed similar Ag concentrations for all three Ag treatments. The soil results are thought to be a consequence of the high and stable Ag concentrations of the extracted LUPW, which were replenished from the large Ag reservoir of the soil phase. In contrast, the Ag concentrations of roots from hydroponic systems were most likely limited by strong adsorption of a significant fraction of the total Ag available in the systems to the container walls.

The data provide also evidence that the high root Ag concentrations are not only a consequence of Ag uptake and internalisation but also reflect adsorption of Ag to root surfaces. In particular, this is demonstrated by the high initial (day 1) Ag concentrations of roots from wheat seedlings exposed to $AgNO_3$ in APW and HS, which subsequently decreased steadily from day 1 to day 14. These observations could be explained by fast initial Ag adsorption to root surfaces followed by slow release of the adsorbed Ag into solution and subsequent re-adsorption onto the container walls. Given that the three hydroponic media overall featured similar Ag distributions at day 14 for all three Ag treatments, the results suggest that all hydroponic exposures were associated with significant adsorption of Ag to the root surfaces. As such, the measured root Ag concentrations are only of limited value to characterise the translocation of Ag in the wheat seedlings based on $[Ag]_{Shoot}/[Ag]_{Root}$ ratios.

Compared to the roots, the shoots featured much lower and more stable Ag concentrations during the exposures. The shoot Ag concentrations were highest for the Ag NP treatment and similar, albeit at a lower level, for the $Ag_2S$ NP and $AgNO_3$ treatments. However, statistically identical Ag concentrations were

determined for the shoots from wheat grown in the Lufa soil and the hydroponic systems for all three Ag treatments. This indicates that hydroponic studies may be a simple and suitable alternative to exposures in soils to characterise Ag accumulation in plant shoots. This conclusion is reinforced by the observation that the bioaccumulation of Ag, as characterised by $[Ag]_{Shoot}/[Ag]_{Medium}$ ratios, was not substantially different for the LUPW and the three different hydroponic media, regardless of the Ag treatment. In addition, there were no statistically significant differences in the dry biomasses of wheat seedlings cultured in the Lufa soil and the hydroponic systems.

Overall, the results show some differences in Ag distribution between the soil exposure and the three hydroponic exposure systems. However, these differences are generally not severe and there are many similarities in the Ag distribution across the four exposure systems for the three different Ag treatments. As such, hydroponic systems can provide a simple and straightforward means to carry out preliminary assessments of Ag distribution in agricultural systems.

# Chapter 5: Xylem- & phloem-based transport of Ag NPs in wheat

## 5.1. Introduction

As observed in previous studies and Chapters 2 and 4, there is ample evidence that silver (Ag) derived from Ag nanoparticles (Ag NPs) released into soils can be taken up through the roots and transported to aboveground plant tissues (Tkalec et al., 2019; Ma et al., 2010; Yin et al., 2011; Geisler-Lee et al., 2013). Plant ecotoxicology studies on the Ag uptake and accumulation from Ag NPs have reported Ag aggregation in the root tips (Geisler-Lee et al., 2013) and limited Ag translocation to the shoots (Ma et al., 2010; Yin et al., 2011; Geisler-Lee et al., 2013). Previous studies suggest that Ag from Ag NPs and $AgNO_3$ can be transported along the apoplast to reach the cortex and vascular tissues (Tkalec et al., 2019) for xylem transport from root-to-shoot. However, the current literature lacks studies on the downward movement of Ag NPs from the shoots-to-roots via the phloem (Ma et al., 2017). One way to trace the phloem system movement is through Ag concentration analysis of roots and shoots in a split root exposure to Ag NPs. To date, two hydroponic split root experiments have reported xylem and phloem movement of copper (Cu) and cerium (Ce) for exposures of maize and cucumber to CuO NPs and $CeO_2$ NPs (Wang et al., 2012; Ma et al., 2017). However, there is little evidence that Ag from Ag NPs is indeed transported in wheat through the phloem.

As well as evidence for phloem transport, split root experiments may also provide information on the uptake and accumulation of Ag from Ag NPs and ionic $Ag^+$ under water stress conditions, by providing only a limited supply of water to one root side. This is of interest as agricultural soils are heterogeneous systems and the roots of a single plant commonly experience different conditions (Kirkham, 1980), whereby water may not always be evenly available. As water can move by capillarity from one part of the root system to another when the water supply is limited (Kirkham, 1980), this transport may potentially have a significant impact on the uptake and translocation of Ag from Ag NPs and $AgNO_3$ in plants.

The current study aimed to investigate the xylem and phloem transport of Ag in wheat plants by splitting the roots of wheat plants between soil treated with Ag and normal untreated soil. The underlying hypothesis of the study approach was that Ag will be transported from the roots in treated soils to the roots in the untreated soils via the shoot of the plant (Figure 1A). To accomplish this, two split root experiments were performed using containers with two soil compartments, where one was treated with Ag NPs or $AgNO_3$ and the other one was untreated (Figure 1B and C). The first split root experiment aimed to obtain information on the xylem- and phloem-based transport of Ag at water-limited conditions. Here, soils were treated with 20 nm polyvinylpyrrolidone (PVP) capped Ag NPs at concentrations of 10 mg $kg^{-1}$ and 50 mg $kg^{-1}$ for 'wet-wet' and 'wet-dry' exposures. The wet-wet exposure encompassed treated wet soil and untreated wet soil kept at 60% water holding capacity, while in the wet-dry exposure consisted of one Ag NP treated wet soil kept at 60% water holding capacity and an untreated dry soil at 30% water holding capacity. Plant tissues of wheat seedlings (*Triticum aestivum L.*) including treated roots, untreated roots and shoots were collected after seven days and analysed for Ag content.

The second split root experiment aimed to compare and quantify Ag uptake by and accumulation in wheat seedlings (*Triticum aestivum L.*) exposed to 20 nm PVP-capped Ag NPs and $AgNO_3$ at Ag concentrations of 10 mg $kg^{-1}$ and under water stress (Figure 1B). Soil, soil pore waters and plant tissue samples including treated roots, untreated roots and shoots were taken at 3 time points over seven days and processed for Ag concentration analysis.

## 5.2. Experimental design & methodology

In the current study, two different split root exposures were carried out in a system with two soil compartments: one contained treated soil and one held untreated soil (Figure 5.1C). For the first test, referred to as 'Ag NP exposure', soils dosed with Ag NPs at concentrations of 10 mg $kg^{-1}$ and 50 mg $kg^{-1}$ were used in 'wet-wet' and 'wet-dry' exposures. For the wet-wet exposures, roots of wheat seedlings were divided between Ag NP treated wet soil and untreated wet soil, both of which were kept at 60% water holding capacity. In contrast, for the

wet-dry exposure roots of wheat seedlings were split between Ag NP treated wet soil kept at 60% water holding capacity and an untreated dry soil at 30% water holding capacity. For the second split root experiment or the 'time series exposure', roots of wheat seedlings were split between soils dosed with Ag NPs or $AgNO_3$ to Ag concentration of 10 mg $kg^{-1}$ and an untreated dry control soil in a wet-dry exposure. These exposure conditions were chosen to mimic conditions of uneven water availability. Here the roots of wheat seedlings were split between Ag NP or $AgNO_3$ treated soil kept at 60% water holding capacity and an untreated control soil at 30% water holding capacity.

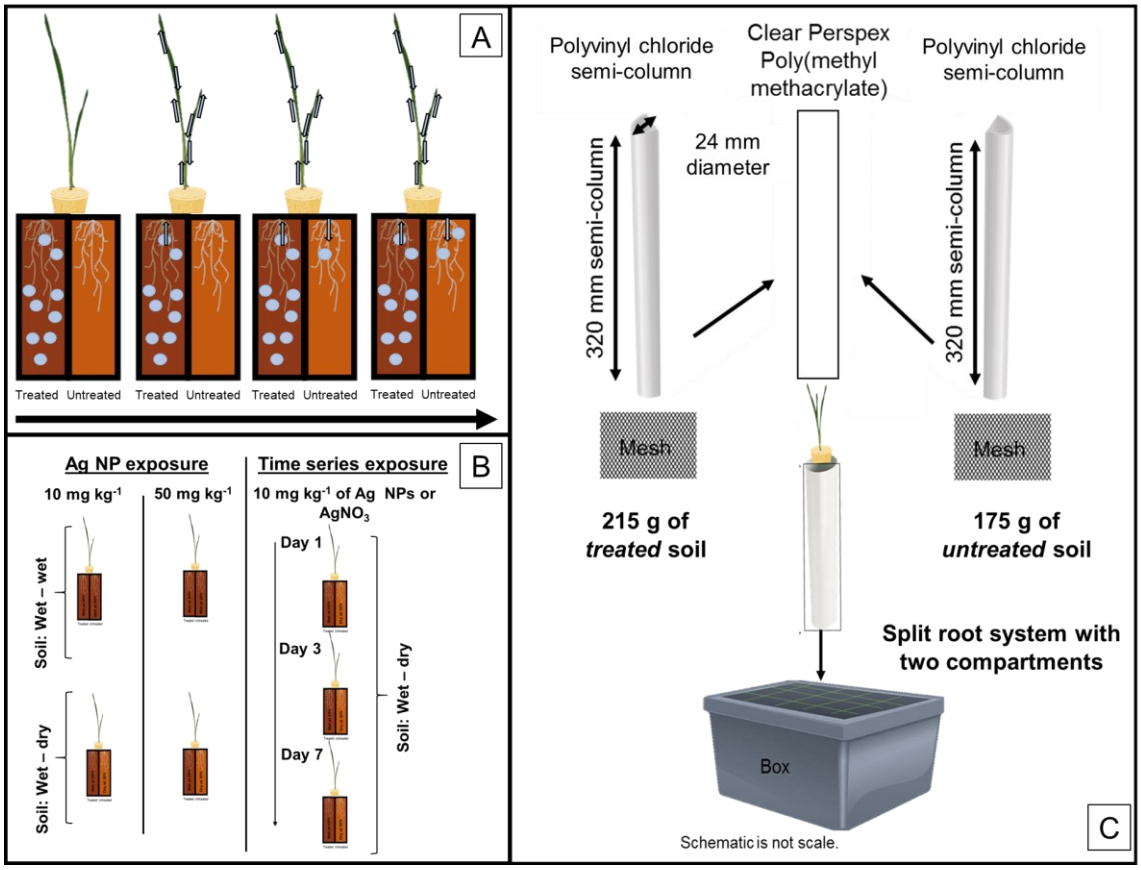



*Figure 5.1.* Schematic diagram of the hypothesis (A), the exposure experiments (B), and experimental setup (C).

### *5.2.1. Ag NPs*

For both split root exposures, 20 nm PVP-coated Ag NPs were synthesised by Applied Nanoparticles, Barcelona, Spain. The hydrodynamic diameter of the NPs was measured by Dynamic Light Scattering (DLS) using a Malvern Zetasizer

Nano ZS90 (Malvern Instruments) instrument. In addition, size, size distribution and particles shape were characterised with a JEOL1010 Transmission Electron Microscope (TEM).

### *5.2.2. Soil*

Lufa 2.2 soil (LUFA-Speyer 2.2, Germany, 2018) is a loamy sand soil with a total organic carbon of 1.61 ± 0.15 %; a $pH_{CaCl_2}$ value of 5.4 ± 0.2; and cation exchange capacity of 9.7 ± 0.4 meq per 100 g. The soil was sieved to a particle size of 2 mm by the distributer and air-dried before the exposure. A 100% water holding capacity of 36 mL per 100 g of soil was determined for Lufa 2.2 using standard techniques (Priha and Smolander, 1999).

### *5.2.3. Exposure system*

Each exposure container consisted of two polyvinyl chloride semi-column compartments with a length of 320 mm and a diameter of 24 mm; a mesh attached to the bottom of each container allowed drainage (Figure 5.1). The two semi-column compartments were separated by a Perspex sheet with dimensions of 14.5 mm x 50 mm x 320 mm (depth x width x height) and secured together with cable ties. One compartment was filled with 215 g of soil treated with Ag NPs or $AgNO_3$ whilst the other was filled with 175 g of untreated soil. After filling, the columns were fixed into gridded boxes.

### *5.2.4. Planting of wheat*

Winter wheat (*Triticum aestivum L.*, Variety: KWS Dacanto) sourced from Københavns Universitet was used in the experiment. The seeds were kept refrigerated at 4°C in the dark and were not pre-treated in any way. Seeds of similar size and visual intactness (~0.8 cm in length and ~0.5 cm in width) were chosen. Seeds were initially germinated on filter paper for three days with 15 mL deionised water under controlled conditions (16 h light/8 h dark photoperiod; 20°C temperature). Following this, the wheat seeds were transferred to soil pots filled with untreated Lufa soil with a wicking system for further 18 days. For this study, one seedling was grown in a single container and represents a single replicate, where each treatment and timepoint encompassed three replicates.

Seedlings with three leaves and of similar fresh weight (≥ 0.65 g) were then transplanted into the split root exposure containers in the following manner. First, the roots were washed three times with deionised water to remove any large soil particles. The roots of seedlings were then separated into the primary root, which was placed in the treated soil, and secondary/lateral roots, which were placed in the untreated soil. The primary root was introduced to the treated side as the primary root is the main pathway for metal transport and higher transport of Ag is expected. Next, all root parts were placed onto about 80% of the soil and covered with roughly 10% of the soil. At this point, the two semi-columns were closed off and isolated from one another by the Perspex sheet and attached to each other to form a unit with cable ties. Next, each exposure system was fitted with a conical cork plug (32 mm diameter at the top and 30 mm diameter on the bottom) with a hole, through which each seedling was threaded. The plugholes were then filled with cotton wool (SLS) to support the vertical position of the seedling, whilst leaving enough space to ensure that growth of the seedling was not impeded. Finally, the last 10% of the soil were added to the semi-columns.

### *5.2.5. Experimental design & test conditions*

The exposure was performed at controlled conditions of 20°C temperature, a 16 h light/8 h dark photoperiod at a light intensity of 350 ± 50 µE/$m^2$/s in a greenhouse chamber at the UK Centre for Ecology and Hydrology, Wallingford. The wet soils were maintained at 60% water holding capacity by weighing the containers and adding deionised water as required every 48 h. The untreated dry soils were not watered as preliminary tests showed that it was kept at 30-35% water holding capacity by water transfer via the roots from the treated wet soils. The positions of the containers and container racks were randomised every three days to minimise position effects in plant growth to make the growth conditions as comparable as possible (Measures et al., 1973).

### *5.2.6. Sample collection*

During sample collection, a small amount of stem and root tissues from a potential zone of cross-contamination were discarded to mitigate the risk of inaccurate results. The cross-contamination zone of approximately 1 cm length was located at the top of the Perspex separator, which split the root system

between the treated and untreated soils. This procedure was performed by initial collection of the shoot sample by carefully cutting the sample down to the zone of possible cross-contamination. This was followed by the removal and disposal of 1 cm of the stem and root tissue from the problematic area. Next, the exposure systems were fully dismantled for root and soil sample collection. After this, each seedling was split into the treated root, untreated root and shoot tissues. Root samples were first washed thoroughly with deionised water, soaked in 0.1 M aqueous ethylenediaminetetraacetic acid (EDTA) solution for approximately 3 mins, and then washed again at least three times with deionised water. The EDTA solution was prepared by dissolving the solid reagent (Fisher BioReagents) in Millipore water and adjustment of the pH value to 8 using NaOH. This solution was used as it is a well-known chelator that complexes a wide variety of metals (Flora and Pachauri, 2010). Prior to use, the EDTA solution was autoclaved at 121°C for 30 mins.

Subsequently, soil samples were obtained by the collection of a 7 g soil aliquot from each treated and untreated compartment. The collected soil and plant tissues were dried at 70ºC in an oven (Heratherm OGS180, Thermo Scientific) for seven days. Once dry, the samples were weighed with a Sartorius Toploader 140 MP8 balance and stored at room temperature.

### *5.2.7. Ag NP exposure*

#### *5.2.7.1. Soil preparation*

The split root exposure systems consisted of two compartments that were filled with soil dosed with Ag NPs and untreated soil for wet-wet and wet-dry exposures. In the wet-wet exposure, the roots of wheat seedlings were split between Ag NP treated soil and an untreated soil at 60% water holding capacity while the wet-dry exposure encompassed one soil side treated with Ag NPs at 60% water holding capacity and one untreated soil at 30% water holding capacity. The dosing of the treated soils was carried out with a fresh aqueous suspension of Ag NPs, which was sonicated for 30 mins before use to break up agglomeration. The Ag NP treatment was introduced into separate 2 kg batch of Lufa soil at nominal Ag concentrations of 10 mg $kg^{-1}$ or 50 mg $kg^{-1}$. The Ag-dosed soils were thoroughly mixed by breaking up wet clumps with the back of a spoon

until they were visibly homogenised with no remaining clumps. At this point, Ag-treated and untreated wet-wet soils were adjusted to 60% by addition of deionised water, while the water holding capacity for wet-dry soils were adjusted to 60% for the Ag NP treated wet soil and to 30% for the untreated dry soil. Finally, the soils were left to equilibrate for 72 h at 20°C in the dark.

*5.2.7.2. Sample collection*

For the Ag NP exposure, soil samples were collected straight after dosing (at day 0) and at day 7 and plant tissues were collected on day 7 in the manner outlined above.

*5.2.8. Time series exposure*

*5.2.8.1. Soil preparation*

The split root exposure systems featured two compartments that were filled with different soils. The first compartment contained Ag-treated wet soil, whilst the second had untreated dry soil. For the time series exposure, the Ag was added in the form of Ag NPs as well as readily soluble $AgNO_3$ (≥ 99% purity; ACS reagent grade, Sigma Aldrich) for comparison.

The treated wet soil was dosed with a freshly prepared aqueous solution of $AgNO_3$ and a fresh aqueous suspension of Ag NPs, which was sonicated for 30 mins before use. The two Ag treatments were introduced to separate 2 kg batches of Lufa soil at nominal Ag concentrations of 10 mg $kg^{-1}$. The Ag-dosed soils were thoroughly mixed by breaking up wet clumps with the back of a spoon until they were visibly homogenised with no remaining clumps. In a final step, the Ag-treated and untreated soils were adjusted to 60% and 30% water holding capacity, respectively with deionised water and then left to equilibrate for 72 h at 20°C in the dark.

The ‘control’ treatments were not dosed with Ag but were otherwise prepared in the same manner as the Ag treatments. As such, they also encompassed one compartment with wet soil and a second compartment with dry soil.

*5.2.8.2. Sample collection*

For the time series exposure, soil and soil pore water samples were collected on days 0, 1, 3 and 7 while plant tissue samples were collected at days 1, 3 and 7 for the Ag NP, $AgNO_3$ and blank control treatments. The soil and plant tissue samples were collected with the methods outlined above.

Soil pore waters were obtained using a sampling protocol described in detail by Lahive et al. (2017). To summarise, 34 g of soil were collected in 50 mL polypropylene centrifuge tubes, transferred to a dark temperature-controlled room (20°C) overnight, before determination of the water holding capacity on an additional small (7 g) soil aliquot. The 34 g of soil were then saturated to 100% water holding capacity, stirred gently and left to equilibrate overnight in a dark room at 20°C.

Approximately 31 g of the water-saturated soil were centrifuged for 1 h at 2000 g at 4°C through $CuSO_4$ preconditioned 25 mL filter inserts (with 0.45 µm PVDF filter membranes) filled with $CuSO_4$ preconditioned glass wool (Sigma Aldrich) and housed in a 50 mL centrifuge system (Thermo Scientific F2519-6). The glass wool and filter inserts were preconditioned by soaking overnight in 0.1 M $CuSO_4$ solution (99.995% purity, Sigma Aldrich) to reduce Ag adsorption. After the extraction, between 5 and 7 mL of soil pore water were separated and stored for determination of the total Ag concentrations. Small (1.5 ml) additional aliquots of the soil pore waters were further centrifuged for 3 h at 20800 g. The top 1 mL of supernatant was then withdrawn for the determination of the truly dissolved Ag concentrations of the soil pore waters. Following collection, all soil pore water samples were acidified with an equal volume of *aqua regia* (3-parts concentrated HCl (≥ 37% purity, TraceSELECT grade, Honeywell) + 1-part concentrated $HNO_3$ (≥ 69% purity, TraceSELECT grade, Honeywell) and stored at 4°C in the dark.

*5.2.9. Sample analysis*

*5.2.9.1. Sample preparation*

The samples were processed and analysed at the Department of Animal Ecology, Vrije Universiteit Amsterdam. The sample preparation for the shoots

and soils was performed in the following manner.

*Step 1.* For the shoot and soil samples, less than 100 mg and 130 mg of material, respectively, were digested without HF for analysis. The samples were first weighed to about ± 0.1 mg accuracy (Sartorius Type 1712 Analytical Balance) on weighing paper and transferred to digestion bombs. To each sample, 2 mL of a mixture consisting of 4-parts concentrated HCl (32 – 35%, Ultrex II Ultrapure, J.T. Baker) + 1-part concentrated $HNO_3$ (70%, Ultrex II Ultrapure, J.T. Baker) were added and the beakers were left open under an extraction hood for 15 mins to release acid fumes. The bomb vessels were then tightly sealed with a wrench and placed in a Binder furnace at 140°C for a digestion time of 7 h. After digestion, the samples were left overnight to cool to room temperature.

*Step 2.* The bombs were carefully opened with a wrench and any acid droplets on the tops or lids of the bombs were collected with a pipette. After this, 4 mL of deionised water were added to each bomb, the solutions were transferred into polystyrene tubes and left to stand for approximately 6 h. The sample tubes were then covered and stored at 4°C in the dark.

For the root samples, up to 30 mg of material were first weighed on weighing paper and transferred to glass vials. To each sample, 500 µL of a 7:1 mixture of $HNO_3$ (70%, Ultrex II Ultrapure, J.T. Baker) and $HClO_4$ (70%, Ultrex II Ultrapure, J.T. Baker) were added. The samples were then digested on DB 200/3 and DB – 3D Dri – Blocks using the following consecutive heating steps: 30 mins at 85°C, 30 mins at 130°C, 45 mins at 160°C and final evaporation to dryness at 180°C. Finally, the samples were stored at room temperature and freshly dissolved in 500 µL 1 M HCl prior to analysis.

All concentrations of the soils and plant tissues are reported for dry weight material.

*5.2.9.2. Graphite furnace atomic absorption spectroscopy (GF AAS)*

All plants and extracted soil pore water samples were analysed with a Perkin Elmer graphite furnace atomic absorption spectrometer (GF AAS; PinAAcle 900Z) equipped with a PinAAcle 900Z autosampler system. For the analyses, the instrument was first set up for Ag measurements and the autosampler tip was

cleaned with 96% ethanol and aligned within the graphite furnace. To improve instrument performance and data quality, a matrix modifier consisting of $Mg(NO_3)_2$ and $Pd(NO_3)_2$, was injected with each sample and standard solution.

Instrument calibration was achieved with four freshly prepared standard solutions with Ag concentrations of 10, 20, 30 and 40 µg $L^{-1}$, which were prepared from a common 4 mg $L^{-1}$ Ag stock (SCP Science). Sample analyses began once a calibration curve with a correlation coefficient of $R^2 > 0.98$ was obtained. The samples were analysed in order of increasing Ag concentrations and sample solutions that exceeded the calibration range were further diluted with 1 M HCl (Ultrex II Ultrapure, J.T. Baker). Between samples, the introduction system was rinsed with 10 µL of a mixture of ethanol and $HNO_3$.

The following quality control measures were adopted for the analyses. The tip alignment in the furnace was checked after every 20 analyses, to ensure samples were dispensing correctly. After every 7 to 13 sample analyses, the 20 µg $L^{-1}$ Ag standard was measured again and the calibration curve was adjusted if necessary or re-determined if the $R^2$ value was less than 0.98. Furthermore, fresh dilute Ag standard solutions were prepared and analysed to define a new calibration curve after every 80 analyses. For further quality control, additional reference material DOLT 4 (NRC - CNRC) for plants was analysed repeatedly (> x10) using the same methods that were applied for the samples/standards. These analyses revealed that the employed methods achieved performance characteristics in terms of reproducibility ± 0.03 µg $L^{-1}$. The Ag detection limit of the instrument was found to be 0.3 ± 0.1 µg $L^{-1}$.

*5.2.9.3. Flame AAS*

Due to the high Ag concentrations of the dosed soils, all soil samples were analysed with a Perkin Elmer AAnalyst 100 flame atomic absorption spectrometer. For the analyses, a calibration curve was produced by measurements of dilute Ag standard solutions with concentrations of 0.5, 1, 2 and 3 mg $L^{-1}$ that were prepared from a common Ag stock solution with 1000 mg Ag $L^{-1}$ (SCP Science). After a calibration curve with a correlation coefficient of $R^2 > 0.98$ was achieved, samples were analysed in order of increasing Ag

concentration. Any samples with Ag concentrations that exceeded the calibration range were diluted with Millipore water. For quality control, additional soil reference material ISE 989 (Wepal/Quasimeme) was analysed repeatedly (> x10) using the same methods that were applied for the samples/standards. These analyses revealed that the employed methods achieved performance characteristics in terms of reproducibility ± 0.03 mg $L^{-1}$. The detection limit of the instrument was 0.01 ± 0.01 mg $L^{-1}$.

### *5.2.10. Statistical analyses*

All statistical analyses were performed with SigmaPlot 13.0 and Minitab 18. For analyses of differences between treatments, media and Ag type, one-way ANOVA and two-way ANOVA analyses with a significance level of $p < 0.05$ were used. First, the Ag concentrations between the control and Na-citrate were compared. After no differences were established between the controls, the control data was compared to the Ag treatments. All errors have been reported as standard deviations.

## 5.3. Results

### *5.3.1. Characterisation of the Ag NPs*

The Ag NPs were supplied as an aqueous suspension of 20 nm PVP-coated Ag NPs. The TEM micrographs revealed an average diameter of 21.6 ± 6.0 nm and particles of spherical shape with a consistent size distribution while the DLS analyses provided an average hydrodynamic diameter of 20.6 ± 5.7 nm (Figure 1C, Appendix C).

### *5.3.2. Validity of the exposure experiment*

According to criteria set out in the OECD guidelines (OECD 208 and 227) for chemical testing of terrestrial plants, both experiments were valid as (i) the germination rate was recorded at 99%, (ii) the controls showed no visible phytotoxic effects such as chlorosis, necrosis, wilting, shoot or stem deformation throughout the experiments and (iii) the mean plant survival was 100% for the duration of the experiments.

### *5.3.3. Ag NP exposure*

Silver concentrations were determined for both wet-wet and wet-dry exposure types at day 0 and day 7 for the soil samples and at day 7 for the plant tissues.

#### *5.3.3.1. Soils*

The Ag concentrations for the treated wet soils dosed with 10 mg $kg^{-1}$ and 50 mg $kg^{-1}$ of Ag NPs were found to be decreasing from day 0 to day 7 for both the wet-wet and wet-dry exposures (Table 5.1). In summary, the Ag concentrations for the soils treated with 10 mg of Ag NPs $kg^{-1}$ for the wet-wet and wet-dry exposures declined from 9.8 mg $kg^{-1}$ and 9.9 mg $kg^{-1}$ respectively to roughly 9.3 mg $kg^{-1}$. Similarly, the Ag concentrations for the soils dosed with 50 mg $kg^{-1}$ of Ag NPs declined from 48.6 mg $kg^{-1}$ and 49.5 mg $kg^{-1}$ for the wet-wet and wet-dry exposures to about 42.8 mg $kg^{-1}$ and 44.2 mg $kg^{-1}$, respectively. The untreated soils for all exposure types had Ag concentrations close to or below the flame AAS detection limit of about 0.06 mg $kg^{-1}$.

*Table 5.1*. Mean Ag concentrations determined for the treated and untreated soils (in mg $kg^{-1}$) of the wet-wet and wet-dry exposure systems of the Ag NP exposure at day 0 and day 7. BLOD: Ag concentrations below the limit of detection. The uncertainties signify the calculated standard deviations (n = 3).

| Time point | Ag concentrations [mg $kg^{-1}$] | |
|---|---|---|
| | **Treated** | **Untreated** |
| *Wet-wet at 10 mg Ag $kg^{-1}$ nominal concentrations* | | |
| **Day 0** | 9.83 ± 0.01 | BLOD |
| **Day 7** | 9.26 ± 0.02 | BLOD |
| *Wet-dry at 10 mg Ag $kg^{-1}$ nominal concentrations* | | |
| **Day 0** | 9.90 ± 0.04 | 0.06 ± 0.01 |
| **Day 7** | 9.32 ± 0.02 | BLOD |
| *Wet-wet at 50 mg Ag $kg^{-1}$ nominal concentrations* | | |
| **Day 0** | 48.55 ± 0.02 | BLOD |
| **Day 7** | 42.83 ± 0.01 | BLOD |
| *Wet-dry at 50 mg Ag $kg^{-1}$ nominal concentrations* | | |
| **Day 0** | 49.49 ± 0.02 | 0.05 ± 0.02 |
| **Day 7** | 44.18 ± 0.03 | 0.06 ± 0.03 |

*5.3.3.2. Plant tissues*

Prior to the statistical analysis, one result each obtained for root samples from treated soils (referred to as treated roots in the following) was excluded from further consideration. In detail, these were treated root data from (i) the wet-wet exposure to 10 mg $kg^{-1}$ Ag NPs and (ii) the wet-dry exposure to 50 mg of Ag NPs $kg^{-1}$. In both cases, the measured Ag concentrations for these samples exceeded the results for the two additional replicates by more than a factor of x2, most likely due to an analytical or procedural error.

For the Ag NP exposure, the treated roots grown in 10 mg $kg^{-1}$ Ag NPs showed identical ($p > 0.1$) Ag concentrations for the wet-wet and wet-dry exposures (Figure 5.2A, Table 1D, Appendix D). The Ag concentrations for the treated roots exposed to 50 mg $kg^{-1}$ of Ag NPs were also similar for the wet-wet and wet-dry exposures but the concentrations were more than 8x higher ($p < 0.001$) compared to those of the treated roots from the 10 mg $kg^{-1}$ Ag NP exposure. In detail, the Ag concentrations determined for the treated roots exposed to 10 mg $kg^{-1}$ of Ag NPs ranged between 33.7 ± 15.7 and 63.3 ± 5.9 µg $g^{-1}$ while the roots treated with 50 mg $kg^{-1}$ of Ag NPs exhibited Ag concentrations between 266.9 ± 9.6 and 531.9 ± 13.5 µg $g^{-1}$.

In contrast, the roots from untreated soils (termed untreated roots in the following) showed identical ($p = 0.1$) but low Ag concentrations for the different exposure types (wet-wet, wet-dry) and Ag NP concentrations (Figure 5.2B, Table 1D, Appendix D). In detail, the Ag concentrations recorded for the untreated roots from the wet-wet exposures were roughly 5.2 µg $g^{-1}$, while those for the wet-dry exposures were about 6.2 µg $g^{-1}$.

The Ag concentrations for the shoots were found to be low and statistically identical ($p = 0.2$) for all exposure types and Ag NP concentrations (Figure 5.3A, Table 2D, Appendix D). In detail, the Ag concentrations for the shoots varied between 0.2 ± 0.1 µg $g^{-1}$ and 0.6 ± 0.2 µg $g^{-1}$. However, analysis of the merged wet-wet and wet-dry shoot data, grouped by Ag NP concentrations, revealed a statistical difference with $p = 0.05$ between the two concentrations (Figure 5.3B). The plants treated with 10 mg $kg^{-1}$ of Ag NPs had Ag concentrations of 0.3 ± 0.3 µg $g^{-1}$ while the shoots exposed to the 50 mg $kg^{-1}$ Ag NP treatment encompassed

Ag concentrations of 0.6 ± 0.2 µg $g^{-1}$.

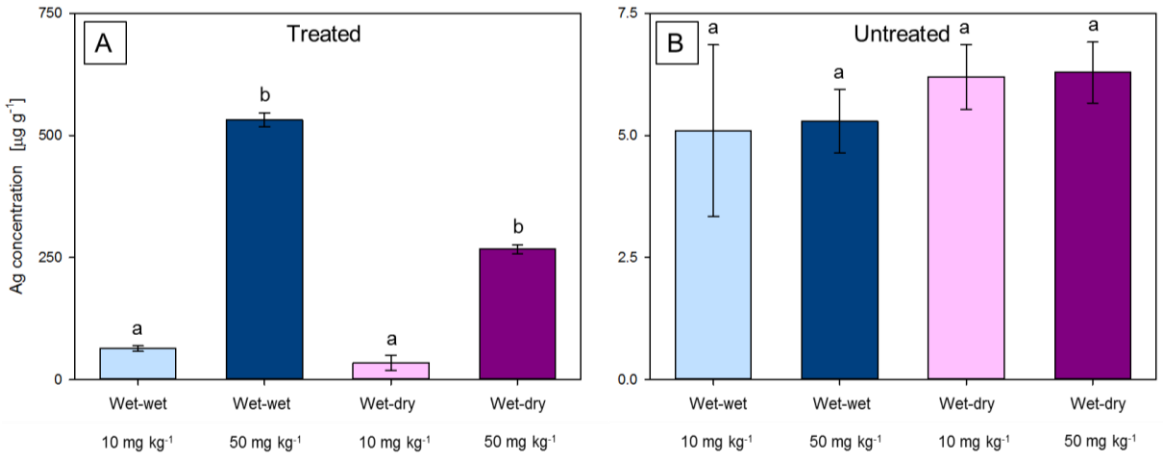



*Figure 5.2.* Mean Ag concentrations measured for the treated (A) and untreated (B) roots from the wet-wet and wet-dry systems of the Ag NP exposures, which were dosed with 10 mg $kg^{-1}$ and 50 mg $kg^{-1}$ of Ag NPs. The error bars signify standard deviation (n = 3). Different letters denote mean values that are statistically different. Note that panels A and B use scaling which differs by a factor of x100.

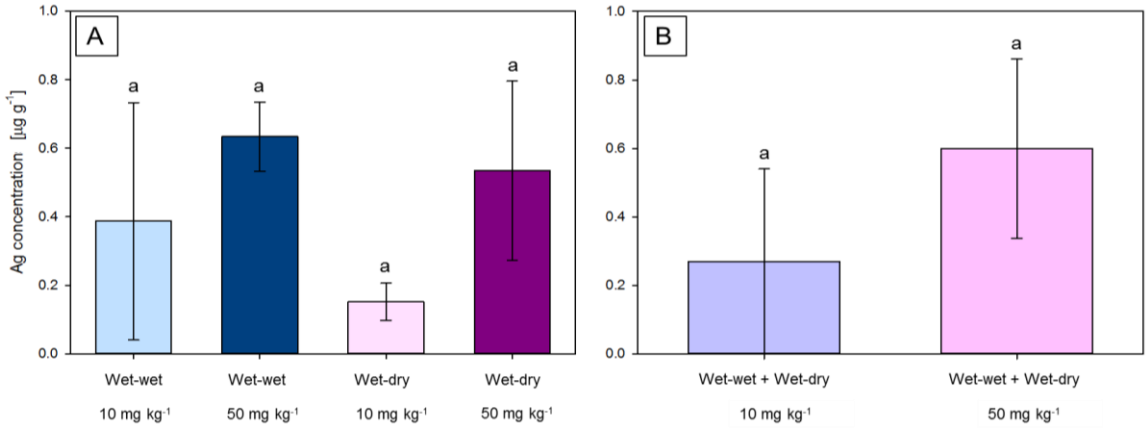



*Figure 5.3.* Mean Ag concentrations measured for shoots for the wet-wet and wet-dry conditions of the Ag NP exposure, which were dosed with 10 mg $kg^{-1}$ and 50 mg $kg^{-1}$ of Ag NPs. Panel (A) shows the mean results for each exposure type. Panel (B) shows the results when the data for wet-wet and wet-dry conditions at a single dosing concentration are pooled. For panel A, the error bars signify standard deviation with n = 3, while for panel B n = 6. Different letters denote mean values that are statistically different.

### *5.3.4. Time series exposure*

Silver concentrations were determined for the soils and soil pore waters from both Ag treatments for days 0, 1, 3 and 7 and on days 1, 3 and 7 for the plant tissues.

#### *5.3.4.1. Soils*

Overall, the Ag concentrations of the soils appear to show a slight decrease for the duration of the experiment for both Ag treatments (Figure 5.4, Table 3D, Appendix D). The Ag NP treated soils thereby generally exhibited somewhat higher Ag concentrations than the soils dosed with $AgNO_3$. This difference is clearly statistically significant for the soils collected on day 3 (with $p < 0.03$) but only marginally apparent for the soils from days 0, 1 and 7 (with $p > 0.15$). In detail, the Ag concentrations for the Ag NP treated soils showed a small but statistically significant ($p > 0.03$) decline from 9.8 ± 0.2 mg $kg^{-1}$ directly after spiking on day 0 to 9.3 ± 0.1 mg $kg^{-1}$ on day 7. In a similar manner, the $AgNO_3$ treated soils revealed a slight reduction ($p > 0.16$) in Ag concentrations from 9.7 ± 0.3 mg $kg^{-1}$ on day 0 to 8.8 ± 0.3 mg $kg^{-1}$ on day 7.

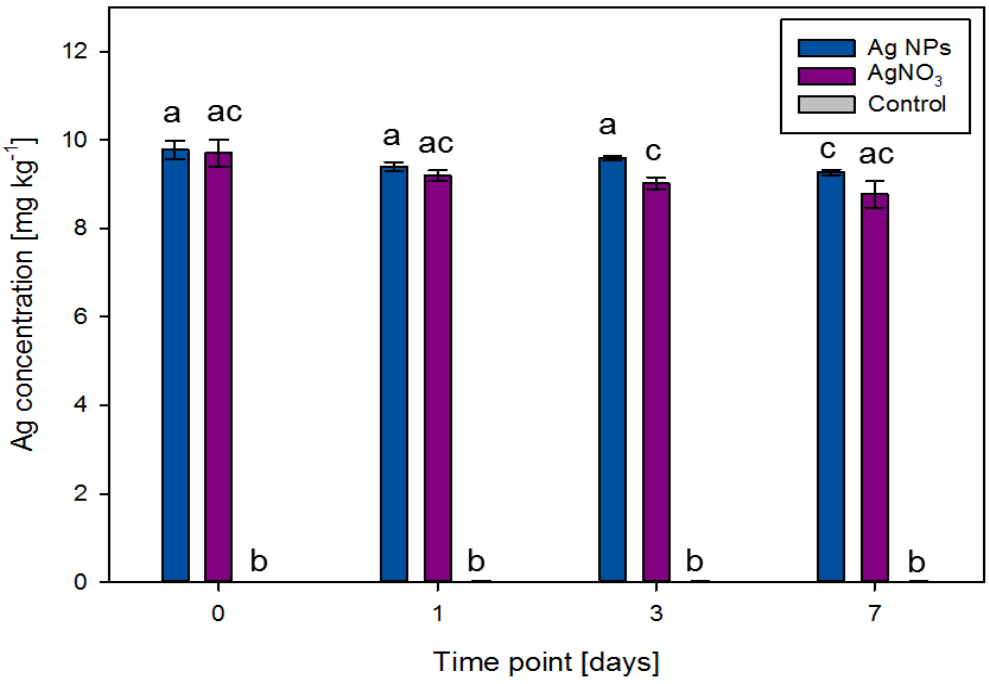



*Figure 5.4.* Mean Ag concentrations measured for the treated wet soils of the time series exposure. The error bars signify standard deviation (n = 3). Different letters denote mean values that are statistically different.

*5.3.4.2. Soil pore waters*

Generally, the total Ag concentrations determined for the soil pore waters from the two Ag treatments exhibited only limited variability with time. Notably, the Ag concentrations were consistently higher ($p < 0.01$) for the Ag NPs than for the $AgNO_3$ treatment (Figure 5.5A, Table 4D, Appendix D). In detail, the total Ag concentrations for the soil pore waters from the Ag NP treatment varied between 13.6 ± 1.1 µg $L^{-1}$ and 16.1 ± 2.8 µg $L^{-1}$. For the pore waters from the $AgNO_3$ treatment, the Ag concentrations were about 3x lower, ranging between 3.7 ± 1.3 µg $L^{-1}$ and 6.1 ± 1.1 µg $L^{-1}$. The Ag concentrations of the soil pore waters from the control treatments and untreated soils were consistently low, with mean results of 0.4 ± 0.2 µg $L^{-1}$ (Table 5.2).

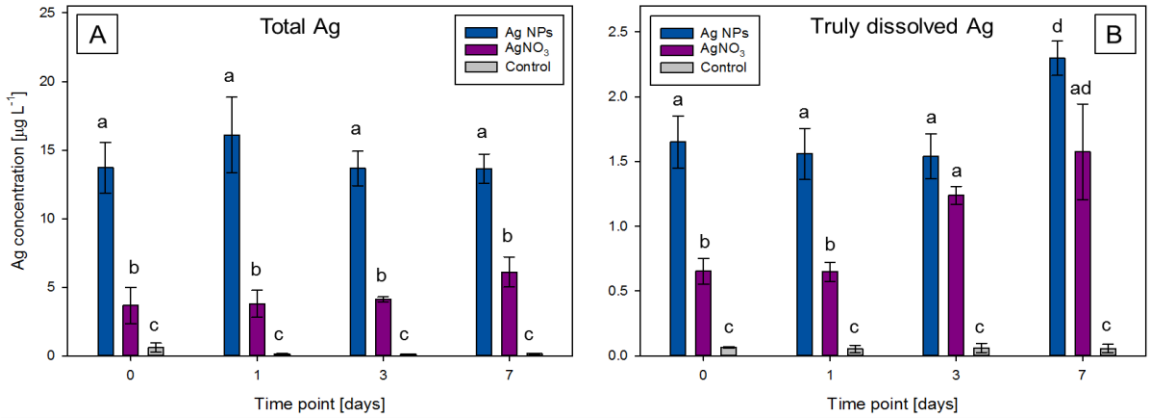



*Figure 5.5.* Total (A) and truly dissolved (B) Ag concentrations measured for the soil pore waters extracted from the treated soils of the time series exposure. The error bars signify standard deviation (n = 3). Different letters denote mean values that are statistically different. Note that the scaling of panels A and B differs by about a factor of x10.

Overall, the truly dissolved Ag concentrations determined for the soil pore waters from the two Ag treatments were about a factor of x10 lower compared to the total Ag contents (Figure 5.5B, Table 4D, Appendix D). Furthermore, the pore waters from the Ag NP treatment generally had truly dissolved Ag concentrations that were consistently higher ($p < 0.004$) than those from the $AgNO_3$ treatment. Finally, the truly dissolved Ag concentrations of the pore waters from both Ag treatments showed a general increase from day 0 to day 7. In detail, the truly

dissolved Ag pore water concentrations for the Ag NP treatment were stable between day 0 and day 3 with mean Ag concentrations of about 1.6 ± 0.2 µg $L^{-1}$; following this, the Ag concentration increased significantly ($p = 0.03$) to 2.3 ± 0.1 µg $L^{-1}$ on day 7. The truly dissolved Ag pore water concentrations for the $AgNO_3$ treatment remained roughly steady at 0.7 ± 0.1 µg $L^{-1}$ for days 0 and 1; following this, the Ag concentration increased ($p < 0.001$) to 1.2 ± 0.1 µg $L^{-1}$ at day 3 and to 1.6 ± 0.4 at day 7. The pore waters of the control treatments and the untreated dry soils exhibited uniformly low truly dissolved Ag concentrations of roughly 0.05 ± 0.02 µg $L^{-1}$ (Table 5.2).

*Table 5.2*. Mean total and truly dissolved Ag concentrations (in µg $L^{-1}$) determined for the soil pore waters of the untreated dry soils during the course of the Ag time series exposure. The uncertainties represent the calculated standard deviations (n = 3).

| Time point | Ag NPs | $AgNO_3$ | Control |
|---|---|---|---|
| | *Total Ag concentration [µg $L^{-1}$]* | | |
| **Day 0** | 0.60 ± 0.33 | 0.60 ± 0.33 | 0.60 ± 0.33 |
| **Day 1** | 0.78 ± 0.09 | 0.42 ± 0.40 | 0.41 ± 0.40 |
| **Day 3** | 0.49 ± 0.28 | 0.61 ± 0.31 | 0.15 ± 0.03 |
| **Day 7** | 0.12 ± 0.01 | 0.15 ± 0.02 | 0.12 ± 0.01 |
| | *Truly dissolved Ag concentration [µg $L^{-1}$]* | | |
| **Day 0** | 0.07 ± 0.01 | 0.07 ± 0.01 | 0.07 ± 0.01 |
| **Day 1** | 0.06 ± 0.01 | 0.04 ± 0.01 | 0.04 ± 0.03 |
| **Day 3** | 0.04 ± 0.01 | 0.04 ± 0.02 | 0.04 ± 0.01 |
| **Day 7** | 0.07 ± 0.02 | 0.02 ± 0.02 | 0.03 ± 0.02 |

### *5.3.4.3. Roots*

For the treated roots, the Ag concentrations appear to be somewhat higher for the Ag NP than for the $AgNO_3$ treatment (Figure 5.6A, Table 5D, Appendix D). Statistical analysis of these results, however, revealed statistically similar treated root Ag concentrations (with p values of 0.06 to 0.1) for the two Ag treatments at days 1 and 3, whilst the Ag levels differed significantly ($p = 0.04$) for day 7. In detail, the treated roots from the Ag NP treatment had marginally variable Ag concentrations ($p = 0.08$), which increased from 71.2 ± 19.6 µg $g^{-1}$ at day 1 to 109.8 ± 32.3 µg $g^{-1}$ at day 3 and then declined to 32.8 ± 4.6 µg $g^{-1}$ at day 7. In contrast, the treated roots from the $AgNO_3$ treatment had statistically less

variable Ag contents (p = 0.15) of between 14.4±1.8 µg $g^{-1}$ and 36.9±12.5 µg $g^{-1}$.

The untreated roots had Ag concentrations that were about a factor of x10 lower than the roots from treated soils for both Ag treatments. Similar to the treated roots, the untreated roots had variable Ag concentrations for the Ag NPs and the $AgNO_3$ treatments (Figure 5.6B, Table 5D, Appendix D). The Ag concentrations of the untreated roots from the two Ag treatments are, however, statistically indistinguishable (p > 0.13) for days 1 and 7 but statistically different (p = 0.02) on day 3. In detail, the untreated roots from the Ag NP treatment had mean Ag concentrations, which increased (p = 0.13) from 5.6 ± 1.8 µg $g^{-1}$ at day 1 to 11.5 ± 1.5 µg $g^{-1}$ on day 3 and then declined significantly (p = 0.04) to 6.21 ± 1.3 µg $g^{-1}$ on day 7. In contrast, the untreated roots from the $AgNO_3$ treatment showed essentially stable Ag concentrations for the duration of the study (with p>0.13) of between 2.2 ± 0.6 and 5.0 ± 1.2 µg $g^{-1}$.

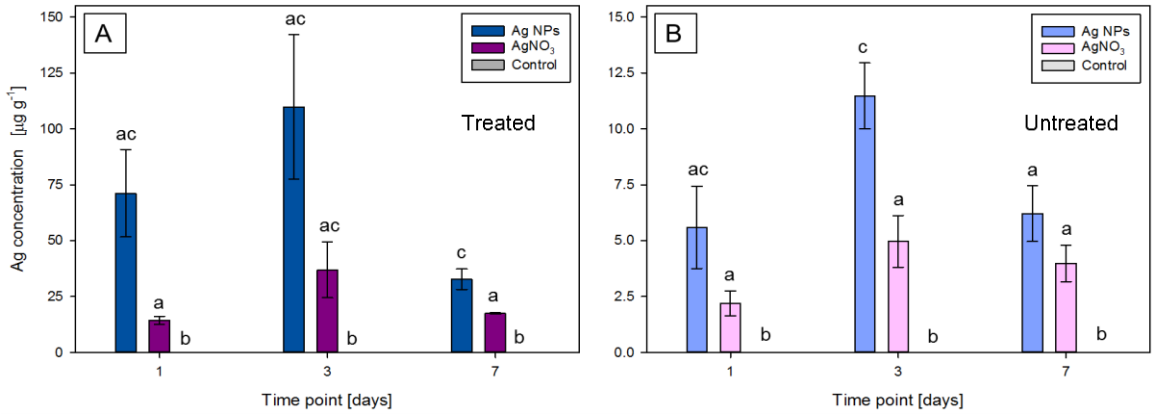



*Figure 5.6.* Mean Ag concentrations measured for the roots grown in the treated soils (A) and untreated (B) soils of the time series exposure. The error bars signify standard deviation (n = 3). Means with different letters are significantly different. Note that the scaling of panels A and B differs by about a factor of x10.

The roots from the treated and untreated sides of the control treatment had low Ag concentrations that were close to the detection limit with results of between 1.4 ± 0.2 ng $g^{-1}$ and 5.8 ± 0.6 ng $g^{-1}$.

### *5.3.4.4. Shoots*

The Ag concentrations of the wheat shoots from both Ag treatments were lower by factors of about x5 and x50 compared to the Ag concentrations of treated and untreated roots, respectively. Furthermore, the shoot Ag concentrations were

found to decrease with time, whereby the shoots from the Ag NP treatment consistently had higher Ag concentrations ($p < 0.001$) (Figure 5.7, Table 6D, Appendix D). In detail, the Ag concentrations of the shoots from the Ag NP treatment decreased gradually from 1.29 ± 0.16 µg $g^{-1}$ on day 1 to 0.54 ± 0.01 µg $g^{-1}$ on day 7. In a similar manner, the shoots from the $AgNO_3$ treatment revealed Ag concentrations that declined from 0.85 ± 0.04 µg $g^{-1}$ on day 1 to 0.45 ± 0.03 µg $g^{-1}$ at day 7. The Ag concentrations of the shoots from the control treatment were more than 100x lower compared to those of shoots from the Ag treatments and ranged between 4.8 ± 0.7 ng $g^{-1}$ and 6.9 ± 1.1 ng $g^{-1}$.

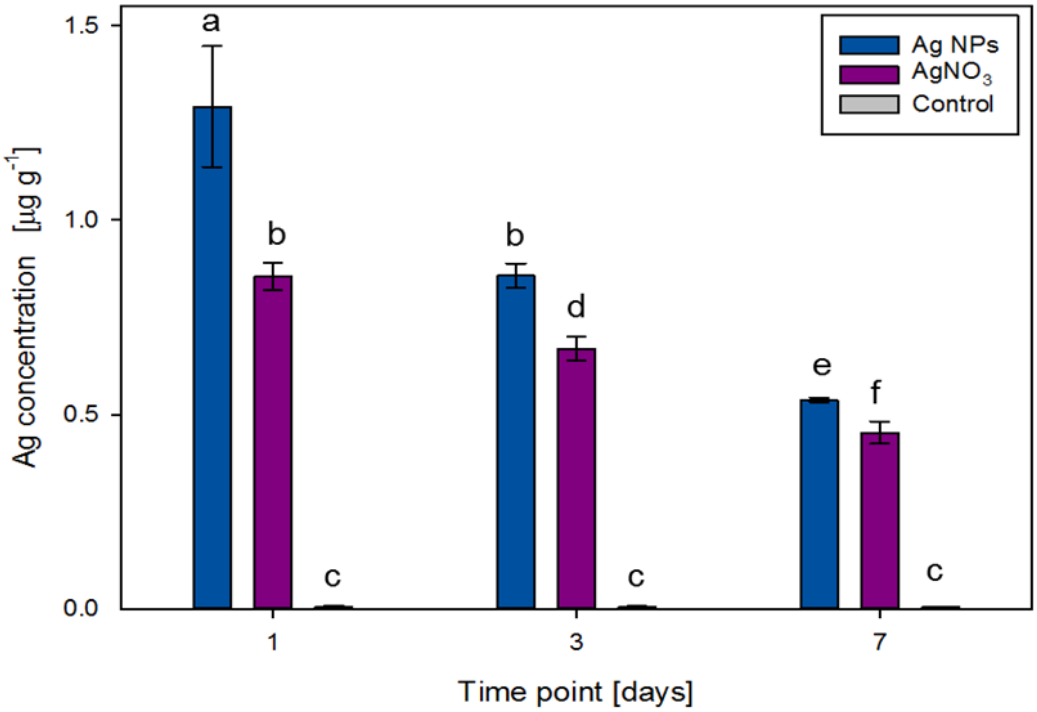



*Figure 5.7.* Mean Ag concentrations measured for shoots from the time series exposure. The error bars signify standard deviation (n = 3). Different letters denote mean values that are statistically different.

## 5.4. Discussion

The following discussion is split into two parts, one discussing the data from the Ag NP exposure and the other focusing on the interpretation of the results of the time series exposure.

### *5.4.1. Ag NP exposure*

#### *5.4.1.1. Soils*

The Ag concentrations of the soils from both exposure types and exposure concentrations decreased from day 0 to day 7 (Table 5.1). In detail, the Ag concentrations for soils from wet-wet and wet-dry exposures treated with 10 mg $kg^{-1}$ and 50 mg $kg^{-1}$ of Ag NPs dropped by about 6% and 11%, respectively, during the course of the experiment. Possible reasons for this decline are discussed in the following.

The decline in soil Ag concentrations is unlikely to be caused by incomplete digestion of the soils (as HF was not used in the digestion procedure) or adsorption of Ag onto undigested soil particles. This conclusion is supported by the high Ag recoveries of > 98% for soils that were sampled directly after spiking on day 0 and the similar decrease of the Ag concentrations for all four exposures (Table 5.1). Furthermore, investigation of the Ag mass balance for the experimental systems revealed that the plants accumulated less than 0.1% of the Ag present in the systems treated with either 10 mg $kg^{-1}$ or 50 mg $kg^{-1}$ of Ag NPs (Table 5.3). This demonstrates that Ag uptake by the plants cannot be the cause for the decrease in Ag concentrations of the soils. It is hence most likely that roughly 6% and 11% of the Ag in soils treated with 10 and 50 mg $kg^{-1}$ of Ag NPs, respectively, was lost to increasing adsorption of Ag from the doped soils to the walls of the polyvinyl chloride containers. This conclusion is in agreement with findings in Chapter 2 and 4 where up to 25% of the Ag added to soils in the form of Ag NPs and $AgNO_3$ was lost to adsorption onto the exposure container walls.

#### *5.4.1.2. Roots from treated soils*

The treated roots exposed to 10 mg $kg^{-1}$ Ag NPs had statistically identical Ag concentrations ($p > 0.1$) regardless of whether the exposures utilised wet-wet or wet-dry conditions. The same observation was made for treated roots from exposures with 50 mg $kg^{-1}$ Ag NPs (Figure 5.2A). This is an expected consequence of the identical Ag concentrations that were established by spiking of the soils with Ag NPs and the otherwise similar exposure conditions. Furthermore, the Ag concentrations of treated roots from soils doped with 50 mg

$kg^{-1}$ Ag NP were about 8x higher than those of treated roots from soils with 10 mg $kg^{-1}$ Ag NPs (Figure 5.2A). The observation of statistically higher Ag concentrations in the former roots ($p < 0.001$) is expected, given that more Ag was added to the respective soils, which will generate higher Ag levels in the soil solutions that are bioavailable to the roots. This agrees with previous findings that root uptake and adsorption of non-essential elements are generally directly linked to increasing elemental concentrations in the soil pore waters (Swartjes 2011).

*5.4.1.3. Shoots & xylem-based transport of Ag*

Whilst the shoots have lower Ag concentrations than both the treated and untreated roots, the data clearly show the presence of excess Ag in the shoots of plants exposed to Ag NPs, as compared to the shoots of control experiments. The latter observation is in accord with the findings of Chapters 2 and 4, as well as previous studies, which demonstrate that plants use the xylem to transport Ag to the shoots (Ma et al., 2010; Geisler-Lee et al., 2013). The transport of Ag from the treated roots-to-shoots is further examined in the following based on the distribution of Ag within the plants and in particular, between treated roots and shoots.

When the results from all four exposure types are compared individually, the shoot Ag concentrations are statistically identical (Figure 5.3A). In particular, the shoots from wet-wet and wet-dry exposures conducted with both 10 mg $kg^{-1}$ and 50 mg $kg^{-1}$ Ag NP have nearly identical Ag concentrations. Furthermore, the concentration ratios of Ag present in the shoots relative to the Ag present in treated roots ($[Ag]_{Shoot}/[Ag]_{T\text{-}root}$) (Table 5.3) are also identical, within error, for the wet-wet and wet-dry conditions at both Ag exposure levels. This demonstrates that the root-to-shoot transfer of Ag by the xylem was not affected by the water supply to the untreated roots.

Notably, when the shoot Ag data for the wet-wet and wet-dry exposures are pooled for each exposure concentration, the shoots from the 50 mg $kg^{-1}$ Ag NP exposures reveal statistically higher Ag concentrations, by about a factor of x2, than the shoots from the 10 mg $kg^{-1}$ Ag NP exposures (Figure 5.3B). To a first order, this finding reflects that the higher soil Ag levels of the 50 mg $kg^{-1}$ Ag NP

exposure produced higher root Ag contents, which are subsequently reflected in higher shoot Ag concentrations following translocation. It is notable, however, that the two Ag exposure levels, with 10 and 50 mg $kg^{-1}$ Ag NPs in soils, were associated with treated root Ag concentrations that differed by about a factor of x8. In contrast, the Ag concentrations of the shoots differed only by about a factor of x2 for the two Ag exposure levels (Figures 5.2A, 5.3B).

*Table 5.3*. Mean $[Ag]_{Shoot}/[Ag]_{T\text{-}root}$ and $[Ag]_{U\text{-}root}/[Ag]_{Shoot}$ ratios for the Ag NP exposure. The uncertainties denote the calculated standard deviations (n = 3).

| Type of exposure | Ag NP concentrations [mg $kg^{-1}$] | $[Ag]_{Shoot}/[Ag]_{T\text{-}root}$ | $[Ag]_{U\text{-}root}/[Ag]_{Shoot}$ |
|---|---|---|---|
| *Wet-wet* | *10* | 0.008 ± 0.009 | 33.8 ± 32.9 |
| *Wet-dry* | *10* | 0.005 ± 0.003 | 47.9 ± 20.2 |
| *Wet-wet* | *50* | 0.001 ± 0.001 | 8.4 ± 1.6 |
| *Wet-dry* | *50* | 0.002 ± 0.001 | 13.1 ± 4.8 |

The finding that the factor of x5 difference in Ag NP exposure levels is approximately mirrored in the Ag concentrations of the treated roots but is clearly attenuated in the shoots is most likely a consequence of controlled Ag transport via the xylem from the roots to the shoots, whereby the Ag transport is more strongly attenuated when more Ag is present in the treated roots. These conclusions are supported by the low shoot Ag concentrations of < 1 mg $kg^{-1}$ and the overall low $[Ag]_{Shoot}/[Ag]_{T\text{-}root}$ ratios of less than 0.01 (Table 5.3). These values are comparable to the results of a previous study, which determined $[Ag]_{Shoot}/[Ag]_{T\text{-}root}$ ratios of 0.04 for wheat exposed to Ag NPs at concentrations of 1 and 10 mg $L^{-1}$ (Vannini et al., 2014). Furthermore, whilst the $[Ag]_{Shoot}/[Ag]_{T\text{-}root}$ ratios obtained here have large uncertainties, the results appear to hint at lower ratios for the exposures carried out at 50 mg $kg^{-1}$ Ag NPs (Table 5.3). As a consequence, less than 4.6% and 0.8% of the total Ag present in the wheat plants was stored in the shoots of wheat plants exposed to 10 and 50 mg $kg^{-1}$ Ag NPs in soils, respectively (Figure 5.8).

Taken together, the current observations provide strong evidence that Ag translocation from the root system to the shoots via the xylem is controlled,

particularly when more Ag is present in the roots. As the water flow rate in the xylem is high (Choat et al., 2010), this restriction is most likely linked to limited transport of Ag within the roots (Su et al., 2019). There are three possible explanations for this conclusion, which are discussed in the following.

First, most of the Ag that was determined in the roots may be adsorbed onto the root surfaces through electrostatic attraction. In a similar manner to Cu and cadmium (Cd), dissolved ionic $Ag^+$ from the pore waters can adsorb to the negatively charged cell walls and membranes of the roots (Liu et al., 2017). Previous evidence for such adsorption is available from a similar experiment, whereby cucumber plants were exposed to $Ce_2O$ NPs (Ma et al., 2017). For the wheat plants studied here, the extent of Ag adsorption is uncertain and further work, including cellular level imaging, is required to better constrain the importance of this process.

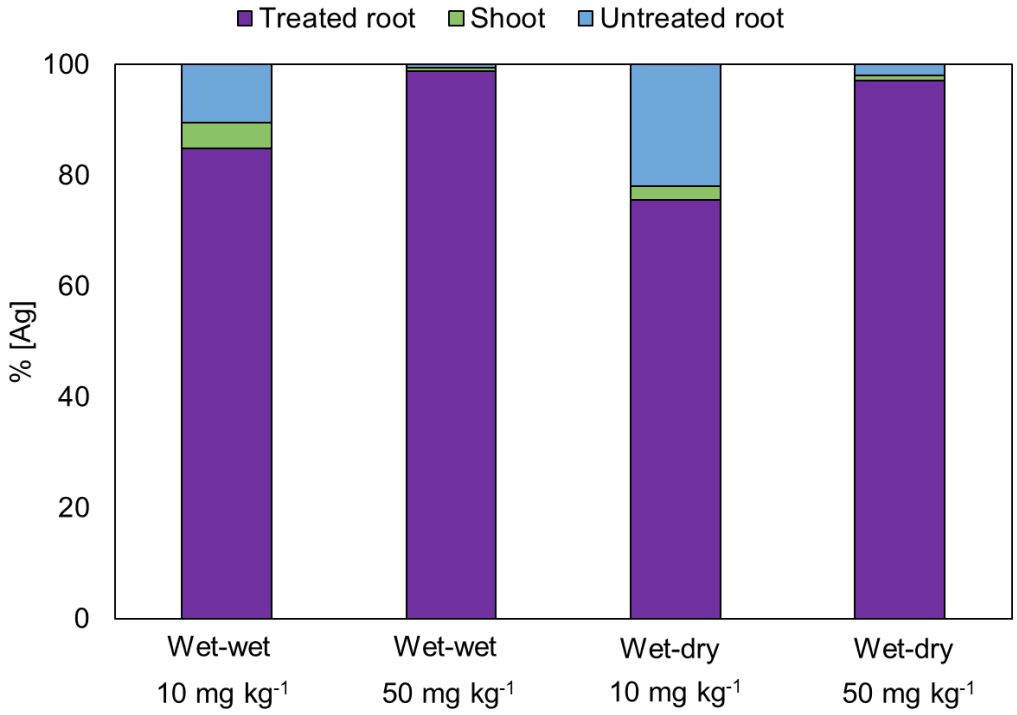



*Figure 5.8.* Silver distribution for the wheat seedlings of the Ag NP exposure (n = 3).

Second, it is also conceivable that the Ag available to the roots was internalised but formed inert Ag species, precipitates and/or aggregates/agglomerates *in planta* that were unable to pass through the Casparian strip/apoplastic barriers and were therefore unavailable for translocation to the shoot. Such a mechanism

is in accord with the work of Stegemeier et al. (2015), who reported that Ag can form aggregates along cell walls and the plasmodesmata of alfalfa plants. A further study reported significant *in planta* transformations for internalised Ag, including partial or total oxidation of Ag NPs and formation of secondary $Ag^+$ ion species such as AgCl and $Ag^+$ ions bound to thiols (Martinez-Criado et al., 2016). Notably, such transformations can reduce the availability of Ag and hinder the transport of the element through the Casparian strip.

Third, it is plausible that the restricted transport is a result of controlled trafficking of Ag within the xylem. Although the mechanisms involved in Ag trafficking remain elusive, it is possible that they are similar to these of Cu and Cd. Previous studies of these elements reported that sequestration of metals from active into non-active tissues by phytochelatins, transporters and other proteins play an important role in metal homeostasis (Chen et al., 2017). For example, heavy metal ATPases and chelating phytochelatins play a key role in the translocation and sequestration, respectively, of root-bound Cd and may also impact Ag (Williams and Mills 2005; Nocito et al., 2011).

*5.4.1.4. Roots in untreated soils & phloem-based transport of Ag*

Considering that the Ag concentrations of the untreated soils were similar to the background levels of control experiments and that direct lateral transport of Ag between the roots of the split root system is not expected to be significant (Wang et al., 2012; Ma et al., 2017), nearly all Ag present in the untreated roots will have been translocated via the phloem from the shoots. Whilst the exact mechanisms for phloem-based transport of Ag are unstudied, they are likely to resemble those inferred for Cu by Wang et al. (2012). As such, Ag is expected to be loaded into the phloem sap together with sugars, amino acids, minerals and secondary metabolites. Once inside the phloem pathway, Ag and other constituents are transported with the phloem sap from the photosynthetic “source” organs (e.g. shoots) to “sink” areas (e.g. young developing shoots and roots) by the hydrostatic pressure gradient.

The untreated roots from all exposure systems had low mean Ag contents, with concentrations that were more than 10x and about 100x lower than those of the treated roots from exposures doped with 10 mg $kg^{-1}$ and 50 mg $kg^{-1}$ Ag NPs,

respectively. Notably, the untreated roots from wet-wet and wet-dry conditions at a particular exposure concentration had nearly identical Ag concentrations (Figure 5.2B). Furthermore, the concentration ratios for Ag in untreated roots versus shoots, $[Ag]_{U\text{-}root}/[Ag]_{shoot}$ (Table 5.3) are identical, within error, for the plants from wet-wet and wet-dry conditions at the two exposure concentrations (Table 5.3). This indicates that the translocation of Ag from treated to untreated roots via both the xylem and the phloem system was not impacted by the water supply to the untreated roots.

Statistical analysis of the root data also shows that all untreated roots had identical Ag concentrations, regardless of exposure conditions and the Ag NP exposure concentrations (Figure 5.2B). As such, the factor of x5 difference in Ag NP exposure levels, which was attenuated to about a factor of x2 difference in shoot Ag concentrations, was completely levelled out in the untreated roots. The latter attenuation is thereby most likely due to controlled transport of Ag via the phloem from shoots-to-roots, whereby the attenuation is more pronounced at higher Ag levels in the shoot source region of Ag. This interpretation is supported by the $[Ag]_{U\text{-}root}/[Ag]_{shoot}$ ratios (Table 5.3). In particular, whilst the ratios are consistently greater than unity, as the untreated roots have higher Ag concentrations than the shoots, they appear to be systematically lower for the plants from the 50 mg $kg^{-1}$ exposures. The limitation of the phloem-based Ag transport is also highlighted by the Ag distributions determined for the plants (Figure 5.8). In detail, the plants exposed to 10 mg $kg^{-1}$ Ag NPs accumulated about 10 to 22% of the total plant Ag inventory in the untreated roots, whilst plants exposed to 50 mg $kg^{-1}$ Ag NPs had only 0.5% to 2% of the Ag budget in the untreated roots.

Taken together, there is hence ample evidence, which points to a restriction of the Ag transport from shoots-to-untreated roots via the phloem system. With a flow rate that typically exceeds 0.07 mm $s^{-1}$, the phloem sap can readily transport constituents by 6 m in 24 h (Choat et al., 2010). As such, the sap flow rate is unlikely to be responsible for the limited transport of Ag from shoots-to-roots. Two alternative mechanisms that provide feasible explanations for the restricted Ag translocation are discussed in the following.

First, the limited transport of Ag may be a consequence of controlled trafficking of Ag in the phloem by proteins that govern the movement of the element. Current understanding of Ag trafficking in plants is sparse but is most likely similar to that of Cu and Cd. Previous studies of these metals reported that phytochelatins and metal-binding proteins, such as metallothioneins, are involved in metal homeostasis and can immobilise Cu and Cd ions (Álvarez-Fernández et al., 2014; van Belleghem et al., 2007). Further studies reported that plants exposed to excess Cu upregulate the expression of metallothionein in leaves to induce scavenging of the element (García-Hernández et al., 1998; Song et al., 2017). Recently, Dimpka et al. (2013) confirmed the induction in the gene expression of metallothionein. Of interest is also the controlled elemental xylem-to-phloem transfer by low-affinity cation transporters (LCT1). Their inactivation has been previously documented to reduce the concentrations of Cd in the phloem (Uraguchi et al., 2011). However, further investigations are required, to identify the proteins, which play a key role in controlling Ag transport in plants.

Second, it is conceivable that the translocation of Ag is restricted by accumulation of the element in larger aggregates or compounds, which do not readily travel through the small pores of the sieve cells and cell walls that must be passed during phloem transport (Su et al., 2019). The phloem sap contains considerable concentrations of different sugars, amino and organic acids, and other constituents, which may react with and bind any Ag in larger molecules, which may limit the free movement of Ag within the phloem system.

### *5.4.2. Time series exposure*

#### *5.4.2.1. Soils*

The Ag concentrations of the soils from the time series exposure declined gradually from day 0 to day 7 for both Ag treatments (Figure 5.4). In detail, the soils exhibited a reduction in Ag concentrations of roughly 5% to 10% during the course of the experiment. Possible causes for this decrease are discussed in the following.

As the day 0 soils, which were sampled directly after dosing, record Ag recoveries of > 97% and given the systematic decrease of the soil Ag

concentrations during the experiment, it is unlikely that the decreasing concentrations are a consequence of incomplete soil digestion or adsorption of Ag onto any undigested particles. Furthermore, as the plants grown in the soils contained less than 0.04% of the total Ag present in the systems at day 7, plant accumulation of Ag is also not a plausible explanation for the observed decline in soil Ag concentrations (Figure 5.4). Given this, the only plausible cause for the reduction in soil Ag concentrations for both treatments is slow and continued adsorption of Ag to the walls of the polyvinyl chloride containers. This conclusion is in agreement with the conclusions drawn for the soils of the Ag NP exposure (Section 5.4.1.1) and the findings of Chapters 2 and 4.

*5.4.2.2. Soil pore waters*

With only limited exceptions, the soil pore waters extracted from the treated wet soils of both Ag treatments exhibited stable total and truly dissolved Ag concentrations during the course of the experiment (Figure 5.5). This indicates that the soils and soil pore waters of both Ag treatments quickly established a dynamic equilibrium with respect to the distribution of Ag, whereby Ag lost to adsorption onto the container walls from the solutions was replenished by the dissolution of further Ag present in the soils.

Overall, the pore waters featured low total and truly dissolved Ag concentrations of less than 20 µg $L^{-1}$ and 2 µg $L^{-1}$, respectively (Figure 5.5). Examination of the Ag distribution of the soil-pore water systems for both Ag treatments revealed that less than 5.5% of the Ag in the system was present in solution. This most likely reflects the low overall solubility of Ag in the soil solutions, regardless of the Ag treatment, in agreement with the findings of Chapter 2 and previous studies. For example, Waalewijn-Kool et al. (2014) reported solubilities of 1.5% for Ag added as Ag NPs and $AgNO_3$ to pore waters at Ag concentrations of 30 to 200 mg $kg^{-1}$.

The low Ag solubilities found here, and by other studies, reflect the physicochemical behaviour of Ag in soil-pore water systems. One the one hand, these feature oxidative dissolution of Ag NPs to soluble $Ag^+$ ions, a reaction that is affected by pH as well as the presence of natural organic matter and cations (Bundschuh et al., 2018; Mitrano et al., 2014; Metreveli et al., 2016). On the other

hand, there are numerous processes, which favour the removal of dissolved Ag from soil pore waters. In particular, Ag can be lost from soil solutions by (i) the formation of highly insoluble precipitates, such as AgCl, $Ag_2S$ and $Ag_2S$ NPs (Qing et al., 2018); (ii) adsorption to the surfaces of organic matter, soil particles and the experimental containers (Diez-Ortiz et al., 2015A; 2015B; Coutris et al., 2012); and (iii) by aggregation and agglomeration of Ag NPs and dissolved $Ag^+$ ions to form larger particles (Jiang et al., 2009).

Of further interest is the observation that the pore waters from soils treated with Ag NPs consistently exhibited higher total Ag concentrations than those derived from soils doped with $AgNO_3$ (Figure 5.5). Similarly, the truly dissolved pore water Ag concentrations that are maintained by the former Ag treatment are also either clearly or marginally higher than those of the latter treatment. In accord with the findings of Chapter 2 and previous studies, these observations most likely reflect that the soluble $Ag^+$ ions supplied by the $AgNO_3$ treatment were rapidly and nearly quantitatively removed from the soil solution by either precipitation reactions (as AgCl or $Ag_2S$) and/or by adsorption to reactive surfaces (Diez-Ortiz et al., 2015A; 2015B; Coutris et al., 2012). In contrast, the Ag NPs that were added to soils presumably dissolved only slowly in the soil solutions (Laycock et al., 2014; Coutris et al., 2012). This acts against rapid and near-quantitative removal of the dissolved Ag and helps the Ag NPs to establish and maintain higher steady-state concentrations of total and truly dissolved Ag for the soil solutions.

Whilst the total dissolved pore water Ag concentrations that were established by both Ag treatments were essentially stable for the duration of the experiment, the truly dissolved Ag contents show a statistically significant increase from day 1 to day 7 (Figure 5.5). The origin of this observed increase is unknown but it may reflect slow disaggregation of larger colloidal dissolved Ag species to form 'truly dissolved' $Ag^+$ ions in the pore waters.

*5.4.2.3. Treated roots*

On first sight, the treated roots from the two Ag treatments appear to record Ag concentrations that are quite variable during the experiment. Closer inspection of the results shows, however, that each Ag treatment is associated with treated

root Ag concentrations that are statistically identical for the duration of the experiment (Figure 5.6A). Furthermore, the overall results indicate somewhat higher Ag concentrations for the roots from the Ag NP treatment ($p = 0.05$). Whilst this difference is statistically most significant for day 7 ($p = 0.04$), the mean treated root Ag concentrations for the two treatments show larger absolute differences for days 1 and 3. These observed differences in the Ag concentrations of the treated roots most likely reflect the overall higher pore water Ag concentrations that were obtained for soils doped with Ag NPs (Figure 5.5).

Furthermore, the $[Ag]_{Root}/[Ag]_{Tot\text{-}PW}$ and $[Ag]_{Root}/[Ag]_{TrD\text{-}PW}$ concentration ratios that were determined for samples from the Ag NP and the $AgNO_3$ treatments are statistically identical, with p-values of 0.76 and 0.32, respectively (Table 5.4). Taken together, these findings are in accord with the results of Chapter 2 and published studies (e.g., Swartjes 2011) and they indicate that adsorption and/or uptake of Ag by the roots was primarily determined by the pore water Ag concentrations rather than by the speciation of the Ag that was added to the soils.

*Table 5.4*. The $[Ag]_{Root}/[Ag]_{Tot\text{-}PW}$ and $[Ag]_{Root}/[Ag]_{TrD\text{-}PW}$ ratios are calculated from the Ag concentrations of roots grown in the TW soils as well as the total (Tot-PW) or truly dissolved (TrD-PW) Ag concentrations of soil pore waters from the treated wet (TW) soils. The uncertainties signify the calculated standard deviation (n = 3).

| Treatment | Time point | $[Ag]_{Root}/[Ag]_{Tot\text{-}PW}$ | $[Ag]_{Root}/[Ag]_{TrD\text{-}PW}$ |
|---|---|---|---|
| Ag NPs | Day 1 | 4420 ± 580 | 45653 ± 7655 |
| | Day 3 | 8034 ± 2156 | 71256 ± 13015 |
| | Day 7 | 2400 ± 448 | 14261 ± 2204 |
| $AgNO_3$ | Day 1 | 3919 ± 2304 | 22160 ± 1813 |
| | Day 3 | 9717 ± 5034 | 29782 ± 9733 |
| | Day 7 | 4225 ± 201 | 11079 ± 2504 |

*5.4.2.4. Shoots & xylem-based transport of Ag*

The Ag concentrations of the shoots decreased by about 50% during the course of the exposure (Figure 5.7). Close examination of the Ag mass balance for the plants indicates stable or decreasing Ag masses of between about 0.03 µg and

0.05 µg for the shoots, which are statistically identical (p = 0.4) for the shoots from the two Ag treatments. Taken together, this suggests that the decreasing shoot Ag concentrations during the experiment are most likely a consequence of Ag dilution during plant growth.

A key observation is the finding that the shoot Ag concentrations for the two Ag treatments differ much less than the Ag concentrations that were determined for the respective pore waters and treated roots (Figures 5.5, 5.6A, 5.7). This is most readily discussed by comparing the Ag concentrations that were measured for the respective compartments (Com) of the two different Ag treatments using the concentration ratio $[Ag]_{Com\text{-}AgNP}/[Ag]_{Com\text{-}AgNO_3}$ (Table 5.5). In the following, this comparison is carried out with the data obtained for samples from day 7. Notably, the total pore waters and treated roots display similar ratios of $[Ag]_{Tot\text{-}PW\text{-}AgNP}/[Ag]_{Tot\text{-}PW\text{-}AgNO_3}$ = 2.3 and $[Ag]_{T\text{-}root\text{-}AgNP}/[Ag]_{T\text{-}root\text{-}AgNO_3}$ = 1.9. In contrast, for the shoots, the corresponding ratio is much closer to unity, with $[Ag]_{Shoot\text{-}AgNP}/[Ag]_{Shoot\text{-}AgNO_3}$ = 1.2. As such, the large Ag concentration difference that is evident for the pore waters and roots from the two treatments is clearly reduced in the shoots. This finding is unlikely to be a consequence of differences in the speciation of Ag within the plants for the two different Ag treatments, as the Ag adsorption and/or uptake by the roots was simply a function of the pore water Ag concentrations. Rather, the observed attenuation of the Ag concentration ratios most likely reflects that the xylem transport of Ag from roots-to-shoots is controlled, particularly when higher Ag concentrations are present in the roots source, in accord with the findings of the Ag NP exposure.

*Table 5.5*. Mean $[Ag]_{Tot\text{-}PW\text{-}Ag\ NP}/[Ag]_{Tot\text{-}PW\text{-}AgNO3}$, $[Ag]_{T\text{-}root\text{-}AgNP}/[Ag]_{T\text{-}root\text{-}AgNO3}$ and $[Ag]_{Shoot\text{-}AgNP}/[Ag]_{Shoot\text{-}AgNO3}$ ratios for day 7 of the time series Ag exposure. The uncertainties denote the calculated standard deviation (n = 3).

| $[Ag]_{Com\text{-}AgNP}/[Ag]_{Com\text{-}AgNO_3}$ | Day 1 | Day 3 | Day 7 |
|---|---|---|---|
| $[Ag]_{Tot\text{-}PW\text{-}Ag\ NP}/[Ag]_{Tot\text{-}PW\text{-}AgNO_3}$ | 4.36 ± 0.68 | 3.31 ± 0.27 | 2.29 ± 0.34 |
| $[Ag]_{T\text{-}root\text{-}Ag\ NP}/[Ag]_{T\text{-}root\text{-}AgNO_3}$ | 5.08 ± 1.69 | 3.45 ± 1.50 | 1.88 ± 0.29 |
| $[Ag]_{Shoot\text{-}Ag\ NP}/[Ag]_{Shoot\text{-}AgNO_3}$ | 1.52 ± 0.25 | 1.28 ± 0.04 | 1.19 ± 0.07 |

The latter conclusion is also supported by the $[Ag]_{Shoot}/[Ag]_{T\text{-}root}$ concentration ratios of the plants (Table 5.6). In detail, both Ag treatments of the time series exposure are associated with low $[Ag]_{Shoot}/[Ag]_{T\text{-}root}$ ratios of between about 0.01 and 0.06. However, whilst the $[Ag]_{Shoot}/[Ag]_{T\text{-}root}$ ratios that were obtained for the two Ag treatments are similar, the mean values determined for each time point appear to be lower for the Ag NP treatment, in accord with more restricted root-to-shoot Ag transport when higher Ag concentrations are present in the root source.

*Table 5.6*. Mean $[Ag]_{Shoot}/[Ag]_{T\text{-}Root}$ and $[Ag]_{U\text{-}Root}/[Ag]_{Shoot}$ ratios for the time series exposure. The uncertainties signify the calculated standard deviation (n = 3).

| Treatment | Time point | $[Ag]_{Shoot}/[Ag]_{T\text{-}root}$ | $[Ag]_{U\text{-}root}/[Ag]_{Shoot}$ |
|---|---|---|---|
| **Ag NPs** | **Day 1** | 0.020 ± 0.005 | 4.4 ± 1.6 |
| | **Day 3** | 0.008 ± 0.002 | 13.5 ± 2.2 |
| | **Day 7** | 0.017 ± 0.002 | 11.5 ± 2.4 |
| **$AgNO_3$** | **Day 1** | 0.060 ± 0.006 | 3.0 ± 0.9 |
| | **Day 3** | 0.021 ± 0.007 | 7.2 ± 2.1 |
| | **Day 7** | 0.026 ± 0.002 | 8.4 ± 2.6 |

In summary, the results of the time series exposure indicate xylem-based transport of Ag from the roots-to-shoots is independent of the form by which Ag was added to the soils. Furthermore and in accord with the results of the Ag NP exposure, the translocation of Ag to shoots appears to be controlled, particularly when higher Ag contents are present in the root source. Possible causes for the limitation of Ag transport were previously discussed in the context of the Ag NP exposure (Section 5.4.1.3). These include adsorption of Ag onto rather than uptake into the roots, the formation of secondary Ag species following internalisation, which restrict the movement of Ag through the Casparian strip to the xylem system, and/or regulation of Ag transport and sequestration by phytochelatins and metalloproteins (Martinez-Criado et al., 2016; Song et al., 2016).

*5.4.2.5. Untreated roots & phloem-based transport of Ag*

The untreated roots from the two Ag treatments had essentially stable Ag concentrations, which were about a factor of x10 lower compared to the treated roots but about a factor of x5 to x10 higher than those of the shoots. Given that the untreated soils displayed only background levels of Ag and lateral root-to-root transport of substances is generally limited (Wang et al., 2012; Ma et al., 2017), it is reasonable to conclude the nearly all Ag present in the untreated roots was translocated via the phloem from the shoots.

Further inspection of the results shows that the untreated roots from the Ag NP and $AgNO_3$ treatments had statistically identical ($p > 0.13$) Ag concentrations at day 1 and the end of the experiment at day 7 (Figure 5.6B). To further investigate the Ag transport within the wheat plants, the Ag concentrations for the untreated roots and the shoots that were obtained for the two Ag treatments are compared using $[Ag]_{U\text{-}Root}/[Ag]_{Shoots}$ ratios (Table 5.6). In detail, the $[Ag]_{U\text{-}Root}/[Ag]_{Shoots}$ ratios varied between 8.4 and 11.6. These data reveal essentially identical ratios ($p = 0.29$) for plants from the two different Ag treatments and values that resemble those from the Ag NP exposure (Table 5.3).

Considering that the two Ag treatments were associated with shoot Ag concentrations, which differed by about 20% (Figure 5.7), the results are in accordance with controlled Ag transport in the phloem system, particularly when higher Ag levels were present. Furthermore, they indicate identical transport and speciation of Ag within the phloem system, regardless of the speciation by which Ag was added to soils. Possible causes for the limitation of Ag transport were previously discussed in the context of the Ag NP exposure (Section 5.4.1.4) and encompass (i) regulated trafficking of Ag in the phloem by phytochelatins, plant transporters and other metal-binding proteins as well as (ii) restricted mobility of Ag by the incorporation into or formation of larger compounds or aggregates, which do not pass readily through the sieve cells or small flow channels of the phloem (Su et al., 2019).

## 5.5. Conclusion

This is the first time the mechanisms of Ag transport were examined for wheat seedlings grown in soil using split root experiments. Two experiments were carried out: (i) the Ag NP exposure employed wheat seedlings that were grown in wet-wet and wet-dry soils dosed with 10 mg $kg^{-1}$ and 50 mg $kg^{-1}$ of Ag NPs; and (ii) the time series exposure investigated wheat seedlings that were exposed to Ag NPs and $AgNO_3$ under water stress at a Ag concentration of 10 mg $kg^{-1}$.

The experiments produced (i) high Ag concentrations of about 20 to 530 mg $kg^{-1}$ for the treated roots, with variations that matched measured or expected variations of pore water Ag concentrations due to different exposure levels and, to a lesser extent, Ag treatments; (ii) low and much less variable Ag concentrations of about 0.1 to 0.5 mg $kg^{-1}$ for the shoots, with a clearly attenuated variability relative to the treated roots; and (iii) intermediate and essentially identical Ag concentrations of about 5 mg $kg^{-1}$ for the untreated roots. The following conclusions can be drawn from the results:

- The low $[Ag]_{Shoot}/[Ag]_{T\text{-}root}$ ratios and the observation that the shoot Ag concentrations were much less variable than the Ag exposure levels demonstrate controlled root-to-shoot transport of Ag via the xylem. Three plausible explanations are suggested for the restricted xylem-based transport of Ag: (i) adsorption of Ag onto the surfaces of the treated roots; (ii) formation of Ag precipitates, aggregates/agglomerates or inert Ag species following internalisation, which restrict the passage of Ag through the Casparian strip; and (iii) sequestration of Ag in the roots by phytochelatins and/or metalloproteins.
- The intermediate and essentially identical Ag concentrations of the untreated roots, despite variable Ag levels in the shoots and employed for the exposures, provide compelling evidence for controlled and limited phloem-based Ag transport to the roots. The attenuation of the Ag translocation is most likely a result of (i) controlled trafficking of Ag by phytochelatins and metal-binding proteins and/or (ii) the small pore sizes of sieve cells and cell walls, which can hinder the transport of larger Ag species that may form in the phloem.

- The results suggest that the xylem- and phloem-based transport of Ag was identical for (i) wet-wet and wet-dry exposure conditions and (ii) both Ag treatments to the soils. This most likely reflects that (i) translocation of Ag was not impacted by variable water supply to roots and (ii) the same Ag speciation was established within the wheat seedlings despite different Ag treatments to the soils.

# Chapter 6: Summary & outlook

This PhD project aimed to expand the current knowledge on the uptake, translocation and accumulation of silver (Ag) by wheat (*Triticum aestivum L.*) through soil and hydroponic exposure studies with Ag nanoparticles (Ag NPs) and $AgNO_3$.

Throughout the thesis, the wheat uptake of Ag from Ag NPs and $AgNO_3$ was found to be primarily governed by the total and truly dissolved Ag concentrations of the soil pore waters and hydroponic solutions. The experiments furthermore confirmed previous work, as Ag NPs were shown to produce higher dissolved Ag concentrations compared to $AgNO_3$ at equivalent Ag treatment concentrations. As a consequence, wheat roots from Ag NP exposures had higher Ag contents than those from $AgNO_3$ treatments at otherwise equivalent conditions (Chapters 2, 4 and 5). However, the bioaccumulation factors that were observed for wheat from the two Ag treatments were identical as documented by (i) the $[^{109}Ag\text{-}E]_{Root}/[^{109}Ag\text{-}E]_{TD\text{-}Pw}$ and $[^{109}Ag\text{-}E]_{Plant}/[^{109}Ag\text{-}E]_{TD\text{-}Pw}$ ratios determined in the study of Chapter 2; the (ii) $[Ag]_{Shoot}/[Ag]_{Medium}$ ratios measured for the multimedia exposures of Chapter 4; and (iii) the $[Ag]_{Root}/[Ag]_{Tot\text{-}PW}$ and $[Ag]_{Root}/[Ag]_{TD\text{-}PW}$ documented for the split root exposures of Chapter 5. These findings indicate that the speciation of Ag in the pore waters was similar for both Ag treatments. Furthermore, similar translocation factors were determined for the Ag treatments in all exposure studies (Chapters 2, 4 and 5); this suggests that Ag speciation within the wheat plants was also identical for both Ag treatments. To confirm these observations, further studies of Ag speciation in soil pore waters/hydroponic media and within plant tissues are desirable, for example by X-ray absorption near edge structure spectroscopy (XANES) (Larue et al., 2014; Doolette et al., 2015; Wang et al., 2016). This would help to further the current understanding of Ag bioavailability to and Ag speciation in wheat.

In terms of Ag accumulation by wheat from Ag NPs and $AgNO_3$, all exposure studies performed in this project showed that Ag was primarily concentrated in the wheat roots. However, the extent of Ag adsorption to the root surfaces versus internalisation is uncertain. This key uncertainty should be addressed in future investigations, for example by using laser ablation inductively coupled plasma mass spectrometry (LA-ICP-MS) for mapping of the Ag distribution in the roots and by

application of transmission electron microscopy (TEM) for detailed observations at the cellular level.

The Ag transport mechanisms in wheat plants were examined in Chapter 5 through split root experiments. These experiments revealed that the translocation of Ag from treated roots to shoots and from shoots to untreated roots was associated with a clear attenuation of Ag concentration differences, which were induced in the treated roots by the applied Ag treatments. These findings point to a regulated Ag transport from both roots-to-shoots via the xylem and from shoots-to-the roots via the phloem pathway. To further understand these processes and their mechanisms, LA-ICP-MS and TEM analyses of treated root tissues would help to identify whether the restricted xylem-based transport of Ag was caused by (i) adsorption of Ag onto the surfaces of the treated roots or (ii) formation of Ag precipitates, aggregates/agglomerates or inert Ag species following internalisation, which limited the passage of Ag through the Casparian strip. These techniques may also help constrain whether the phloem-based Ag transport was limited by the small pore sizes of sieve cells and cell walls. Furthermore, of interest are molecular analyses of relevant protein expressions, to study how the sequestration and transport of Ag in wheat is regulated by metalloproteins and phytochelatins.

Of interest are also the similar Ag concentrations determined for the shoots of wheat that were exposed to $AgNO_3$, Ag NPs and $Ag_2S$ NPs in both Lufa soil and three different hydroponic systems (Chapter 4). Notably, the direct comparison of the Ag uptake determined for wheat plants grown in soil and hydroponic media showed that, to a first-order, the latter provides a simple and straightforward means to conduct preliminary studies of Ag uptake by crops in real agricultural systems.

The examination of the biological effects of Ag from Ag NPs and $AgNO_3$ on wheat produced to two main findings. On the one hand, either neutral or positive effects were observed in Chapters 3 and 4, as the seed mass, aboveground dry biomass, and shoot dry biomass were either not impacted or improved by the Ag treatments. On the other hand, in the long-term study of Chapter 3, which utilised low and hence realistic Ag exposure levels, wheat plants exposed to Ag NPs and $AgNO_3$ exhibited retardation in development by about 15 to 20 days for two later growth stages. If further work can confirm that this negative impact on plant development was indeed

related to Ag uptake by the wheat plants, it will be important to conduct additional molecular, microbiome and reactive oxygen species analyses to investigate the mechanisms, which trigger the retardation.

Finally, one of the key results of Chapter 2 is the finding that at soil Ag levels, which exceeded the predicted environmental concentrations by a factor of x3, wheat grains had unproblematic Ag concentrations even at advanced growth stages. In detail, the grains showed the lowest Ag levels among the plant tissues, with concentrations that were about 300x to 1000x lower than the maximum guideline concentrations set by the European Food Safety Authority. Importantly, this indicates that the application of sewage sludge, which contains Ag NPs (or Ag derived from these), to agricultural soils is unlikely to generate Ag levels in grains that are problematic for human consumption. However, the Ag levels in terrestrial environments are set to increase to almost twice the levels that were tested in Chapter 2 by 2050, due to enhanced use of Ag NPs (Giese et al., 2018). As such, it will be prudent to conduct further environmentally relevant studies to investigate and constrain the Ag uptake by crops. Needed in particular, are additional investigations that monitor the uptake, translocation and accumulation of Ag by other important edible crops, including rice and corn, as well crop exposures to Ag, which are conducted in alkaline soils.

# Bibliography


1. Abd-Alla, M. H., Nafady, N. A., & Khalaf, D. M. (2016). Assessment of silver nanoparticles contamination on faba bean-Rhizobium leguminosarum bv. viciae-Glomus aggregatum symbiosis: implications for induction of autophagy process in root nodule. *Agriculture, Ecosystems & Environment*, *218*, 163-177.
2. Abdel-Azeem, E. A., & Elsayed, B. A. (2013). Phytotoxicity of silver nanoparticles on Vicia faba seedlings. *NY Sci. J*, *6*(12), 148-156.
3. Adams, N. W., & Kramer, J. R. (1999). Silver speciation in wastewater effluent, surface waters, and pore waters. *Environmental Toxicology and Chemistry: An International Journal*, *18*(12), 2667-2673.
4. Alloway, B. J. (2013), Heavy Metals in Soils: Trace Metals and Metalloids in Soils and their Bioavailability, Environmental Pollution 22, 535-542.
5. Alloway, B. J. (1990). Soil processes and the behaviour of metals. Heavy metals in soils., 7-28.
6. Álvarez-Fernández, A., Díaz-Benito, P., Abadía, A., López-Millán, A. F., & Abadía, J. (2014). Metal species involved in long distance metal transport in plants. *Frontiers in plant science*, *5*, 105.
7. American Society for Testing and Materials. (2006). Standard terminology relating to nanotechnology. E 2456-06. West Conshohocken, PA.
8. Arndt, S. K., Irawan, A., & Sanders, G. J. (2015). Apoplastic water fraction and rehydration techniques introduce significant errors in measurements of relative water content and osmotic potential in plant leaves. *Physiologia plantarum*, *155*(4), 355-368.
9. Aruoja, V., Dubourguier, H. C., Kasemets, K., & Kahru, A. (2009). Toxicity of nanoparticles of CuO, ZnO and TiO 2 to microalgae Pseudokirchneriella subcapitata. *Science of the total environment*, *407*(4), 1461-1468.
10. Babu, K., Deepa, M., Shankar, S. G., & Rai, S. (2008). Effect of nano-silver on cell division and mitotic chromosomes: a prefatory siren. *Internet J Nanotech*, *2*, 2-5.

11. Bao, D., Oh, Z. G., & Chen, Z. (2016). Characterization of silver nanoparticles internalized by Arabidopsis plants using single particle ICP-MS analysis. *Frontiers in plant science*, *7*, 32.
12. Barberon, M., & Geldner, N. (2014). Radial transport of nutrients: the plant root as a polarized epithelium. *Plant physiology*, *166*(2), 528-537.
13. Barrena, R., Casals, E., Colón, J., Font, X., Sánchez, A., & Puntes, V. (2009). Evaluation of the ecotoxicity of model nanoparticles. *Chemosphere*, *75*(7), 850-857.
14. Bashan, Y. and de-Bashan, L.E., (2005). Fresh-weight measurements of roots provide inaccurate estimates of the effects of plant growth-promoting bacteria on root growth: a critical examination. *Soil biology and biochemistry*, *37*(10), pp.1795-1804.
15. Benn, T. M., & Westerhoff, P. (2008). Nanoparticle silver released into water from commercially available sock fabrics. *Environmental science & technology*, 42(11), 4133-4139.
16. Benn, T., Cavanagh, B., Hristovski, K., Posner, J. D., & Westerhoff, P. (2010). The release of nanosilver from consumer products used in the home. *Journal of environmental quality*, 39(6), 1875-1882.
17. Berendsen, R.L., Pieterse, C.M. and Bakker, P.A., 2012. The rhizosphere microbiome and plant health. *Trends in plant science*, *17*(8), pp.478-486.
18. Bermudez, E., Mangum, J. B., Wong, B. A., Asgharian, B., Hext, P. M., Warheit, D. B., & Everitt, J. I. (2004). Pulmonary responses of mice, rats, and hamsters to subchronic inhalation of ultrafine titanium dioxide particles. *Toxicological sciences*, *77*(2), 347-357.
19. Blaser, S. A., Scheringer, M., MacLeod, M., & Hungerbühler, K. (2008). Estimation of cumulative aquatic exposure and risk due to silver: contribution of nano-functionalized plastics and textiles. *Science of the total environment*, *390*(2), 396-409.
20. Borm, P. J., Robbins, D., Haubold, S., Kuhlbusch, T., Fissan, H., Donaldson, K., & Krutmann, J. (2006). The potential risks of nanomaterials: a review carried out for ECETOC. *Particle and fibre toxicology*, *3*(1), 1.
21. Boyle, R. W. (1968). The geochemistry of silver and its deposits (Geological Survey of Canada Bulletin No. 160, 264 pp). Ottawa: Department of Energy Mines and Resources.

22. Brar, S. K., Verma, M., Tyagi, R. D., & Surampalli, R. Y. (2010). Engineered nanoparticles in wastewater and wastewater sludge–Evidence and impacts. *Waste management*, *30*(3), 504-520.
23. British Standards Institution. (2007). Terminology for nanomaterials. PAS 136:2007. London, UK.
24. Brunner, T. J., Wick, P., Manser, P., Spohn, P., Grass, R. N., Limbach, L. K., ... & Stark, W. J. (2006). In vitro cytotoxicity of oxide nanoparticles: comparison to asbestos, silica, and the effect of particle solubility. *Environmental science & technology*, *40*(14), 4374-4381.
25. Bundschuh, M., Filser, J., Lüderwald, S., McKee, M. S., Metreveli, G., Schaumann, G. E., ... & Wagner, S. (2018). Nanoparticles in the environment: where do we come from, where do we go to?. *Environmental Sciences Europe*, *30*(1), 1-17.
26. Chen, F., Luo, Z., Fan, Y. F., Wu, K., Pan, Y. X., Liu, X., ... & Song, Y. F. (2016). Five metal elements homeostasis-related genes in Synechogobius hasta: molecular characterization, tissue expression and transcriptional response to Cu and Fe exposure. *Chemosphere*, *159*, 392-402.
27. Cheng, Y., Yin, L., Lin, S., Wiesner, M., Bernhardt, E., & Liu, J. (2011). Toxicity reduction of polymer-stabilized silver nanoparticles by sunlight. *The Journal of Physical Chemistry C*, *115*(11), 4425-4432.
28. Choat, B., Medek, D. E., Stuart, S. A., Pasquet-Kok, J., Egerton, J. J., Salari, H., ... & Ball, M. C. (2011). Xylem traits mediate a trade-off between resistance to freeze–thaw-induced embolism and photosynthetic capacity in overwintering evergreens. *New Phytologist*, *191*(4), 996-1005.
29. Christian, P., Von der Kammer, F., Baalousha, M., & Hofmann, T. (2008). Nanoparticles: structure, properties, preparation and behaviour in environmental media. *Ecotoxicology*, 17(5), 326-343.
30. Colvin, V. L. (2003). The potential environmental impact of engineered nanomaterials. *Nature biotechnology*, *21*(10), 1166-1170.
31. Cornelis, G., Hund-Rinke, K., Kuhlbusch, T., Van den Brink, N., & Nickel, C. (2014). Fate and bioavailability of engineered nanoparticles in soils: a review. *Critical Reviews in Environmental Science and Technology*, *44*(24), 2720-2764.

32. Cornelis, G., Pang, L., Doolette, C., Kirby, J. K., & McLaughlin, M. J. (2013). Transport of silver nanoparticles in saturated columns of natural soils. *Science of the Total Environment*, *463*, 120-130.
33. COT, C. COC (2005) Joint statement on nanomaterial toxicology. *FSA: London.* Accessed 10/01/2017.
34. Council of Europe. (2013). Metals and Alloys Used in Food Contact Materials and Articles.
35. Croteau, M. N., Dybowska, A. D., Luoma, S. N., & Valsami-Jones, E. (2011). A novel approach reveals that zinc oxide nanoparticles are bioavailable and toxic after dietary exposures. *Nanotoxicology*, *5*(1), 79-90.
36. Croteau, M. N., Dybowska, A. D., Luoma, S. N., Misra, S. K., & Valsami-Jones, E. (2014). Isotopically modified silver nanoparticles to assess nanosilver bioavailability and toxicity at environmentally relevant exposures. *Environmental Chemistry*, *11*(3), 247-256.
37. de Laeter, J. R., Böhlke, J. K., De Bièvre, P., Hidaka, H., Peiser, H. S., Rosman, K. J. R., & Taylor, P. D. P. (2003). Atomic weights of the elements. Review 2000 (IUPAC Technical Report). *Pure and applied chemistry*, *75*(6), 683-800.
38. Dhawan, A., Sharma, V., & Parmar, D. (2009). Nanomaterials: a challenge for toxicologists. *Nanotoxicology*.
39. Dietz, K. J., & Herth, S. (2011). Plant nanotoxicology. *Trends in plant science, 16(*11), 582-589.
40. Diez-Ortiz, M., Lahive, E., George, S., Ter Schure, A., Van Gestel, C. A., Jurkschat, K., ... & Spurgeon, D. J. (2015). Short-term soil bioassays may not reveal the full toxicity potential for nanomaterials; bioavailability and toxicity of silver ions (AgNO3) and silver nanoparticles to earthworm Eisenia fetida in long-term aged soils. *Environmental pollution*, *203*, 191-198.
41. Diez-Ortiz, M., Lahive, E., Kille, P., Powell, K., Morgan, A. J., Jurkschat, K., ... & Spurgeon, D. J. (2015). Uptake routes and toxicokinetics of silver nanoparticles and silver ions in the earthworm Lumbricus rubellus. *Environmental toxicology and chemistry*, *34*(10), 2263-2270.
42. Dimkpa, C. O., McLean, J. E., Martineau, N., Britt, D. W., Haverkamp, R., & Anderson, A. J. (2013). Silver nanoparticles disrupt wheat (Triticum

aestivum L.) growth in a sand matrix. *Environmental science & technology*, *47*(2), 1082-1090.

43. Doolette, C. L., McLaughlin, M. J., Kirby, J. K., & Navarro, D. A. (2015). Bioavailability of silver and silver sulfide nanoparticles to lettuce (Lactuca sativa): Effect of agricultural amendments on plant uptake. *Journal of Hazardous Materials*, *300*, 788-795.
44. Dybowska, A. D., Croteau, M. N., Misra, S. K., Berhanu, D., Luoma, S. N., Christian, P., ... & Valsami-Jones, E. (2011). Synthesis of isotopically modified ZnO nanoparticles and their potential as nanotoxicity tracers. *Environmental pollution*, *159*(1), 266-273.
45. Dybowska, A., Misra, S. K., & Valsami-Jones, E. (2016). Labelling Nanoparticles with Non-Radioactive Isotopes. In *Isotopes in Nanoparticles: Fundamentals and Applications* (pp. 455-492). Pan Stanford.
46. EFSA Panel on food contact materials, enzymes, flavourings and processing aids (CEF). (2011). Scientific Opinion on the safety evaluation of the substance, silver zeolite A (silver zinc sodium ammonium alumino silicate), silver content 2–5%, for use in food contact materials. *EFSA Journal*, *9*(2), 1999.
47. El-Temsah, Y. S., & Joner, E. J. (2012). Impact of Fe and Ag nanoparticles on seed germination and differences in bioavailability during exposure in aqueous suspension and soil. *Environmental toxicology*, *27*(1), 42-49.
48. Fabrega J., Luoma S.N., Tyler C.R., Galloway T.S., Lead J.R. (2011). Silver nanoparticles: Behaviour and effects in the aquatic environment. *Environment International* 37:517-531
49. FAO. (2020). Cereal Supply and Demand Brief. http://www.fao.org/worldfoodsituation/csdb/en/
50. Farré, M., Gajda-Schrantz, K., Kantiani, L., & Barceló, D. (2009). Ecotoxicity and analysis of nanomaterials in the aquatic environment. *Analytical and bioanalytical chemistry*, *393*(1), 81-95.
51. Federici, G., Shaw, B. J., & Handy, R. D. (2007). Toxicity of titanium dioxide nanoparticles to rainbow trout (Oncorhynchus mykiss): gill injury, oxidative stress, and other physiological effects. *Aquatic Toxicology*, 84(4), 415-430.

52. Flora, S. J., & Pachauri, V. (2010). Chelation in metal intoxication. *International journal of environmental research and public health*, *7*(7), 2745-2788.
53. Flora, S. J., & Pachauri, V. (2012). Chelation in metal intoxication. *International journal of environmental research and public health*, *7*(7), 2745-2788.
54. Florini, K., Walsh, S., Balbus, J. M., & Denison, R. (2006). Nanotechnology: getting it right the first time. *Nanotech. L. & Bus., 3,* 39.
55. Friend, D. J. C. (1965). Ear length and spikelet number of wheat grown at different temperatures and light intensities. *Canadian Journal of Botany*, *43*(3), 345-353.
56. Fung, M. C., & Bowen, D. L. (1996). Silver products for medical indications: risk-benefit assessment. *Journal of toxicology: Clinical toxicology*, *34*(1), 119-126.
57. Gan, W., Xu, B., & Dai, H. L. (2011). Activation of thiols at a silver nanoparticle surface. *Angewandte Chemie International Edition*, *50*(29), 6622-6625.
58. García-Hernández, M., Murphy, A., & Taiz, L. (1998). Metallothioneins 1 and 2 have distinct but overlapping expression patterns in Arabidopsis. *Plant Physiology*, *118*(2), 387-397.
59. Geisler-Lee, J., Brooks, M., Gerfen, J. R., Wang, Q., Fotis, C., Sparer, A. …& Geisler, M. (2014). Reproductive toxicity and life history study of silver nanoparticle effect, uptake and transport in Arabidopsis thaliana. *Nanomaterials*, *4*(2), 301-318.
60. Geisler-Lee, J., Wang, Q., Yao, Y., Zhang, W., Geisler, M., Li, K., ... & Ma, X. (2012). Phytotoxicity, accumulation and transport of silver nanoparticles by Arabidopsis thaliana. *Nanotoxicology*, *7*(3), 323-337.
61. Giese, B., Klaessig, F., Park, B., Kaegi, R., Steinfeldt, M., Wigger, H., ... & Gottschalk, F. (2018). Risks, release and concentrations of engineered nanomaterial in the environment. *Scientific reports*, *8*(1), 1-18.
62. Gottschalk, F., & Nowack, B. (2011). The release of engineered nanomaterials to the environment. *Journal of Environmental Monitoring*, *13*(5), 1145-1155.

63. Gottschalk, F., Sonderer, T., Scholz, R. W., & Nowack, B. (2009). Modeled environmental concentrations of engineered nanomaterials (TiO2, ZnO, Ag, CNT, fullerenes) for different regions. *Environmental science & technology*, 43(24), 9216-9222.
64. Gottschalk, F., Sun, T., & Nowack, B. (2013). Environmental concentrations of engineered nanomaterials: review of modeling and analytical studies. *Environmental Pollution*, 181, 287-300.
65. Grusak, M. A. (2002). Enhancing mineral content in plant food products. *Journal of the American College of Nutrition*, *21*(sup3), 178S-183S.
66. Gubbins, E. J., Batty, L. C., & Lead, J. R. (2011). Phytotoxicity of silver nanoparticles to Lemna minor L. *Environmental Pollution*, *159*(6), 1551-1559.
67. Gulson, B., & Wong, H. (2006). Stable isotopic tracing: A way forward for nanotechnology. *Environmental health perspectives*, 1486-1488.
68. Guo, G., Lei, M., Wang, Y., Song, B., & Yang, J. (2018). Accumulation of As, Cd, and Pb in sixteen wheat cultivars grown in contaminated soils and associated health risk assessment. *International Journal of Environmental Research and Public Health*, *15*(11), 2601.
69. Gupta, S. D., Agarwal, A., & Pradhan, S. (2018). Phytostimulatory effect of silver nanoparticles (Ag NPs) on rice seedling growth: an insight from antioxidative enzyme activities and gene expression patterns. *Ecotoxicology and environmental safety*, *161*, 624-633.
70. Handy, R. D., Henry, T. B., Scown, T. M., Johnston, B. D., & Tyler, C. R. (2008). Manufactured nanoparticles: their uptake and effects on fish—a mechanistic analysis. *Ecotoxicology*, *17*(5), 396-409.
71. Handy, R. D., Owen, R., & Valsami-Jones, E. (2008). The ecotoxicology of nanoparticles and nanomaterials: current status, knowledge gaps, challenges, and future needs. *Ecotoxicology*, *17*(5), 315-325.
72. Hansen, S. F., Hansen, O. F. H., & Nielsen, M. B. (2020). Advances and challenges towards consumerization of nanomaterials. *Nature Nanotechnology*, *15*(12), 964-965.
73. Hao, Y., Yu, F., Lv, R., Ma, C., Zhang, Z., Rui, Y., Liu, L., Cao, W. and Xing, B. (2016). Carbon nanotubes filled with different ferromagnetic alloys affect

the growth and development of rice seedlings by changing the C: N ratio and plant hormones concentrations. *PLoS One*, *11*(6), p.e0157264.

74. Hart, J. J., Welch, R. M., Norvell, W. A., Sullivan, L. A., & Kochian, L. V. (1998). Characterization of cadmium binding, uptake, and translocation in intact seedlings of bread and durum wheat cultivars. *Plant physiology*, *116*(4), 1413-1420.
75. Hartmann, N. B., Skjolding, L. M., Hansen, S. F., Baun, A., Kjølholt, J., Gottschalk, F. (2014). Environmental fate and behaviour of nanomaterials. The Danish Environmental Protection Agency. ISBN nr. 978-87-93178-87-8
76. Hawthorne, J., Musante, C., Sinha, S. K., & White, J. C. (2012). Accumulation and phytotoxicity of engineered nanoparticles to Cucurbita pepo. *International journal of phytoremediation*, *14*(4), 429-442.
77. Hernández, D., Cepriá, G., Laborda, F., & Castillo, J. R. (2019). Detection and determination of released ions in the presence of nanoparticles: selectivity or strategy?. *Electroanalysis*, *31*(2), 405-410.
78. Hood, E. (2004). Nanotechnology: looking as we leap.
79. Imseng, M., Wiggenhauser, M., Keller, A., Müller, M., Rehkämper, M., Murphy, K., ... & Bigalke, M. (2019). Towards an understanding of the Cd isotope fractionation during transfer from the soil to the cereal grain. *Environmental pollution*, *244*, 834-844.
80. Jeevanandam, J., Barhoum, A., Chan, Y. S., Dufresne, A., & Danquah, M. K. (2018). Review on nanoparticles and nanostructured materials: history, sources, toxicity and regulations. *Beilstein journal of nanotechnology*, *9*(1), 1050-1074.
81. Jhanzab, H. M., Razzaq, A., Jilani, G., Rehman, A., Hafeez, A., & Yasmeen, F. (2015). Silver nano-particles enhance the growth, yield and nutrient use efficiency of wheat. *Int J Agron Agri Res*, *7*, 15-22.
82. Jiang, H. S., Qiu, X. N., Li, G. B., Li, W., & Yin, L. Y. (2014). Silver nanoparticles induced accumulation of reactive oxygen species and alteration of antioxidant systems in the aquatic plant Spirodela polyrhiza. *Environmental toxicology and chemistry*, *33*(6), 1398-1405.
83. Jiang, J., Oberdörster, G., & Biswas, P. (2009). Characterization of size, surface charge, and agglomeration state of nanoparticle dispersions for

toxicological studies. *Journal of Nanoparticle Research*, *11*(1), 77-89.

84. Jin, X., Shi, C., Yu, C. Y., Yamada, T., & Sacks, E. J. (2017). Determination of leaf water content by visible and near-infrared spectrometry and multivariate calibration in miscanthus. *Frontiers in plant science*, *8*, 721.
85. Kabata-Pendias, A., & Pendias, H. (2011). Trace elements in soils and plants, Vol. 4. Boca Raton: CRC press., 268 - 273
86. Kaegi, R., Sinnet, B., Zuleeg, S., Hagendorfer, H., Mueller, E., Vonbank, R., ... & Burkhardt, M. (2010). Release of silver nanoparticles from outdoor facades. *Environmental pollution*, *158*(9), 2900-2905.
87. Kahru, A., & Dubourguier, H. C. (2010). From ecotoxicology to nanoecotoxicology. *Toxicology*, *269*(2), 105-119.
88. Kaveh, R., Li, Y. S., Ranjbar, S., Tehrani, R., Brueck, C. L., & Van Aken, B. (2013). Changes in Arabidopsis thaliana gene expression in response to silver nanoparticles and silver ions. *Environmental science & technology*, *47*(18), 10637-10644.
89. Keller, A. A., McFerran, S., Lazareva, A., & Suh, S. (2013). Global life cycle releases of engineered nanomaterials. *Journal of Nanoparticle Research*, *15*(6), 1-17.
90. Khan, F. R., Laycock, A., Dybowska, A., Larner, F., Smith, B. D., Rainbow, P. S., & Valsami-Jones, E. (2013). Stable isotope tracer to determine uptake and efflux dynamics of ZnO nano-and bulk particles and dissolved Zn to an estuarine snail. *Environmental science & technology*, *47*(15), 8532-8539.
91. Kim, Y. X., Ranathunge, K., Lee, S., Lee, Y., Lee, D., & Sung, J. (2018). Composite transport model and water and solute transport across plant roots: an update. *Frontiers in plant science*, *9*, 193.
92. Kirby, E. J. M., Curtis, B. C., Rajaram, S., & Gómez Macpherson, H. (2002). Bread wheat: Improvement and Production.
93. Kirkham, M. B. (1980). Movement of cadmium and water in split-root wheat plants. *Soil Science*, *129*(6), 339-344.
94. Klaine, S. J., Alvarez, P. J. J., Batley, G. E., Fernandes, T. F., Handy, R. D., Lyon, D. Y., Mahendra, S., McLaughlin, M. J. and Lead, J. R. (2008), Nanomaterials in the environment: Behaviour, fate, bioavailability, and effects. *Environmental Toxicology and Chemistry*, 27: 1825–1851. doi:10.1897/08-090.1

95. Klaine, S. J., Edgington, A., & Seda, B. (2013). Nanomaterials in the Environment. In *Encyclopedia of Aquatic Ecotoxicology* (pp. 767-780). Springer Netherlands.
96. Klitzke, S., Metreveli, G., Peters, A., Schaumann, G. E., & Lang, F. (2015). The fate of silver nanoparticles in soil solution—Sorption of solutes and aggregation. *Science of the Total Environment*, *535*, 54-60.
97. Kraas M, Schlich K, Knopf B, Wege F, Kagi R, Terytze K, Hund-Rinke K (2017) Long-term effects of sulfidized silver nanoparticles in sewage sludge on soil microflora. Environ Toxicol Chem 36:3305–3313
98. Kumari, M., Mukherjee, A., & Chandrasekaran, N. (2009). Genotoxicity of silver nanoparticles in Allium cepa. *Science of the Total Environment*, *407*(19), 5243-5246.
99. Kvitek, L., Karlikova, M., Soukupova, J., Panacek, A., Prucek, R., Kozakova, S., & Bardakci, B. (2011). Nanocomposites on the bases of silicate materials and silver nanoparticles. In *Nanocon. Conf. Olomouc.* (Vol. 2011, pp. 25-30).
100. Lahive, E., Matzke, M., Durenkamp, M., Lawlor, A. J., Thacker, S. A., Pereira, M. G., ... & Lofts, S. (2017). Sewage sludge treated with metal nanomaterials inhibits earthworm reproduction more strongly than sludge treated with metal metals in bulk/salt forms. *Environmental Science: Nano*, *4*(1), 78-88
101. Larner, F., & Rehkämper, M. (2012). Evaluation of Stable Isotope Tracing for ZnO Nanomaterials. New Constraints from High Precision Isotope Analyses and Modeling. *Environmental science & technology*, 46(7), 4149-4158.
102. Larner, F., Dogra, Y., Dybowska, A., Fabrega, J., Stolpe, B., Bridgestock, L. J., ... & Valsami-Jones, E. (2012). Tracing bioavailability of ZnO nanoparticles using stable isotope labeling. *Environmental science & technology*, *46*(21), 12137-12145.
103. Larue, C., Castillo-Michel, H., Sobanska, S., Cécillon, L., Bureau, S., Barthès, V., ... & Sarret, G. (2014). Foliar exposure of the crop Lactuca sativa to silver nanoparticles: evidence for internalization and changes in Ag speciation. *Journal of hazardous materials*, *264*, 98-106.
104. Larue, C., Laurette, J., Herlin-Boime, N., Khodja, H., Fayard, B.,

Flank, A. M., ... & Carriere, M. (2012). Accumulation, translocation and impact of TiO2 nanoparticles in wheat (Triticum aestivum spp.): influence of diameter and crystal phase. *Science of the total environment*, *431*, 197-208.

105. Laycock, A., Stolpe, B., Römer, I., Dybowska, A., Valsami-Jones, E., Lead, J. R., & Rehkämper, M. (2014). Synthesis and characterization of isotopically labeled silver nanoparticles for tracing studies. *Environmental Science: Nano*, *1*(3), 271-283.
106. Lea, M. C. (1889). Allotropic forms of silver. *American Journal of science*, (222), 476-491.
107. Lecoanet, H. F., Bottero, J. Y., & Wiesner, M. R. (2004). Laboratory assessment of the mobility of nanomaterials in porous media. *Environmental science & technology*, *38*(19), 5164-5169.
108. Lee, W. M., Kwak, J. I., & An, Y. J. (2012). Effect of silver nanoparticles in crop plants Phaseolus radiatus and Sorghum bicolor: media effect on phytotoxicity. *Chemosphere*, *86*(5), 491-499.
109. Levard, C., Hotze, E. M., Lowry, G. V., & Brown Jr, G. E. (2012). Environmental transformations of silver nanoparticles: impact on stability and toxicity. *Environmental science & technology*, *46*(13), 6900-6914.
110. Levard, C., Reinsch, B. C., Michel, F. M., Oumahi, C., Lowry, G. V., & Brown Jr, G. E. (2011). Sulfidation processes of PVP-coated silver nanoparticles in aqueous solution: impact on dissolution rate. *Environmental science & technology*, *45*(12), 5260-5266.
111. Li, X., Lenhart, J. J., & Walker, H. W. (2010). Dissolution-accompanied aggregation kinetics of silver nanoparticles. *Langmuir*, *26*(22), 16690-16698.
112. Li, Y., Chen, H., Wang, F., Zhao, F., Han, X., Geng, H., ... & Yao, J. (2018). Environmental behavior and associated plant accumulation of silver nanoparticles in the presence of dissolved humic and fulvic acid. *Environmental Pollution*, *243*, 1334-1342.
113. Lin, D., & Xing, B. (2007). Phytotoxicity of nanoparticles: inhibition of seed germination and root growth. *Environmental Pollution*, *150*(2), 243-250.
114. Liu, G., Zhang, M., Jin, Y., Fan, X., Xu, J., Zhu, Y., ... & Qian, H. (2017). The effects of low concentrations of silver nanoparticles on wheat

growth, seed quality, and soil microbial communities. *Water, Air, & Soil Pollution*, *228*(9), 348.

115. Liu, J., & Hurt, R. H. (2010). Ion release kinetics and particle persistence in aqueous nano-silver colloids. *Environmental science & technology*, *44*(6), 2169-2175.

116. Liu, W. X., Liu, J. W., Wu, M. Z., Li, Y., Zhao, Y., & Li, S. R. (2009). Accumulation and translocation of toxic heavy metals in winter wheat (Triticum aestivum L.) growing in agricultural soil of Zhengzhou, China. *Bulletin of environmental contamination and toxicology*, *82*(3), 343-347.

117. Lowry, G. V., Gregory, K. B., Apte, S. C., & Lead, J. R. (2012). Transformations of nanomaterials in the environment.

118. Lugtenberg, B. and Kamilova, F., 2009. Plant-growth-promoting rhizobacteria. *Annual review of microbiology*, *63*, pp.541-556.

119. Luoma, S. N. (2008). Silver nanotechnologies and the environment. *The Project on Emerging Nanotechnologies Report, 15.*

120. Ma, X., Geisler-Lee, J., Deng, Y., & Kolmakov, A. (2010). Interactions between engineered nanoparticles (ENPs) and plants: phytotoxicity, uptake and accumulation. *Science of the total environment*, *408*(16), 3053-3061.

121. Ma, Y., He, X., Zhang, P., Zhang, Z., Ding, Y., Zhang, J., ... & Zheng, L. (2017). Xylem and phloem based transport of CeO2 nanoparticles in hydroponic cucumber plants. *Environmental Science & Technology*, *51*(9), 5215-5221.

122. Mackevica, A., Olsson, M. E., & Hansen, S. F. (2016). Silver nanoparticle release from commercially available plastic food containers into food simulants. *Journal of Nanoparticle Research*, *18*(1), 5.

123. Mackevica, A., Olsson, M. E., & Hansen, S. F. (2017). The release of silver nanoparticles from commercial toothbrushes. *Journal of hazardous materials*, *322*, 270-275.

124. Marschner, H. (1995). Mineral nutrition of higher plants 2nd edition. *Academic, Great Britain*.

125. Marschner, H., Kirkby, E. A., & Cakmak, I. (1996). Effect of mineral nutritional status on shoot—root partitioning of photoassimilates and cycling of mineral nutrients. *Journal of experimental botany*, 1255-1263.

126. Martinez-Criado, G., Villanova, J., Tucoulou, R., Salomon, D., Suuronen, J. P., Labouré, S., ... & Dabin, Y. (2016). ID16B: a hard X-ray nanoprobe beamline at the ESRF for nano-analysis. *Journal of synchrotron radiation*, *23*(1), 344-352.

127. Mazumdar, H., & Ahmed, G. U. (2011). Phytotoxicity effect of silver nanoparticles on Oryza sativa. *IJ ChemTech. Res*, *3*(3), 1494-1500.

128. McGillicuddy, E., Murray, I., Kavanagh, S., Morrison, L., Fogarty, A., Cormican, M., ... & Morris, D. (2017). Silver nanoparticles in the environment: Sources, detection and ecotoxicology. *Science of the Total Environment*, *575*, 231-246.

129. Measures, M., Weinberger, P., & Baer, H. (1973). Variability of plant growth within controlled-environment chambers as related to temperature and light distribution. *Canadian Journal of Plant Science*, *53*(1), 215-220.

130. Metreveli G, Frombold B, Seitz F, Grün A, Phillippe A, Rosenfeldt RR, Bundschuh M, Schulz R, Manz W, Schaumann GE (2016) Impact of chemical composition of ecotoxicological test media on the stability and aggregation status of silver nanoparticles. Environ Sci Nano 3:418–433

131. Metrno DM, Ranville JF, Bednar A, Kazor K, Hering AS, Higgins CP (2014) Tracking dissolution of silver nanoparticles at environmentally relevant concentrations in laboratory, natural, and processed waters using single particle ICP-MS (spICP-MS). Environ Sci Nano 1(3):248–259

132. Miao, A. J., Quigg, A., Schwehr, K., Xu, C., & Santschi, P. (2007). Engineered silver nanoparticles (ESNs) in coastal marine environments: bioavailability and toxic effects to the phytoplankton Thalassiosira weissflogii. In 2nd International Conference on the Environmental Effects of Nanoparticles and Nanomaterials: Sept 24 (Vol. 25).

133. Mirzajani, F., Askari, H., Hamzelou, S., Farzaneh, M., & Ghassempour, A. (2013). Effect of silver nanoparticles on Oryza sativa L. and its rhizosphere bacteria. *Ecotoxicology and environmental safety*, *88*, 48-54.

134. Misra, S. K., Dybowska, A., Berhanu, D., Croteau, M. N., Luoma, S. N., Boccaccini, A. R., & Valsami-Jones, E. (2011). Isotopically modified nanoparticles for enhanced detection in bioaccumulation studies. *Environmental science & technology*, 46(2), 1216-1222.

135. Mueller, N. C., & Nowack, B. (2008). Exposure modelling of engineered nanoparticles in the environment. *Environmental science & technology*, 42(12), 4447-4453.

136. Musante, C., & White, J. C. (2012). Toxicity of silver and copper to Cucurbita pepo: differential effects of nano and bulk-size particles. *Environmental toxicology*, *27*(9), 510-517.

137. Nair, P. M. G., & Chung, I. M. (2014). Physiological and molecular level effects of silver nanoparticles exposure in rice (Oryza sativa L.) seedlings. *Chemosphere*, *112*, 105-113.

138. Nair, P. M. G., & Chung, I. M. (2015). Physiological and molecular level studies on the toxicity of silver nanoparticles in germinating seedlings of mung bean (Vigna radiata L.). *Acta physiologiae plantarum*, *37*(1), 1-11.

139. Navarro, E., Baun, A., Behra, R., Hartmann, N. B., Filser, J., Miao, A. J., & Sigg, L. (2008). Environmental behavior and ecotoxicity of engineered nanoparticles to algae, plants, and fungi. *Ecotoxicology*, *17*(5), 372-386.

140. Nejatzadeh-Barandozi, F., Darvishzadeh, F., & Aminkhani, A. (2014). Effect of nano silver and silver nitrate on seed yield of (Ocimum basilicum L.). *Organic and medicinal chemistry letters*, *4*(1), 11.

141. Nocito, F. F., Lancilli, C., Dendena, B., Lucchini, G., & Sacchi, G. A. (2011). Cadmium retention in rice roots is influenced by cadmium availability, chelation and translocation. *Plant, cell & environment*, *34*(6), 994-1008.

142. Nowack, B., Krug, H. F., & Height, M. (2011). 120 years of nanosilver history: implications for policy makers.

143. OECD Guideline for Testing of Chemicals 208. (1984). Terrestrial Plants, Growth Test. ... Determination of the Effects of Pollutants on Soil Flora - Effects of Chemicals on the Emergence and Growth of Higher Plants.

144. OECD Guideline for Testing of Chemicals 227. (2006). Terrestrial Plants Test. Vegetative Vigour Test

145. Oukarroum, A., Barhoumi, L., Pirastru, L., & Dewez, D. (2013). Silver nanoparticle toxicity effect on growth and cellular viability of the aquatic plant Lemna gibba. *Environmental Toxicology and Chemistry*, *32*(4), 902-907.

146. Pachapur, V. L., Larios, A. D., Cledón, M., Brar, S. K., Verma, M., & Surampalli, R. Y. (2016). Behavior and characterization of titanium dioxide

and silver nanoparticles in soils. *Science of the Total Environment*, *563*, 933-943.

147. Pais, I., & Jones Jr, J. B. (1997). *The handbook of trace elements*. CRC Press.

148. Pal, S., Tak, Y. K., & Song, J. M. (2007). Does the antibacterial activity of silver nanoparticles depend on the shape of the nanoparticle? A study of the gram-negative bacterium Escherichia coli. *Applied and environmental microbiology*, *73*(6), 1712-1720.

149. Panda, K. K., Achary, V. M. M., Krishnaveni, R., Padhi, B. K., Sarangi, S. N., Sahu, S. N., & Panda, B. B. (2011). In vitro biosynthesis and genotoxicity bioassay of silver nanoparticles using plants. *Toxicology in vitro*, *25*(5), 1097-1105.

150. Parveen, A., & Rao, S. (2015). Effect of nanosilver on seed germination and seedling growth in Pennisetum glaucum. *Journal of Cluster Science*, *26*(3), 693-701.

151. Patlolla, A. K., Berry, A., May, L., & Tchounwou, P. B. (2012). Genotoxicity of silver nanoparticles in Vicia faba: a pilot study on the environmental monitoring of nanoparticles. *International journal of environmental research and public health*, *9*(5), 1649-1662.

152. Peralta-Videa, J. R., Zhao, L., Lopez-Moreno, M. L., de la Rosa, G., Hong, J., & Gardea-Torresdey, J. L. (2011). Nanomaterials and the environment: a review for the biennium 2008–2010. *Journal of Hazardous Materials*, *186*(1), 1-15.

153. Percival, J. (1974). *The Wheat Plant: A Monography*. Duckworth.

154. Pérez-de-Luque, A. (2017). Interaction of nanomaterials with plants: what do we need for real applications in agriculture?. *Frontiers in Environmental Science*, *5*, 12.

155. Perry, M. W., Belford, R. K., Anderson, W. K., & Garlinge, J. R. (2000). The structure and development of cereal plant. *The wheat book*, 23-37.

156. Poehlman, J. M. (2013). *Breeding field crops*. Springer Science & Business Media.

157. Pokhrel, L. R., & Dubey, B. (2013). Evaluation of developmental responses of two crop plants exposed to silver and zinc oxide nanoparticles. *Science of the Total Environment*, *452*, 321-332.

158. Pradas del Real, A. E., Vidal, V., Carrière, M., Castillo-Michel, H. A., Levard, C., Chaurand, P., & Sarret, G. (2017). Ag nanoparticles and wheat roots: a complex interplay. *Environmental Science & Technology*.

159. Priha, O., & Smolander, A. (1999). Nitrogen transformations in soil under Pinus sylvestris, Picea abies and Betula pendula at two forest sites. *Soil Biology and Biochemistry*, *31*(7), 965-977.

160. Qian, H., Peng, X., Han, X., Ren, J., Sun, L., & Fu, Z. (2013). Comparison of the toxicity of silver nanoparticles and silver ions on the growth of terrestrial plant model Arabidopsis thaliana. *Journal of environmental sciences*, *25*(9), 1947-1956.

161. Quik, J. T., van De Meent, D., & Koelmans, A. A. (2014). Simplifying modeling of nanoparticle aggregation–sedimentation behavior in environmental systems: A theoretical analysis. *Water research*, *62*, 193-201.

162. Ratte, H. T. (1999). Bioaccumulation and toxicity of silver compounds: a review. *Environmental Toxicology and Chemistry: An International Journal*, *18*(1), 89-108.

163. Rauscher, H., Roebben, G., Amenta, V., Boix, S. A., Calzolai, L., Emons, H., Quiros, P. L. (2014). Towards a review of the EC Recommendation for a definition of the term “nanomaterial”. *Eur Union*. doi, 10(2788), 36237.

164. Ravindran, A., Prathna, T. C., Verma, V. K., Chandrasekaran, N., & Mukherjee, A. (2012). Bovine serum albumin mediated decrease in silver nanoparticle phytotoxicity: root elongation and seed germination assay. *Toxicological & Environmental Chemistry*, *94*(1), 91-98.

165. Ray, P. C., Yu, H., & Fu, P. P. (2009). Toxicity and environmental risks of nanomaterials: challenges and future needs. *Journal of Environmental Science and Health Part C*, *27*(1), 1-35.

166. Rayment, G. E., & Higginson, F. R. (1992). *Australian laboratory handbook of soil and water chemical methods*. Inkata Press Pty Ltd..

167. Rico, C. M., Peralta-Videa, J. R., & Gardea-Torresdey, J. L. (2015). Chemistry, biochemistry of nanoparticles, and their role in antioxidant defense system in plants. In *Nanotechnology and Plant Sciences* (pp. 1-17). Springer International Publishing.

168. Römer, I., White, T. A., Baalousha, M., Chipman, K., Viant, M. R., & Lead, J. R. (2011). Aggregation and dispersion of silver nanoparticles in exposure media for aquatic toxicity tests. *Journal of Chromatography A*, *1218*(27), 4226-4233.

169. Royal Society (2004) Nanoscience and nanotechnologies: opportunities and uncertainties. Report by The Royal Society and Royal Academy of Engineering, London. http://www.nanotec.org.uk/finalReport.htm Accessed 18/01/2017

170. Rui, M., Ma, C., Tang, X., Yang, J., Jiang, F., Pan, Y., ... & Xing, B. (2017). Phytotoxicity of silver nanoparticles to peanut (Arachis hypogaea L.): physiological responses and food safety. *ACS Sustainable Chemistry & Engineering*, *5*(8), 6557-6567.

171. Woodland, S. J., Rehkämper, M., Halliday, A. N., Lee, D. C., Hattendorf, B., & Günther, D. (2005). Accurate measurement of silver isotopic compositions in geological materials including low Pd/Ag meteorites. *Geochimica et cosmochimica acta*, *69*(8), 2153-2163.

172. Sah, S., Sorooshzadeh, A., Rezazadeh, H. S., & Naghdibadi, H. A. (2011). Effect of nano silver and silver nitrate on seed yield of borage. *Journal of Medicinal Plants Research*, *5*(5), 706-710.

173. Salama, H. M. H. (2012). Effects of silver nanoparticles in some crop plants, Common bean (*Phaseolus vulgaris* L.) and corn (*Zea mays* L.). *International Research Journal of Biotechnology,* 3(10), 190-197.

174. Schlich, K., Klawonn, T., Terytze, K., & Hund-Rinke, K. (2013). Hazard assessment of a silver nanoparticle in soil applied via sewage sludge. *Environmental Sciences Europe*, *25*(1), 1-14.

175. Schönbächler, M., Carlson, R. W., Horan, M. F., Mock, T. D., & Hauri, E. H. (2007). High precision Ag isotope measurements in geologic materials by multiple-collector ICPMS: an evaluation of dry versus wet plasma. *International Journal of Mass Spectrometry*, *261*(2), 183-191.

176. Scientific Committee on Emerging and Newly Identified Health Risks. (2007). The appropriateness of the risk assessment methodology in accordance with the Technical Guidance Documents for new and existing substances for assessing the risks of nanomaterials, 21–22 June (2007). European Commission, Brussels, Belgium.

177. Sekine, R., Khurana, K., Vasilev, K., Lombi, E., & Donner, E. (2015). Quantifying the adsorption of ionic silver and functionalized nanoparticles during ecotoxicity testing: test container effects and recommendations. *Nanotoxicology*, *9*(8), 1005-1012.

178. Setter, T. L., & Carlton, G. (2000). The structure and development of the cereal plant Chapter 2. *The wheat book, principles and practice. Agriculture Western Australia, Midland*, 23-36.

179. Sharma, P., Bhatt, D., Zaidi, M. G. H., Saradhi, P. P., Khanna, P. K., & Arora, S. (2012). Silver nanoparticle-mediated enhancement in growth and antioxidant status of Brassica juncea. *Applied biochemistry and biotechnology*, *167*(8), 2225-2233.

180. Sharma, S., Kandel, N., Chaudhary, P., & Rai, P. (2020). A review on integrated nutrient management on wheat (*Triticum Aestivum L.*).

181. Sillen, W. M., Thijs, S., Abbamondi, G. R., Janssen, J., Weyens, N., White, J. C., & Vangronsveld, J. (2015). Effects of silver nanoparticles on soil microorganisms and maize biomass are linked in the rhizosphere. *Soil Biology and Biochemistry*, *91*, 14-22.

182. Smith, I. C. and Carson, B. L. (1977). Trace Metals in the Environment, Vol. 2, Ann Arbor Scientific Publications, Ann Arbor, MI, 469

183. Somenahally, A. C., Hollister, E. B., Loeppert, R. H., Yan, W., & Gentry, T. J. (2011). Microbial communities in rice rhizosphere altered by intermittent and continuous flooding in fields with long-term arsenic application. *Soil Biology and Biochemistry*, *43*(6), 1220-1228.

184. Sondi, I., & Salopek-Sondi, B. (2004). Silver nanoparticles as antimicrobial agent: a case study on E. coli as a model for Gram-negative bacteria. Journal of colloid and interface science, 275(1), 177-182.

185. Song, G., Gao, Y., Wu, H., Hou, W., Zhang, C., & Ma, H. (2012). Physiological effect of anatase TiO2 nanoparticles on Lemna minor. *Environmental toxicology and chemistry*, *31*(9), 2147-2152.

186. Song, M. H., Kim, S., Reddy, D. H. K., Wei, W., Bediako, J. K., Park, S., & Yun, Y. S. (2017). Development of polyethyleneimine-loaded core-shell chitosan hollow beads and their application for platinum recovery in sequential metal scavenging fill-and-draw process. *Journal of hazardous materials*, *324*, 724-731.

187. Song, U., Jun, H., Waldman, B., Roh, J., Kim, Y., Yi, J., & Lee, E. J. (2013). Functional analyses of nanoparticle toxicity: a comparative study of the effects of $TiO_2$ and Ag on tomatoes (Lycopersicon esculentum). *Ecotoxicology and environmental safety*, *93*, 60-67.

188. Stampoulis, D., Sinha, S. K., & White, J. C. (2009). Assay-dependent phytotoxicity of nanoparticles to plants. *Environmental science & technology*, *43*(24), 9473-9479.

189. Stegemeier, J. P., Reinsch, B. C., Lentini, C. J., Dale, J. G., & Kim, C. S. (2015B). Aggregation of nanoscale iron oxyhydroxides and corresponding effects on metal uptake, retention, and speciation: II. Temperature and time. *Geochimica et Cosmochimica Acta*, *148*, 113-129.

190. Stegemeier, J. P., Schwab, F., Colman, B. P., Webb, S. M., Newville, M., Lanzirotti, A., ... & Lowry, G. V. (2015A). Speciation matters: Bioavailability of silver and silver sulfide nanoparticles to alfalfa (Medicago sativa). *Environmental science & technology*, *49*(14), 8451-8460.

191. Su, Y., Ashworth, V., Kim, C., Adeleye, A. S., Rolshausen, P., Roper, C., ... & Jassby, D. (2019). Delivery, uptake, fate, and transport of engineered nanoparticles in plants: a critical review and data analysis. *Environmental Science: Nano*, *6*(8), 2311-2331.

192. Sun, T. Y., Bornhöft, N. A., Hungerbühler, K., & Nowack, B. (2016). Dynamic Probabilistic Modeling of Environmental Emissions of Engineered Nanomaterials. *Environmental science & technology*, 50(9), 4701-4711.

193. Sun, T. Y., Gottschalk, F., Hungerbühler, K., & Nowack, B. (2014). Comprehensive probabilistic modelling of environmental emissions of engineered nanomaterials. *Environmental Pollution*, 185, 69-76.

194. Swartjes, F. A. (2011). Introduction to contaminated site management. In *Dealing with contaminated sites* (pp. 3-89). Springer, Dordrecht.

195. Syu, Y. Y., Hung, J. H., Chen, J. C., & Chuang, H. W. (2014). Impacts of size and shape of silver nanoparticles on Arabidopsis plant growth and gene expression. *Plant physiology and biochemistry*, *83*, 57-64.

196. Tangahu, B. V., Sheikh Abdullah, S. R., Basri, H., Idris, M., Anuar, N., & Mukhlisin, M. (2011). A review on heavy metals (As, Pb, and Hg) uptake by plants through phytoremediation. *International Journal of Chemical Engineering*, *2011*.

197. The Royal Society and Royal Academy of Engineering (2004). Nanoscience and nanotechnologies: Opportunities and Uncertainties, published 29 July 2004, http://www.nanotec.org.uk/finalReport.htm

198. Thuesombat, P., Hannongbua, S., Akasit, S., & Chadchawan, S. (2014). Effect of silver nanoparticles on rice (Oryza sativa L. cv. KDML 105) seed germination and seedling growth. *Ecotoxicology and environmental safety*, *104*, 302-309.

199. Tkalec, M., Štefanić, P. P., & Balen, B. (2019). Phytotoxicity of silver nanoparticles and defence mechanisms. In *Comprehensive Analytical Chemistry* (Vol. 84, pp. 145-198). Elsevier.

200. Tottman D.R., Makepeace R.J. (1979) An explanation of the decimal code for the growth stages of cereals, with illustrations. *Annals of Applied Biology*, 93, 221–234.

201. Tourinho, P. S., Van Gestel, C. A., Lofts, S., Svendsen, C., Soares, A. M., & Loureiro, S. (2012). Metal-based nanoparticles in soil: Fate, behavior, and effects on soil invertebrates. *Environmental Toxicology and Chemistry*, 31(8), 1679-1692.

202. Tripathi, D. K., Singh, S., Singh, S., Pandey, R., Singh, V. P., Sharma, N. C., ... & Chauhan, D. K. (2017). An overview on manufactured nanoparticles in plants: uptake, translocation, accumulation and phytotoxicity. *Plant Physiology and Biochemistry*, *110*, 2-12.

203. Tyne, W., Lofts, S., Spurgeon, D. J., Jurkschat, K., & Svendsen, C. (2013). A new medium for Caenorhabditis elegans toxicology and nanotoxicology studies designed to better reflect natural soil solution conditions. *Environmental toxicology and chemistry*, *32*(8), 1711-1717.

204. Ueno, D., Iwashita, T., Zhao, F. J., & Ma, J. F. (2008). Characterization of Cd translocation and identification of the Cd form in

xylem sap of the Cd-hyperaccumulator Arabidopsis halleri. *Plant and Cell Physiology*, *49*(4), 540-548.

205. Uraguchi, S., Kamiya, T., Sakamoto, T., Kasai, K., Sato, Y., Nagamura, Y., ... & Fujiwara, T. (2011). Low-affinity cation transporter (OsLCT1) regulates cadmium transport into rice grains. *Proceedings of the national academy of sciences*, *108*(52), 20959-20964.

206. Uraguchi, S., Mori, S., Kuramata, M., Kawasaki, A., Arao, T., & Ishikawa, S. (2009). Root-to-shoot Cd translocation via the xylem is the major process determining shoot and grain cadmium accumulation in rice. *Journal of experimental botany*, *60*(9), 2677-2688.

207. Van Belleghem, F., Cuypers, A., Semane, B., Smeets, K., Vangronsveld, J., d'Haen, J., & Valcke, R. (2007). Subcellular localization of cadmium in roots and leaves of Arabidopsis thaliana. *New Phytologist*, *173*(3), 495-508.

208. Vance, M. E., Kuiken, T., Vejerano, E. P., McGinnis, S. P., Hochella Jr, M. F., Rejeski, D., & Hull, M. S. (2015). Nanotechnology in the real world: Redeveloping the nanomaterial consumer products inventory. *Beilstein journal of nanotechnology*, *6*, 1769.

209. Vannini, C., Domingo, G., Onelli, E., De Mattia, F., Bruni, I., Marsoni, M., & Bracale, M. (2014). Phytotoxic and genotoxic effects of silver nanoparticles exposure on germinating wheat seedlings. *Journal of plant physiology*, *171*(13), 1142-1148.

210. Waalewijn-Kool, P. L., Klein, K., Forniés, R. M., & van Gestel, C. A. (2014). Bioaccumulation and toxicity of silver nanoparticles and silver nitrate to the soil arthropod Folsomia candida. *Ecotoxicology*, *23*(9), 1629-1637.

211. Wan, Y., & Layton, J. (2006). Wheat (Triticum aestivum L.). *Agrobacterium Protocols*, 245-254.

212. Wang, J., Koo, Y., Alexander, A., Yang, Y., Westerhof, S., Zhang, Q., ... & Alvarez, P. J. (2013). Phytostimulation of poplars and Arabidopsis exposed to silver nanoparticles and Ag+ at sublethal concentrations. *Environmental science & technology*, *47*(10), 5442-5449.

213. Wang, P., Lombi, E., Sun, S., Scheckel, K. G., Malysheva, A., McKenna, B. A., ... & Kopittke, P. M. (2017). Characterizing the uptake,

accumulation and toxicity of silver sulfide nanoparticles in plants. *Environmental Science: Nano*.

214. Wang, P., Menzies, N. W., Lombi, E., Sekine, R., Blamey, F. P. C., Hernandez-Soriano, M. C., ... & Kopittke, P. M. (2015). Silver sulfide nanoparticles ($Ag_2S$-NPs) are taken up by plants and are phytotoxic. *Nanotoxicology*, *9*(8), 1041-1049.

215. Wang, X., Luo, X., Wang, Q., Liu, Y., & Naidu, R. (2020). Predicting the combined toxicity of binary metal mixtures (Cu–Ni and Zn–Ni) to wheat. *Ecotoxicology and Environmental Safety*, *205*, 111334.

216. Wang, Z., Xie, X., Zhao, J., Liu, X., Feng, W., White, J. C., & Xing, B. (2012). Xylem-and phloem-based transport of CuO nanoparticles in maize (Zea mays L.). *Environmental science & technology*, *46*(8), 4434-4441.

217. Weiss, E., & Zohary, D. (2011). The Neolithic Southwest Asian founder crops: their biology and archaeobotany. *Current Anthropology*, *52*(S4), S237-S254.

218. Wen, Y., Zhang, L., Chen, Z., Sheng, X., Qiu, J., & Xu, D. (2016). Co-exposure of silver nanoparticles and chiral herbicide imazethapyr to Arabidopsis thaliana: enantioselective effects. *Chemosphere*, *145*, 207-214.

219. Wiggenhauser, M., Bigalke, M., Imseng, M., Müller, M., Keller, A., Murphy, K., ... & Frossard, E. (2016). Cadmium isotope fractionation in soil–wheat systems. *Environmental science & technology*, *50*(17), 9223-9231.

220. Wijnhoven, S. W., Peijnenburg, W. J., Herberts, C. A., Hagens, W. I., Oomen, A. G., Heugens, E. H., ... & Dekkers, S. (2009). Nano-silver–a review of available data and knowledge gaps in human and environmental risk assessment. *Nanotoxicology*, *3*(2), 109-138.

221. Williams, L. E., & Mills, R. F. (2005). P1B-ATPases–an ancient family of transition metal pumps with diverse functions in plants. *Trends in plant science*, *10*(10), 491-502.

222. Wombacher, F., & Rehkämper, M. (2003). Investigation of the mass discrimination of multiple collector ICP-MS using neodymium isotopes and the generalised power law. *Journal of analytical atomic spectrometry*, *18*(11), 1371-1375.

223. Wu, Y., & Hendershot, W. H. (2009). Cation exchange capacity and proton binding properties of pea (Pisum sativum L.) roots. *Water, air, and soil pollution*, *200*(1-4), 353-369.

224. Wu, Y., & Hendershot, W. H. (2010). The effect of calcium and pH on nickel accumulation in and rhizotoxicity to pea (Pisum sativum L.) root–empirical relationships and modeling. *Environmental pollution*, *158*(5), 1850-1856.

225. Y. Qing, L. C., Li, R., Liu, G., Zhang, Y., Tang, X., Wang, J., ... & Qin, Y. (2018). Potential antibacterial mechanism of silver nanoparticles and the optimization of orthopedic implants by advanced modification technologies. *International journal of nanomedicine*, *13*, 3311.

226. Yan, A., & Chen, Z. (2019). Impacts of silver nanoparticles on plants: a focus on the phytotoxicity and underlying mechanism. *International Journal of Molecular Sciences*, *20*(5), 1003.

227. Yang, J., Jiang, F., Ma, C., Rui, Y., Rui, M., Adeel, M., ... & Xing, B. (2018). Alteration of crop yield and quality of wheat upon exposure to silver nanoparticles in a life cycle study. *Journal of agricultural and food chemistry*, *66*(11), 2589-2597.

228. Yasur, J., & Rani, P. U. (2013). Environmental effects of nanosilver: impact on castor seed germination, seedling growth, and plant physiology. *Environmental Science and Pollution Research*, *20*(12), 8636-8648.

229. Yin, L., Cheng, Y., Espinasse, B., Colman, B. P., Auffan, M., Wiesner, M., ... & Bernhardt, E. S. (2011). More than the ions: the effects of silver nanoparticles on Lolium multiflorum. *Environmental science & technology*, *45*(6), 2360-2367.

230. Yu, S. J., Yin, Y. G., & Liu, J. F. (2013). Silver nanoparticles in the environment. *Environmental Science: Processes & Impacts*, 15(1), 78-92.

231. Zadoks, J. C., Chang, T. T., & Konzak, C. F. (1974). A decimal code for the growth stages of cereals. *Weed research*, 14(6), 415-421.

232. Zuverza-Mena, N., Armendariz, R., Peralta-Videa, J. R., & Gardea-Torresdey, J. L. (2016). Effects of silver nanoparticles on radish sprouts: root growth reduction and modifications in the nutritional value. *Frontiers in plant science*, *7*.

233. Zuverza-Mena, N., Martínez-Fernández, D., Du, W., Hernandez-Viezcas, J. A., Bonilla-Bird, N., López-Moreno, M. L., ... & Gardea-Torresdey, J. L. (2017). Exposure of engineered nanomaterials to plants: Insights into the physiological and biochemical responses-A review. *Plant Physiology and Biochemistry*, *110*, 236-264.

# Appendices

## Appendix A

*Table 1A*. Mean $^{109}$Ag-E concentrations for the soils (µg kg$^{-1}$) and their standard deviation (n = 2).

| Growth stage No | $^{109}$Ag NPs | $^{109}$AgNO$_3$ | Blank control | Citrate control |
|---|---|---|---|---|
| **0** | 68.9 ± 0.8 | 68.2 ± 0.3 | 0.0023 ± 0.0004 | 0.0023 ± 0.0007 |
| **1** | 65.9 ± 1.1 | 63.0 ± 1.1 | 0.0013 ± 0.0002 | 0.0009 ± 0.0005 |
| **2** | 64.6 ± 1.2 | 56.1 ± 1.1 | 0.0012 ± 0.0005 | 0.0011 ± 0.0005 |
| **4** | 50.1 ± 1.0 | 51.3 ± 0.3 | 0.0010 ± 0.0005 | 0.0011 ± 0.0005 |
| **6** | 51.3 ± 0.4 | 51.6 ± 0.7 | 0.0012 ± 0.0002 | 0.0011 ± 0.0001 |
| **8** | 51.5 ± 0.7 | 51.0 ± 0.4 | 0.0015 ± 0.0001 | 0.0015 ± 0.0004 |

*Table 2A*. Mean total $^{109}$Ag-E concentrations for the soil pore waters (µg L$^{-1}$) and their standard deviation (n = 2).

| Growth stage No | $^{109}$Ag NPs | $^{109}$AgNO$_3$ | Blank control |
|---|---|---|---|
| **4** | 0.8 ± 0.7 | 0.5 ± 0.8 | 0.002 ± 0.001 |
| **6** | 1.7 ± 0.7 | 0.3 ± 0.1 | 0.001 ± 0.005 |
| **8** | 1.9 ± 2.8 | 0.2 ± 0.2 | 0.002 ± 0.007 |

*Table 3A*. Mean truly dissolved $^{109}$Ag-E concentrations for the soil pore waters (µg L$^{-1}$) and their standard deviation (n = 2).

| Growth stage No | $^{109}$Ag NPs | $^{109}$AgNO$_3$ | Blank control |
|---|---|---|---|
| **4** | 0.09 ± 0.04 | 0.03 ± 0.02 | 0.009 ± 0.014 |
| **6** | 0.09 ± 0.05 | 0.03 ± 0.01 | 0.001 ± 0.001 |
| **8** | 0.11 ± 0.01 | 0.02 ± 0.02 | 0.002 ± 0.001 |

*Table 4A.* Mean $^{109}$Ag-E concentrations for the different plant tissues (µg kg$^{-1}$) and their standard deviations (n = 2).

| Growth stage No | Shoot | Root | Seed | Grain |
|---|---|---|---|---|
| | | **$^{109}$Ag NPs** | | |
| **1** | 0.41 ± 0.09 | 6.72 ± 1.12 | 0.70 ± 0.71 | |
| **2** | 0.23 ± 0.01 | 6.63 ± 0.54 | 1.35 ± 0.07 | |
| **4** | 0.29 ± 0.03 | 4.72 ± 1.35 | | |
| **6** | 0.27 ± 0.16 | 3.47 ± 1.35 | | 0.13 ± 0.03 |
| **8** | 0.33 ± 0.20 | 3.25 ± 0.46 | | 0.17 ± 0.01 |
| | | **$^{109}AgNO_3$** | | |
| **1** | 0.05 ± 0.02 | 1.35 ± 0.01 | 0.54 ± 0.53 | |
| **2** | 0.09 ± 0.01 | 1.64 ± 0.13 | 0.42 ± 0.15 | |
| **4** | 0.27 ± 0.26 | 0.68 ± 0.19 | | |
| **6** | 0.12 ± 0.06 | 1.08 ± 0.01 | | 0.06 ± 0.05 |
| **8** | 0.09 ± 0.03 | 0.69 ± 0.02 | | 0.07 ± 0.02 |
| | | **Blank control** | | |
| **1** | 0.0011 ± 0.0013 | 0.0006 ± 0.0008 | 0.0003 ± 0.0002 | |
| **2** | 0.0004 ± 0.0004 | 0.0001 ± 0.0001 | 0.0005 ± 0.0006 | |
| **4** | 0.0007 ± 0.0001 | 0.0010 ± 0.0008 | | |
| **6** | 0.0008 ± 0.0002 | 0.0011 ± 0.0002 | | 0.0006 ± 0.0004 |
| **8** | 0.0008 ± 0.0003 | 0.0007 ± 0.0002 | | 0.0002 ± 0.0001 |
| | | **Citrate control** | | |
| **1** | 0.0025 ± 0.0016 | 0.0018 ± 0.0021 | 0.0003 ± 0.0002 | |
| **2** | 0.0011 ± 0.0006 | 0.0007 ± 0.0008 | 0.0007 ± 0.0005 | |
| **4** | 0.0006 ± 0.0005 | 0.0031 ± 0.0010 | | |
| **6** | 0.0002 ± 0.0003 | 0.0014 ± 0.0016 | | 0.0001 ± 0.0001 |
| **8** | 0.0011 ± 0.0004 | 0.0007 ± 0.0008 | | 0.0005 ± 0.0002 |

*Table 4A.* Mean $[^{109}Ag\text{-}E]_{TD\text{-}PW}/[^{109}Ag\text{-}E]_{Total\text{-}Pw}$ ratios for samples from GSs 4, 6 and 8 and their standard deviations (n = 2).

| Growth stage No | $^{109}$Ag NPs | $^{109}AgNO_3$ | p-value |
|---|---|---|---|
| **4** | 0.08 ± 0.01 | 0.04 ± 0.03 | 0.67 |
| **6** | 0.05 ± 0.02 | 0.10 ± 0.04 | 0.23 |
| **8** | 0.06 ± 0.17 | 0.12 ± 0.00 | 0.28 |

## Appendix B

*Table 1B*. Mean total dry biomass yield (%) for GSs 1 to 8 and their standard deviation. The * indicates which treatments show statistical significance (n = 5 for the Ag treatments and n = 3 for the controls).

| Growth stage No | $^{109}$Ag NPs | $^{109}AgNO_3$ | Blank control | Citrate control | P-value |
|---|---|---|---|---|---|
| **1** | 114 ± 21 | 86 ± 12 | 100 ± 7 | 108 ± 10 | 0.18 |
| **2** | 90 ± 5 | 90 ± 5 | 100 ± 13 | 131 ± 21 | 0.23 |
| **3** | 94 ± 24 | 87 ± 31 | 100 ± 17 | 69 ± 28 | 0.67 |
| **4** | 130 ± 49 | 73 ± 17 | 100 ± 14 | 78 ± 32 | 0.21 |
| **5** | 104 ± 12 | 147* ± 28 | 100 ± 16 | 63* ± 16 | 0.04 |
| **6** | 123 ± 12 | 69 ± 22 | 100 ± 31 | 100 ± 28 | 0.07 |
| **7** | 144 ± 24 | 122 ± 18 | 100 ± 11 | 107 ± 33 | 0.14 |
| **8** | 81 ± 12 | 74 ± 15 | 100 ± 16 | 82 ± 26 | 0.46 |

*Table 2B.* Mean aboveground dry biomass yield (%) for GSs 1 to 8 and their standard deviation (n = 5 for the Ag treatments and n = 3 for the controls).

| Growth stage No | $^{109}$Ag NPs | $^{109}AgNO_3$ | Blank control | Citrate control | P-value |
|---|---|---|---|---|---|
| **1** | 111 ± 18 | 88 ± 12 | 100 ± 5 | 108 ± 7 | 0.20 |
| **2** | 91 ± 6 | 90 ± 8 | 100 ± 13 | 130 ± 16 | 0.13 |
| **3** | 116 ± 14 | 101 ± 24 | 100 ± 18 | 96 ± 9 | 0.37 |
| **4** | 112 ± 5 | 97 ± 17 | 100 ± 22 | 105 ± 15 | 0.53 |
| **5** | 116 ± 11 | 123 ± 13 | 100 ± 5 | 106 ± 29 | 0.12 |
| **6** | 136 ± 12 | 109 ± 15 | 100 ± 14 | 121 ± 10 | 0.05 |
| **7** | 111 ± 16 | 92 ± 16 | 100 ± 24 | 119 ± 17 | 0.40 |
| **8** | 79 ± 13 | 76 ± 15 | 100 ± 10 | 103 ± 6 | 0.06 |

*Table 3B*. Mean shoot dry biomass (g) for GSs 1 to 8 and their standard deviation (n = 5 for the Ag treatments and n = 3 for the controls).

| Growth stage No | $^{109}$Ag NPs | $^{109}AgNO_3$ | Blank control | Citrate control | P-value |
|---|---|---|---|---|---|
| **1** | 0.010 ± 0.002 | 0.010 ± 0.002 | 0.008 ± 0.004 | 0.010 ± 0.001 | 0.20 |
| **2** | 0.042 ± 0.005 | 0.043 ± 0.005 | 0.047 ± 0.006 | 0.062 ± 0.006 | 0.83 |
| **3** | 0.279 ± 0.033 | 0.241 ± 0.059 | 0.240 ± 0.042 | 0.231 ± 0.022 | 0.45 |
| **4** | 3.864 ± 0.174 | 3.356 ± 0.603 | 3.457 ± 0.772 | 3.637 ± 0.507 | 0.38 |
| **5** | 3.490 ± 0.339 | 3.702 ± 0.398 | 3.020 ± 0.158 | 3.197 ± 0.886 | 0.07 |
| **6** | 3.988 ± 0.337 | 3.216 ± 0.512 | 2.903 ± 0.356 | 3.510 ± 0.450 | 0.08 |
| **7** | 3.512 ± 0.583 | 2.896 ± 0.723 | 3.187 ± 0.791 | 3.693 ± 0.690 | 0.70 |
| **8** | 2.854 ± 0.580 | 2.772 ± 0.722 | 3.793 ± 0.119 | 3.224 ± 0.288 | 0.06 |

*Table 4B*. Mean grain dry biomass (g) for GSs 6 to 8 and their standard deviation. The * indicates which treatments show statistical significance (n = 5 for the Ag treatments and n = 3 for the controls).

| Growth stage No | $^{109}$Ag NPs | $^{109}AgNO_3$ | Blank control | Citrate control | P-value |
|---|---|---|---|---|---|
| **6** | 0.3 ± 0.1 | 0.2 ± 0.1 | 0.25 ± 0.06 | 0.30 ± 0.01 | 0.205 |
| **7** | 0.6 ± 0.3 | 0.5 ± 0.2 | 0.48 ± 0.11 | 0.67 ± 0.09 | 0.356 |
| **8** | 0.7* ± 0.2 | 0.6* ± 0.1 | 0.70 ± 0.39 | 1.40* ± 0.01 | 0.001 |

*Table 5B*. Mean shoot length (cm) for GSs 1 to 8 and their standard deviation. The * indicates which treatments show statistical significance (n = 5 for the Ag treatments and n = 3 for the controls).

| Growth stage No | $^{109}$Ag NPs | $^{109}AgNO_3$ | Blank control | Citrate control | P-value |
|---|---|---|---|---|---|
| **1** | 8.4 ± 0.7 | 8.6 ± 0.8 | 6.4 ± 1.3 | 6.1 ± 1.0 | 0.05 |
| **2** | 26.8 ± 4.4 | 26.7 ± 4.0 | 27.9 ± 2.6 | 28.9 ± 3.2 | 0.07 |
| **3** | 31.2 ± 1.0 | 28.6 ± 3.0 | 36.1 ± 3.0 | 34.9 ± 1.8 | 0.09 |
| **4** | 46.6 ± 4.7 | 45.1 ± 3.6 | 46.6 ± 1.9 | 45.2 ± 5.7 | 0.92 |
| **5** | 47.7 ± 7.9 | 54.5* ± 3.7 | 50.7 ± 3.1 | 45* ± 1.1 | 0.02 |
| **6** | 47.2 ± 0.6 | 47.9 ± 4.1 | 55.7 ± 4.7 | 54.4 ± 3.5 | 0.17 |
| **7** | 50.1 ± 0.9 | 50.1 ± 4.1 | 54.4 ± 3.2 | 58.2 ± 6.7 | 0.46 |
| **8** | 47.8 ± 1.4 | 50.5 ± 1.9 | 54.0 ± 2.1 | 56.2 ± 2.8 | 0.06 |

*Table 6B*. Mean grain length (cm) for GSs 6 to 8 and their standard deviation. The * indicates which treatments show statistical significance (n = 5 for the Ag treatments and n = 3 for the controls).

| Growth stage No | $^{109}$Ag NPs | $^{109}AgNO_3$ | Blank control | Citrate control | P-value |
|---|---|---|---|---|---|
| **6** | 8.2 ± 1.8 | 8.3 ± 2.3 | 10.3 ± 3.0 | 9.0 ± 0.6 | 0.77 |
| **7** | 8.3 ± 1.1 | 7.8 ± 1.3 | 10.1 ± 0.5 | 9.0 ± 1.4 | 0.10 |
| **8** | 9.0 ± 0.7 | 8.2* ± 0.4 | 10.2 ± 1.0 | 9.8* ± 0.1 | 0.01 |

*Table 7B*. Mean plant growth rate (days) for GSs 1 to 8 and their standard deviation. The * indicates which treatments show statistical significance (n = 5 for the Ag treatments and n = 3 for the controls).

| Growth stage No | $^{109}$Ag NPs | $^{109}AgNO_3$ | Blank control | Citrate control | P-value |
|---|---|---|---|---|---|
| **1** | 6.00 ± 0.01 | 6.0 ± 0.02 | 6.0 ± 0.01 | 6.0 ± 0.01 | 1.000 |
| **2** | 14.60 ± 0.80 | 14.8 ± 0.75 | 14.0 ± 0.03 | 14.0 ± 0.01 | 1.000 |
| **3** | 33.00 ± 2.00 | 35.4 ± 2.80 | 32.3 ± 2.36 | 33.3 ± 3.30 | 0.597 |
| **4** | 109.40 ± 8.09 | 112.2 ± 9.58 | 98.3 ± 3.09 | 98.7 ± 3.30 | 0.088 |
| **5** | 122.2* ± 0.40 | 124.6* ± 0.80 | 103.7* ± 1.25 | 104* ± 0.82 | 0.001 |
| **6** | 129.60 ± 9.31 | 127.8 ± 9.15 | 115.7 ± 6.60 | 114.3 ± 4.71 | 0.118 |
| **7** | 142.8* ± 6.37 | 144.8* ± 6.40 | 127.7* ± 5.19 | 127.7* ± 5.19 | 0.033 |
| **8** | 181.20 ± 10.83 | 185.2 ± 8.70 | 161.7 ± 8.96 | 174.7 ± 9.43 | 0.149 |

## Appendix C

In this Appendix, all media refer to Lufa soil, Lufa pore water (LUPW), Lufa hydroponic solution (LUHS), artificial pore water (APW) and 25% Hoagland solution (HS).

*Table 1C*. Mean Ag concentrations for all media in mg kg $^{-1}$ or mg L$^{-1}$ and their standard deviation (n = 3). BLOD indicates below the limit of detection data.

| Time points | Lufa soil | LUPW | LUHS | APW | HS |
|---|---|---|---|---|---|
| | | | *Ag NPS* | | |
| **0** | 9.8 ± 0.8 | 0.030 ± 0.002 | 0.017 ± 0.001 | 0.020 ± 0.001 | 0.020 ± 0.004 |
| **1** | 8.1 ± 0.9 | 0.028 ± 0.001 | 0.015 ± 0.001 | 0.008 ± 0.001 | 0.011 ± 0.007 |
| **3** | 7.6 ± 0.4 | 0.026 ± 0.001 | 0.014 ± 0.002 | 0.012 ± 0.002 | 0.008 ± 0.001 |
| **7** | 7.8 ± 0.2 | 0.025 ± 0.002 | 0.007 ± 0.001 | 0.007 ± 0.001 | 0.006 ± 0.002 |
| **14** | 7.6 ± 0.3 | 0.031 ± 0.003 | 0.011 ± 0.002 | 0.008 ± 0.002 | 0.013 ± 0.002 |
| | | | *$Ag_2S$ NPs* | | |
| **0** | 11.7 ± 1.2 | 0.007 ± 0.001 | 0.009 ± 0.001 | 0.010 ± 0.001 | 0.009 ± 0.002 |
| **1** | 11.0 ± 0.6 | 0.006 ± 0.005 | 0.009 ± 0.001 | 0.007 ± 0.003 | 0.007 ± 0.007 |
| **3** | 10.6 ± 0.9 | 0.006 ± 0.001 | 0.007 ± 0.001 | 0.005 ± 0.001 | 0.002 ± 0.001 |
| **7** | 11.0 ± 0.5 | 0.011 ± 0.004 | 0.004 ± 0.003 | 0.003 ± 0.001 | 0.002 ± 0.001 |
| **14** | 10.6 ± 1.3 | 0.020 ± 0.009 | 0.002 ± 0.001 | 0.003 ± 0.001 | 0.004 ± 0.004 |
| | | | *$AgNO_3$* | | |
| **0** | 8.5 ± 0.3 | 0.018 ± 0.005 | 0.020 ± 0.001 | 0.020 ± 0.001 | 0.020 ± 0.001 |
| **1** | 8.3 ± 0.3 | 0.023 ± 0.005 | 0.018 ± 0.005 | 0.010 ± 0.002 | 0.009 ± 0.007 |
| **3** | 8.0 ± 0.4 | 0.015 ± 0.002 | 0.016 ± 0.005 | 0.012 ± 0.002 | 0.019 ± 0.011 |
| **7** | 7.4 ± 0.8 | 0.011 ± 0.004 | 0.011 ± 0.007 | 0.008 ± 0.004 | 0.004 ± 0.001 |
| **14** | 7.2 ± 0.6 | 0.017 ± 0.002 | 0.007 ± 0.003 | 0.006 ± 0.001 | 0.007 ± 0.001 |
| | | | *Blank* | | |
| **0** | BLOD | 0.000 ± 0.000 | BLOD | 0.000 ± 0.000 | 0.000 ± 0.000 |
| **1** | BLOD | 0.000 ± 0.000 | 0.000 ± 0.000 | 0.000 ± 0.000 | 0.000 ± 0.000 |
| **3** | BLOD | 0.000 ± 0.000 | 0.000 ± 0.000 | 0.000 ± 0.000 | 0.000 ± 0.000 |
| **7** | BLOD | 0.000 ± 0.000 | 0.000 ± 0.000 | 0.000 ± 0.000 | 0.000 ± 0.000 |
| **14** | BLOD | 0.000 ± 0.000 | 0.000 ± 0.000 | 0.000 ± 0.000 | 0.000 ± 0.000 |
| | | | *Coating control* | | |
| **0** | BLOD | 0.000 ± 0.000 | 0.000 ± 0.000 | 0.000 ± 0.000 | BLOD |
| **1** | BLOD | 0.000 ± 0.000 | 0.000 ± 0.000 | 0.000 ± 0.000 | 0.000 ± 0.000 |
| **14** | BLOD | 0.000 ± 0.000 | 0.000 ± 0.000 | BLOD | 0.000 ± 0.000 |

*Table 2C*. Mean Ag concentrations for the root tissues in µg $g^{-1}$ and their standard deviation (n = 3). BLOD indicates below the limit of detection data.

| Time points | Lufa soil | LUHS | APW | HS |
|---|---|---|---|---|
| | | *Ag NPS* | | |
| **1** | 6.9 ± 2.0 | 4.1 ± 1.9 | 5.8 ± 1.8 | 12.4 ± 3.8 |
| **3** | 6.8 ± 2.3 | 2.0 ± 0.3 | 5.0 ± 2.6 | 9.6 ± 3.9 |
| **7** | 18.8 ± 3.8 | 4.6 ± 2.3 | 8.7 ± 5.0 | 9.1 ± 0.6 |
| **14** | 56.2 ± 9.5 | 5.2 ± 1.0 | 9.6 ± 3.1 | 8.9 ± 3.8 |
| | | *$Ag_2S$ NPs* | | |
| **1** | 1.0 ± 0.2 | 0.1 ± 0.2 | 0.1 ± 0.0 | 0.3 ± 0.2 |
| **3** | 2.1 ± 1.1 | 1.1 ± 0.5 | 2.9 ± 1.7 | 3.2 ± 3.0 |
| **7** | 1.6 ± 0.1 | 1.8 ± 0.9 | 1.8 ± 0.2 | 2.1 ± 0.9 |
| **14** | 4.2 ± 0.4 | 2.8 ± 1.3 | 2.1 ± 0.9 | 2.9 ± 0.6 |
| | | *$AgNO_3$* | | |
| **1** | 9.9 ± 0.8 | 12.7 ± 1.6 | 83.8 ± 28.5 | 130.3 ± 20.2 |
| **3** | 15.2 ± 2.5 | 5.7 ± 0.4 | 55.8 ± 25.4 | 76.2 ± 20.3 |
| **7** | 27.4 ± 2.2 | 6.4 ± 1.5 | 44.8 ± 30.7 | 42.7 ± 21.3 |
| **14** | 32.5 ± 7.2 | 7.7 ± 4.7 | 24.0 ± 10.0 | 13.1 ± 6.1 |
| | | *Blank* | | |
| **1** | BLOD | 0.0003 ± 0.0002 | 0.0004 ± 0.0000 | 0.0003 ± 0.0002 |
| **3** | 0.0002 ± 0.0000 | 0.0002 ± 0.0000 | 0.0005 ± 0.0000 | 0.0003 ± 0.0002 |
| **7** | 0.0002 ± 0.0002 | 0.0002 ± 0.0002 | 0.0002 ± 0.0000 | 0.0003 ± 0.0001 |
| **14** | 0.0002 ± 0.0001 | 0.0002 ± 0.0000 | 0.0002 ± 0.0000 | 0.0003 ± 0.0001 |
| | | *Coating control* | | |
| **1** | 0.0003 ± 0.0001 | BLOD | 0.0001 ± 0.0000 | 0.0004 ± 0.0001 |
| **14** | 0.0003 ± 0.0002 | 0.0001 ± 0.0000 | 0.0002 ± 0.0001 | 0.0002 ± 0.0000 |

*Table 3C*. Mean Ag concentrations for the shoot tissues in µg $g^{-1}$ and their standard deviation (n = 3). BLOD indicates below the limit of detection data.

| Time points | Lufa soil | LUHS | APW | HS |
|---|---|---|---|---|
| | | *Ag NPS* | | |
| **1** | 0.36 ± 0.17 | 0.13 ± 0.04 | 0.47 ± 0.10 | 0.54 ± 0.11 |
| **3** | 0.48 ± 0.24 | 0.44 ± 0.46 | 1.67 ± 0.75 | 1.25 ± 0.39 |
| **7** | 0.45 ± 0.21 | 0.43 ± 0.28 | 0.64 ± 0.25 | 0.74 ± 0.39 |
| **14** | 0.78 ± 0.09 | 0.58 ± 0.27 | 0.74 ± 0.39 | 1.22 ± 0.41 |
| | | *$Ag_2S$ NPs* | | |
| **1** | 0.32 ± 0.16 | 0.02 ± 0.02 | 0.01 ± 0.02 | 0.14 ± 0.11 |
| **3** | 0.29 ± 0.09 | 0.03 ± 0.02 | 0.24 ± 0.14 | 0.17 ± 0.16 |
| **7** | 0.12 ± 0.02 | 0.14 ± 0.09 | 0.28 ± 0.03 | 0.07 ± 0.04 |
| **14** | 0.35 ± 0.15 | 0.26 ± 0.23 | 0.18 ± 0.05 | 0.15 ± 0.09 |
| | | *$AgNO_3$* | | |
| **1** | 0.14 ± 0.03 | 0.10 ± 0.06 | 0.36 ± 0.34 | 0.57 ± 0.24 |
| **3** | 0.14 ± 0.06 | 0.13 ± 0.05 | 1.07 ± 0.09 | 0.26 ± 0.06 |
| **7** | 0.18 ± 0.06 | 0.42 ± 0.27 | 0.46 ± 0.18 | 0.44 ± 0.36 |
| **14** | 0.16 ± 0.04 | 0.18 ± 0.05 | 0.31 ± 0.05 | 0.33 ± 0.06 |
| | | *Blank* | | |
| **1** | BLOD | BLOD | BLOD | 0.0012 ± 0.0003 |
| **3** | 0.0004 ± 0.0004 | 0.0001 ± 0.0000 | 0.0001 ± 0.0000 | 0.0002 ± 0.0001 |
| **7** | 0.0002 ± 0.0000 | 0.0003 ± 0.0001 | 0.0002 ± 0.0001 | 0.0001 ± 0.0001 |
| **14** | 0.0002 ± 0.0001 | 0.0002 ± 0.0000 | 0.0002 ± 0.0001 | 0.0002 ± 0.0000 |
| | | *Coating control* | | |
| **1** | BLOD | BLOD | BLOD | BLOD |
| **14** | 0.0001 ± 0.0001 | 0.0004 ± 0.0002 | 0.0003 ± 0.0002 | 0.0003 ± 0.0002 |

*Table 4C*. Mean dry biomass for all media in g and their standard deviation (n = 3).

| Time points | Lufa soil | LUHS | APW | HS |
|---|---|---|---|---|
| | | *Ag NPS* | | |
| **1** | 0.014 ± 0.002 | 0.014 ± 0.002 | 0.016 ± 0.002 | 0.011 ± 0.002 |
| **3** | 0.018 ± 0.002 | 0.017 ± 0.003 | 0.020 ± 0.002 | 0.015 ± 0.001 |
| **7** | 0.031 ± 0.001 | 0.038 ± 0.004 | 0.025 ± 0.007 | 0.024 ± 0.000 |
| **14** | 0.067 ± 0.007 | 0.084 ± 0.009 | 0.078 ± 0.011 | 0.074 ± 0.005 |
| | | *$Ag_2S$ NPs* | | |
| **1** | 0.011 ± 0.002 | 0.010 ± 0.002 | 0.013 ± 0.000 | 0.010 ± 0.001 |
| **3** | 0.019 ± 0.002 | 0.021 ± 0.004 | 0.019 ± 0.002 | 0.016 ± 0.000 |
| **7** | 0.031 ± 0.003 | 0.034 ± 0.004 | 0.036 ± 0.001 | 0.026 ± 0.003 |
| **14** | 0.056 ± 0.004 | 0.071 ± 0.006 | 0.071 ± 0.008 | 0.074 ± 0.012 |
| | | *$AgNO_3$* | | |
| **1** | 0.012 ± 0.002 | 0.009 ± 0.004 | 0.012 ± 0.002 | 0.014 ± 0.003 |
| **3** | 0.016 ± 0.001 | 0.016 ± 0.000 | 0.013 ± 0.001 | 0.016 ± 0.003 |
| **7** | 0.026 ± 0.005 | 0.026 ± 0.005 | 0.028 ± 0.005 | 0.032 ± 0.001 |
| **14** | 0.042 ± 0.002 | 0.063 ± 0.013 | 0.067 ± 0.008 | 0.066 ± 0.009 |
| | | *Blank* | | |
| **1** | 0.008 ± 0.001 | 0.009 ± 0.001 | 0.012 ± 0.002 | 0.013 ± 0.001 |
| **3** | 0.017 ± 0.002 | 0.010 ± 0.002 | 0.013 ± 0.001 | 0.019 ± 0.002 |
| **7** | 0.022 ± 0.003 | 0.022 ± 0.003 | 0.024 ± 0.003 | 0.030 ± 0.002 |
| **14** | 0.049 ± 0.003 | 0.054 ± 0.008 | 0.054 ± 0.008 | 0.053 ± 0.011 |
| | | *Coating control* | | |
| **1** | 0.009 ± 0.001 | 0.009 ± 0.000 | 0.010 ± 0.001 | 0.015 ± 0.003 |
| **14** | 0.040 ± 0.004 | 0.044 ± 0.007 | 0.054 ± 0.008 | 0.073 ± 0.004 |

*Table 5C*. Mean Ag distribution for all media and all compartments (n = 3).

| Ag distribution | Lufa soil | LUHS | APW | HS |
|---|---|---|---|---|
| | | *Ag NPs* | | |
| **% medium** | 78 | 53 | 39 | 35 |
| **% LUPW** | 0.01 | | | |
| **% root** | 0.12 | 24 | 39 | 26 |
| **% shoot** | 0.003 | 0.7 | 5.8 | 13.6 |
| **% adsorption** | 22 | 22 | 16 | 25 |
| | | *$Ag_2S$ NPs* | | |
| **% medium** | 88 | 18 | 28 | 36 |
| **% LUPW** | 0.01 | | | |
| **% root** | 0.01 | 43 | 25 | 24 |
| **% shoot** | 0.001 | 7.4 | 4.6 | 3.9 |
| **% adsorption** | 12 | 31 | 42 | 37 |
| | | *$AgNO_3$* | | |
| **% medium** | 83 | 9 | 30 | 19 |
| **% LUPW** | 0.01 | | | |
| **% root** | 0.04 | 58 | 57 | 70 |
| **% shoot** | 0.0004 | 13.1 | 7.5 | 1.5 |
| **% adsorption** | 17 | 20 | 5 | 9 |

*Table 6C*. Mean $[Ag]_{Shoot}/[Ag]_{Root}$ ratios determined for samples from days 7 and 14 (n = 3).

| Treatment | Lufa soil | LUHS | APW | HS |
|---|---|---|---|---|
| **Ag NPS** | 0.02 ± 0.01 | 0.03 ± 0.03 | 0.08 ± 0.02 | 0.09 ± 0.03 |
| **$Ag_2S$ NPs** | 0.08 ± 0.02 | 0.08 ± 0.03 | 0.12 ± 0.04 | 0.04 ± 0.01 |
| **$AgNO_3$** | 0.01 ± 0.002 | 0.09 ± 0.03 | 0.01 ± 0.01 | 0.02 ± 0.02 |

*Table 7C*. Mean $[Ag]_{Shoot}/[Ag]_{Medium}$ ratios determined for samples from days 7 and 14 (n = 3).

| Treatment | LUPW | LUHS | APW | HS |
|---|---|---|---|---|
| **Ag NPS** | 22 ± 8 | 33 ± 32 | 95 ± 43 | 191 ± 116 |
| **$Ag_2S$ NPs** | 20 ± 18 | 70 ± 59 | 81 ± 26 | 27 ± 6 |
| **$AgNO_3$** | 13 ± 5 | 182 ± 131 | 68 ± 43 | 78 ± 52 |

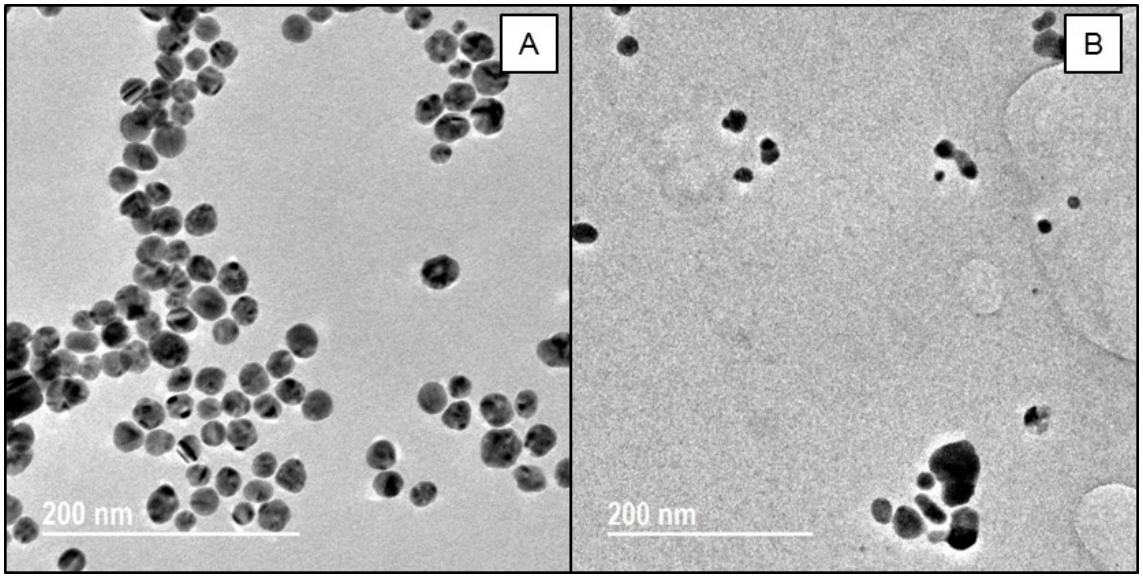



*Figure 1C*. TEM micrographs of the Ag NPs (A) and the $Ag_2S$ NPs (B).

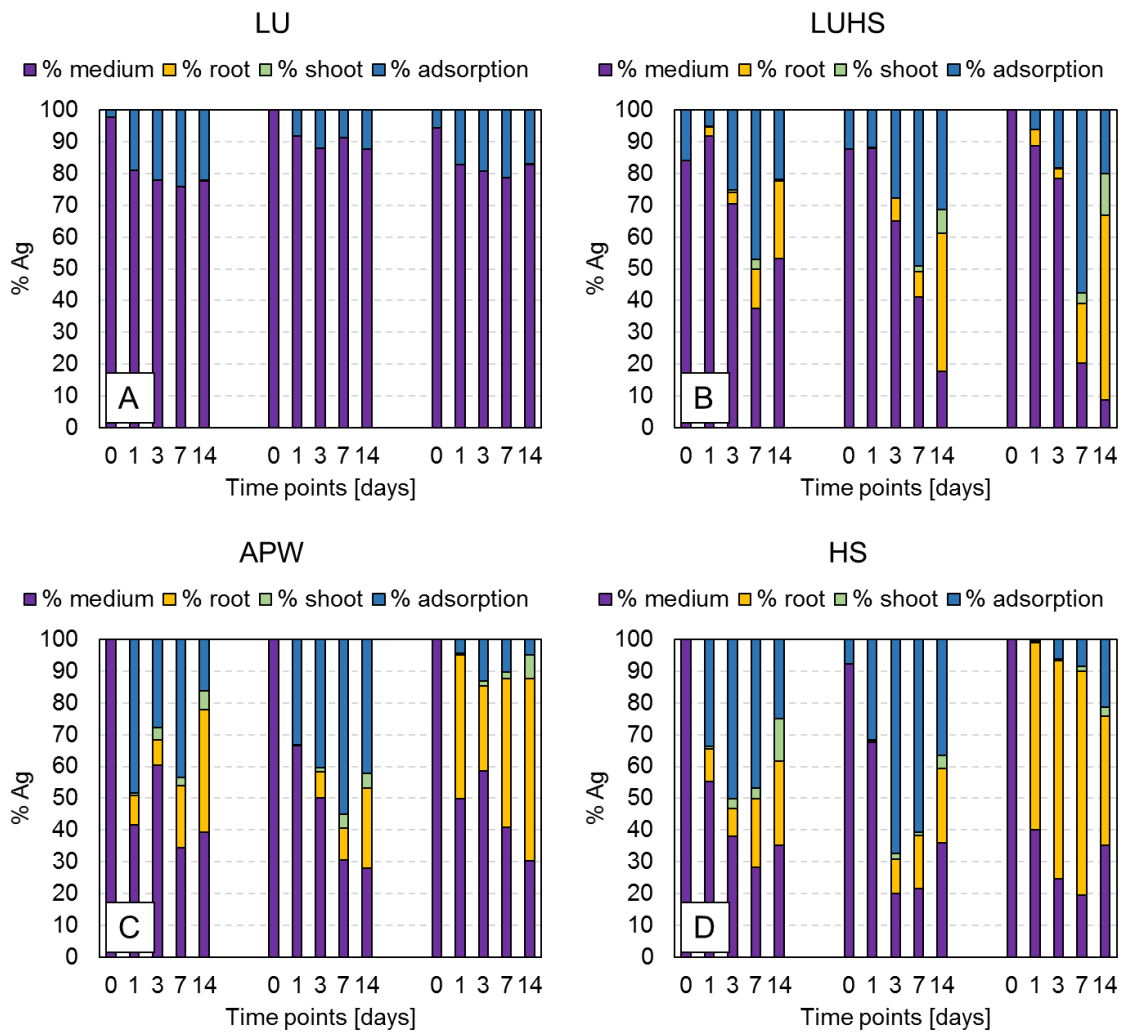



*Figure 2C*. Mean Ag distribution for the Lufa soil (LU), Lufa hydroponic solution (LUHS), artificial pore water (APW) and Hoagland solution (HS) systems between day 1 and 14. The distributions were determined by mass balance calculations for the different compartments, which are exposure medium (soil or hydroponic solution) as well as root and shoot tissues (n = 3). For each system, the maximum value of 100% was defined by the Ag mass that as introduced into the system at the beginning of the exposure. Any Ag that was not found in any of the medium or plant tissue compartments was assumed to be adsorbed to the container walls. As the extracted LUPW contains less than 0.01% of the Ag for exposures carried out in Lufa soil (LU), this reservoir cannot be seen at the scale of the figure and it is hence ignored.

## Appendix D

*Table 1D*. Mean Ag concentrations for the treated and untreated roots in µg $g^{-1}$ and their standard deviation for the Ag NP exposure (n = 3).

| Time point | Ag concentrations [mg $kg^{-1}$] | |
|---|---|---|
| | **Treated roots** | **Untreated roots** |
| | *Wet-wet at 10 mg Ag $kg^{-1}$* | |
| **Day 7** | 63.3 ± 5.9 | 5.1 ± 1.8 |
| | *Wet-dry at 10 mg Ag $kg^{-1}$* | |
| **Day 7** | 33.7 ± 15.7 | 6.2 ± 0.7 |
| | *Wet-wet at 50 mg Ag $kg^{-1}$* | |
| **Day 7** | 531.9 ± 13.5 | 5.3 ± 0.7 |
| | *Wet-dry at 50 mg Ag $kg^{-1}$* | |
| **Day 7** | 266.9 ± 9.6 | 6.3 ± 0.6 |

*Table 2D*. Mean Ag concentrations for the shoots in µg $g^{-1}$ and their standard deviation for the Ag NP exposure (n = 3).

| Time point | Ag concentrations [mg $kg^{-1}$] |
|---|---|
| | **Shoots** |
| | *Wet-wet at 10 mg Ag $kg^{-1}$* |
| **Day 7** | 0.4 ± 0.3 |
| | *Wet-dry at 10 mg Ag $kg^{-1}$* |
| **Day 7** | 0.2 ± 0.1 |
| | *Wet-wet at 50 mg Ag $kg^{-1}$* |
| **Day 7** | 0.6 ± 0.1 |
| | *Wet-dry at 50 mg Ag $kg^{-1}$* |
| **Day 7** | 0.6 ± 0.2 |

*Table 3D*. Mean Ag concentrations for the soils in mg $kg^{-1}$ and their standard deviation for the time series exposure. BLOD signifies below the limit of detection (n = 3).

| Time point | Ag NPs | $AgNO_3$ | Control |
|---|---|---|---|
| | | *Treated soil* | |
| **Day 0** | 9.8 ± 0.2 | 9.7 ± 0.3 | 0.05 ± 0.03 |
| **Day 1** | 9.4 ± 0.1 | 9.2 ± 0.1 | BLOD |
| **Day 3** | 9.6 ± 0.1 | 9.0 ± 0.1 | BLOD |
| **Day 7** | 9.3 ± 0.1 | 8.8 ± 0.3 | BLOD |
| | | *Untreated soil* | |
| **Day 0** | 0.05 ± 0.03 | 0.05 ± 0.03 | 0.05 ± 0.03 |
| **Day 1** | 0.02 ± 0.02 | 0.05 ± 0.04 | 0.05 ± 0.02 |
| **Day 3** | BLOD | BLOD | 0.02 ± 0.01 |
| **Day 7** | 0.05 ± 0.01 | 0.05 ± 0.03 | BLOD |

*Table 4D*. Total and truly dissolved Ag concentrations in the treated pore waters in mg $L^{-1}$ and their standard deviation for the time series exposure (n = 3) .

| Time point | Ag NPs | $AgNO_3$ | Control |
|---|---|---|---|
| | | *Total Ag concentration [mg $L^{-1}$]* | |
| **Day 0** | 13.72 ± 1.86 | 3.67 ± 1.34 | 0.60 ± 0.33 |
| **Day 1** | 16.10 ± 2.75 | 3.80 ± 0.99 | 0.15 ± 0.01 |
| **Day 3** | 13.67 ± 1.26 | 4.13 ± 0.18 | 0.15 ± 0.01 |
| **Day 7** | 13.65 ± 1.07 | 6.11 ± 1.09 | 0.16 ± 0.03 |
| | | *Truly dissolved Ag concentration [mg $L^{-1}$]* | |
| **Day 0** | 1.65 ± 0.20 | 0.65 ± 0.10 | 0.07 ± 0.01 |
| **Day 1** | 1.56 ± 0.20 | 0.65 ± 0.07 | 0.05 ± 0.03 |
| **Day 3** | 1.54 ± 0.17 | 1.24 ± 0.07 | 0.06 ± 0.03 |
| **Day 7** | 2.30 ± 0.13 | 1.57 ± 0.37 | 0.06 ± 0.03 |

*Table 5D*. Mean Ag concentrations for the treated and untreated roots in µg $g^{-1}$ and their standard deviation for the time series exposure (n = 3).

| Time point | Ag NPs | $AgNO_3$ | Control |
|---|---|---|---|
| | | *Treated roots* | |
| **Day 1** | 71.17 ± 19.59 | 14.38 ± 1.84 | 0.001 ± 0.002 |
| **Day 3** | 109.79 ± 32.28 | 36.88 ± 12.47 | 0.002 ± 0.001 |
| **Day 7** | 32.75 ± 4.56 | 17.449 ± 0.26 | 0.001 ± 0.002 |
| | | *Untreated roots* | |
| **Day 1** | 5.60 ± 1.84 | 2.19 ± 0.56 | 0.006 ± 0.001 |
| **Day 3** | 11.47 ± 1.47 | 4.96 ± 1.16 | 0.005 ± 0.002 |
| **Day 7** | 6.21 ± 1.25 | 3.98 ± 0.82 | 0.006 ± 0.003 |

*Table 6D*. Mean Ag concentrations for the shoots in µg $g^{-1}$ and their standard deviation for the time series exposure (n = 3).

| Time point | Ag NPs | $AgNO_3$ | Control |
|---|---|---|---|
| **Day 1** | 1.29 ± 0.155471 | 0.855 ± 0.0350572 | 0.007 ± 0.001 |
| **Day 3** | 0.86 ± 0.031625 | 0.670 ± 0.03052 | 0.006 ± 0.002 |
| **Day 7** | 0.54 ± 0.005912 | 0.454 ± 0.0286957 | 0.005 ± 0.001 |